NASA-CR-165, 917

NASA Contractor Report 165917

NASA-CR-165917
19820025528

DESIGN CONCEPTS AND COST STUDIES FOR MAGNETIC SUSPENSION AND BALANCE SYSTEMS

H. L. Bloom, et al.

KENTRON INTERNATIONAL, INC.
Hampton Technical Center
Hampton, Virginia 23666

GENERAL ELECTRIC COMPANY (Subcontractor)
Energy Systems Programs Department
Schenectady, New York 12345

Contract NAS1-16000
July 1982

National Aeronautics and Space Administration

Langley Research Center
Hampton, Virginia 23665

FOREWORD

This report represents the final results of a 5-month Study to develop design concepts and estimates of costs and schedules for Magnetic Suspension and Balance Systems.

During the course of this Study, documents defining the then-current methods, approaches and results have been issued at the times of the Orientation Meeting on November 20, 1980, the Mid-Term Review on January 28, 1981, and the Final Review on February 27, 1981. In addition, limited amounts of such information have been included in Monthly Progress Reports. Since the requirements initially published for the Study have been evolving and have been supplemented frequently during its execution, the consequent study results have undergone continual changes. This report represents the results of the latest version of requirements and corrections of information presented at the Final Review, and, therefore, supersedes all other documents previously issued as part of this Study.

The following General Electric personnel have contributed to the work performed under this Contract: H.L. Bloom, General Electric Program Manager, and, in alphabetical order, R. Baheti, H. Betzweiser, L. Coffman, W. Court, M. Cusano, J. Donato, K. Haefner, W. Hedrick, J. Heinrich, E. Hotchkiss, A. Kalafala, C. Linkinhoker, D. Mercaldi, P. Michaelson, P. Ostermann, W. Overstreet, R. Perrault, J. Pilcher, R. Pohl, R. Quay, K. Sands, D. Scott, R. Shafer, R. Smith, T. Sullivan, J. Sweeney, A. Wait, J. Welch, R. Willig.

TABLE OF CONTENTS

TABLE OF CONTENTS (cont.)

TABLE OF CONTENTS (cont.)

TABLE OF CONTENTS (cont.)

LIST OF ILLUSTRATIONS

LIST OF ILLUSTRATIONS (cont.)

LIST OF ILLUSTRATIONS (cont.)

LIST OF ILLUSTRATIONS (cont.)

1.0 INTRODUCTION & SUMMARY

The utilization of magnetic suspension and balance systems for wind tunnel models has been demonstrated in small scale applications[1,2,3], and has been analyzed in preliminary "scale-up" studies[4,5]. Results of these programs indicate that the application of such systems to large-scale, high Reynolds Number wind tunnels is feasible. In order to develop comprehensive plans for logical development of magnetic suspension and balance systems which accommodate the test section and model sizes compatible with high Reynolds Number, design concepts of such systems must first be defined. These concepts must be supported by preliminary estimates of the timing and costs to design, acquire and operate the eventual systems.

General Electric, under contract to Kentron International Incorporated, and in close interaction with Mr. Neil Holmberg and other key NASA-Langley personnel, has carried out the definition of a family of MSBS concepts. These design concepts and estimates of related programmatic data are the subjects of this report.

The point of departure for the Study was a set of requirements defined in the project Statement of Work issued October 28, 1980.[*] As the Study proceeded, these requirements were supplemented and complemented by additional and alternative requirements; those relating to decreased forced model oscillations, control system provision for disturbances in continuous flow wind tunnels, and realistic limitations on the wide spectrum of possible magnet design approaches.

While the Study Team attempted to respond to the logical changes in requirements, there was insufficient time to carry all changes through all of the steps of establishing the design concepts corresponding to each change. Consequently, not all calculations and estimates are shown for the subsystems in each Case/Alternative. However, interpolations and extrapolations of data were made in those cases where detailed calculations were not performed, so that the final cost estimates could be presented.

As a result of the 3 test section/model cases specified in the MSBS Statement of Work combined with 2 possible levels of wind tunnel flow disturbance, and 2 reduced levels of forced model oscillation requirements, GE investigated, to various depths, the 21 combinations of requirements shown in Figure 1.1.

*Summarized in Section 2 MSBS Requirements

Figure 1.1

REQUIREMENT ALTERNATIVES

Requirements of RFP Paragraphs 2.2.3, 2.2.4, 2.2.6 (Duty Cycle, Forces and Moments, Model Angular Displacement, Positioning Accuracy) Plus One of Columns Below							
	A	B	C	D	E	F	G
Forced Model Sinusoidal Oscillations:	As in RFP Para. 2.2.5	10% of Para. 2.2.5	0	0	As in Para. 2.2.5	10% of Para. 2.2.5	0
Control Force and Frequency to Overcome Disturbance;							
Force:	.5% of Static Force	.5%	.5%	.5%	.1%	.1%	.1%
Frequency:	50 Hz	50 Hz	50 Hz	10 Hz	By Simulation	By Simulation	By Simulation
<u>Case 1</u> 8'x8' Test Section Mach. No. 0.9	X	X	X	X	X	X	X
<u>Case 2</u> 8'x8' Test Section Mach. No. 0.3	X	X	X	X	X	X	X
<u>Case 3</u> 4'x4' Test Section Mach. No. 0.9	X	X	X	X	X	X	X

This broad investigation served to identify the most rigorous requirements and their effects. For instance, implementation for Case 1 (8x8 foot test section, transonic) of the full set of requirements specified in the Statement of Work, supplemented by the requirement to control the model under maximum wind tunnel disturbance levels - that is, Case 1, Alternative A, in Figure 1.1 - resulted in a peak power demand from the utility of nearly 20,000 MVA and called for approximately 6 acres of helium storage tanks, among other out-size implementation data. Furthermore, a preliminary cost estimate came to nearly one billion dollars, half of which would be for power supplies, for such a system. These results clearly indicated the need to review Statement of Work requirements for possible easing.

Major reductions in the implementation data occurred when agreement was obtained to reduce the forced model oscillation requirements of the Statement of Work to one-tenth of the values specified in the Statement of Work. For Case 1, Alternative B, power requirements dropped to one-half of Alternative A, with corresponding decreases in other areas. Elimination of the forced model oscillation mode, Alternative C, produced further, but less dramatic reductions. Finally, reduction of the wind tunnel disturbance level to the .1%, felt by NASA to be more representative of current tunnels, and utilizing GE's control simulation to determine the magnitude and rate of corrective control force, were judged to provide the most logical combination of disturbance requirements. Study effort was, therefore, finally concentrated on the three cases 1, 2 and 3, and three levels of forced model oscillations (100% of Statement of Work requirements, 10% of those requirements, and 0%), Alternatives E, F and G in Figure 1.1.

More detailed discussion of MSBS requirements is found in Section 2.0 of this report.

The above-noted variations in requirements, while imposing a broad spectrum of subsystem requirements, nevertheless represented a consistent system concept, which is depicted in Figure 1.2. As shown in the figure, the control of the model position and attitude is vested in the Control System computer, which is interfaced by its keyboard and displays.

The Control System computer commands the power supplies of each set of magnets, either via keyboard inputs or model attitude and position feedback, to vary power to the magnets for the purposes of establishing or holding selected positions and attitudes and/or rates.

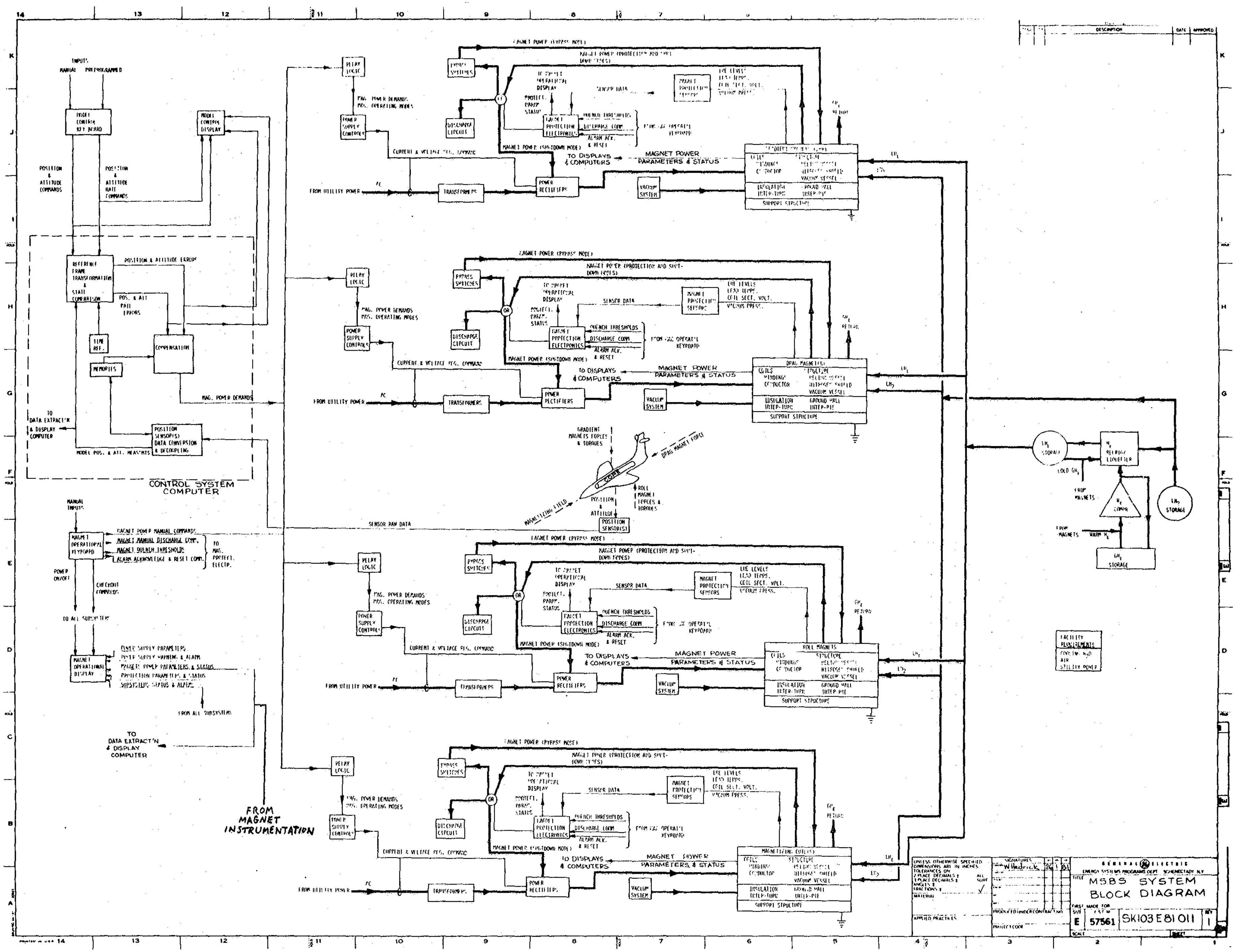

Figure 1.2

MSBS SYSTEM BLOCK DIAGRAM

Model Position Sensors feed model position and attitude data to the Control System computer to close the control loop, and magnet power instrumentation provides data to the Data Extraction and Display Computer to enable calculation of aerodynamic forces and moments.

Other magnet sensors support the magnet protection system, which monitors the magnet parameters that warn of impending failures in magnets, their support services and equipment, and automatically, or on-command, carries out magnet discharge, bypass, or shutdown operations.

Within this overall system, the changes in requirements, responsive variations in subsystems and resulting programmatic effects contributed a feedback loop to the process of developing the final versions of MSBS design concepts.

While the iterations among requirements, the configuration concepts meeting them, the characteristics that size the concepts and cost estimates for such concepts were proceeding, significant decisions were made in the selection of subsystems. Figure 1.3 lists the key subsystem concept tradeoffs and analyses that were carried out and, in the case of tradeoffs, notes the selection made. In all subsystem concepts, selections utilize available hardware or existing technology.

In the magnet area, the results of earlier studies and discussions with key participants in magnetic suspension programs enabled early narrowing of candidate gradient magnet arrangements to the "+" and the "x". Subsequent trades, discussed in Section 2.0, resulted in selection of the "+" arrangement, primarily on a cost and system effectiveness basis. Section 2.0 also pinpoints the economic reasons for selecting bipolar coils, the design simplification accruing from using coils with AC and DC operating capability as opposed to separate AC and DC coils in the necessarily close proximity to each other, and the state of art limitations that led to the decision for modularization.

The analyses of the mode of conductor stabilization and conductor configuration is given in Section 2.0. Key features of the magnet system are given in Figure 1.4.

The Cryogenics concept is discussed in Section 4.0. Its features are summarized in Figure 1.5.

The use of 4.2°K liquid helium, with liquid nitrogen intercooling and vacuum insulated dewars, is currently standard in large superconducting magnet

Figure 1.3 SUBSYSTEM CONCEPTS ANALYZED AND EVALUATED

- Magnets:

  Arrangement - "X" vs "+"*
  Coils - Bipolar* vs Monopolar, Modularized AC/DC Coils* vs Separate AC and DC Coils
  Conductor - Stabilization Modes, Configurations
  Cooling - Pool Boiling* vs Forced Flow, Dewar Arrangements
  Structures - Helium Vessel Materials (Metallic vs Non-Metallic)*, Segmented vs Monolithic

- Power Supplies:

  Silicon Controlled Rectifier (SCR)-Based* vs Rotating Machinery vs Energy Storage

- Cryogenic System

  Storage Capacity and Refrigeration/Liquefacation Capacity

- Control System, Displays, Computer

  Back-up Computer* vs Back-up Capability in Data Extraction Computer

- Position Sensors

  Two EPS's and an Optical System
  Point Detectors vs Imaging Sensors vs Solid State Arrays*

*Denotes Selection Resulting from Tradeoff

Figure 1.4 MAGNET SYSTEM KEY FEATURES

- 20 Magnets in Symmetric Configuration
  - 4 Z (Vertical Axis) and 4 Y (Horizontal Axis) Gradient Coils in "+" Arrangement
  - 2 Magnetization Coils
  - 2 Drag Coils
  - 8 Roll Coils
- Bipolar Z, Y and Roll Coils
- Case 1 and Case 2 Conductors are 50,000 AMP, Cryostable, Pie or Layer Wound with Standard Insulation, and Mechanically Constrained
- Case 3 Conductors for Gradient and Roll Coils are 1,000 AMP, Epoxy-Impregnated, Adiabatically Stable. Other Coils as Above.
- Reinforced Non-metallic (G-10) Magnet Dewars for Alternate E. Metallic Dewars Possible for Alternatives F and G

FIGURE 1.5

KEY FEATURES OF THE CRYOGENICS SUBSYSTEMS

- o System includes helium, nitrogen and vacuum subsystems.
- o Liquid helium in magnet dewars @ 4.2^{o}K and 1 to 2 Atm. Nitrogen @ 77^{o}K to cooldown helium in liquefier/refrigerator, second stage cooling of current leads. Vacuum for dewar jackets, liquid helium transfer lines and storage dewars.
- o Liquefier/refrigerator sized for continuous, 24 hour, operation; specified MSBS duty cycle plus 14 hour replenishment mode.
- o Liquid helium storage sized for 50% contingency.
- o Design and Componentry are State-of-Art.

  -Cases 1 and 2, Alternative E require liquefier/refrigerator plants (22,000 and 9,500 liters/hr., respectively), 2 to 5 times larger than largest plant being built. All other cases and alternatives use plants of sizes currently in use.
- o Nitrogen boiloff is vented to atmosphere.
- o Vacuum provided by roughing pump @ 10^{-3} torr. At coil assembly diffusion pump reduces vacuum to 10^{-6} torr.
- o Initial cooldown by helium gas @ $\sim 20^{o}$K, followed by liquid helium.

  -Plan 7 days for cooldown.

applications. In sizing the cryogenic subsystems, the cost effective operating mode calls for balancing the liquid helium storage capacity, the liquefaction/refrigeration capacity, and the liquid helium requirement of the duty cycle specified in the Statement of Work. The aim is to maintain the liquefier/refrigerators in continuous full capacity operation, which supplies only a portion of the liquid helium used during the 10 hours of specified operations and performs the remaining replenishment during the 14 hours of standby.

Power Supplies, Magnet Protection and MSBS Instrumentation are discussed in Section 5.0. These subjects have customarily been treated together because of their close interactions in an operating superconducting magnet system. In the event of any of several types of system failures, the potential catastrophic damage to such magnets by the power transmitted from the power supplies imposes the need for both warning of incipient failures (provided by specific instrumentation), and action to prevent damage (provided by the protection system). So as not to fragment an area, other instrumentation (for diagnostics, performance measurement) is included in this portion of the project.

Figure 1.6 summarizes the major features of the Power Supplies, Protection and Instrumentation.

Four quadrant, bipolar power supplies are provided to enable full current and voltage reversals in the gradient and roll magnets. Two quadrant, monopolar supplies are provided for the drag and magnetization coils. It was determined that SCR Invertor/Convertor would best serve the needs of MSBS, although for the higher power Cases and Alternatives, high peak power demands on the utility may necessitate consideration of a "buffer" energy storage unit or in-house peak power generation. The use of 50,000 amps, when combined with high voltage (> 1000 volts) calls for specialized design, but makes use of existing technology and components.

The large-scale power supplies call for high-rated power switches. The MSBS concepts utilize an existing type of GE switch in a series/parallel network to meet these requirements. Also, for the large scale discharge resistors, the present concept utilizes parallel resistors of existing, but smaller capacity to take advantage of the cost savings involved in multi-unit purchases.

The Control System concept discussed in Section 6.0, has been developed in two 3 degree of freedom modes - longitudinal (pitch, heave and drag), and lateral (yaw, slip and roll) and has been subjected to preliminary verification in GE's control simulation. The results indicate that required position and

FIGURE 1.6

POWER SUPPLIES, PROTECTION AND INSTRUMENTATION KEY FEATURES

- Bipolar Power Supplies (for gradient and roll magnets).
- Monopolar Power Supplies (for drag and magnetization coils).

} Silicon controlled rectifier - based

- Separate power supplies and discharge resistors for each magnet module.
- 50,000 AMP is maximum current required, several magnets require 1,400 to 750 AMP.
- Cases 1, 2 and 3, Alternative E, require maximum voltages of 2,250 to 8,000 volts, maximum of remaining cases and alternatives is < 1,000 volts, many magnets require < 100 volts.
- Power switching by existing switches requires series/parallel switch network for large power supplies.
- Discharge resistors sized for 30 second discharge - Maximum required rating 379 megajoules, many <50 megajoules, many <10.
- Instrumentation includes voltage taps, thermocouples, liquid helium level sensors, Ion vacuum gages, strain gages, liquid helium carbon glass sensors, AC and DC current transducers.

attitude accuracies have been met for both stable and unstable aerodynamic configurations. The Control System concept, developed on the basis of linearized force-current relationships for the magnets, has also been shown to be effective with a non-linearized relationship. Other features of the Control System, listed in Figure 1.7, identify the selected Control System Computer (PDP 11/60) and some of the key interfaces and peripherals for the computer.

Position Sensors are discussed in Section 7.0. By terms of the Statement of Work, two Electronic Position Sensors have been included in the study, based on scale-up of the MIT EPS. The scale-up approach has not resulted in satisfactory solutions. While position accuracies of the scaled-up sensors meets the requirements of the Statement of Work, attitude accuracies do not. Furthermore, the scale-up approach did not provide the nearly 10 to 1 separation between resonant frequencies and the basic 20 KHz operating frequency that is achieved in the MIT sensor. It is felt, however, that these shortcomings do not eliminate the Electromagnetic Position Sensor as an MSBS sensor - only that a simple scale-up is not feasible.

A more serious problem of the Electromagnetic Position Sensor is the fact that it will require the use of non-metallic test section walls to avoid shielding the model core/coil signals. However, the current availability of such high strength composites as G-10 glass fiber/epoxy and of polycarbonates such as Lexan can overcome this problem.

The key features of the Electromagnetic Position Sensor and the Electro-Optical Position Sensor are noted in Figure 1.8. The Electro-Optical Position Sensor makes use of an already developed application (star trackers) of existing hardware (Charge Injection Device area array cameras). Not only do the multiple cameras offer high reliability through redundancy, but also allow the option of video display of the model. The Electro-Optical Position Sensor is independent of model and core shape and size, as well as test section size (within a wide range).

Section 8.0 is a discussion of the brief task defined in the Statement of Work to identify the data available from the MSBS Magnet System Instrumentation. Such data would be used by NASA to extract and display the aerodynamic data of the model being tested, and to perform an error analysis of the results. In addition, this task discusses methods of system-independent calibration of the data extraction process. It is concluded that, in the worst case of uncertainties in measurement of magnet currents, the measurements of magnet forces

FIGURE 1.7

CONTROL SYSTEM KEY FEATURES

- Six degree of freedom performance meets accuracies specified in Statement of Work. Verified in simulation of 2 three degree of freedom modes - longitudinal (pitch, heave, drag) and lateral (yaw, slip, roll).
- Performance verified in simulation for stable and unstable aerodynamic configurations.
- Performance verified insimulation for linearized force - current relationship, and non-linear.
- Control algorithm bandpass is 20 Hz.
- Analog to digital converter required for electromagnetic position sensor.
- Digital interface required for electro-optical position sensor.
- On-line data storage (24 variables, 50 samples/second - maximum) capability is 2 hours.
- Computer is PDP 11/60 minicomputer, backup is a stripped down PDP 11/60.
- Software is FORTRAN supplemented with macro-level software for functions requiring faster computation times.
- Control computation (600 multiples and 600 additions) accomplished in 4 to 5 miliseconds.
- Monitor and display of magnet coil currents, coil status, status of other subsystems, model position and attitude, time plots of control outputs, TV (optional).

Figure 1.8

KEY FEATURES OF THE POSITION SENSORS

- MSBS Concept includes 2 Electro-magnetic Position Sensors (scale-up from MIT EPS) and an Electro-Optical Position Sensor (using area array solid state cameras).

- Position Sensors based on scale-up of EPS meet position accuracies, not attitude accuracies. Redesign required. Requires non-metallic test section wall.
  - Use dual coils at each location on sensor, and separately powered - for redundancy reliability

- Electro-Optical Position Sensor System uses 10 Charge Injection Device cameras, 9 model mounted "targets".
  - Provides option for video viewing
  - Use microprocessor for command generation and data processing, control system computer for backup

and torques would be uncertain by $\pm$ .2%.

In the case of position and attitude measurements, it is concluded that meeting the position and attitude holding accuracies specified in the Statement of Work requires measurement accuracies of about 1/2 the holding values. These are well within the capabilities of the Electro-Optical Position Sensor, and can probably be met by an Electromagnetic Position Sensor designed from "scratch".

Force and torque calibration by the technique of applying forces and torques mechanically while measuring the magnet currents required to balance the applied forces and torques is the "classical" approach. While it has been used, and is backed by existing computer programs to handle the non-linear relationships involved, the inverse procedure could provide direct, high resolution force and moment readouts. Both approaches are recommended at this time.

Interfaces that must be provided for MSBS at the operating site are discussed in Section 9.0 and indicated in Figure 1.9. The electrical power interface to the power supplies for charging the magnets is a primary concern, particularly for the MSBS Alternative E. Resolution of the utility's capability to accommodate peak power demands must be completed early in the project. The power supplies potential impact on other non-MSBS equipment which may be sensitive to electromagnetic interference will require protective measures.

MSBS magnets must, of necessity, be installed in close proximity to the test section without depending on the wind tunnel for support. Provision must, therefore, be made for space around the test section, and mounting surfaces must be emplaced. The exposure of personnel to the magnets during MSBS operations requires control on work location and duration, and care must be exercised on the location of magnetically susceptible electronics and tools.

The Control System requires, primarily, nominal electrical power and wiring to the Data Extraction Computer.

The Cryogenics Subsystems major requirement is for sufficient indoor and outdoor space to accommodate the large volume of components, primarily tank farm and liquefier/refrigerators. There is also a need for a substantial amount of electrical power.

Position Sensors interfaces call for minimal Radio Frequency Intereference in the 5 to 20 KHz range in the proximity of the Electromagnetic Position Sensor, and the previously discussed restriction to non-metallic test section walls for that sensor. The Electro-Optical Position Sensors interfaces are

Figure 1.9

KEY AREAS OF MSBS INTERFACE REQUIREMENTS

MSBS Subsystem	Interface Area
Power Supply Interfaces	Electrical Power, Cooling Water, Cooling Air, Interface Cabling and Wiring, Separation Distance or Shielding of EMI-Sensitive Equipment
Magnets Interfaces	Installation Mounting Pads, Clear Space around Test Section, Exposure Levels of Personnel, Proximity of Electronic Equipment and Magnetically Susceptible Tools
Control System Interfaces	Electrical Power, Interface Wiring for Data Extraction and Display Computer
Cryogenics Interfaces	Outdoor Space for Tank Farm, Indoor Installation Space, Minimum Helium Piping Run, Electrical Power, Minimal RFI, Non-metallic Test Section Walls (for EPS)
Position Sensors	Visual Access to Model and Illumination of Model (for Electro-Optical Position Sensor)

limited to the earlier-noted visual access and model illumination.

Section 10.0 assembles all the subsystem concepts into the MSBS concept pictured in Figure 1.10. Dimensions are given for all Cases specified in the Statement of Work, Cases 1, 2 and 3. It is noted that the large (> 30 ft.) diameter of the drag and magnetization coils for Cases 1 and 2 would require their transportation to the installation site via water routes. Section 10.0 also shows sketches of the total indoor installation of Case 1 Alternative F, and calculates the installation areas for the other Cases and Alternatives, as well as the sizes of required outdoor areas.

The estimated schedule for carrying out a program to bring an MSBS into operation is given in Section 11.0. The 60 month schedule covers Preliminary Design, Final Design, Fabrication, Testing, Installation and Checkout. To meet the 60 month schedule, it will be necessary to perform advance procurements of the magnet conductor, which is obtainable only from sources with limited production capability. Initiation of advance procurement vendor surveys, proposal requests, and subcontract negotiations are also required for the power supplies and liquefier/refrigerators in order to assure adequate time to select the best combination of vendor competence and minimal price.

Cost Estimates are provided in Section 12.0 for all specified Cases, Alternatives E, F and G and are summarized in Figure 1.11. Costs have been assembled by Work Breakdown Structure (shown in Appendix B) number, and are also spread, by 6 month increments over the 5 year schedule.

Conclusions and Recommendations, Section 13.0, states that all three Cases, Alternatives E, F and G are feasible from a technical point of view. No judgement is made on economic feasibility, although the power supplies and cryogenics for Cases 1 and 2 are relatively expensive.

This section notes that the larger ratings of power supplies, the liquefier/refrigerators of the largest sizes, and non-metallic dewars are considered at the limits of state-of-the-art. However, custom design and standard componentry are expected to be successful in the first two areas and developments are in process in the third which are expected to solve its problems in time for potential MSBS application.

A key conclusion in Section 13.0 is that reduction or elimination of forced model oscillation requirements has demonstrated significant beneficial effects on the MSBS conductor, power and cryogenic requirements, and on the

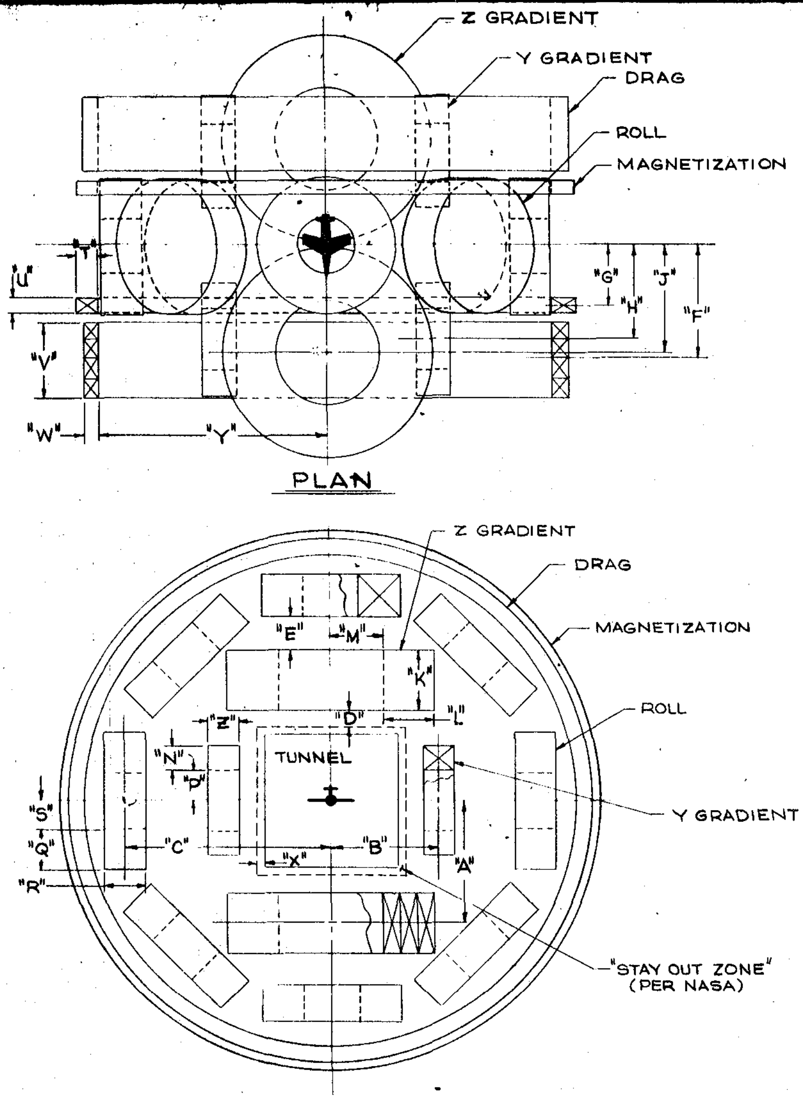

ZONE	LTR	DESCRIPTION	DATE	APPROVED
	1	DIM C, CASE III - 1.6 was 1.11 DIM R, CASE III - .80 was .20		

DIMENSIONS (m)			
DIM	CASE I	CASE II	CASE III
A	2.26	2.26	.94
B	2.08	2.08	.94
C	3.6	3.6	1.6 (1)
D	.30	.30	.07
E	.60	.60	.15
F	2.04	2.04	1.17
G	1.03	1.03	.57
H	1.53	1.53	.88
J	1.80	1.80	.47
K	.89	.89	.20
L	.79	.22	.09
M	.94	.94	.30
N	.37	.12	.04
P	.56	.56	.24
Q	.53	.53	.09
R	.53	.53	.80 (1)
S	.50	.50	.30
T	.27	.27	.08
U	.26	.26	.13
V	1.61	1.61	.53
W	.25	.07	.07
X	.30	.30	.15
Y	4.50	4.50	1.30
Z	.53	.53	.20

DRAWING NOT TO SCALE

UNLESS OTHERWISE SPECIFIED DIMENSIONS ARE IN INCHES— TOLERANCES ON: 2-PLACE DECIMALS ± 3-PLACE DECIMALS ± ANGLES ± FRACTIONS ± ALL SURF. √
MATERIAL—
APPLIED PRACTICES—
SIGNATURES: W Hedrick
PRODUCED UNDER CONTRACT NO.
PROJECT CODE

GENERAL ELECTRIC — ENERGY SYSTEMS PROGRAMS DEPT. · SCHENECTADY, N.Y.

TITLE: MSBS LAYOUT

SIZE: D | FSCM: 57561 | SK103D81013 | REV: 1

Figure 1.10

MSBS CONCEPT

Figure 1.11

MSBS TOTAL COST* ESTIMATES ($K)

ALTERNATIVE	E	F	G
Case 1	447,082	89,352	88,448
Case 2	153,246	52,601	52,343
Case 3	48,542	29,252	29,136

*1981 Dollars, Fee not included

project costs.

Section 13.0 also re-states conclusions on the advantages of the epoxy-impregnated coils for Case 3, the need for additional work on arrangement of Roll Control Coils and wing core materials, the design effort required to verify feasibility of an Electromagnetic Position Sensor for MSBS, and the capability and versatility of the Electro-Optical Position Sensor.

Conclusions are also given on the feasibility of the Control System, as demonstrated by simulation, and on the magnitudes of the major MSBS interfaces.

Recommendations are then given in Section 13.0. The key recommendations are that subsequent MSBS effort consider the following:

- Reduction in frequency and/or amplitude of forced model oscillation
- Reduction in the maximum load duty cycle
- Reduction in the number of simultaneous forced model oscillation modes
- Review of eddy current losses in metallic dewars, and obtain non-metallic dewar data
- Investigation of cost effective support structure design approaches
- Investigation of alternative model cores
- Investigation of alternative cost effective power supply approaches
- Investigation of peak power "buffering"
- Performance of aero data error analysis
- Initiation of new EPS design concept
- Initiation of Electro-Optical Position Sensor design
- Continuation of Control System Studies

This section also discusses a review of attempting to establish a figure of merit for magnet coil fabrication methods.

The final portions of this report are Appendices reporting on A) The Scale-up of Epoxy Impregnated Coils - which established the sizes conceived for the 4x4 foot test section as being close to the limit of today's technology; B) The Work Breakdown Structure and Task Descriptions - for the subsequent phases of MSBS; and C) Verification Testing Program - to explain such a program to those who have not been involved in the superconducting magnet industry.

Section 1 References

1. Covert, E.E., Finston, M., Vlajinac, M., and Stephens, T. - "Magnetic Balance and Suspension Systems for Use with Wind Tunnels", Progress in Aerospace Science 14, Pergamon Press, 1973.

2. Britcher, C.P. - The Magnetic Suspension and Balance System in the Cryogenic Wind Tunnel, BSc Honours Project Report, University of Southampton April, 1978, N80-71565#

3. Daum, F. - Summary of ARL Symposium on Magnetic Wind Tunnel Model Suspension and Balance Systems, ARL66-0135, July,1966 .

4. Zapata, R.N. - "Magnetic Suspension Techniques for Large Scale Aerodynamic Testing", Wind Tunnel Design and Testing Techniques, AGARD-CP-174, N76-25213, March, 1976 .

5. Britcher, C.P., Fortescue, P.W., Allcock, G.A., and Goodyer, M.J.- Preliminary Investigations of Design Philosophies and Features Applicable to Large Magnetic Suspension and Balance Systems, University of Southampton, November, 1979, NASA-CR-162433, November 1979

2.0 MSBS REQUIREMENTS

The requirements for MSBS fall into two major categories. The Statement of Work for Design Concepts and Cost Studies for Magnetic Suspension and Balance Systems, Rev. A, (SOW) imposes requirements on the configuration and performance of the magnet system in the form of static and dynamic forces which the coils must produce, the need for visual access to the model, and reliability to prevent loss of control of the model as a result of single point failures. The SOW also requires that standard design practices and proven off-the-shelf hardware shall be used to the maximum possible extent. GE has expanded this requirement into a series of specific, quantitative design requirements intended to ensure that the selected approaches result in minimum technical, cost, and schedule risk and maximum system reliability. Additional requirements have also been imposed where needed to constrain the design. These requirements are summarized in Figure 2.1a and b and described in more detail below.

2.1 SOW CONFIGURATION AND PERFORMANCE REQUIREMENTS

Section 2.2 of the SOW specifies the performance and configuration of the MSBS. Paragraph 2.2.1 requires that the arrangement of the coils allow for the 8 by 8 foot and 4 by 4 foot test sections and a clear wall area for viewing windows of a size and location to be determined. Paragraph 2.2.3.1 defines the duty cycle required of the MSBS. Paragraph 2.2.3.2 and 2.2.3.3 specify the values of static forces and moments which the coils must be able to produce for each of the three cases to be studied. Paragraph 2.2.4 specifies the range of model angular displacement range required in the tunnel. Requirements for amplitude and frequency of forced model sinusoidal oscillations are given in Paragraph 2.2.5. Paragraph 2.2.6 specifies the accuracy with which the MSBS must position models. Paragraph 2.2.9 defines the model characteristics that must be accommodated by the MSBS, and Paragraph 2.2.10 lists the aerodynamic parameters for which the MSBS must provide data. Finally, Paragraph 2.11 imposes requirements for reliability which the MSBS systems, must meet. These requirements have been analyzed and implemented as described in the following sections.

Figure 2.1a MSBS REQUIREMENTS

- Tunnel Test Section per RFP Paragraph 2.2.1
  + 1' Stayout Zone for 8' x 8'; 1/2' for 4' x 4' and Non-Magnetic Walls
- Operational Duty Cycle per Paragraph 2.2.3
- Static Force and Moment Requirements per Paragraph 2.2.3
- * Aero Disturbances ∿ .1% Static Forces @ 10-50 Hz
- Angular Displacements per Paragraph 2.2.4
- * Forced Sinusoidal Oscillations 10% of Paragraph 2.2.5 + Control Forces via Simulation
- Model Positioning Accuracies per Paragraph 2.2.6
- Model Cylindrical Core Dimensions per Paragraph 2.2.7
- Model Roll Control Magnetic Cores ∿ 10% of Mean Chord
- Model Characteristics per Paragraph 2.2.9
- Model Failsafe Criterion per Paragraph 2.2.11
  - Redundancy in Subsystem Components
  - Modularity of Subsystems
  - Operations Sequencing
  - Selection Based on Effectiveness and Cost
- Hardware Design - "Off the Shelf" per Paragraph 3.1
  + "Existing Technology", where necessary

*Alternatives Approved by Project Manager

Figure 2.1b MSBS REQUIREMENTS (DETAILED)*

Para. 2.2.3.1 — Operational Duty Cycle - Maximum Design Conditions
2 Hrs/Day, 25% of Maximum
8 Hrs/Day, (Stand by 14 hrs/day)

Para. 2.2.3.2 — Static Force Requirements

	8' x 8' Test Section		4' x 4' Test Section
	Case I	Case II	Case III
	Required	Required	Required
Lift	9790N	2760N	2450N
Drag	4180N	1160N	1045N
Side	1380N	400N	355N
Para. 2.2.3.3	**Static Moment Capability**		
Pitch	420m-N	120m-N	105m-N
Yaw	140m-N	40m-N	35m-N
Roll	140m-N	40m-N	35m-N

Para. 2.2.4 — Model Angular Displacement Range

	Desirable	Acceptable
Angle of Attack α	$\pm 45^\circ$	$\pm 30^\circ$
Angle of Sideslip β	$\pm 20^\circ$	$\pm 10^\circ$
Angle of Roll ϕ	$\pm 360^\circ$ or $\pm 180^\circ$	$\pm 20^\circ$

Para. 2.2.5 — Forced Model Sinusoidal Oscillations

Mode	Amplitude	Frequency, Hz
Pitch	1.00°	5
Yaw	1.00°	3.5
Roll	2.50°	3
Heave	.75cm	5
Slip	1.0 cm	3

Para. 2.2.6 — Model Positioning Accuracies

X	$\pm$.025cm
Y	$\pm$.025cm
Z	$\pm$.025cm
α	$\pm .02^\circ$
β	$\pm .02^\circ$
ϕ	$\pm .02^\circ$

*From Statement of Work, Reference 6 of Section 1.0

2.1.1 Test Section Allowance and Model Visual Access

The test section walls, in all cases, allow sufficient length and width to accommodate visual access to the models under a wide range of attitudes and positions. SOW requirements, however, did not specify limitations on wall materials or on external dimensions of the test section. These are discussed in Section 2.2.1. It was tentatively assumed that visual access to the model would be provided on the sides of the test section, in the approach typically used in wind tunnels. If the "+" arrangement of gradient coils is selected, (discussed in Section 3.2.1), the Y gradient coils would be required to be separated by the length of the model to provide the required access. In the event the "X" arrangement is used (see Section 3.2.1), visual access could make use of the fact that gradient coil axes are angled above and below the test section horizontal centerline, thus increasing the potential visual accessibility.

Incorporation of roll control coil arrays may restrict access to the windows to some degree. In eight coil arrays, with the coils located on top and bottom, sides, and at 45^o, direct access to the windows is available through the clear bore of the side roll coils. On the other hand, if the roll coils are located a sufficient distance from the walls and gradient coils to provide the required field of view, observation equipment may be located between the roll coils and other coils or the wall. Any equipment located in this region would, of course, have to be able to operate in a high magnetic field.

2.1.2 Operational Duty Cycle

The duty cycle specified in the SOW provides for the testing operations of two hours at maximum design conditions and 8 hours at 25% of maximum conditions, but does not account for the remaining 14 hours per day (see Section 2.2.2).

2.1.3 Static Forces and Moments

The requirements for static forces and moments are summarized in Figure 2.1b. These requirements were translated into values of fields and gradients to provide a basis for magnetic analysis. Field gradient requirements were determined from the expression

$$F_i = \mu_o MV \frac{\partial Hi}{\partial X} \cos\Theta$$

where F_i = force (N)

$\mu_o = 4\pi \times 10^{-7}$ (N/A^2)

V = magnetic core volume (m^3)

M = sample magnetization (A/m)

$\partial H_i/\partial X$ = gradient of H_i in direction X (A/m/m)

θ = maximum angle between model axis and wind tunnel axis

i = X, Y, or Z as appropriate

To calculate the fields required to produce static torques, the torque exerted by the magnetization coil must be taken into account. For the static pitch and yaw torque the required torque and the applied lateral field are related by the expression

$$T_{reg} = \mu_o VMH_{app}\cos\Theta - \mu_o MV\overline{H}_m \sin\Theta$$

where T_{reg} = required torque (N-m)

$\mu_o = 4\pi \times 10^{-7}$ (N/A^2)

V = magnetic core volume (m^3)

M = core magnetization (A/m)

H_{app} = applied lateral field (A/m)

Θ = maximum angle between model axis and wind tunnel axis (pitch or yaw angle respectively)

$\overline{H}_m$ = average field of the magnetization coil at the model

The applied field required to produce the required net torque, in either pitch or yaw, increases rapidly as the angle of pitch or yaw increases, since $\cos\Theta$ decreases and $\sin\Theta$ increases. The requirement for the gradient coils was, therefore, designed to achieve the minimum acceptable rather than the desirable angles of pitch and yaw, as explained in Section 2.1.4. Achievement of larger angles is possible but will significantly affect the size and cost of the system, since an increase in the size of the gradient coils will result in an increase in the size of the roll, magnetization, and drag coils.

Since the magnetization coils cannot exert a torque about the x-axis, the roll torque is given by

$$T_{roll} = \mu_o MH_{roll} \cos\phi$$

where H_{roll} is the field exerted by the roll coils. Where the roll coil system has 8-fold symmetry, the maximum value of ϕ is 22.5°.

The field and gradient values calculated as described above do not account fully for additional contributions to force and torque which arise from cross-coupling of forces and torques at non-zero angles of pitch and yaw. Expressions for these additional contributions have been employed in analyzing the effects of cross-coupling on control system requirements, as described in Section 6. Although the gradient coil designs were not revised to account for these additional contributions, a design margin was maintained in coil performance so that they can be taken into account in subsequent design phases without significant changes in coil size. Preliminary analysis of cross-coupling has shown that the additional force terms are relatively small at the required angles of pitch and yaw ($< 25\%$), and sufficient margin is available to compensate for this. The additional torque terms are very large, but the dominant contribution comes from the magnetization coils and has been explicitly accounted for in deriving the torque field requirements, as explained above.

The field and gradient requirements for the three specified cases are summarized in Figure 2.2.

2.1.4 Model Angular Displacement Range

Figure 2.1 also summarizes the desirable ranges for model angular displacement. Initially, coil sizing and magnetic analysis was aimed at achieving the desired values of $\pm 45^{o}$ in pitch and $\pm 20^{o}$ in yaw. However, during the study, it became evident that the torque exerted by the magnetization coil would limit the angular range which could be attained. The minimum acceptable values of pitch and yaw angles were therefore selected. It was determined that attainment of a 45^{o} pitch angle would require that the number of amp-turns in the Z-gradient coils be increased by about 10%. Because the peak field in these coils is near the maximum allowable value of 8T as shown in Section 3.3.5, the coil cross-section would have to be increased by $\sim$ 20% to keep the peak field below 8T. This would, in turn, require that the roll coils be moved outward and increased in size, and that the magnetization and drag coils be increased in size. Thus, the choice of the minimum acceptable values of pitch and yaw angles represents not a technological limit but a judgement based on the impact of these parameters on system size and cost.

Figure 2.2

FIELD AND GRADIENT REQUIREMENTS

	$\partial Hz/\partial x$ (A/m/m) Lift	$\partial Hy/\partial z$ (A/m/m) Lateral	$\partial Hx/\partial x$ (A/m/m) Drag	Hz (A/m) Pitch	Hy (A/m) Yaw	Hroll*(A/m)
Case 1	$7.4x10^5$	$7.8x10^4$	$3.2x10^5$	$1.6x10^5$	$4.6x10^4$	$5x10^4$
Case 2	$2.1x10^5$	$2.3x10^4$	$8.9x10^4$	$1.5x10^5$	$4.4x10^4$	$1.4x10^4$
Case 3	$1.2x10^6$	$1.5x10^5$	$5.2x10^5$	$5.2x10^4$	$1.5x10^4$	$1x10^5$

*Average through-wing field assuming $\overline{M} = 1/4\ M_S$

The use of a fully symmetric roll coil system appears highly desirable in order to limit coupling between roll torques and pitch and yaw torques. Furthermore, an eight-coil system using soft-iron transverse wing cores appeared, in preliminary analysis, to be the only approach potentially capable of achieving the required roll torque magnitudes.

2.1.5 Forced Model Sinusoidal Oscillations

The requirements for forced model sinusoidal oscillations are summarized in Figure 2.1. The forced oscillation requirements have proved to be the most significant single design driver for not only the magnet system but also related systems such as power supplies and cryogenics because they lead to high levels of coil voltage, peak reactive power, and AC losses. Because of the impact these requirements have on the design and cost of MSBS, several alternative operating modes, including reduction of the oscillation frequencies by a factor of ten and elimination of forced oscillation capability altogether, have been evaluated. These alternative modes and their impact on MSBS design are described more fully in Section 3.2.9.

Analysis of the requirements for oscillatory heave and slip forces was carried out with a very simple model of forced vibration with inertial damping. Aerodynamic damping effects were not considered. If the position of the model as a function of time is given by

$$x = x_o \sin\omega t \qquad (1)$$

where x = generalized coordinate (m)

x_o = maximum amplitude (m)

ω = $2\pi f$ (radians/sec)

t = time (sec)

then

$$\dot{x} = x_o \omega \cos\omega t \qquad (2)$$

$$\ddot{x} = -x_o \omega^2 \sin\omega t \qquad (3)$$

$$\text{Now } F = m\ddot{x} \qquad (4)$$

$$\text{so } F = -m x_o \omega^2 \sin\omega t \qquad (5)$$

and the maximum value of F is given by

$$F_{max} = -mx_o\omega^2 \qquad (6)$$

where F_{max} = maximum force (N)

m = model mass (kg)

The requirements for magnet operation are then calculated from

$$\frac{I_{Fdyn}}{I_{Fstatic}} = \frac{F_{dyn}}{F_{static}} \qquad (7)$$

so

$$I_{Fdyn} = I_{Fstatic} \times \left(\frac{F_{dyn}}{F_{static}}\right) \qquad (8)$$

where

$$I_{Fstatic} = \left(\frac{(NI)_{force}}{(NI)_{total}}\right) \times \left(I_{total}\right) \qquad (9)$$

Here I_{Fdyn} = peak current for dynamic force

$I_{Fstatic}$ = current for maximum static force

F_{dyn} = maximum dynamic force

F_{static} = maximum static force

$(NI)_{force}$ = amp-turns needed to produce maximum static force

$(NI)_{total}$ = total amp-turns in coil

where (9) takes into account the fact that the gradient coils produce both forces and torques, so that only a portion of the ampere-turns are needed to produce force. Then the maximum rate of current change is given by

$$\left.\frac{dI}{dt}\right)_{max} = I_{Fdyn}\,\omega \qquad (10)$$

The values required for forced heave and slip motions are shown in Figure 2.3. The values for roll torque were calculated in exactly the same way, using the required oscillatory roll amplitude and roll moment of inertia as appropriate.

Figure 2.3

FORCED OSCILLATION REQUIREMENTS (ALTERNATIVE E*)

Mode	Amplitude	Frequency (Hz)	Coil	dI/dt_{max}		
				Case 1	Case II	Case III
Heave	.75 cm	5	Z	$8x10^4$	$2.9x10^5$	440
Pitch (including change in lift force with attack of angle)	1.0^0	5	Z	$1.2x10^5$	$2.5x10^5$	2035
Slip	1.00 cm	3	Y	$1.3x10^5$	$4.4x10^5$	1040
Yaw	1.0^0	3.5	Y	$1x10^5$	$3.5x10^5$	4400
Roll	2.5^0	3	Roll	$2x10^4$	$3.6x10^4$	500

*For Alternate F, all values are reduced by 1000x

An additional oscillatory force which must be supplied is the change in lift force which occurs when the model is oscillated in pitch. It was assumed that the lift forces varies linearly with angle of attack. The magnitude of the change in lift forces is then simply

$$\frac{\Delta F_{lift}}{F_{lift}} = \frac{\Delta\alpha}{\alpha_{max}}$$

where $\Delta\alpha$ = oscillatory pitch angle

α_{max} = max. angle of attack

Then

$$\frac{\Delta F_{lift}}{F_{lift}} = \frac{1}{30}$$

So

$$\frac{\Delta I_{lift}}{I_{lift}} = \frac{1}{30}$$

or

$$\Delta I_{lift} = \frac{I_{lift}}{30}$$

The required values for this mode are also shown in Figure 2.3.

The oscillatory pitch and yaw torques were determined in a somewhat different manner. As described previously, both the magnetization and gradient coils exert significant torques on the model, and the net static torque required is the difference of these values. Oscillation in pitch or yaw can be achieved by changing the torque exerted by the magnetization coil, by the gradient coil, or both. It is somewhat inconvenient to vary both, so one or the other is selected. Initially, variation of the magnetization coil current was considered to ease the requirements on the gradient coils. However, this proved to be unnecessary and also placed an additional burden on the cryogenics, power supply, and control systems. It was, therefore, decided during the study that the oscillatory pitch and yaw would be supplied by the Z and Y gradient coils respectively.

The equation of motion for the forced oscillation for a simple harmonic applied torque is given in Reference (1) by

$$\Theta^{(t)} = \frac{T}{k - Iv^2} (\cos vt - \cos\omega_n t) \qquad (11)$$

where $\Theta^{(t)}$ = pitch or yaw angle (rad)

T = applied pitch or yaw torque

K = $\frac{dT}{d\Theta}$ (N-m/rad)

I = moment of inertia $Kg\text{-}m^2$

v = driving frequency (rad/sec)

ω_n = natural frequency = $\frac{K}{I}$ (rad/sec)

so that

$$T = \frac{\Theta(t)\ (K - Iv^2)}{\cos vt - \cos\omega_n t}$$

and the magnitude of the applied torque required can in principle be determined from this relationship. For the present case, v and ω are nearly the same for both pitch and yaw, which results in a "beat" behavior with the correct amplitude but a lower effective frequency than the desired 5 or 3.5 Hz. Thus, the driving torque must be a more complex function of time to produce the required simple harmonic motion. This case is beyond the scope of simple analysis and was determined by control system simulation as described in Section 6. As expected, the maximum values of dI/dt determined by simulation are considerably larger than those estimated earlier from simple analysis.

This has resulted in some inconsistencies between the values shown in Figure 2.3 and the values used in Section 3.3 to calculate reactive power and AC losses for the coils. No attempt has been made to resolve these inconsistencies. However, the system impact of making the correction on reactive power and cryogenic requirements, the two major cost drivers, would be only a few percent since the largest errors occur in the Y-coils which require the least power and cooling. Thus, the inconsistencies have a negligible effect on Alternate F and none on Alternate G.

2.1.6 System Reliability

The SOW requires that the MSBS be failsafe such that any single failure shall not cause loss of control of the model. For the magnet system, the basic approach to the reliability requirement is the realization that, under any condition which would result in loss of a coil's field, the model can be brought back to a position of zero pitch and yaw angle and minimum lift, and the aerodynamic loads reduced accordingly, in a time which is short compared to the length of time during which the coil field drops to zero. Redundant instrumentation would be used in all coils, and loss of redundancy would be considered a failure mode. The malfunctioning coil can then be discharged, along with another coil in the set if needed to maintain field symmetry, and the model supported with the remaining coils in the set until the wind tunnel can be fully shut down. This approach is predicated on the assumption that the probability is small of a second coil failing during the period when the tunnel is being shut down. Relatively little data is available on failure rates for large superconducting magnets[2][3], but this appears to be a reasonable assumption.

Although the SOW specified protection of the model as the criterion for reliability, protection of the superconducting magnets is also critical, due to their cost. For this reason, the power supplies for superconducting magnets are required to be equipped with Protection Systems. The protection system must provide the means for detecting incipient failures that could cause loss of the magnet, and for automatically discharging the magnet.

As an illustration of the inherent reliability of the system, consider the following example: assume the model is oriented at the maximum angles of yaw, attack, and roll, and is being tested in one or more forced oscillation modes. The protection system senses a malfunction in one of the Z-gradient coils. The control system immediately ceases forced oscillation and begins to change the currents in the coils to return the model to zero angles of attack, yaw, and roll (or any other attitude which may be convenient and does not require more than 1/2 of the maximum steady-state force in any degree of freedom). As is shown in Section 3.3, all of the coils are designed for current ramp rates of $\frac{dI/dt}{I_{max}} \geq 2$ because of the requirements for forced sinusoidal oscillation.

Thus, the achievement of _any_ attitude within the range of motion of the model (neglecting requirements to reduce the rate near the end of the cycle to prevent overshoot) will require at most 1/2 second. During this time the temperature rise, even for an uncooled fully normal region, is a few degrees Kelvin at most, completely negligible in comparison to maximum allowable temperature of ∿ 200K during a discharge. After the model has reached the desired attitude, the control system would direct the malfunctioning coil to be discharged through its protection resistor. This process takes 15-30 seconds at a voltage which is extremely modest ($\lesssim$ 1000) compared to the maximum coil operating voltage. Simultaneously (if required) the other Z-coil on either top or bottom would be discharged to maintain field symmetry along the wind tunnel axis. The remaining two Z-coils on the top or bottom can provide the required lift force to support the model during the 3 to 10 minutes for tunnel shutdown.

In keeping with the example given above, the protection system is required to provide complete discharge of any magnet in 30 seconds.

The above approach to system reliability appears adequate for virtually all reasonable failure modes at the magnet system level including non-recovering normal zones as a result of conductor motion or other events, loss of coolant, loss of power, and loss of cryostat vacuum. The impact of abrupt, catastrophic loss of vacuum (as opposed to a "slow leak") has not been analyzed but is unlikely to be more severe than loss of coolant and could, in any event, be handled by a more rapid rampdown within the capability of the power supply. Gross magnet motion as a result of catastrophic structural failure is considered to be a non-credible situation. Complete loss of facility power as a result of a grid blackout would require the Protection System to switch all magnets automatically into a "bypass" mode in which the current is shunted through a low-resistance air-cooled bus internal to the power supply and decays slowly over a period of time (∿ hours). This failure mode is of concern because, while the coil fields are not lost, the capability to adjust and control this is. The model may thus be "overloaded" as the wind dies down due to loss of power and be thrown against the tunnel walls. This mode of failure will require more study to define adequate measures at the top system level, such as use of an uninterruptible power or some other non-magnetic mechanism for model control.

Complete loss of Position Sensing capability could seriously impact model safety. The requirement is thus established for separately powering the dual Electromagnetic Position Sensors. If the Electro-Optical Position Sensors are used solely, the multiple CID cameras should be separately powered.

In the Control System, the requirement for reliability calls for a redundant data bus and a backup computer.

2.2 GE-IMPOSED REQUIREMENTS

GE has, based on experience in large superconducting magnet design and knowledge of the state of the art, imposed requirements in addition to those given explicitly in the SOW. These additional requirements provide quantitative limits and criteria for design and are intended to implement the general requirements given in SOW para. 3.1 to use standard design practices and proven "off the shelf" hardware where possible.

2.2.1 Tunnel Interfaces and Constraints

The location and configuration of the MSBS coils is constrained by the nature of the allowed interfaces with the tunnel, which include requirements for stayout zones and limitations on the physical interfaces between the coils and the tunnel. In addition, the operating characteristics of the coils impose constraints on the design of the remainder of the facility. The requirements for AC operation of the coils (for forced oscillation and/or dynamic model control) constrain the choice of materials for the test section walls, while the stray fields produced by the coil array restrict the use of materials elsewhere in the facility, the placement of other equipment, and the personnel access allowed during facility operation.

The SOW specifies the tunnel sizes as 8'x8' for Cases 1 and 2 and 4'x4' for Case 3. To these have been added the "stay out" zones of 1' on all sides for Cases 1 and 2 and 6" for Case 3. In addition, the magnet system must meet the requirements of physical independence of the tunnel. As is shown in Section 3.3, the "stay-out" zone has been maintained in sizing and locating all coils, and independent systems have been supplied for mechanical support and other requirements.

The constraints which the requirement for AC coil operation place on the materials for the test section were evaluated by calculating the time constants for field diffusion through test section walls of various materials and thicknesses. The test section was modeled as an infinite cylinder which should make the results somewhat conservative. The characteristic time for a change in the field was taken to be $\tau \sim 1/f$, where f is the frequency of the field, and any configuration which had a time constant greater than τ was assumed to be clearly unacceptable because substantial distortion of the waveform would occur.

For the present case, if a control bandwidth of $\sim$ 20 Hz is assumed, the characteristic time is $\sim$ .05 seconds.

The results of the analysis are shown in Figure 2.4. It is evident that 1" stainless steel is marginal for the 8'x8' tunnel and probably acceptable for the 4'x4' tunnel. The use of aluminum is clearly out of the question unless it is used in the form of a laminate made of very thin sheets insulated from each other. The resistance used for aluminum is characteristic of an 1100 alloy. Other aluminum alloys are available with resistivities up to ten times as large which would reduce the time constants by an order of magnitude but would not change the conclusion.

Even for those configurations in which the time constant of the wall is acceptably small, the AC field is substantially attenuated as a result of the losses in the wall and the reflection due to the mismatch in dielectric constant between the wall and air. For the 8'x8' and 4'x4' tunnels, the attenuations are respectively a factor of 6 and 3, meaning that the AC field generated by the coils must be 3 to 6 times as large as the field required to provide dynamic control or forced oscillation. This increase can probably be tolerated if only dynamic control is required but would lead to prohibitive power and cryogenic demands if full forced oscillation is required. The need for this increase in AC field over that required at the model has <u>not</u> been taken into account in costing the system.

Figure 2.4

TIME CONSTANTS FOR FIELD DIFFUSION THROUGH TEST SECTION WALLS

8 x 8 Foot Test Section

τ(sec) @ 77°K / Material	Wall Thickness ω = 1"	Wall Thickness ω = 2"	Wall Thickness ω = 3"
Aluminum	5.5	11.0	16.5
Stainless Steel	0.04	0.08	0.12

4 x 4 Foot Test Section

τ(sec) @ 77°K / Material	Wall Thickness ω = 1"	Wall Thickness ω = 2"	Wall Thickness ω = 3"
Aluminum	3	6	9
Stainless Steel	.025	.05	.075

(Steel) = 5×10^{-7} Ω.m at 77 K

(Al) = 3×10^{-9} Ω.m at 77 K

An even more fundamental constraint on the test section wall material may be imposed by the desire to use electromagnetic position sensors (EPS), as explained in Section 7. EPS would operate at $\sim$ 20 kHz, so that a characteristic time would be $\sim 5 \times 10^{-4}$ sec. Any metal wall would virtually completely shield the EPS signal from the tunnel interior, thus rendering EPS totally useless. It therefore appears that, particularly if EPS is to be used, NASA must evaluate the impact of using non-metallic walls for the test section.

Because of the various orientations of the coils, the MSBS coil system will produce substantial stray fields in all directions. Figure 2.5 shows the magnitude of the DC field along each of the coordinate axes out to a distance of 10m from the center of the model. It is evident that substantial fields ($\sim$ .06-.07T) occur even at this distance along the Y and Z axes. Although no accepted standards exist at present, these fields may be large enough to require limitation of long-term exposure[4]. They will also constrain the location of any equipment which can be affected by a DC field. The AC component of the magnetic field will be comparable in magnitude to the DC component for full forced oscillation and less than 1% of the DC component for dynamic control only. Sensitive electronic instruments which must be placed close to the tunnel will require shielding, and lead wires must also be twisted and shielded to minimize noise. Finally, the DC field and gradient at 10m are sufficient to magnetize and attract ferro-magnetic hardware, and care will have to be taken prior to energization to ensure that the area is cleared of all loose objects to avoid hazard to both personnel and equipment.

Figure 2.5. MSBS Stray Fields

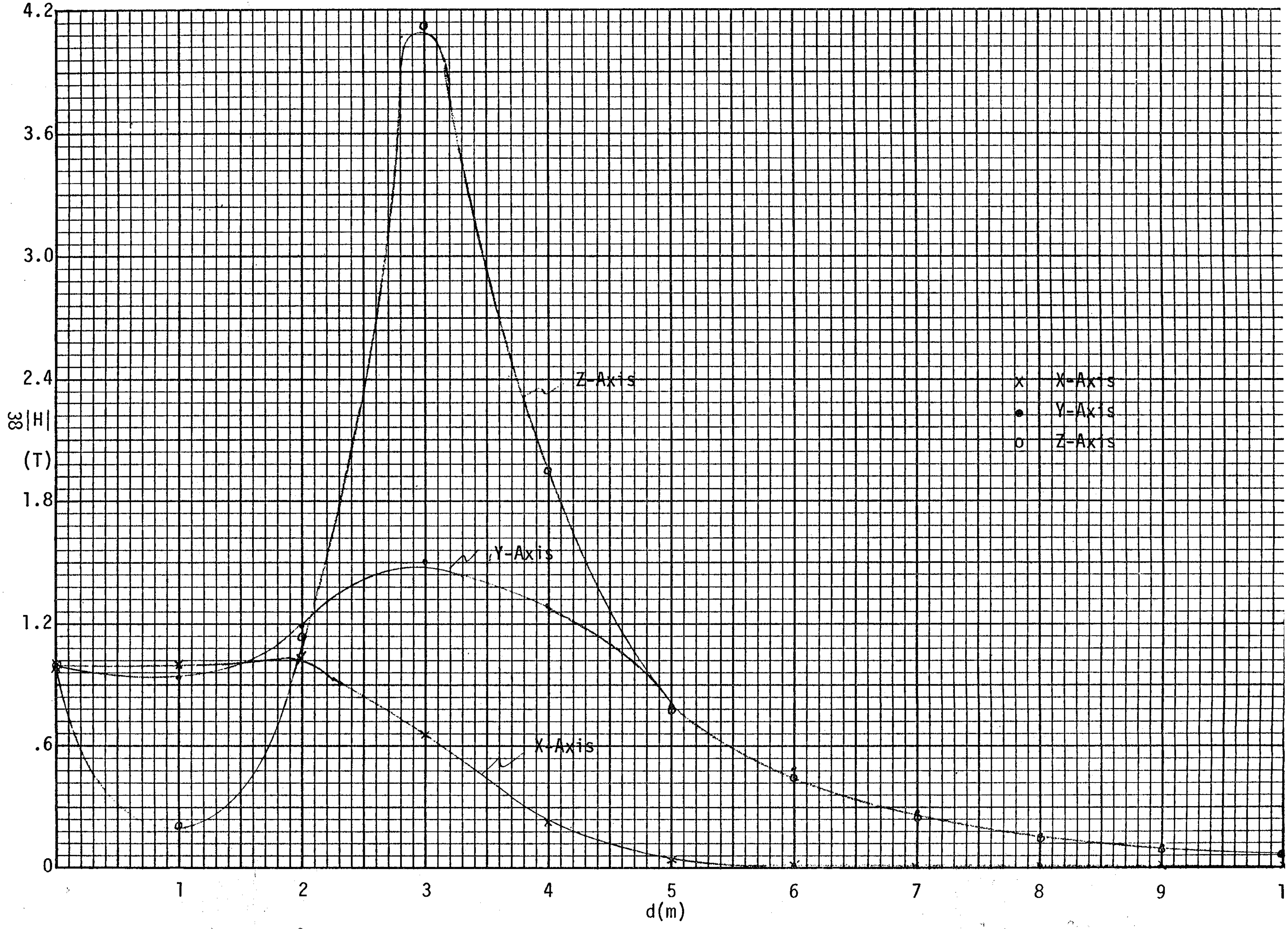

2.2.2 Duty Cycle

GE has added a 14 hour "standby" mode to the maximum and 25% operations specified in the SOW, during which the helium liquefier/refrigerator system maintains the magnets at or near superconducting temperatures, and refills the liquid helium storage dewar. A tradeoff is required to determine the cost-effective "mix" of liquefier/refrigerator capacity and dewar capacity. An alternative approach of maintaining the magnets at liquid nitrogen temperature between operating cycles was not evaluated, due to lack of time.

2.2.3 Flow Disturbances

Since the Control System must maintain model position and attitude in the face of tunnel flow disturbances, a review of such disturbances was made in order to establish their magnitude. Based on currently available data, dynamic pressure in the test section of a wind tunnel could, typically, vary from ±.1% to ±.5%. At the suggestion of the Program Manager, the requirement for control of forces disturbing the model was established as ±.1% of static forces given in SOW paragraph 2.2.3.2.

Section 2 References

1. Freberg, C.R., Kemler, E.N., Elements of Mechanical Vibration, Wiley, New York (1949), p. 32

2. Montgomery, D.B., Proc. 6th Symposium on Engineering Problems in Fusion Research, San Diego, 1975, p. 122

3. Hsieh, S.Y. et al, ibid, p. 116

4. Alpen, E.L. in Proceedings of the Bio-magnetics Effects Workshop LBL-7452, Lawrence Berkeley Laboratory, p. 19 (April 1978)

3.0 MAGNET SYSTEM CONCEPT

The magnet system for MSBS provides the magnetic fields and field gradients which, in turn, produce the forces and torques required to control and manipulate the model in the required six degrees of freedom: lift, lateral, and drag force and pitch, yaw, and roll torque. Concepts have been developed for the three cases specified by NASA which, although different in detail, share a number of common features. All three systems consist of fully symmetric arrays of 4 each Z (vertical axis) and Y (horizontal axis), 2 each magnetization and drag, and 8 roll coils. The symmetry of the coil arrays enhances the reliability of the magnet system by allowing control of the model to be maintained even during discharge of a coil. The Z, Y, and roll coils are fully bipolar, which reduces the coil size without significantly impacting power supply costs. All coils for Cases 1 and 2 are wound with a 50-kA low-loss cryostable conductor being developed under the DOE/LASL ohmic heating coil program and use straightforward layer or pie winding approaches and simple readily available insulation. The Z, Y, and roll coils for Case 3 use the GE epoxy-impregnated coil technology and use a 1000A, six-strand cabled conductor. Use of non-metallic helium and vacuum vessels was found to be necessary to eliminate eddy current losses for the full forced oscillation requirements, and G-10 dewars with 304L reinforcement were originally selected based partially on technology being developed by LASL. Reduction or elimination of forced oscillation requirements could eliminate the need for non-metallic dewars, which would be a significant advantage. Technical risks are judged to be low overall because all the approaches chosen are generally based on technology which exists or which present developments will make available in the next one to two years. Areas which will require particular attention during both design and fabrication are the insulation system and service stack because of the high voltages required, and the non-metallic case and helium vessel, because of the relative difficulty of achieving low leak rate and high thermal efficiency. The principal cost and schedule risks are judged to be fabrication of the conductor and the non-metallic case and dewar components and insulation. The vendors for the first and last items at present are small firms whose capabilities are heavily taxed by the volume of material required for large coils. Competent vendors are available for case and dewar components, but more complete definition of their designs could have a significant cost and schedule impact.

3.1 MAGNET SYSTEM REQUIREMENTS

The majority of system requirements discussed in Section 2.0 are Magnet System Requirements. As shown in Figure 3.1, all requirements for static and dynamic force and torque have been met, with the exception of roll torque in Cases 1 and 3, for which reasonable engineering configurations will produce only about half the required value.

Primary magnet design requirements, such as coil shapes, maximum allowable peak field strength, allowable peak voltages at the magnet terminals, and structural design limits for the magnet system have been defined on the basis of current experience in the design and fabrication of large superconducting magnets. Other magnet requirements, such as the magnetization coil field strength, and the magnet current requirements to enable model control are based on analytical derivations.

3.1.1 Coil Shape

Large superconducting magnets have been built or are presently being built in a variety of configurations including circular (solenoidal), oval, D-shaped, racetrack, and saddle shaped. These shapes are generally dictated by the geometry of the device and the required field distribution. However, any deviation from a solenoidal geometry generally leads to substantially increased support structure requirements in the non-circular sections, which tend to complicate the design and fabrication of the coil and reduce the overall current density. It is possible that the design of the magnetic system, particularly the gradient coils, could be improved through the use of non-circular coils. However, it was not possible within the scope of the present study to incorporate variable coil shapes. Therefore, it was required that all the coils be solenoidal.

3.1.2 Coil Peak Voltage

The maximum allowable peak field is required to be less than 8T. Although coils of physical size comparable to the MSBS coils at fields up to 12T have been considered[1], 8T represents the state of the art with respect to large coils which will be demonstrated in the next several years. Moreover, limitation of the peak field to 8T ensures the applicability of NbTi conductor technology, which is much more mature than that of Nb_3Sn and makes available a much broader range of relatively well characterized conductor designs.

Figure 3.1

IMPLEMENTATION OF MAGNET SYSTEM REQUIREMENTS

Para. 2.2.3.2 Static Force Requirements

	8' x 8' Test Section						4' x 4' Test Section		
	Case I			Case II			Case III		
	Required		Achieved	Required		Achieved	Required		Achieved
Lift	9790N	>	9790N (1)	2760N	>	2760N (1)	2450N	>	2450N (1)
Drag	4180N		4180N	1160N		1160N	1045N		1045N
Side	1380N	>	1380N (2)	400N	>	400N (2)	355N	>	355N (2)

Para. 2.2.3.3 Static Moment Capability

	Case I Required	Case I Achieved	Case II Required	Case II Achieved	Case III Required	Case III Achieved
Pitch	420m-N	420m-N (3)	120m-N	120m-N (3)	105m-N	105m-N (3)
Yaw	140m-N	140m-N (4)	40m-N	40m-N (4)	35m-N	35m-N (4)
Roll	140m-N	~70m-N (5)	40m-N	~40m-N (5)	35m-N	14m-N (5)

Para. 2.2.4 Model Angular Displacement Range

	Desirable	Acceptable	Achieved
Angle of Attack α	$\pm 45^0$	$\pm 30^0$	$\pm 30^0$
Angle of Sideslip β	$\pm 20^0$	$\pm 10^0$	$\pm 10^0$
Angle of Roll $\emptyset$	$\pm 360^0$	$\pm 20^0$	$\pm 360^0$ (6)
	$\pm 180^0$		

(1) At maximum angle of attack
(2) At maximum angle of yaw
(3) Net torque available at maximum angle of attack
(4) Net torque available at maximum angle of yaw
(5) Requires all - iron wings with thickness = 11% of mean chord

Figure 3.1

IMPLEMENTATION OF MAGNET SYSTEM REQUIREMENTS

(continued)

Para. 2.2.5 Forced Model Sinusoidal Oscillations

	Amplitude			Frequency Hz	
Mode	Required		Achieved	Required	Achieved
Pitch	1.0^{0}	>	1.0^{0}	5	5
Yaw	1.0^{0}	>	1.0^{0}	3.5	3.5
Roll	2.5^{0}		2.5^{0}	3	3
Heave	.75cm		.75cm	5	5
Slip	1.0cm		1.0cm	3	3

3.1.3 Coil Terminal Voltage

As described in Section 3.3, the requirements for forced model oscillation and model control lead to high peak terminal voltages. In order to develop criteria for modularization of coils, a limit for allowable voltages had to be selected. The value selected was 10 kV, which is the nominal maximum terminal voltage of the 20 MJ prototype ohmic heating coil being fabricated for the Los Alamos Scientific Labratory. This value is not a fundamental limit in any sense; in fact, full scale tokamak ohmic heating coils will operate at terminal voltages up to ten times as large. However, it is a value for which adequate design approaches will be demonstrated on a time scale relevant to MSBS.

3.1.4 Coil Structural Design Limits

The MSBS magnet system must be capable of supporting the magnetic loads required to suspend and balance aerodynamic shapes to the static and dynamic forces described in Para. 2.2.3.2, 2.2.4 and 2.2.5 of the SOW. The functional requirements involved in attaining the above requirements are:

- Magnetic Forces
  - Steady-State
  - Sinusoidal
- Gravity Loads
- External Pressure Due to Internal Vacuum
- Thermal and Electrical Cycling
- Heat Loads
- Transportation
- Handling

The structural requirements of the MSBS includes evaluation of thermal and mechanical stresses and cyclic life of the coils, coil support structure and external structure to ground. Design limits are based on experience gained on current or previous magnet contracts.

The stresses calculated for this study are primary membrane or primary bending stresses. Local stress intensities have not been calculated. Figure 3.2 summarizes the basic stress limits used to size the MSBS structure.

3.1.5 Magnetic Core Characteristics

As explained in Section 2.1.3, the field produced by the magnetization coils exerts a torque on the model at non-zero pitch and yaw angles. As a result, the gradient coils must produce relatively large transverse fields in order to achieve the required torques and angular range. It is therefore important that magnetization coils be designed to produce the smallest field which will saturate the model core, and must be capable of being saturated at the lowest possible field. The use of single crystal iron for the core would be advantageous magnetically but would be relatively expensive and would also entail difficulties in machining and handling because of its extreme softness. High quality polycrystalline ingot iron, which can be saturated at an effective field of 500-1000 Oe ($4x10^4$ to $8x10^4$ A/m) as shown in Figure 3.3 is a reasonable choice for the core material. The minimum applied field to achieve saturation is about 1500g ($6x10^4$ A/m), because of the demagnetizing field, as described in Section 3.3.3.

It should be noted that, for the purposes of analysis, the saturation magnetization of the core has been taken as 2T. In fact, the saturation magnetization of high-purity iron at room temperature is about 2.17T. This represents a margin of almost 10% which will compensate for the non-uniform magnetization of the cylindrical core. Alternatively, if an ellipsoidal core of equivalent volume could be used, this would provide a 10% margin on the performance of the magnetic system, and the size and cost of the coils could be reduced accordingly.

Figure 3.2
BASIC STRESS LIMITS

Primary membrane or Primary bending	:	2/3 min. yield strength
Primary bending + Primary membrane	:	yield strength
Buckling behavior	:	5
Fatigue	:	endurance limit on sinusoidal oscillations - 10 on coil energizations
Conductor strain	:	.10%

There are also alternative materials with saturation magnetizations significantly higher than pure iron. The magnetic characteristics of one such material, vanadium permendur, are shown in Figure 3.3. Use of this material, which has a saturation magnetization in excess of 2.4T, would allow the size and cost of the coils to be reduced by an additional 10%. The cost impact of this alternate material would be relatively modest with respect to the cost of a typical model, probably less than $5,000. This and other high-saturation alloys also have better mechanical properties and higher resistivity than high-purity iron. A further evaluation of alternate core materials should be performed.

3.1.6 Magnet Control Requirements

The magnitude and frequency of coil current changes to maintain stable model suspension impacts the coil system design, since they lead to requirements for coil terminal voltages, reactive power, and AC losses, just as do the forced oscillation requirements. It was assumed, as a starting point, that the coil system had to supply forces to counteract the .5% of the steady-state forces due to dynamic pressure changes in the wind tunnel at frequencies up to 50 Hz. Subsequently, these maximum values were replaced by a value of .1% of the steady state force. Later in the study, a more realistic analysis of the impact of this value on magnet requirements was performed by applying it as a step input in the model control simulation and determining the requirements for current ramp rates. The simulation results indicate that the maximum required rate of current change for the lower disturbance level and control force obtained by simulation is about $3x10^3$ A/sec, a reduction of about a factor of 25. As explained in Section 3.2.9, this has a very dramatic effect on the reactive power requirements for the system.

3.2 DESIGN APPROACHES

Various design approaches have been considered for the overall coil arrangement and operating modes, coil case, and dewar designs, conductor stabilization and cooling approaches, and support structure. The selected approaches are sufficient to establish feasibility and appear to have significant advantages although, as indicated in later sections, a good deal of design optimization remains to be done to minimize the overall cost of the system.

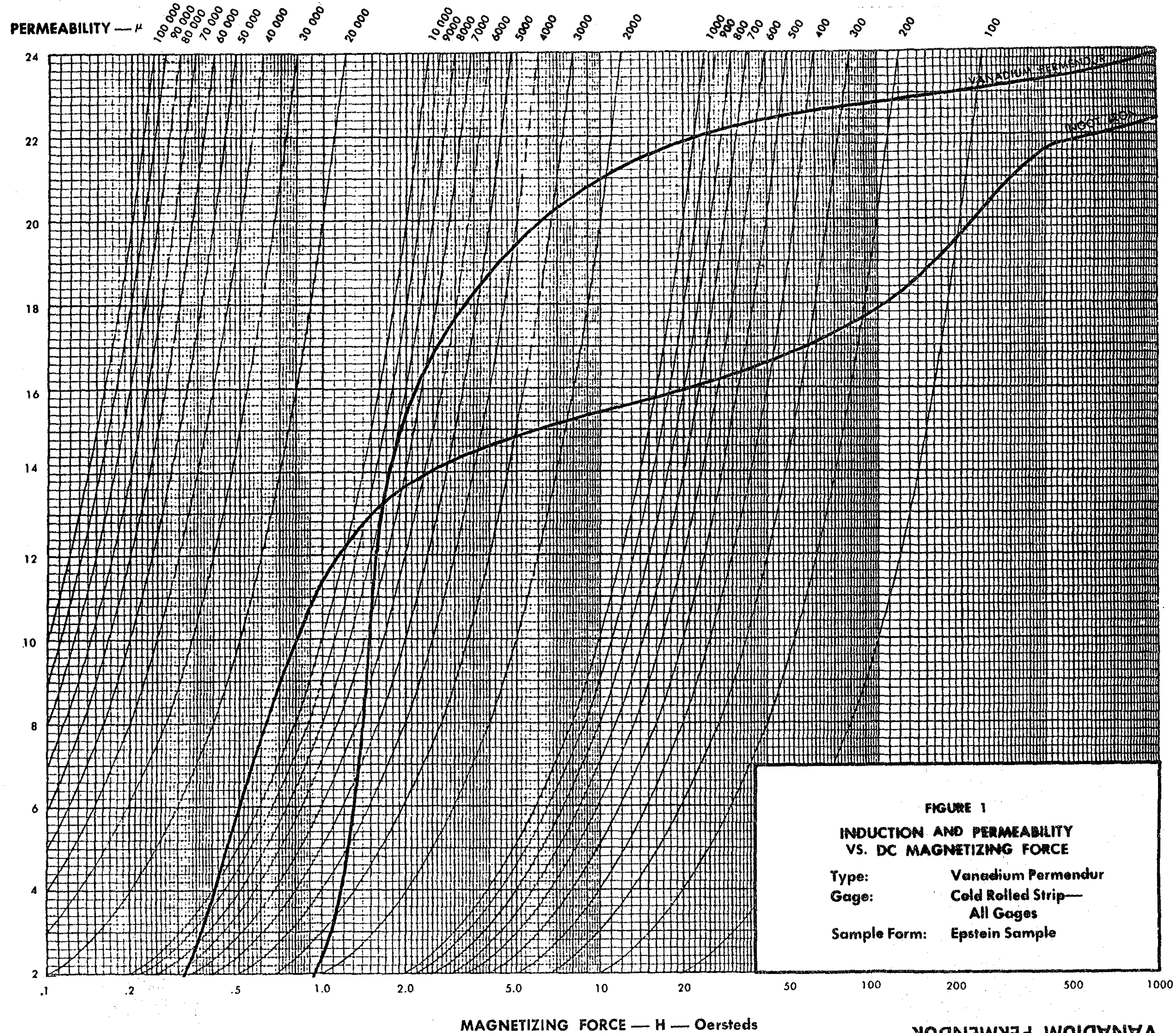

FIGURE 1

INDUCTION AND PERMEABILITY VS. DC MAGNETIZING FORCE

Type:	Vanadium Permendur
Gage:	Cold Rolled Strip— All Gages
Sample Form:	Epstein Sample

3.2.1 Gradient Coil Arrangement

A variety of gradient coil arrangements have been suggested and employed in small-scale MSBS systems[2]. These arrangements generally have in common the use of coils coaxial with the tunnel to magnetize the model and provide a force to resist the drag force, and differ primarily in the number and arrangement of the coils which produce vertical and lateral forces and torques (referred to here as gradient coils). Generally, the choice of a gradient coil arrangement which has high symmetry enhances the flexibility of the system and also improves its inherent reliability, as discussed in Section 2.1.6. On this basis, two arrangements of gradient coils were selected for comparison, as shown in Figure 3.4.

The first is referred to as the "plus" configuration, in which four gradient coils are placed in pairs with coil axes vertical on the top and bottom of the tunnel and four additional coils are placed in pairs with coil axes horizontal on the sides of the tunnel. Each set of four coils is located symmetrically with respect to the model center. The top and bottom, or Z gradient coils are, in general, different in size than the side, or Y, gradient coils. The Z coils provide lift, heave, and pitch, while the Y coils provide lateral force and yaw.

The second configuration considered is referred to as the X configuration, in which eight identical gradient coils are placed around the tunnel with their axes at some angle in the Y-Z plane. Again, the coils are located symmetrically with respect to the model center. By proper manipulation of the coil currents, all the required gradient coil functions can be supplied.

A brief parametric study of coil orientation and position showed that the preferred position for the gradient coils was at 45° to the tunnel but displaced along a 45° line so that the edges of the coils nearly touched above and below the tunnel.

Coil parameters were generated for each configuration and analyzed with the computer program BARC. These parameters are clearly not optimized and, in fact, differ significantly from the final values given in Section 3.3. However, they form a reasonable basis for comparison because they are derived from equivalent assumptions on performance requirements, coil envelope sizes, operating currents and current densities, and other characteristics.

Magnetic Arrangement

"X" CONFIGURATION

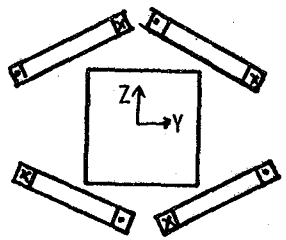

Other Four Coils Located Directly Behind Four Shown

"+" CONFIGURATION

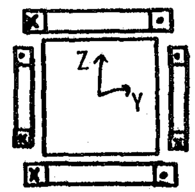

	"X" Configuration			"+" Configuration			
	Gradient	Magnetization	Drag	Z Gradient	Y Gradient	Magnetization	Drag
Number of Coils	8	2	2	4	4	2	2
NI (10^6 Amp-Turns)/Coil	10	13.3	24.3	6.1	2.05	13.3	18
Operating Current (kA)	10	10	10	10	10	10	10
No. of Turns	1000	1330	2430	610	205	1330	1800
Inner Radius (M)	.75	5.5	4.72	1.34	.605	5.5	4.1
Winding Cross-Section(MxM)	.5x1.0	.82x.82	1.1x1.1	.96x.32	.32x.32	.82x.82	.95x.95
Peak Field (T)	~8T	~7T	~9.5T	~6T	~5T	~7T	~8T
Self-Inductance (mh)	2350	39715	98215	1400	75	39715	47593
Stored Energy/Coil (MJ)	118	1985	4910	70	3.7	1985	2379

The basic parameter used to compare the two configurations is the total winding volume of the coils. This is a direct measure of the magnetic efficiency and, more importantly, the cost of the magnet system. The winding volume determines directly the cost of the conductor and other components and the cost of coil winding, which are major cost elements. It also drives the cost of the coil case, dewar, and structure which depend on the linear dimensions of the coil and thus on the volume, although to some power less than unity. Finally, the winding volume drives the cost of related systems such as the power supplies and cryogenics. The cost of power supplies varies almost linearly with the power required, which in turn scales with the coil inductance. The inductance varies as the square of the number of turns or, for a fixed current, with the square of the coil volume. The cost of the cryogenic system scales almost linearly with capacity. The required capacity scales almost linearly with coil volume, since the dominant refrigeration load, the AC losses in the winding, varies directly with volume.

Analysis of the selected "plus" and "X" configurations showed that the "plus" system is smaller in winding volume by more than 25%. It should be noted that the magnetization and drag coils, which are nearly identical for the two systems, comprise the bulk of the winding volume for each system, and winding volume of the "plus" gradient coils is only about 50% of that of the "X" system. On this basis, the "plus" system is an obvious choice. However, the two systems were also compared qualitatively on a number of other bases. The criteria for comparison included:

- visual access
- reliability
- maintainability
- field homogeneity

Visual access to the model is a specified requirement. The "X" system provides horizontal visual access to the model naturally, with adequate space for a window ∿ 2m x 2m between the coils. The "plus" system provides access naturally only along the edges of the tunnel, which may prove inconvenient. It was therefore assumed in developing the "plus" model that horizontal access equal to at least the length of the model must be provided by moving the Y coils apart. However, the increase in total winding volume associated with this change is small (a few percent), and the winding volume of the "plus" system is still substantially smaller. Thus visual access alone favors the "X" system but it not a strong driver.

Reliability is also a specified requirement, as explained in Section 2.1.6. In this system, reliability is achieved through the symmetry of the coil array and the ability to rapidly reduce the loads on the model quickly. Since the symmetry of both systems is the same, no advantage in reliability is inherent in either arrangement.

Maintainability of the magnet system is essential to high availability and productivity. In this study it has been assumed that an acceptable level of maintainability can be attained by providing spare gradient coils. It should be noted that no apportionment of MTBF or MTTR has been made, nor has the time required to replace a coil been estimated. Since all gradient coils are identical, only one spare is required for the "X" system. Two spare coils, one Z and one Y, must be provided for the "plus" system. However, the cost of the two coils for the "plus" system, as measured by the winding volume, should not be significantly larger than the cost of the single "X" spare. Thus, maintainability, as measured by the cost of sparing, favors the "X" system only slightly.

High homogeneity of fields and gradients in the tunnel working volume is advantageous because it limits the coupling between various modes of motion. For the systems considered here, the large size of the coils and the large coil-to-model distances, compared to the size of the model, lead to relatively homogeneous fields and gradients for both configurations.

In summary, a reasonable quantitative comparison of initial cost of the "X" and "plus" systems indicates that, for the configurations derived from the specified requirements, the "plus" system has a clear cost advantage. Evaluation of several other factors which could not be easily quantified favor the "X" system only slightly, if at all. The "plus" system was therefore selected for further study.

3.2.2 Gradient Coil Operating Modes

The gradient coil system must provide the full required forces and torques in both directions. This implies that the coils must generate both senses of fields and gradients. Two modes of coil operation are then possible:

- The coils can be monopolar, so that the maximum field and gradient are produced by two coils (e.g. top front and bottom rear Z coils) with the other two coils off. This mode has the advantage that the power supplies must operate in only two quadrants. It has the disadvantage that the coils must be sized so that two coils can produce the maximum field and gradient. This makes the gradient coils more than twice as large as for the bipolar mode described below. As a consequence, the peak inductive power is more than four times as large as for the bipolar mode, since the power varies directly with coil inductance, which in turn varies with the square of the coil volume (for a fixed operating current).

- The coils can be bipolar, so that all four coils contribute to both senses of field and gradient. This mode has corresponding advantages and disadvantages, i.e. the power supplies must operate in all four quadrants, but the coils can be smaller because all four of them are "working" at all times.

This tradeoff analysis was thought to be relevant because, for relatively modest power levels ($\lesssim$ 1 MW), bipolar power supplies were expected to be significantly more expensive than monopolar supplies.

It was found that, based on ROM estimates, the cost impact of reduced coil size far outweighed the cost impact of bipolar power supplies. Moreover, as the rating of the power supply increases to the levels ultimately found to be required for Case 1 (see Section 5), the cost of the power supply scales linearly with power and is nearly independent of whether the supply is monopolar or bipolar. Thus, the choice of bipolar power supplies and coils is an obvious one and was incorporated in the magnet system model.

3.2.3 Reliability Approach

High reliability is an essential requirement for virtually all of the ultimate applications of large superconducting magnets such as power production by MHD and fusion. Present large magnet programs will serve to define the design approaches and provide the operating experience needed to provide this reliability. At present, however, the data base on large superconducting magnets is limited. Because of the catastrophic consequences of a model flyaway, the problem of reliability for MSBS requires very careful consideration.

One approach(3) to magnet system reliability for MSBS involves the division of each coil into modules, with a separate power supply for each module, and the incorporation of additional, redundant windings so that the full capability of any coil can be maintained even after failure of one of the modules. If a coil is divided into N modules, for example, one additional module would be added, and each of the N+1 modules would operate at $\frac{N}{N+1}$% of its rated current.

This approach to system reliability was evaluated carefully for the chosen magnet system configuration. The number of modules N+1 in each coil, which is obviously the most important parameter in evaluating this approach, was chosen as 4 on the basis of judgement. It was concluded that this approach could clearly provide the required reliability, but that the impact on system cost and complexity makes the approach very unattractive. First, the size of each coil is increased by 33%, and the need for four sets of current leads per coil adds to the complexity of fabricating, operating, and monitoring each coil. The total reactive power required increases significantly since the power scales as the square of the coil volume, and the need for four separate power supplies also significantly increases the complexity of the system. Finally, the four sets of current leads increase the lead cooling requirement, which is not the largest load on the cryogenic system but is significant, by a factor of four.

Because of the impact which the use of modularization and redundancy has on MSBS, evaluation of other approaches to system reliability was necessary. An appreciation of the reliability inherent in the symmetry of the coil system led to the development of an approach based on rapid reduction of the model loads and controlled, symmetric manipulation of the coils in the event of a coil malfunction. This approach has been described in Section 2.1.6 and has been adopted because the required reliability can be achieved without additional system cost and complexity.

3.2.4 Low-Loss Coil Design Approaches

As a result of the requirements for dynamic control and forced model oscillation, the MSBS coils are subject to relatively large dB/dt and the need to minimize AC losses to limit the impact on stability and cryogenic requirements becomes a significant design driver. Several design approaches to limit AC losses were considered.

The first approach was a conventional stainless steel cryostat. For the sizes and section thicknesses required, it was estimated that the eddy current losses in the Z coil cases would be on the order of 200 kW during the simultaneous application of all dynamic test modes. This was viewed as an unreasonably large cryogenic load. The resulting He vapor would probably also have an intolerable effect on coil stability due to degradation of boiling heat transfer. The possibility of segmenting the coil cases to reduce the size of the eddy current path was also considered. However, no state-of-the-art approach which could maintain the required structural integrity could be found. Other approaches were therefore investigated.

The second approach considered, as shown in Figure 3.5, involves dividing the coil into two sections, one designed to generate only "DC" components of field and force, the other AC components for control and forced sinusoidal oscillation (the static components are, of course, not truly DC, but they are assumed to change at a rate which is very slow compared to the AC components). The DC section of the coil, including the case, is surrounded by a copper shield which prevents the AC field from penetrating the DC winding and causing AC losses. This approach has been previously proposed for energy storage coils.

In an idealized application, the current density is adjusted azimuthally around the shield to give a very small field within. In this application, however, a number of practical difficulties ensue. The shielding achieved by the configuration shown is relatively imperfect, and substantial changes in coil cross-section (to nearly circular rather than rectangular) would be needed to improve it. Furthermore, the shield cannot operate on self-generated eddy currents, but must be powered to be effective, and the Joule heating in the shield appears to be comparable to that in the case. The Lorentz forces on the shield and the requirements for active cooling would significantly complicate the mechanical and thermal design of the system. Finally and most fundamentally, the changing flux which links the DC coil would cause very large AC voltages (tens of kilovolts) to appear at the DC coil terminals. These voltages would have to be bucked by the DC coil power supply to prevent AC currents from flowing in the DC coil. The DC coil power supply then becomes, in fact, an AC supply with very large peak power requirements. Thus the approach of a shielded coil, while it has some conceptual benefit, is subject to a number of practical drawbacks.

The final approach considered, and the one ultimately adopted, is a configuration in which all continuous cold structure is made of a non-metallic material, typically either epoxy or polyester reinforced with fiberglass. The use of metal, if needed, is limited to bolts and stiffening members of small dimensions. The technology of non-metallic liquid helium vessels has been developed and applied somewhat sporadically in the past but is presently under more active and systematic development because it is required for at least two

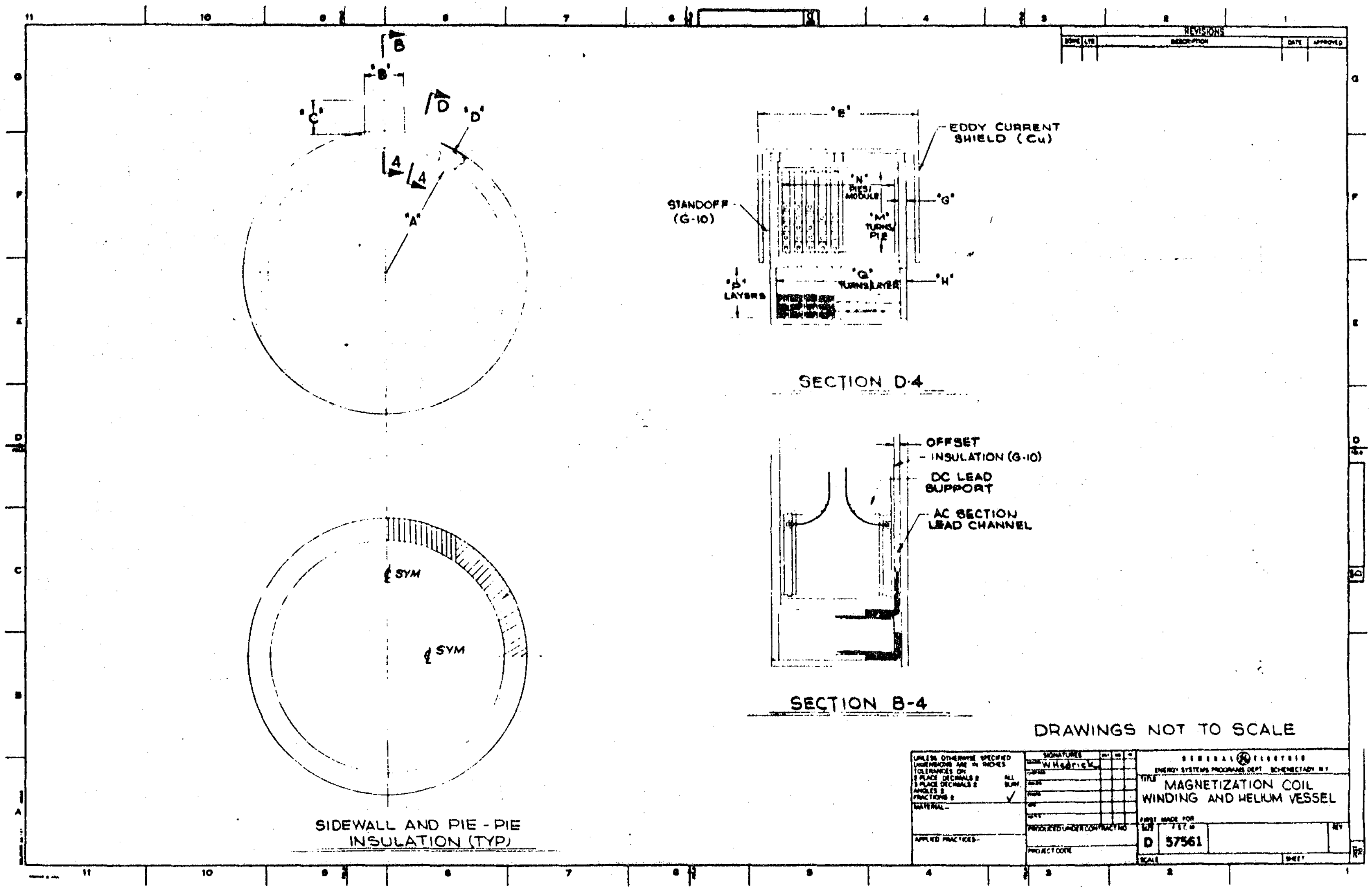

Figure 3.5
Magnetization Coil Winding and Helium Vessel

other applications of large superconducting magnets:

- ohmic heating coils for tokamak fusion reactors
- energy storage coils for electrical network stabilization

Los Alamos Scientific Laboratory, which is responsible under the Department of Energy for both of these areas, is presently procuring two non-metallic dewars of physical size comparable to those required for MSBS (∿ 3m diameter, ∿ 2 meters high). LASL has kindly provided specifications and other data used in the procurement of these dewars. GE has reviewed this information and has concluded that the use of non-metallic dewars for MSBS is feasible. However, there are two key differences between the LASL application and MSBS which will require careful design attention and probably component development and verification testing:

- The dewar assembly which, unlike the LASL application, may require helium-tight joints which operate at low temperatures.
- The need for transmission of large coil-to-coil forces, which is not presently required in the LASL applications.

These issues are discussed in more detail in Section 3.4. The configurations of the non-metallic dewars are described in more detail in Section 3.3.7.

3.2.5 Model Core Material

Although not strictly within the scope of the study, the use of a permanent magnet rather than a soft iron core was considered briefly. The use of a permanent magnet core has two attractive features:

- It allows the magnetization coil to be eliminated. The magnetization coil, although relatively small in cross-section, is large in diameter and has a significant winding volume. In addition, elimination of the magnetization coil eliminates the torque it exerts on the model and greatly eases the requirements for applied lateral fields to produce pitch and yaw.
- If the coercive force of the core is large compared to externally applied fields, the magnetization will remain collinear with the core and the degree of cross-coupling between various force and torque components will be reduced.

These potential advantages must be balanced against the fact that, since the magnetization of the core is reduced by at least a factor of two, the fields and gradients produced by the coil system must be larger by the same factor to produce the required forces and torques.

For the purposes of comparison, it was assumed that a permanent magnet core with a remanant magnetization of 1T could be used. Such properties can be achieved in state-of-the-art R_2Co_{17}-type magnets, which have $B_r \geq 1T$ and $Hc \geq 4 \times 10^5$ A/m (5000 Oe).

Elimination of the magnetization coil reduces the initial winding volume (number of ampere-meters) by about 10.7%. However, the winding volume of the drag coil is at least doubled (if the added amp-meters were the same distance from the model as the original ones, the volume would be exactly doubled. Since they are inevitably further away, it is more than doubled, in general). The amp-meters in the gradient coils associated with the production of force are also doubled. The amp-meters associated with the production of torque are increased due to the reduced magnetization, but are also decreased by a (large) factor which reflects the elimination of the torque resulting from the magnetization coil. The roll coils, which provide both magnetizing and torque field, are essentially unchanged. However, if it is assumed that PM cores are to be used for the wing cores also, then the assumption that the full wing volume can be used for the core is in serious jeopardy because of the poor mechanical properties of typical PM alloys.

The net effect of the elimination of the magnetization coils is as follows:

- Magnetization Coil: $N_{new} = 0$
- Drag Coil: $N_{new} \geq 2\ N_{old}$
- Z Coil: $N_{new} \geq 1.9\ N_{old}$
- Y Coil: $N_{new} \geq 1.4\ N_{old}$
- Roll Coils: $N_{new} = N_{old}$
- Total System: $N_{new} \geq 1.6\ N_{old}$

where N_{new} and N_{old} denote the total number of ampere-meters without and with the magnetization coil, respectively. Thus, the elimination of the magnetization coil would cause a net <u>increase</u> of about 60% in the winding volume of the magnet system. Not accounted for in this analysis is the fact that some of the coils, in particular the Z coils, are near the peak field limit of 8T in the existing configuration. If the coil cross-section were doubled, the peak field would likely exceed 8T, and the overall current density would have to be reduced with a corresponding further increase in coil cross-section. This would tend to exacerbate the difference between the two systems.

Finally, the inductances of the remaining coils in the system increase by $(\frac{Nnew}{Nold})^2$. The peak reactive power, which is already very large and the major cost driver in the system, would be increased by about a factor of 2.5. Thus the use of a permanent magnet core and the elimination of the magnetization coil is a very unattractive alternative.

3.2.6 Conductor Cooling and Stability Approaches

Numerous design criteria are employed in the design of conductors for superconducting magnets. The most prominent of these are the thermal stability criteria. They are used as a guide to conductor design by providing an estimate of the maximum stable current that can be expected under full operating conditions. These criteria are obviously important because the maximum field that can be obtained is limited by the maximum current that can be carried by the conductor without quenching the entire magnet.

The conductor selection for a superconducting magnet is a major driver in the design of the magnet because it is intimately related to the other subsystems (refrigeration, protection, power supplies, structure, insulation, dewar, current leads). Because of the number of factors involved the task of designing a thermally stable conductor is usually divided, for convenience and systematic exposition, into four separate technical tasks:

1. Minimize the amount of heat generated inside the conductor as well as the abruptness with which it occurs.
2. Minimize the amount external heat that reaches the conductor as well as the speed with which it enters.
3. Maximize the heat transfer rate within the conductor.
4. Maximize the heat removal rate from the surface of the conductor.

Each of these tasks is carried out within the constraints of the particular magnet system. The first of these tasks amounts to designing the conductor so as to reduce the AC losses, flux dumps and internal frictional heating. The second of these tasks is concerned almost exclusively with minimizing the effect of friction. The third task is in competition with the AC losses because increasing the heat transfer rate within the conductor also tends to increase the AC losses. The fourth task has the largest system impact of the four tasks. Because of this, selection of the coolant scheme and the stability criterion are given special attention.

3.2.6.1 Coolant Scheme

For the MSBS magnet system, pool boiling with saturated liquid helium at 4.2°K is proposed for reasons of reliability and availability. Virtually all the large superconducting magnets built to date, and most of those being designed at present, employ pool boiling. With this cooling scheme the conductor is cooled by natural convection.

Other possible coolant schemes included supercritical forced flow helium and superfluid helium. Both offer the potential for higher overall current densities than pool boiling. However, neither has any record of performance or design data base at present, and neither can be considered state of the art. Supercritical forced flow cooling also has the following disadvantages:

- pressurization and pumping of the helium (albeit at relatively modest velocities) is required. This adds to the cost and complexity of the cryogenic system. Moreover, large-scale efficient helium pumps have yet to be demonstrated.
- the use of forced-flow cooling for NbTi conductors at fields near 8T is difficult because the small thermal margin available ($\sim$ 1.4K) makes achievement of an acceptable stability margin difficult without resorting to very short hydraulic paths and complex manifolding. The use of Nb_3Sn in this application is viewed as highly undesirable, as explained in Section 3.1.2.

The use of superfluid helium requires a relatively complex cryogenic system including a double-walled He vessel and a low-temperature heat exchanger to keep the He bath at about 1.8K. A system of this type has not yet been demonstrated on any scale even approaching that of MSBS.

It should be pointed out that large magnets using both these cooling approaches are presently under development, and either technology could be implemented in MSBS if it were demonstrated to have significant technical and cost advantages in the near future. However, neither technique appears sufficiently promising at present to justify development specifically for MSBS.

3.2.6.2 Stability Criterion for Large Superconducting Coils

The most conservative thermal stability criterion has been chosen for designing the conductors in the MSBS magnet systems, viz the full cryogenic stability criterion. It is the most conservative criterion because it involves the least technical risk.

The five major thermal stability criterion for saturated liquid helium are compared and ranked according to risk in Figure 3.6. In this figure, the first three criteria were developed by considering steady-state conditions:

(1) Full cryogenic stability criterion
(2) Equal-area criterion
(3) Minimum propagating zone criterion

Criterion (1) requires that the heat generated by the conductor when fully resistive (non-superconducting) be less than the heat removed by the coolant at every point along the length. This requirement leads to the lowest heat flux from the conductor's surface and also the lowest operating current density. It has the advantage of simplicity because the number of critical parameters is reduced to a minimum. For criterion (1) the maximum heat flux that can be removed by helium is the only major uncertainty. In large ventilated pool boiling magnets this critical heat flux ranges from 0.1 W/cm^2 to 0.3 W/cm^2 and can not be predicted to better than 30% with present design tools. This would not be a problem if it were cost effective to allow this kind of design margin in the heat flux.

As it is, the overall cost of the magnet is closely tied to this parameter and some form of advance component testing is usually required to provide a cost-effective design.

Criterion (2) does not require that heat generation be below the minimum cooling provided by the helium. It requires, however, that long lengths of resistive conductor be capable of recovering by heat conduction out of the cold-end of the normal zone. Because this process of recovery may take several seconds (typical recovery rates are 1.0 meter/second) much more helium vapor is generated than if recovery occurs on a local basis. Slightly higher current densities are obtained compared to criterion (1).

Criterion (3) is an extension of the theory behind criterion (2) to short resistive regions. For normal lengths of limited extent (usually less than 50 cm) significantly higher current densities are obtained. However,

FIGURE 3.6

COMPARISON OF THERMAL STABILITY CRITERIA FOR CONDUCTORS COOLED BY NATURAL CONVECTION WITH SATURATED LIQUID HELIUM

Thermal Stability Criteria	Typical Heat Flux Limit	Typical Current Density Limit	Typical Restrictions on Disturbance Energy for an 8 Tesla Conductor*: Magnitude	Extent	Major Unknown and Range at 8 Tesla	Relative Measure of Risk
Theories Assuming Steady-State Conditions						
• Full cryogenic stability criterion	0.2 W/cm^2	2.5 kA/cm^2	NONE	Several turns	Critical heat flux (0.1 - 0.3 W/cm^2)	1
• Equal-area criterion	0.3	3.0	NONE	One turn	" "	2
• Minimum propagating zone (MPZ) criterion	0.6	4.0	$e_D < 40$ mJ/cm^3	$\ell < 10$ cm	Magnitude of disturbance energy per unit volume (10 - 1000 mJ/cm^3)	10
Theories Assuming Dynamic Conditions						
• Critical current margin (CCM) criteria	1.0 W/cm^2	5.0 kA/cm^2	$e_D \frac{A}{S} < 20$ mJ/cm^2	NONE	Magnitude of disturbance energy per unit volume (20-2000 mJ/cm^3)	40
• Combined criterion (MPZ and CCM)	1.6	7.0	$e_D < [40 + 20\,S/A] \cdot \frac{mJ}{cm^3}$	$\ell < 10$ cm	" "	60

* e_D = Disturbance Energy per Unit Volume

ℓ = Length of Conductor Affected

S/A = Cooled Perimeter/Cross-Sectional Area the magnitude of the disturbance energies that can be tolerated have to be several magnitudes smaller than what could be tolerated under criterion (1) and (2). This is true, in general, for all of the criterion that allow current densities higher than that permitted by criterion (2).

There are two criteria in Figure 3.6 that were developed for application to dynamic conditions:

(4) Critical current margin criterion
(5) Combined criterion

These criteria take advantage of the transient nature of the energy disturbances in the conductor to obtain higher current densities that might be allowed under the steady state criteria. Employing either of these two criteria involves a high degree of risk for two reasons:

- There is not a sufficient data base and experience with transient heat transfer to helium.
- There is not a sufficient understanding of the controlling factors and sources of the spontaneous energy disturbances.

3.2.6.3 Stability Criteria for Small Superconducting Coils

All the stability criteria described in the previous section are intended to counteract the effect of energy inputs due to conductor motion, which are generally thought to be inevitable in large magnets due to large Lorentz forces and unavoidable tolerance buildup and looseness in the windings. For "smaller" magnets (up to $\sim$ 1-2 MJ stored energy) the physical size and forces are such that it is conceivable to design the coil to eliminate frictional motion rather than deal with its consequences. The Z, Y, and roll coils for Case 3 fall into this category.

This is the basic principal underlying so-called adiabatically stable coils. Such coils typically do not contain large amounts of copper or cooled surface, and their ability to tolerate disturbance is limited to the (very small) adiabatic heat capacity of the conductor material. On the other hand, the absence of large amounts of copper and helium in the windings allows such coils to operate at current densities up to ten times as large as those for cryostable coils.

A number of fabrication approaches have been employed for high current density adiabatically stable coils. These include both dry windings, in which the conductor is either wound under high tension and held in place by friction, or wound with a low-friction interface material and allowed to move with minimal heat generation, and impregnated windings in which the conductors are held in place by epoxy, grease, wax, or some other substance. Virtually all of these approaches result in a highly undesirable phenomenon known as "training". "Training" manifests itself as a series of coil quenches, usually beginning well below the expected performance level of the coil. In extreme cases the coil may quench hundreds of times without ever reaching rated performance. "Training" is generally thought to result from microscopic conductor motions due to Lorentz force. Each quench is the result of one or more conductors moving and generating frictional heat. If all the conductors ultimately find stable, well-supported positions, the coil reaches rated performance; if not, it does not.

"Training" is clearly unacceptable for a system such as MSBS. The change in forces which would result from a change in field direction would almost certainly cause the coil to "untrain" and quench. The result of this would be extreme inconvenience in operation and low system availability.

Fortunately, a technology is available which is a notable exception to the behavior described above. GE has developed design and fabrication techniques for epoxy-impregnated adiabatically stable coils which routinely perform to the full critical current of the conductor without training. A summary of GE experience in this technology is shown in Figure 3.7. This unparalleled record of success has been achieved through careful analysis and design of coil windings and support structure to completely eliminate frictional motion, and careful fabrication to implement these key design features.

GE has recently broadened the applicability of this technology by developing a technique to introduce porosity in the epoxy-impregnated windings. This is achieved by inserting shims during winding which are removed after impregnation. The presence of liquid helium in the windings increases their heat capacity dramatically and allows the coils to remain superconducting at very high field ramp rates (up to 7 T/sec has been demonstrated). This capability makes the porous impregnated windings ideal for use in the Case 3 Z, Y, and roll coils, as described in Section 3.3.

FIGURE 3.7
EPOXY-IMPREGNATED WINDINGS

ITEM	MAGNET	TYPE	STORED ENERGY (mJ)	SIZE ODx LENGTH (m)	PEAK FIELD (T)	COIL CURRENT DENSITY (KA/cm^2)	Cu/Sc RATIO	PERFORMANCE	CROSS SECTION (cm x cm)	PEAK TRANSVERSE STRESS (psi)
1	CYLINDRICAL	POTTED	0.02	0.16 x 0.06	7.3	23	1.6	SHORT SAMPLE	4.5 x 6.4	
2	CYLINDRICAL	POTTED	0.02	0.16 x 0.06	7.3	23	1.6	SHORT SAMPLE	4.5 x 6.4	
3	CYLINDRICAL	POTTED	0.02	0.16 x 0.06	7.9	25	1.6	SHORT SAMPLE	4.1 x 6.4	
4	RACETRACK	POTTED	0.14	0.24 x 0.81	7.3	23	1.6	SHORT SAMPLE	8.3 x 3.8	-5300
5	RACKTRACK	POTTED	0.12	0.16 x 1.46	6.1	30	1.6	SHORT SAMPLE	4.6 x 3.0	
6	RACETRACK	POTTED	0.21	0.22 x 1.54	6.9	27	1.6	SHORT SAMPLE	6.6 x 3.3	
7	RACETRACK	POTTED	0.45	0.25 x 1.66	7.8	22	1.6	SHORT SAMPLE	7.6 x 5.2	
8	RACETRACK	POTTED	0.21	0.22 x 1.54	6.9	27	1.6	SHORT SAMPLE	6.6 x 3.3	
9	RACETRACK	POTTED	0.12	0.16 x 1.46	6.1	30	1.6	SHORT SAMPLE	4.6 x 3.0	
10	20-MVA GENERATOR ROTOR WINDING	POTTED	1.16	0.25 x 1.66	7.9	17	1.6	SHORT SAMPLE		-5950
11	CYLINDRICAL	POROUS	0.02	0.16 x 0.06	7.3	22	1.6	SHORT SAMPLE	5.0 x 6.6	
12	CYLINDRICAL	POROUS	0.03	0.18 x 0.07	7.5	18	1.8	SHORT SAMPLE	7.2 x 5.7	
13	RACETRACK FOR 20-MVA GENERATOR	POROUS	0.08	0.22 x 0.38	7.8	17	1.8	UNDER CONSTR.	7.2 x 7.5	-8800
14	EBT-P	POROUS	1.1	0.54 x 0.10 (EACH MODULE)	7.7	16	1.6			-6700

3.2.7 Dewar Configuration Approaches

Because of the large number of coils in the MSBS array, the possibility of mounting more than one coil in a single dewar was considered. Potential advantages of putting multiple coils in a single dewar include:

- improved thermal efficiency
- improved structural efficiency by allowing coil-to-coil forces to be transmitted by cold members
- reduced cryogenic system complexity by limiting the number of cryogenic lines needed
- reduced overall system size

Potential disadvantages include:

- more difficult transportation assembly and handling due to increased assembly
- reduced access to the tunnel

Several possible configurations were evaluated based on these considerations.

The possibility of putting the entire array in a common cryogenic envelope with cutouts for access was briefly considered. This approach would offer very high structural efficiency, since the large coil-to-coil forces could be carried by cold-structure, with only gravity forces transmitted to room temperature. However, this approach has at least two major disadvantages:

- the dewar and coil assembly would be much too large to be transported and would have to be assembled and tested largely on site. This would increase the cost and delivery time of the system very significantly because of the relatively high cost and low productivity of on-site labor.
- the large panels required would need extensive stiffening to carry the required pressure loads. Stiffening would also be required for the access cutouts. This would significantly complicate the design and fabrication of the assembly and increase its cost.

This approach was rejected, primarily because of the need for significant on-site labor.

The opposite extreme, the use of individual dewars for each coil, was considered and rejected because many cold-to-warm transitions would be needed to carry coil-to-coil forces, which complicate the system and increases the heat load.

The configuration ultimately selected combines certain coils in common dewars in a somewhat "natural" fashion and allows the largest forces to be carried by highly efficient cold structure. Each drag coil-magnetization coil set at either end of the test section is contained in a single dewar. The size of the dewar is increased only slightly over the size needed for the drag coil alone because the magnetization coil cross-section is relatively small. In this way the axial forces between the drag and magnetization coils, which are the largest in the system, can be carried by cold structure. Each pair of Z-gradient coils, above or below the tunnel, is also housed in a common dewar which is shaped somewhat like a "figure-eight". Since no vertical access has been assumed, no cutouts or penetrations are required. The coils can be close together for high magnetic efficiency, and the large repulsive forces along the tunnel axis can be carried by cold tension members. The Y-gradients are housed in individual dewars because they must be separated laterally to allow visual access to the model. The roll coils are also housed in individual dewars because their differing orientations would make a common dewar a very difficult design and assembly program. The dewar approach is more fully described in Section 3.3.8.

3.2.8 Structural Approaches

The magnet system consists of pairs of drag and magnetization coils, four Z gradient coils, four Y gradient coils and 8 roll coils. The major structural elements of the system are coil case, coil support, system support, vacuum vessel and LN_2 shield. Each major element could be designed according to a number of approaches and each approach was traded off against a number of considerations. The approaches and considerations are:

- Coil Supports
  - Bolt vs Weld to Coil Case
  - Truss Type
  - Continuous Type
  - Continuous vs Segmented Coil Interface Structure

- System Support
  - Truss Type
  - Feet Type

- Vacuum Vessel
  - One Large Enclosing System
  - Individual
  - SS304L (stainless steel) vs G10 (glass fiber/epoxy laminate)
- LN_2 Shield
  - SS304L
  - G10
- Coil Case
  - Continuous Thick Wall SS304L
  - Continuous Thin Wall SS304L with G10 Reinforcement
- Considerations
  - Magnetic & Gravity Loads
  - Eddy Current Losses
  - Heat Loads
  - Manufacturing & Cost
  - Field Assembly
  - Transportation

The larger drag and magnetization magnets and their support structures are used to transmit the system loads to ground. The Z and Y gradient magnets and the roll magnets are individually supported and attached to the magnetization and drag coil structure. The initial approach was for an all metallic construction, i.e. coil case, coil structure and inter-coil structure of SS304L material. As the magnetics analysis progressed, it became evident that eddy current losses was a serious problem and an all metallic construction would not suffice. The final concept is a combination of SS304L for warm structure and G-10 for cold structure.

Figure 3.8 is a summary comparison of the concepts considered, the selection criteria and the concept selected. A rating system of P (poor), A (average) and G (good) was used to evaluate the concepts. A rating of "P" indicates the concept is feasible but will have an undesireable effect, an "A" rating indicates the concept is feasible but can be improved, a "G" rating indicates the concept may be improved somewhat. Along the left-hand column the concepts under each major heading has been numbered. The last column on the right-hand side is the concept selected.

3.2.9 Alternative Operating Scenarios

As shown in Section 3.3, the peak reactive power and AC losses which result from the control and forced sinusoidal oscillation requirements are

FIGURE 3.8
CONCEPTS SELECTED & RATIONALE

Major Structural Element	Magnetic Loads	Eddy Current Losses	Heat Loads	Manufacture & Cost	Field Assy.	Transportation	Selection
Coil Support							
1 - Bolt	G	P	P	A	G	G	
2 - Weld	G	P	P	A	P	G	
3 - Truss	P	G	G	A	G	G	6
4 - Continuous	G	P	P	A	N/A	G	
5 - Cont. Interface	G	P	P	A	G	G	
6 - Seg. Interface	G	G	G	A	G	G	
System Support							
1 - Truss	P	N/A	N/A	A	A	A	2
2 - Feet	G	N/A	N/A	A	G	A	
Vacuum Vessel							
1 - One Large	N/A	N/A	P	A	A	P	2
2 - Individual	N/A	N/A	G	A	G	G	
LN_2 Shield (SS304L)							
1 - Continuous	N/A	P	A	A	A	A	
2 - Segmented	N/A	A	A	P	P	A	3
3 - G-10	N/A	G	A	A	A	A	
Coil Case							
1 - Continuous Thick Wall SS304L	G	P	A	G	N/A	G	
2 - Continuous Thin Wall SS304L	A	P	A	G	N/A	G	3
3 - All G-10	A	G	A	A	N/A	G	

significant design and cost drivers for MSBS. A number of alternative operating scenarios intended to reduce these values have been briefly evaluated by scaling from the baseline case. The results are summarized in Figure 3.9.

As explained in Section 3.1.6, it was initially assumed that dynamic control for MSBS required application of currents to oppose forces of up to .5% of the steady-state forces at 50 Hz. It was apparent at the outset that this was a very conservative assumption because the inertia of the model would prevent it from responding measurably to forces applied at this high frequency. Subsequent discussions with NASA indicated that a force of .1% of steady state at ∿ 10 Hz was more typical. This value was analyzed more realistically by applying it as a step input in simulation and determining the current ramp rate needed to keep the model within the position accuracy specified in the SOW. These values are reflected in Alternatives (E) and (F) and are expected much more nearly to approximate the real situation.

The requirements for forced model sinusoidal oscillation give rise to > 50% of the peak reactive power needed for MSBS. To provide a basis for comparison, cases in which the oscillation frequency was reduced by 10X (for all modes) and eliminated were evaluated. It is evident from equations (6) and (10) in Section 2.1.5 that $(dI/dt)_{max}$ which is directly proportional to peak power, scales as ω^3. Reducing the frequency by 10X therefore reduces the peak power by ∿ 1000X, a very significant reduction. This reduction is observed in Figure 3.13 for Alternatives (E) and (F). Elimination of forced oscillation has very little additional effect, as is apparent from a comparison of cases (F) and (G).

In light of the significant reduction in peak power requirements which can be achieved through a 10X reduction in the forced oscillation frequency, NASA may wish to consider whether this mode could produce useful data.

3.3 MAGNET SYSTEM CONCEPT

The magnet system concept selected to satisfy the requirements described in Sections 2.0 and 3.1, on the basis of the tradeoffs discussed in Section 3.2, is shown in Figure 3.10. The system consists of twenty separate superconducting magnets arranged around the tunnel test section in a highly symmetric array. There are five types of coils, each having a distinct function.

Figure 3-9

TOTAL REACTIVE POWER FOR THE MAGNET SYSTEM (MVAR)

	Alternate E Full Forced Oscillation Frequencies Control from Simulation of .1% Disturbance	Alternate F 10% Forced Oscillation Frequencies Control from Simulation of .1% Disturbance	Alternate G No Forced Oscillation Control from Simulation of .1% Disturbance
Case 1	5364	205	199
Case 2	1043	16.4	16
Case 3	112	10.8	10.8

A Number of Alternatives Have Been Investigated In An Attempt To Define More Attractive Operating Scenarios

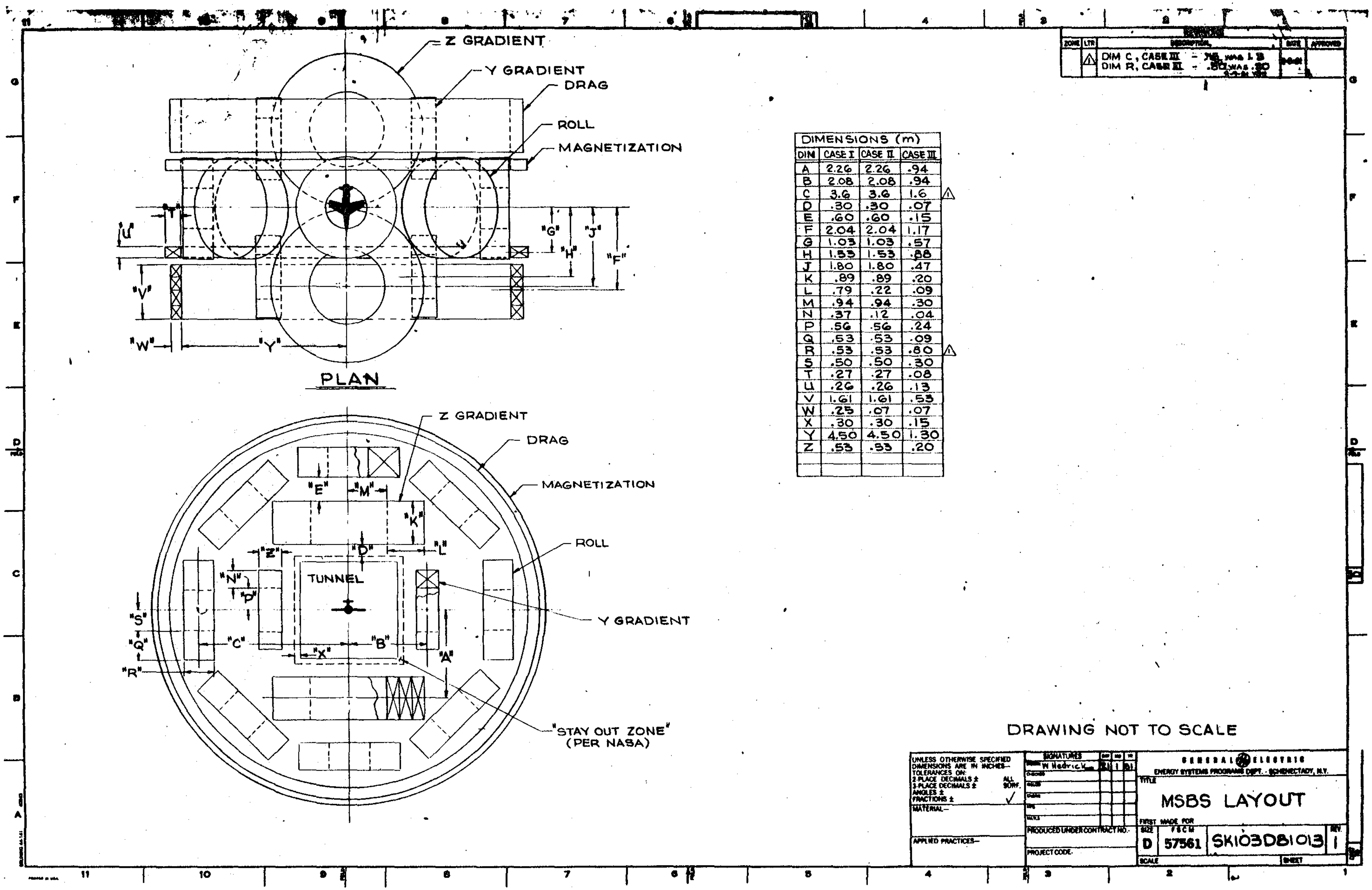

DIMENSIONS (m)			
DIM	CASE I	CASE II	CASE III
A	2.26	2.26	.94
B	2.08	2.08	.94
C	3.6	3.6	1.6 △1
D	.30	.30	.07
E	.60	.60	.15
F	2.04	2.04	1.17
G	1.03	1.03	.57
H	1.53	1.53	.88
J	1.80	1.80	.47
K	.89	.89	.20
L	.79	.22	.09
M	.94	.94	.30
N	.37	.12	.04
P	.56	.56	.24
Q	.53	.53	.09
R	.53	.53	.80 △1
S	.50	.50	.30
T	.27	.27	.08
U	.26	.26	.13
V	1.61	1.61	.53
W	.25	.07	.07
X	.30	.30	.15
Y	4.50	4.50	1.30
Z	.53	.53	.20

Figure 3.10
MSBS Layout

The magnetization coils are two large solenoids, located symmetrically fore and aft of the model. They are monopolar DC coils which provide the field required to keep the magnetic core in the model saturated. They are described more fully in Section 3.3.3.

The drag coils are also two large solenoids, located symmetrically fore and aft of the model. They are designed to produce a pure axial gradient (no net field) at the model to provide the axial force needed to resist the wind drag on the model. The drag coils are monopolar and operate with a small AC component superimposed on a DC background to provide control of the model position along the wind tunnel axis. They are described further in Section 3.3.4.

The four Z-gradient coils are four large solenoids located above and below the tunnel, symmetrically fore and aft of the model. They produce both fields and gradients which supply lift force and pitching torque. These coils are fully bipolar and operate with a substantial AC component to provide control and forced oscillation capabilities. They are described more fully in Section 3.3.5

The four Y-gradient coils are solenoids located in pairs on either side of the tunnel test section, symmetrically fore and aft of the model. Like the Z-coils, they produce both fields and gradients which in turn supply lateral force and yawing torques. Because of the relatively modest requirements for force and torque, they are much smaller than the Z-coils. They must also provide control and forced oscillation capabilities and must therefore be capable of AC operation. They are more fully described in Section 3.3.6.

The roll coils are eight solenoids located around the axial center of the model, in a symmetric array with one coil every 45°. They produce a field configuration which simultaneously magnetizes the wings of the model and applies a field perpendicular to the wings to produce rolling torques. They must be capable of AC operation to provide oscillatory roll and roll control. They are described more completely in Section 3.3.7.

Two types of conductor are used in the MSBS coils. All the coils for Cases 1 and 2, and the Case 3 magnetization and drag coils, use a 50-kA cryostable low-loss cabled conductor being developed for application in the LASL 20 MJ prototype ohmic heating coils. The Case 3 Z, Y, and roll coils use a 1000-A adiabatically stable cabled conductor which has been used by GE in the rotor coils for the 20 MW Air Force generator. Both conductors are described more fully in Section 3.3.2.

The dewars for the MSBS coils are constructed from non-metallic materials (fiberglass-reinforced plastic) to eliminate eddy current losses which would be intolerably large in metal vessels. The helium vessels are reinforced by segmented metal structure which restrains and transmits coil forces. Design approaches have been selected based on non-metallic dewars currently being produced by LASL. However, the differences in configuration and application are significant enough that some development of fabrication and closure methods may be required. The support structure for the coils is a relatively conventional cylindrical superstructure which reacts coil-to-coil forces at room temperature and carries the gravity forces to ground. The dewars and support structure are more fully described in Section 3.3.8.

3.3.1 System Analysis

A magnetic model of MSBS was developed to facilitate analysis tasks in support of the system design. This model incorporates the full cross-section and current density of each coil. This allows accurate calculation of fields and forces within the windings and will be essential for further design work. Analysis of the model was performed with the computer code BARC8, which was obtained from ORNL and is capable of handling large arrays of arbitrarily shaped planar coils. Analysis was performed in four major areas:

- magnetic forces
- coil peak fields
- field homogeneity
- coil inductances

3.3.1.1 Magnetic Forces

Magnetic forces were calculated for all coils in the system for nominal static operating conditions (maximum static forces and moments). In order to establish the symmetry of the forces for various modes of system operation, forces for all coils were also calculated for the following cases:

- currents in Z-coils reversed, corresponding to a reversal of static lift force and pitching torque
- currents in Y-coils reversed, corresponding to a reversal of static lateral force and yawing moment
- currents in both Z and Y coils reversed

These analyses clearly established the need for rigid, bi-directional coil supports rather than monodirectional link-type supports such as might be used to support gravity loads.

Oscillatory forces resulting from forced model oscillations were calculated on two coils, one Z and one Y, and derived by symmetry for the other coils in the system. Since the changes in current for forced oscillation are small, the oscillatory forces should be small (a few percent of the static forces), and the analysis confirmed this. As a result, the structure is designed almost entirely on the basis of static forces, as discussed in Section 3.3.8. Typical results of the magnetic force analysis are given in Section 3.3.8.

3.3.1.2 Coil Peak Fields

Calculation of the peak field of a solenoidal coil is normally a straight forward matter, because it always occurs on the inner surface of the winding (the exact axial location depends on the ratio of coil radius to thickness). However, in a complex magnet array such as MSBS, the superposition of the self-field of a coil and fields generated by other coils can cause the peak field to occur elsewhere. Careful scanning of the field in the windings is required to ensure that it is within design limits at all points.

In the present system it was clear from inspection that high peak fields would occur in the Z-coils, because of their high self field and their proximity to the magnetization and drag coils. A scan of the field at the winding in all three dimensions (axial, radial, circumferential) indicated that the peak field occurs at the 180° point (near the center of the test section rather than at the end) on the winding ID and just above the axial centerline. The peak field is about .5T greater than the peak self field of the Z coil. Detailed peak field scans were also performed for the magnetization and drag coils. The peak field in the magnetization coil was found to be about 4.6T, considerably larger than the peak self field of about 1.7T because of the proximity of the drag coils. Likewise, the drag coil peak field is about 4.5T compared to a peak self field of about 3T. Both peaks occur at the winding inner diameter, at the ends of the coils which face each other, and about 20° off the horizontal centerline where the coils pass closest to the Z-coils. This is as expected. A peak field scan was not performed for the Y or roll coils, but their peak fields were estimated from the Z coil data.

3.3.1.3 Field Homogeneity

The homogeneity of the magnetic fields in MSBS is expected to be relatively good in the region of the model because the system is highly symmetric and the coil-to-model distance is relatively large compared to the axial length of the coils. Two sample analyses were performed to verify this.

The variation of the magnetization coil field along the x and z axes was determined. It was found that, over the length of the model, the magnetization coil field is constant along the x-axis to within less than one percent. The change in the magnetization coil field in going from z=0 to z=20 cm (the value at maximum angle of attack) at any point along the length of the model is about 1.15%. Thus the magnetization coil field is very homogeneous even though, as explained in Section 3.3.3, the magnetization coils are not a Helmholtz pair and no special effort was exerted to achieve high homogeneity.

The variation of the vertical field gradient, $\partial Hz/\partial x$, with position was also examined. It was found that, over the 20cm maximum range of vertical excursion of any point on the model, $\partial Hz/\partial x$ varies by less than 1%.

3.3.1.4 Coil Inductances

The single turn self and mutual inductances of the MSBS coil system were calculated using standard formulas (4). The results are shown in Figure 3.11. For this analysis the coils were modeled as single filaments. A sample calculation for two coils using the full cross-section indicates that the error introduced by the filamentary model is less than 10%.

As is apparent from inspection of the results, the inductive coupling between coils in the system is relatively small compared to the coil self-inductance. The effect of inductive coupling has therefore been ignored in analyzing power requirements and AC losses in the coils. The one exception to this is the coupling between the drag and magnetization coils, which would be expected to be large since the coils are coaxial and close together. In order to account for this, the magnetization coils are wound with low-loss conductor even though they are nominally DC coils.

3.3.2 Conductor Concepts

The MSBS coil conductor must satisfy the following requirements:

- it must meet the stability limits given in Section 3.2.6

Figure 3.11

MSBS TABLE OF SELF & MUTUAL INDUCTANCES
FOR SINGLE TURN COILS (MICRO-HENRYS)

2	3	4	5	6	7	8	9	10	11	12	13	
2.76	.0488	.0605	.0488	0.152	<<.049	.0464	<<.049	0.162	0.240	.0878	0.174	2
	1.715	.0488	.0097	<<.049	0.01	<<.049	.0075	.0349	0.054	.0239	.0395	3
		2.76	.0488	.0464	<<.049	.152	<<.049	0.162	0.240	.0878	0.174	4
			1.715	<<.049	.0075	<<.049	0.01	.0349	0.054	.0239	.0395	5
				2.76	.0488	.0605	.0488	0.240	0.162	0.174	.0878	6
					1.715	.0488	.0097	.054	.0349	0.0395	.0239	7
						2.76	.0488	0.240	0.162	0.174	.0878	8
							1.715	.054	.0349	0.0395	.0239	9
								19.55	4.775	8.625	3.163	10
									19.55	3.163	8.625	11
										13.168	2.164	12
											13.168	13

NOTE: Coils Identified in Figure 3.26

- it must operate at a high current sufficient to limit coil inductive voltages to acceptable levels
- it must have losses sufficiently low to allow stable operation and produce reasonable cryogenic loads
- it must have proven performance and be readily available

Two conductor concepts must be selected, one for the large cryostable coils and one for the Case 3 adiabatically stable coils.

3.3.2.1 Cryostable Conductor

A brief review of the state of the art indicates that the only cryostable conductor which appears able to satisfy conductor requirements is the 50 kA conductor being developed for use in the Los Alamos Scientific Laboratory (LASL) 20 MJ prototype ohmic coil. It is designed to achieve stable operation at high field ramp rates ($\sim$ 15T/sec) with low losses. This conductor is shown in Figure 3.12. The principal parameters, as given in Ref. 5, are shown in Figure 3.13.

The conductor consists of 36 7-strand subcables around a steel core which provides structural support. Each strand in the subcables is individually insulated with a film insulation to prevent eddy currents from flowing between strands. The NbTi filaments are concentrated in the center of the strand, which allows a tighter twist and reduces losses. The surrounding copper is subdivided by high resistance copper-nickel barriers to limit eddy current losses.

Stability tests[6] have confirmed analysis[5] which indicated that the conductor is essentially fully cryogenically stable at 50 kA and 7.5T. Since the maximum field in MSBS is slightly lower ($\sim$ 7.2T), full stability can be expected.

3.3.2.2 Adiabatically Stable Conductor

The conductor selected for the adiabatically stable coils for Case 3 has been successfully used by GE in racetrack coils for the 20 MW Air Force superconducting generator. This conductor must operate stably at field ramp rates of up to 7T/sec. The conductor parameters are shown in Figure 3.13, and a cross-section of the conductor is shown in Figure 3.19.

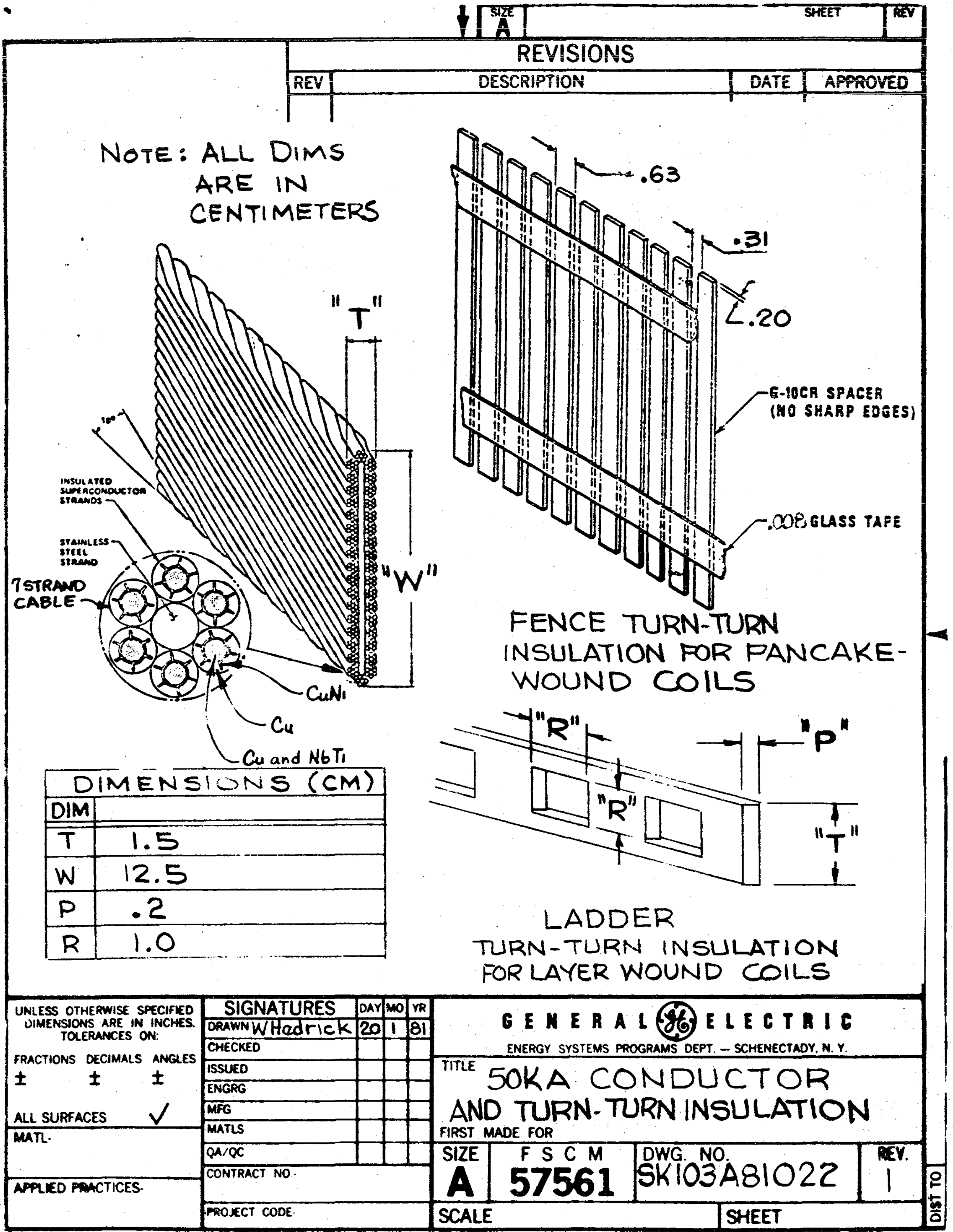

DIMENSIONS (CM)	
DIM	
T	1.5
W	12.5
P	.2
R	1.0

Figure 3.12

Figure 3-13

MSBS CONDUCTOR PARAMETERS

	Cryostable	Adiabatic (Epoxy - Impregnated)
Configuration	6x36 Cable Around Core, Insulated Strands	6-Strand Coreless Cable, Insulated Strands
Operating Current (kA)	50	.750 or 1.4
Critical Current (kA)	70 @ 7.5T	~1.0 @ 8T
Conductor Dimensions (cm)	12.5 x 1.5	.284 x .178
Strand Configuration	NbTi/Cu with Cu Ni Fins and Cu Sectors	NbTi/Cu
Strand Diameter (mm)	2	.9
Filament Size (μm)	21	~30
Heat Transfer Rate (w/cm^2)	.26	N/A

Both Conductors Are State-of-the-Art and Available

The conductor consists of six individually insulated strands cabled without a core into a compact 3x2 configuration. Each strand is a conventional multifilamentary NbTi/Cu composite. The small strand size limits the losses to a reasonable level. The performance of the conductor has been confirmed by successful testing of all four racetrack coils.

3.3.3 Magnetization Coils

The magnetization coils must provide a DC field sufficient to saturate the model core. As shown in Figure 3.14 the magnetization coil is a large horizontal-axis solenoid. The 50 kA conductor is pie-wound in order to provide well-defined vertical paths for helium circulation and venting of helium vapor. Circumferentially grooved G-10 sheet on the inner and outer rings provides for helium circulation also around the coil perimeter. The interpie and sidewall insulation is G-10 sheet grooved to provide helium circulation between pies. This type of insulation has been used on the GE LCP coil. The groove sizes has been selected based on Sydoviak's correlation[7] to ensure no degradation in heat transfer.

The coil is enclosed in a non-metallic case which is reinforced by segmented supports bolted together around the coil circumference. Electrical and instrumentation leads and helium vapor exit through a service stack at the top of the coil. Use of commercial vapor-cooled leads has been assumed although they are not an off-the-shelf product for this high current.

The coil supports interface with the drag coil support structure through cold members within a common dewar. On the other end, the support structure connects to the external room temperature support cylinder through a thermal standoff not shown.

As explained in Section 3.1.5, the model core can be saturated by a field of about 1.2×10^4 A/m. However, the drag coil produces an axial field which varies from 1.36×10^4 A/m (1700 Oe) at one end of the core to -1.36×10^4 (-1700 Oe) at the other. In order to ensure that the net field at all points along the core is at least 1.2×10^4 A/m, the magnetization coils are designed to produce 2.56×10^4 A/m. The resulting coil parameters are shown in Figure 3.15. Some AC losses may occur in the coil, even though it is nominally DC, because of inductive coupling with the drag coil. However, these are expected to be small compared to other losses in the system and have been ignored.

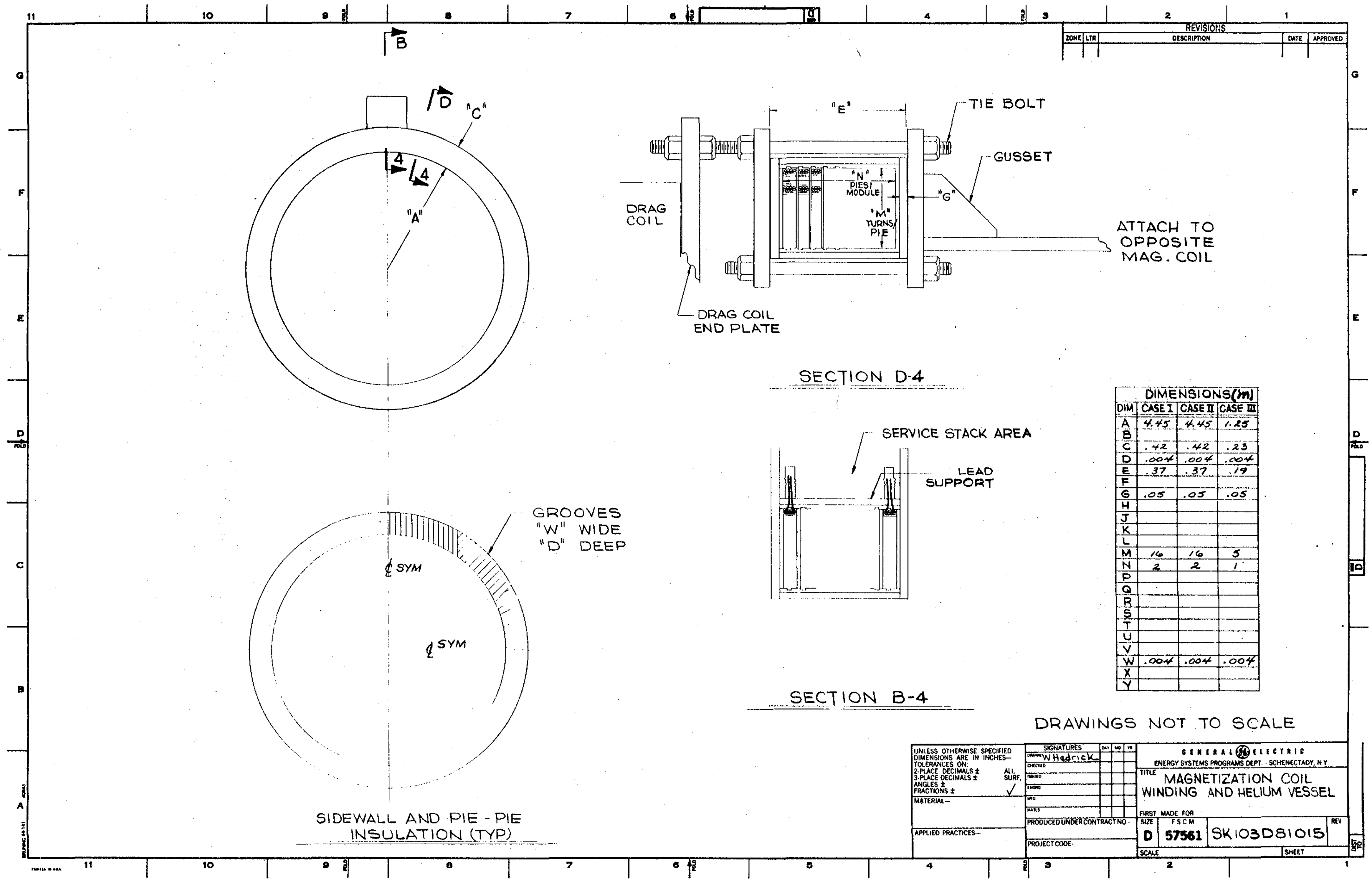

DIMENSIONS (m)			
DIM	CASE I	CASE II	CASE III
A	4.45	4.45	1.25
B			
C	.42	.42	.23
D	.004	.004	.004
E	.37	.37	.19
F			
G	.05	.05	.05
H			
J			
K			
L			
M	16	16	5
N	2	2	1
P			
Q			
R			
S			
T			
U			
V			
W	.004	.004	.004
X			
Y			

Figure 3.14
Magnetization Coil Winding and Helium Vessel

FIGURE 3-15

MAGNETIZATION COIL OPERATION PARAMETERS

	CASE 1		CASE 2		CASE 3	
	ALTERNATE E Full Forced Oscillation Frequencies Control from Simulation of .1% Disturbance	ALTERNATE F 10% Forced Oscillation Frequency Control from Simulation of .1% Disturbance	ALTERNATE E	ALTERNATE F	ALTERNATE E	ALTERNATE F
NUMBER OF COILS	2	2	2	2	2	2
MODULES/COIL	1	1	1	1	1	1
AMP. TURNS/MODULE (10^6A)	1.6	1.6	1.6	1.6	.50	.50
OPERATING CURRENT (kA)	50	50	50	50	50	50
WINDING CURRENT DENSITY (A/cm^2)	1500	1500	1500	1500	1500	1500
PEAK FIELD (T)	4.6	4.6	4.6	4.6	3.0	3.0
STORED ENERGY (MJ)	26	26	26	26	.6	.6
$(dI/dt)_{max}$ (A/sec)	$\sim$0	$\sim$0	$\sim$0	$\sim$0	$\sim$0	$\sim$0
PEAK VOLTAGE/MODULE (kV)	$\sim$0	$\sim$0	$\sim$0	$\sim$0	$\sim$0	$\sim$0
PEAK REACTIVE POWER/COIL (MW)	$\sim$0	$\sim$0	$\sim$0	$\sim$0	$\sim$0	$\sim$0
PEAK AC LOSSES/COIL (w)	$\sim$0	$\sim$0.	$\sim$0	$\sim$0	$\sim$0	$\sim$0
DISCHARGE VOLTAGE (v) (T_{max} = 200K)	40	40	40	40	1	1

As shown in Figure 3-14, the winding for Cases 1 and 2 is identical, two pies of 16 turns each, because the physical sizes of the model and tunnel are unchanged. For Case 3, the 4'x 4' tunnel, only 5 turns of 50 kA conductor are required to produce the needed field. The resulting single pie layout is possible but inconvenient for the purpose of routing leads. However, a lower current could clearly be used, which would make the winding layout more conventional and also decrease the cryogenic load which results from lead losses.

The magnetization coils as presently conceived are relatively straightforward in design and compact in cross-section but are so large in diameter ($\sim$ 33 ft with cryostat) that they can be shipped only by barge. This is certainly feasible, given the relative case of water access to both the GE fabrication facility in Schenectady and the Langley site. However, it is relatively expensive and time-consuming. An alternative configuration in which the magnetization coils lie forward and aft of the Z-coils and fit relatively tightly around the tunnel was therefore briefly considered. In this configuration the coils could be reduced in diameter to $\sim$ 20 ft and might be shippable overland through the use of special routing. However, the ampere-turn requirements for the coil would increase by at least a factor of 2.5 as a result of the large increase in axial distance from the coil to the model. The winding volume and cost of the coil would increase significantly despite the smaller diameter, and this would substantially or totally offset any savings in shipping cost.

A third possible approach, fabrication of the coil on-site at Langley, has not been evaluated. However, previous studies have concluded that on-site fabrication carries a very significant cost penalty and should be avoided if at all possible.

3.3.4 Drag Coils

The drag coils supply a field gradient at the model which produces an axial force to resist the drag force of the wind. The gradient requirements are given in Section 2.1.3 for the three specified cases. The configuration selected, as shown in Figure 3.16 is a large horizontal axis solenoid. It was initially assumed that the drag coils should be a Helmholtz pair (separation radius) to ensure a uniform gradient at the model. However, geometrical constraints drove the coils to relatively large separation, and the large radii then resulted in large amp-turn, peak field, stored energy, and stress values. Subsequent analysis showed that the use of Helmholtz coils was a totally artificial constraint and that a somewhat elongated solenoid could provide

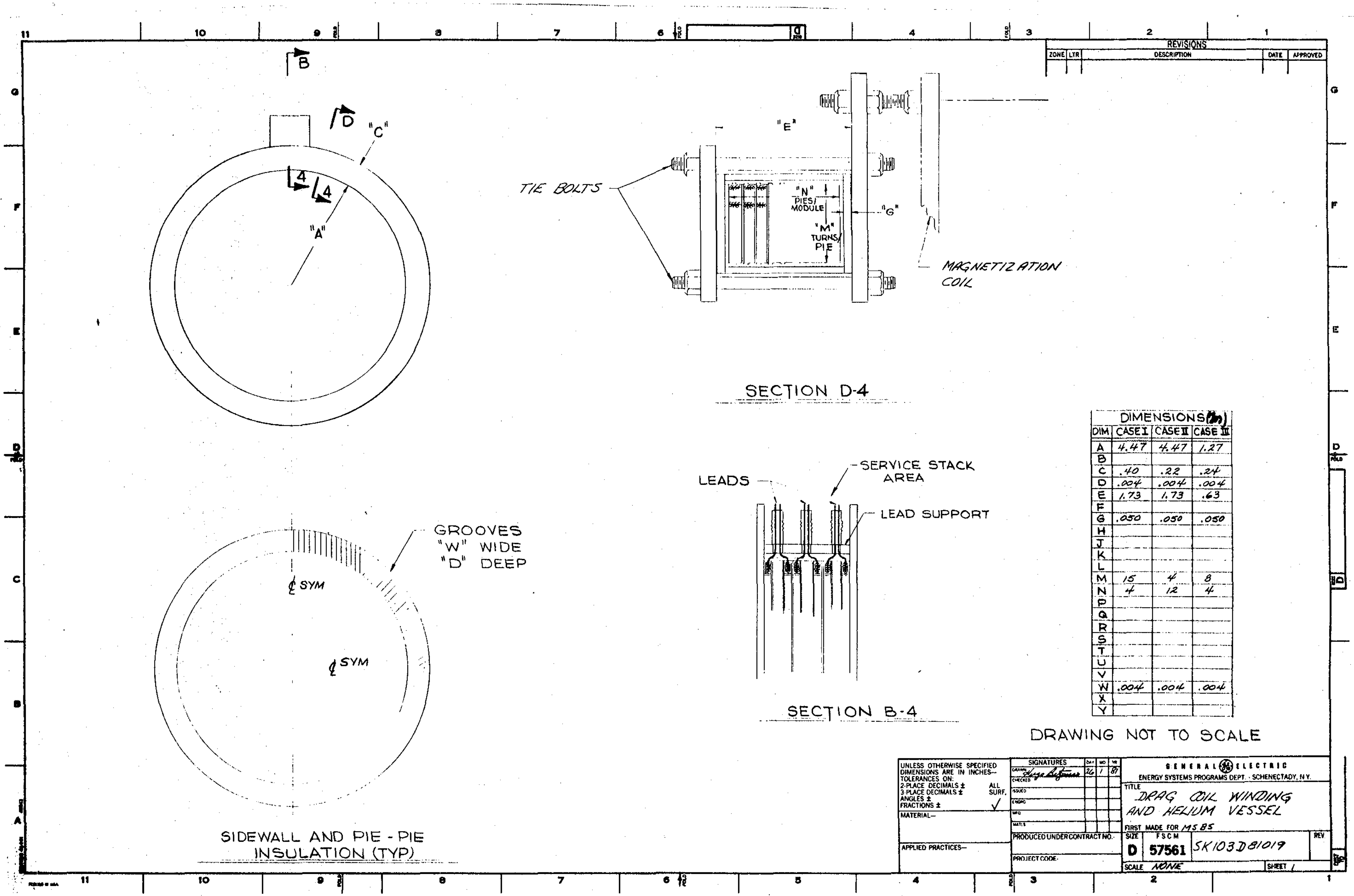

Figure 3.16
Drag Coil Winding and Helium Vessel

adequate homogeneity with substantially reduced values of the above magnetic parameters. The resulting configuration, as shown in Figure 3.16, is essentially identical in concept to the magnetization coil. The coils are supported structurally by the magnetization coils at one end and by external warm structure (not shown) at the other.

Magnetic analysis to determine the amp-turns needed to produce the required gradient was performed with a simple GE program called COIL which calculates fields at any point for a single solenoid. The effect of the other coil was accounted for simply by symmetry. The resulting parameters for the three cases are shown in Figure 3.17.

The drag coil is not required to provide forced oscillation but must provide longitudinal control of the model by means of dynamic adjustment in current. The maximum required rate of current change, based on the initial assumption of control pulses of .5% of steady state at 50 Hz as described in Section 3.1.6, is 3.10^3 A/sec, as indicated in Figure 3.17. This value is derived by the method described in Section 2.1.5.

The required rate of current change and coil inductance lead to relatively modest inductive voltages, as indicated in Figures 3.17. For Cases 1, 2 and 3, a single module is sufficient to limit the terminal voltage to an acceptable value.

The AC losses in the drag coil were estimated by using the expressions derived by Walker for the 50 kA conductor[5] In applying these expressions, care must be taken to distinguish between the full bipolar field sweep required for the ohmic heating coil and the relatively small dynamic field changes ($\Delta B/Bo < .1$) required for the MSBS application. This difference has a significant effect on the hysteresis losses which depend on the magnitude of the field change and are much smaller in the latter case than in the former.

The peak local AC losses were calculated using these expressions. The peak average losses were then estimated by averaging the field change or rate of field change over the cycle and the volume of the coil. The resulting values which are accurate to within a factor of two, are shown in Figure 3.17 for the three cases.

The drag coils are also too large to be shipped overland. Like the magnetization coils, however, they would increase substantially in winding cross-section and cost if they were moved to a larger axial distance from the model and reduced in diameter.

FIGURE 3-17

DRAG COIL OPERATING PARAMETERS

	CASE 1		CASE 2		CASE 3	
	ALTERNATE E	ALTERNATE F	ALTERNATE E	ALTERNATE F	ALTERNATE E	ALTERNATE F
NUMBER OF COILS	2	2	2	2	2	2
MODULES/COIL	1	1	1	1	1	1
AMP. TURNS/MODULE (10^6A)	9	9	2.4	2.4	1.6	1.6
OPERATING CURRENT (kA)	50	50	50	50	50	50
WINDING CURRENT DENSITY (A/cm^2)	1500	1500	1500	1500	1500	1500
PEAK FIELD (T)	4.5	4.5	1.5	1.5	3.0	3.0
STORED ENERGY (MJ)	379	379	53	53	5.1	5.1
$(dI/dt)_{max}$ (A/sec)	3×10^3	3×10^3	3×10^3	3×10^3	3×10^3	3×10^3
PEAK VOLTAGE/MODULE (kV)	.9	.9	.063	.063	.012	.012
PEAK REACTIVE POWER/COIL (MW)	45	45	3.2	3.2	.6	.6
PEAK AC LOSSES/COIL (w)	133	133	40	40	9	9
DISCHARGE VOLTAGE (v) (T_{max} = 200K)	500	500	71	71	7	7

3.3.5 Z-Gradient Coils

The Z-gradient coils supply both fields and gradients at the model to produce static and dynamic lift forces and static and dynamic pitching torques. The requirements are discussed in Section 2.1.3. As shown in Figure 3.18, the Z-coil configuration for Cases 1 and 2 is a large vertical axis solenoid. The 50 kA conductor is layer wound in this case, again to provide clear vertical channels for helium vapor ventilation. The interlayer insulation is a straightforward grooved sheet of 1.0cm overall thickness with .4cm x .4cm grooves on both sides. The webs are solid to provide good layer-to-layer isolation; lateral helium flow is not needed. The insulation material in this case is fiberglass reinforced polyester which has sufficient flexibility to be bent on the required radii. The coil case and reinforcement are very similar to that used for the drag coil. The case is attached, through a thermal standoff not shown, to a support cylinder which in turn attaches to the large support cylinder around the array.

The Z-coil for Case 3 is quite different in construction. The physical size and stored energy of the coil are small enough that an adiabatically stable coil can be used, and the design shown in Figure 3.19 is based on the epoxy-impregnated coil technology developed by GE. The 6-strand cabled conductor is layer-wound with glass cloth and metallic shims between layers, as shown in Figure 3-20. After impregnation, the shims are removed, leaving helium flow passages through the winding. The coil modules are then interference fit into a support ring and the entire assembly surrounded by a helium vessel, super-insulation, and vacuum vessel as shown in Figure 3.19. As for Cases 1 and 2, the vessel walls must be non-metallic to eliminate eddy current losses. The coil is attached to external support structure through a circumferential ring as shown.

Magnetic analysis to determine the amp-turns required for fields and gradients was initially performed with the computer program COIL. Again, by making use of symmetry, the requirements can be reduced to calculating the field at a single point in space, usually taken for convenience as one end of the model. The magnetic parameters which result from this analysis are shown in Figure 3.21.

The Z-coils must supply AC fields and gradients to produce forced model oscillation in heave and pitch, as well as dynamic control for these two degrees of freedom. The total maximum rate of current change, as shown in Figure 3.21, is 2×10^5 A/sec. This value is calculated based on the revised assumption for control requirements.

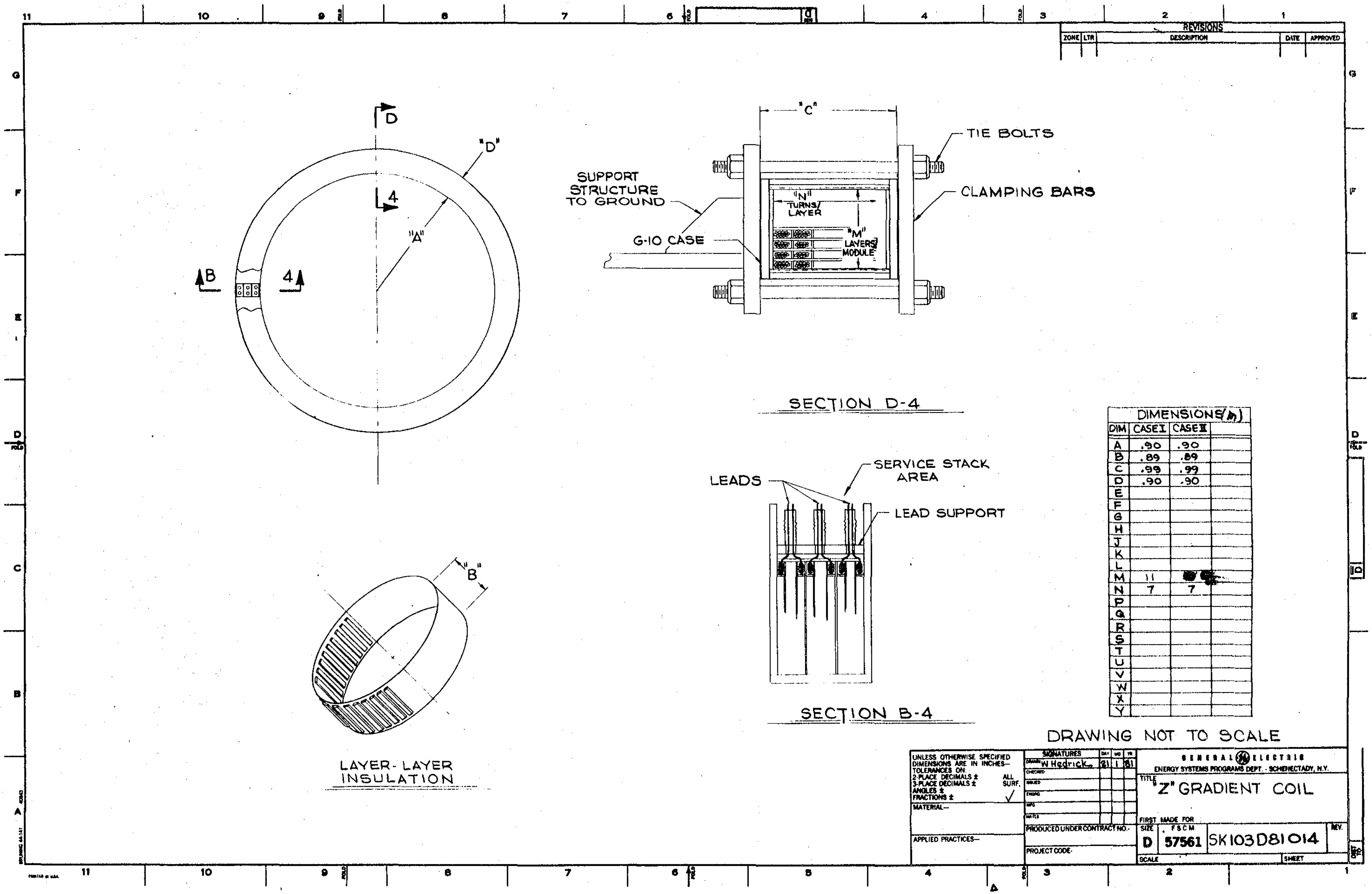

Figure 3.18
"Z" Gradient Coil

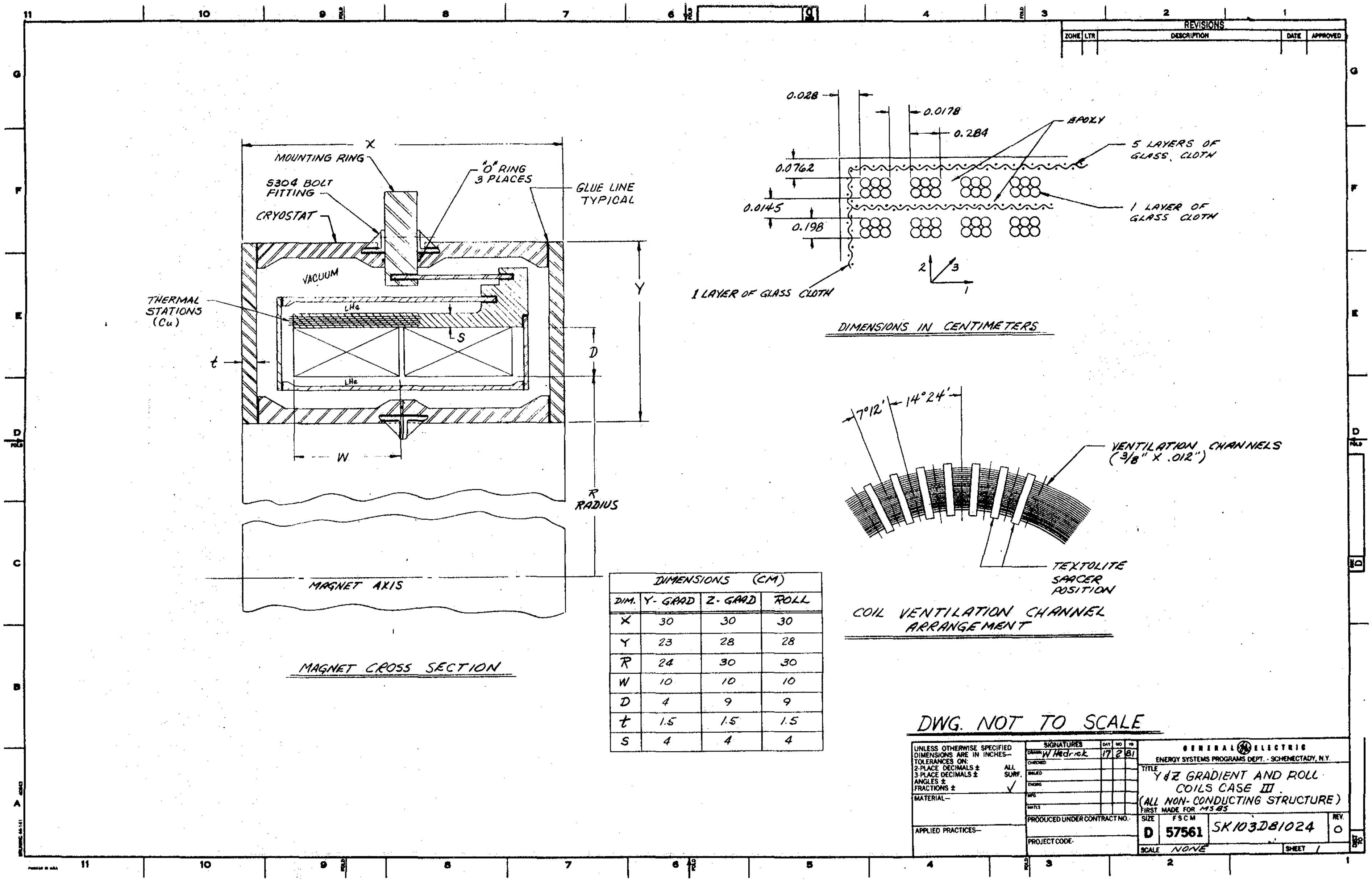

DIMENSIONS (CM)			
DIM.	Y-GRAD	Z-GRAD	ROLL
X	30	30	30
Y	23	28	28
R	24	30	30
W	10	10	10
D	4	9	9
t	1.5	1.5	1.5
S	4	4	4

Figure 3.19
Y&Z Gradient and Roll Coils Case III
(All Non-Conducting Structure)

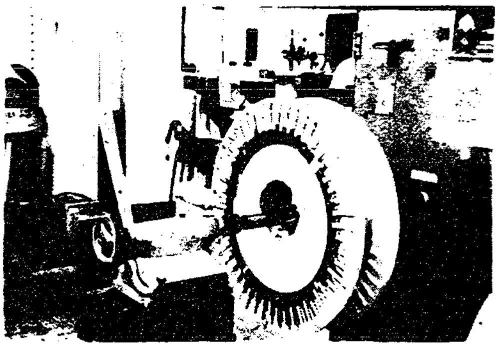

Insulated coil form on winding stand.

Coil winding in progress.

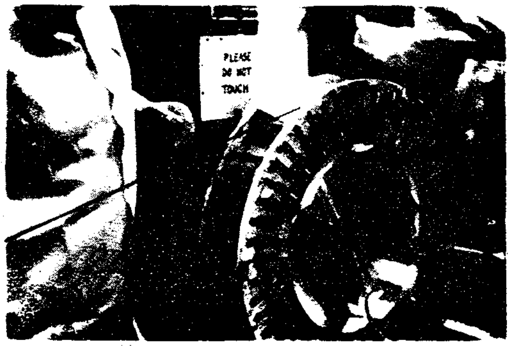

Ventilation shims being added during winding.

Figure 3.20
Coil Winding in Progress

FIGURE 3-21

Z GRADIENT COIL OPERATING PARAMETERS

	CASE 1		CASE 2		CASE 3	
	ALTERNATE E	ALTERNATE F	ALTERNATE E	ALTERNATE F	ALTERNATE E	ALTERNATE F
NUMBER OF COILS	4	4	4	4	4	4
MODULES/COIL	3	1	1	1	2	1
AMP. TURNS/MODULE (10^6A)	3.7	11.1	3.2	3.2	.40	.40
OPERATING CURRENT (kA)	50	50	50	50	.75	.75
WINDING CURRENT DENSITY (A/cm²)	1500	1500	1500	1500	9000	9000
PEAK FIELD (T)	7.7	7.7	3.0	3.0	6.5	6.5
STORED ENERGY (MJ)	148	148	24	24	1.4	1.4
$(dI/dt)_{max}$ (A/sec)	2×10^5	3.2×10^3	5.0×10^5	3.5×10^3	900	46
PEAK VOLTAGE/MODULE (kV)	8.0	.384	4.8	.033	2.25	.23
PEAK REACTIVE POWER/COIL (MW)	1200	19.2	240	1.7	3.4	.17
PEAK AC LOSSES/COIL (w)	29000	1000	12000	400	250	1.5
DISCHARGE VOLTAGE (v) (T_{max} = 200K)	200	200	32	32	620	620

The inductive voltages which result from this rapid change in current are extremely large, as indicated in Figure 3.21. In order to limit the terminal voltage for Case 1 to 10 kV, it is necessary to divide the coil into three modules. For Case 2, one module is sufficient. For Case 3, the voltage across the coil is $\sim$ 4500v. However, the voltage on the epoxy-impregnated winding must be limited to $\sim$ 2000v based on previous experience. Two modules are therefore required.

The AC losses for these coils were estimated by the methods described in the previous section. The losses during simultaneous use of all forced oscillation modes is very large, as shown in Figure 3.21 and correspond (for Case 1) to the boiloff of about 15 ℓ/sec of liquid helium (about 1% of the He volume in the coil) and the generation of about 100 ℓ/sec of vapor at 4.2K. This appears tolerable from a conductor stability point of view as long as good ventilation is maintained, but the loss rate should be checked by testing since it is not amenable to exact analysis, and it places a significant load on the cryogenic system.

Figure 3.21 also shows design and analysis results for a modified version of Cases 1 and 3 in which forced oscillation rates are reduced. As expected, the coil voltage, reactive power, and AC losses are reduced dramatically, making Alternative F very attractive with respect to power supply and cryogenic requirements. The same benefits apply to Alternative G since, as discussed earlier, elimination of forced model oscillation offers reductions in the above parameters slightly better than Alternative F.

3.3.6 Y-Gradient Coils

The Y-gradient coils, like the Z-coils, produce both fields and gradients. They supply static and dynamic lateral forces and yaw torques. For Cases 1 and 2, pie-wound horizontal axis coils are used, as shown in Figure 3.22. These coils are much smaller than the Z-coils because of the smaller lateral force and torque requirements. The design of the coils is similar to the magnetization and drag coils previously described, and the coils are supported in the same way as the Z-coils. For Case 3, an adiabatically stable coil identical in design but smaller in size than the Case 3 Z-coil is used. Its dimensions are given in Figure 3.19.

Figure 3.23 lists the electrical parameters for the Y-coils, which were derived as described in the previous section. The peak voltage, reactive

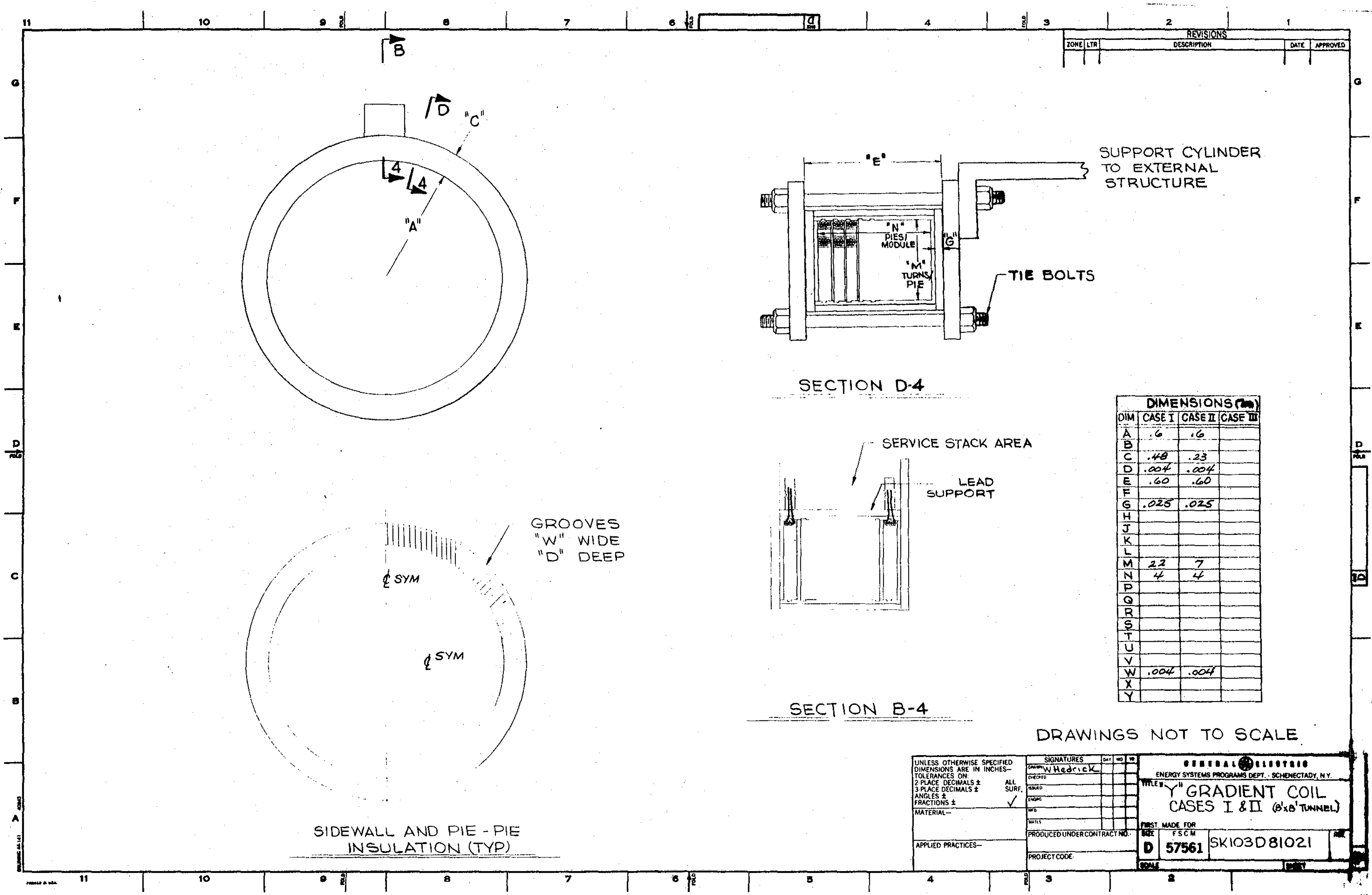

DIMENSIONS			
DIM	CASE I	CASE II	CASE III
A	.6	.6	
B			
C	.48	.23	
D	.004	.004	
E	.60	.60	
F			
G	.025	.025	
H			
J			
K			
L			
M	22	7	
N	4	4	
P			
Q			
R			
S			
T			
U			
V			
W	.004	.004	
X			
Y			

Figure 3.22
"Y" Gradient Coil Cases I&II

FIGURE 3-23

Y GRADIENT COIL OPERATING PARAMETERS

	CASE 1		CASE 2		CASE 3	
	ALTERNATE E	ALTERNATE F	ALTERNATE E	ALTERNATE F	ALTERNATE E	ALTERNATE F
	Full Forced Oscil-ation Freq. Control .1% Control Derived from Simulation	10% Forced Oscila-tion Freq. .1% Con-trol Derived from Simulation				
NUMBER OF COILS	4	4	4	4	4	4
MODULES/COIL	1	1	1	1	1	1
AMP. TURNS/MODULE (10^6A)	4.4	4.4	1.4	1.4	.40	.40
OPERATING CURRENT (kA)	50	50	50	50	1.4	1.4
WINDING CURRENT DENSITY (A/cm^2)	1500	1500	1500	1500	20000	20000
PEAK FIELD (T)	5.0	5.0	2.0	2.0	5.0	5.0
STORED ENERGY (MJ)	14	14	2.7	2.7	.7	.7
$(dI/dt)_{max}$ (A/sec)	1.1×10^5	3.1×10^3	2.0×10^5	3.2×10^3	900	42
PEAK VOLTAGE/MODULE (kV)	1.2	.036	.220	.003	.66	.03
PEAK REACTIVE POWER/COIL (MW)	61	1.9	11	.2	.36	.04
PEAK AC LOSSES/COIL (w)	2900	130	940	31	90	.25
DISCHARGE VOLTAGE (v) (T_{max} = 200K)	20	20	3	3	500	500

power, and AC losses are all considerably smaller than for the Z-coil because of the smaller physical size and lower dI/dt.

3.3.7 Roll Coils

The roll coils supply a field which produces a roll torque on the model. An array of eight coils as suggested by Britcher et al[3] was adopted after a very brief review of possible approaches[8,9] indicated that this approach, which requires the use of magnetic cores along the length of the wings, was the only one which appeared to be capable of generating the required moments. The roll coils are similar in construction to the other coils in the system. For Cases 1 and 2, the coils are pie or layer wound with 50 kA conductor and insulation identical to that used for the other coils as shown in Figure 3.24 The case and coil support structure concepts are also identical. For Case 3, the roll coils are epoxy-impregnated ventilated coils identical in design to the Case 3 Z and Y coils, as shown in Figure 3.19. The principal difference in the roll coil concept is the variety of service stack orientations needed to maintain proper lead cooling and removal of helium vapor. The roll coils are attached to the external support structure through thermal standoffs and crylindrical supports like the Z and Y coils.

In the present configuration, six of the coils are pie wound, while the two coils on the top and bottom of the system, adjacent to the Z-coils, are layer wound to achieve good helium ventilation. An alternative which has not been investigated but which appears feasible is a 22.5 degree rotation of the system, which would allow all eight coils to be pie wound and still maintain adequate helium ventilation. This would reduce the cost of design and manufacturing somewhat by making all eight coils identical.

The roll coils represent perhaps the most difficult magnetic design task in MSBS. The use of a fully symmetric system minimizes coupling with other torque and force modes in the system, but results in a relatively inefficient use of the magnetic wing cores because both the magnetizing and through-wing fields drop to very small values near the model fuselage. Moreover, the roll coils are located at such a large distance from the model that the maximum net magnetization and through wing fields at the model wing tips are only about 48000 A/m and 41600 A/m respectively. The former value is much too low to assure saturation of the wing cores, even at the tips. However, further increases in these values are difficult to achieve practically because the

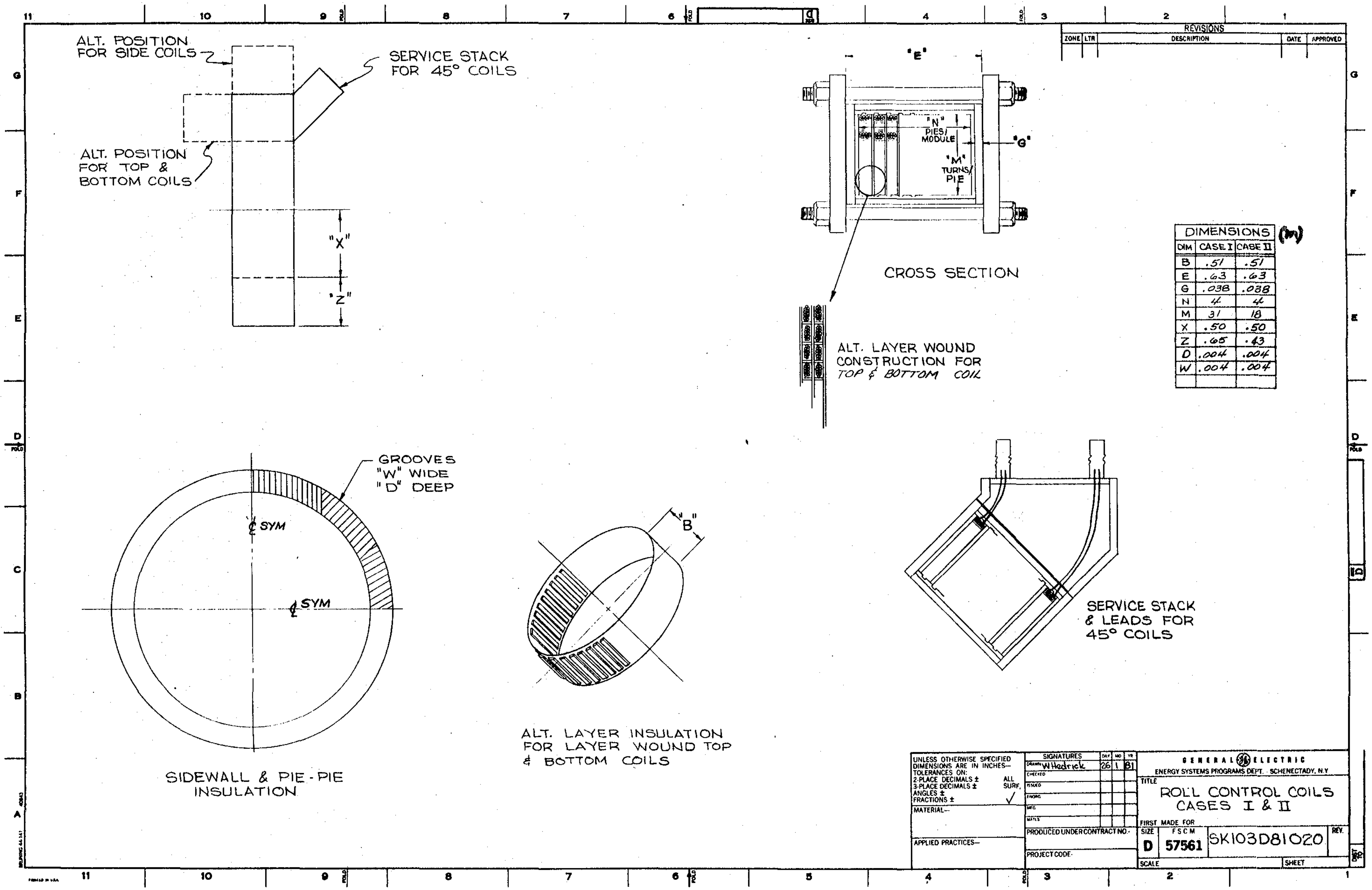

DIM	CASE I	CASE II
B	.51	.51
E	.63	.63
G	.038	.038
N	4	4
M	31	18
X	.50	.50
Z	.65	.43
D	.004	.004
W	.004	.004

Figure 3.24
Roll Control Coils Cases I&II

roll coils are near their peak allowable field and an increase in amp-turns would require a reduction in overall current density and a significant increase in the size of the coils. This problem is aggravated by the fact that the outside diameter of the coils cannot be increased, since coils have little clearance at their OD in the present configuration, and adding amp-turns at the far end of the coil is relatively inefficient. Such a change would also force a rearrangement and increase in size of the magnetization and drag coils to avoid mechanical interferences.

The non-uniformity of the magnetizing field along the wing cores makes magnetic analysis and design difficult. Within the limited scope of the present study only a greatly simplified analysis could be performed. This analysis was based upon the following assumptions:

- The entire cross-section of the model wing was available for magnetic core material.
- The wings occupy 75% by length of the total wing span.
- The wing is relatively thick ($\sim$ 10% - 12% of the mean chord).
- The wing magnetic core can be approximated by an ellipsoid of the same dimensions to calculate the demagnetizing factor. The resulting demagnetization factor along the length, for length $\simeq$ width and thickness $\simeq$ 11% of length, is about .11[14].
- The volume-average magnetization in the wing cores is 1/4 Ms ($\sim$ .5T). This is based on a simple analysis of the magnetization curve for pure iron (Figure 3.3), assuming $\mu = 10^4$ for low fields.
- The torque can be calculated based on the product of the average magnetization and the average through-wing field.

The electrical parameters for the selected configuration are shown in Figure 3.25. As indicated, the configuration for Case 3 is presently unacceptable because peak fields greater than 8T occur on the windings. Furthermore, the high inductance of the coil leads to an unreasonably large number of modules to limit the operating voltage to an acceptable value. The elimination of forced oscillation, as indicated, alleviates the voltage problem but obviously does not improve the difficulties with peak field or static torque.

The production of the required roll torques for Cases 1 and 3 is a difficult one and an acceptable engineering solution has not yet been found. Further optimization of the present configuration, with the roll coil array located outside the gradient coils, will produce some improvement but seems

FIGURE 3-25

ROLL COIL OPERATING PARAMETERS

	CASE 1		CASE 2		CASE 3	
	ALTERNATE E	ALTERNATE F	ALTERNATE E	ALTERNATE F	ALTERNATE E	ALTERNATE F
NUMBER OF COILS	8	8	8	8	8	8
MODULES/COIL	1	1	1	1	8	2
AMP. TURNS/MODULE (10^6A)	6.2	6.2	3.6	3.6	.78	3.2
OPERATING CURRENT (kA)	50	50	50	50	.75	.75
WINDING CURRENT DENSITY (A/cm^2)	1500	1500	1500	1500	9000	9000
PEAK FIELD (T)	8	8	5	5	> 8	> 8
STORED ENERGY (MJ)	31	31	18	18	8.0	8.0
$(dI/dt)_{max}$ (A/sec)	2.3×10^4	3×10^3	3.9×10^4	3×10^3	500	45
PEAK VOLTAGE/MODULE (kV)	.575	.075	.082	.006	2.0	.72
PEAK REACTIVE POWER/COIL (MW)	28.8	3.8	4.1	.3	12	1.1
PEAK AC LOSSES/COIL (w)	700	72	200	20	500	5
DISCHARGE VOLTAGE (v) (T_{max} = 200K)	40	40	20	20	3500	3500

unlikely to yield the required values. The most obvious alternative, the placement of the roll coils inside the gradient coils immediately adjacent to the tunnel, will help somewhat but is limited by the fact that as the coils are moved closed to the tunnel, they must be reduced in diameter to maintain the eight-fold symmetry. Use of a high-saturation permanent magnet core could ensure $M \simeq 1T$, which would ease the requirements on the coils, but is subject to fabrication difficulties due to the poor mechanical properties of these materials. Further study of the roll control problem is needed.

3.3.8 Dewar and Support Structure

The dewars and support structure for the MSBS magnetic system provide the liquid helium environment for the superconducting coils with acceptably low heat load, and support the static and dynamic loads on the coils. Preliminary tradeoffs have been performed as described in Sections 3.2.7 and 3.2.8, to select dewar and structure concepts which best satisfy the requirements identified in Section 3.1.4. Materials have been selected for the dewars and support structure based on GE experience on other large superconducting magnets. Structural analysis has demonstrated that design limits have been met.

3.3.8.1 Material Selection

For this project, GE has made use of material evaluations performed for the Oak Ridge National Laboratory (ORNL) Large Coil Program (LCP), MIT's Component Development and Integration Facility (CDIF) magnet, ORNL Elmo Bumpy Torus magnets, and Lawrence Livermore National Laboratory (LLNL) MFTF-B magnets. The evaluations considered the following characteristics:

- Cryostallographic Stability
- Permeability
- Tensile Properties
- Impact Resistance
- Fatigue Strength
- Crack Growth Resistance
- Fracture Toughness
- Fabricability
- Availability and Cost

The materials considered were stainless steels 304, 304L, 316, 316LN, 310S, Kromarc 58, Nitronic 40, Nitronic 30 metals, G-10 polyester reinforced glass, and phenolic resin composites. The choice of base material welding consumables, and welding processes used for fabricating the MSBS metallic structure has been based upon technical requirements and cost. Designing to low stresses allows the choice of low cost, and readily available, AISI 304L austenitic stainless steel plate for the "warm" structure.

Typical mechanical properties* for 304L at 4°K and room temperature are:

		4°K	Room Temp.
Yield strength @ .2% strain (KSI)	=	55	35
Ultimate strength (KSI)	=	240	100
Elongation @ .2% Yield (%)	=	40	40
Reduction in area @ .2% Yield (%)	=	55	55
Charpy impact, V notch (ft-#)	=	50	50

*Note: After completion of this study, a report "Materials for Cryogenic Wind Tunnel Testing" by RL Tobler, National Bureau of Standards, NBSIR79-1624, was obtained. Data and references therein may be beneficial for subsequent design efforts.

Type A286 steel will be used for threaded bar. Type A286 has been chosen for its high strength and good toughness at both room temperature and 4°K and also because of its similar expansion coefficient to austenitic stainless steel.

The choice of coil case, LN_2 shield, interlayer, interturn, and ground wall insulating materials for the MSBS coils is dictated by considerations of electrical properties, fabricability, and mechanical properties at cryogenic temperature. Glass-cloth epoxy laminate (type G-10) has been chosen because it has been extensively used as insulation in both conventional electrical generation equipment and superconducting machinery with good success. Fiberglass reinforced polyester may offer some advantages in fabricability and cost for large sections and could be used as an alternative. G-10 is being used for the CDIF and LCP superconducting magnets to serve both structural and insulating purposes for these magnets where high strength is a primary requirement. Extensive data on this material and other glass cloth reinforced laminates are found in Reference 15.

3.3.8.2 Design Loads

The mechanical loads that ultimately design the MSBS coil system include steady-state and oscillatory magnetic loads, gravity loads, pressure loads, heat loads, thermal and electrical cycling, and transportation and handling. The loads used in the analysis discussed in this report were magnetic loads, pressure loads, cyclic effects on fatigue. Transportation and handling loads have not been considered at this time because, in general, fixtures can be designed and procedures written that will limit the loads. Figure 3.26 shows the net forces on the coil system for Case 1 peak lift condition. Figure 3.27 shows the in-plane and out-of-plane loads for coil 6, lower downstream Z gradient coil, for the Case 1 peak lift conditions. Data similar to that shown in Figure 3.27 can be plotted for all 12 coils shown in Figure 3.30. The forces required to oscillate the model were calculated for Case 1 peak lift conditions. These forces, similar to Figure 3.26 were used to calculate cyclic stresses in support structure.

The loads for Case 2 are about 10% of Case 1 for the gradient coils and about 50% for drag and magnetization coils. The loads for Case 3 are about 50% of Case 1.

3.3.8.3 Analysis Approach

The structural analysis approach combined simplified finite element models with hand calculations of published formulae. The design iteration was one which began with conventional thick walled metal coil cases which were thinned down while being reinforced with G10 until the case wall was entirely non-metal. The liquid nitrogen (LN_2) thermal shield and vacuum vessel followed the same pattern. These design iterations were principally a result of efforts to reduce the eddy current losses.

The coil case wall thicknesses were determined by considering the side wall to be a uniformly loaded circular plate with a concentric hole and the outer ring as a uniformly loaded long narrow rectangular plate. In past experience, similar approximations were made for the coil designed for the Oak Ridge Large Coil Program (LCP), and compared to the LCP finite element results and found to be a reasonable approximation. The wall thicknesses for the all stainless steel 304L coil case are given in Figure 3.28. When the case walls were reduced in thickness to lessen the eddy current effects, the case was reinforced with G-10 and side wall stiffeners and tie rods. The coil case wall thicknesses for this design are shown in Figure 3.29.

3.3.8.4 Structures Concepts

A trade-off between a tubular truss and a cylinder for supporting the Y and Z gradient coils was made using Case 1 peak lift loads and the sinusoidal

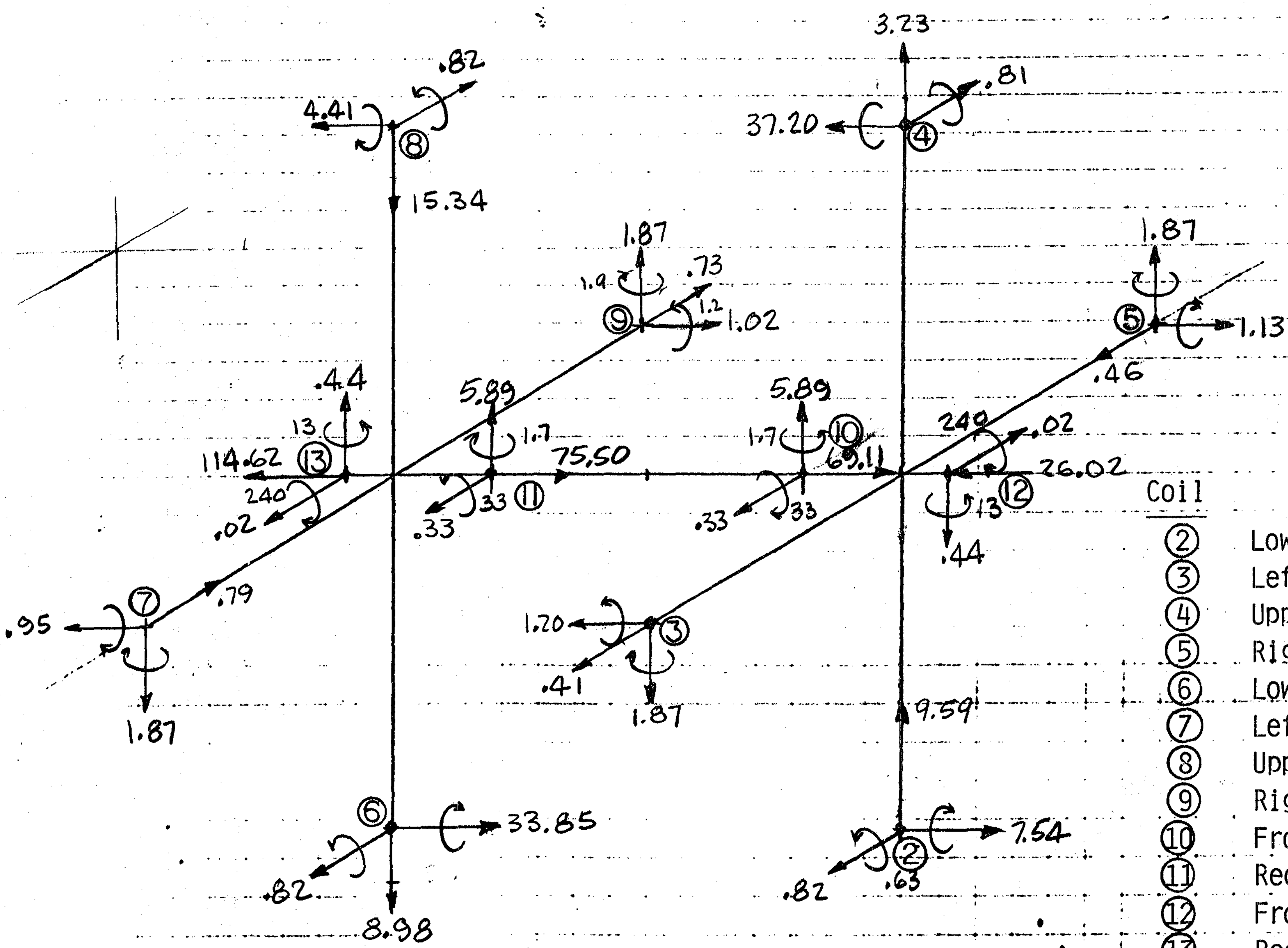

Coil	Ident
②	Lower Front Z
③	Left Front Y
④	Upper Front Z
⑤	Right Front Y
⑥	Lower Back Z
⑦	Left Back Y
⑧	Upper Back Z
⑨	Right Back Y
⑩	Front Mag.
⑪	Rear Mag.
⑫	Front Drag
⑬	Rear Drag

Fig. 3.26. Case I Peak Lift Forces and Moments

Forces-MN; Moments-Mn-m

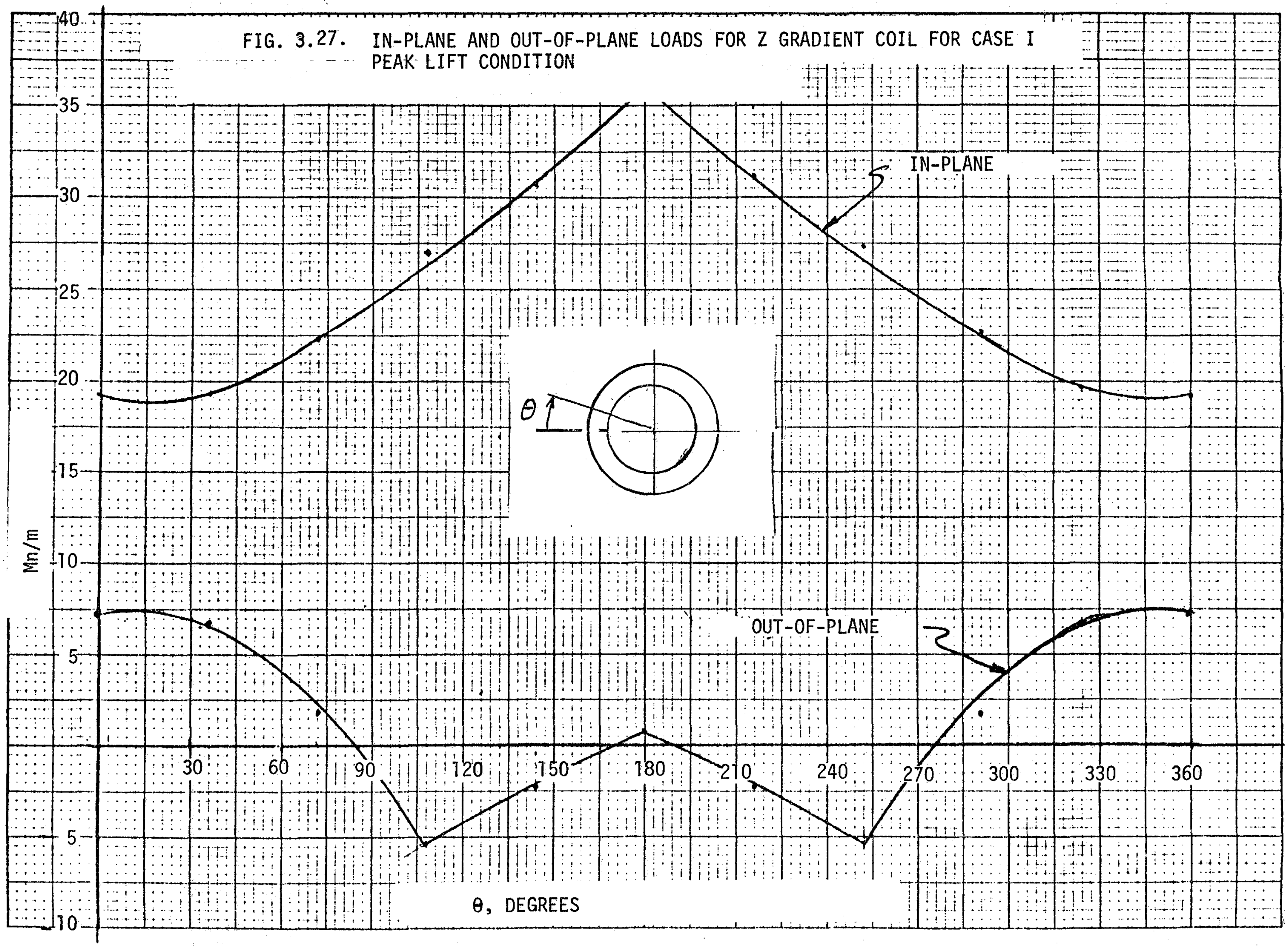

FIG. 3.27. IN-PLANE AND OUT-OF-PLANE LOADS FOR Z GRADIENT COIL FOR CASE I PEAK LIFT CONDITION

Figure 3.28

COIL CASE WALL THICKNESS FOR 304L CASE I LOADS

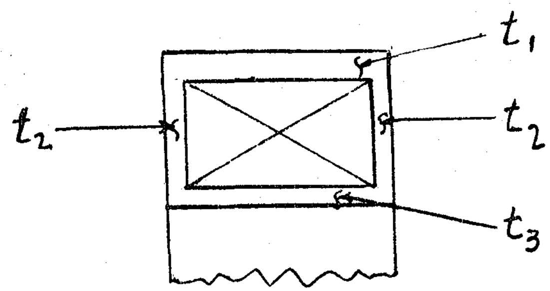

	Case 1			Case 2			Case 3		
COIL	t_1	t_2	t_3	t_1	t_2	t_3	t_1	t_2	t_3
Drag	1.375	1.0*	1.0	1.0	1.0*	1.0	.75	.5*	1.0
Mag.	1.375	1.0*	1.0	1.0	1.0*	1.0	.75	.5*	1.0
Z Grad.	1.25	.75	1.0	.625	.50	1.0	NA	NA	NA
Y Grad.	.5	.5	.5	.375	.375	.500	NA	NA	NA
Roll	1.25	.75	1.0	.625	.50	1.0	NA	NA	NA

inches

*Also requires rib stiffeners

Figure 3.29

COIL CASE WALL THICKNESS FOR THIN 304L WITH G-10 REINFORCEMENT OR G-10 ALONE

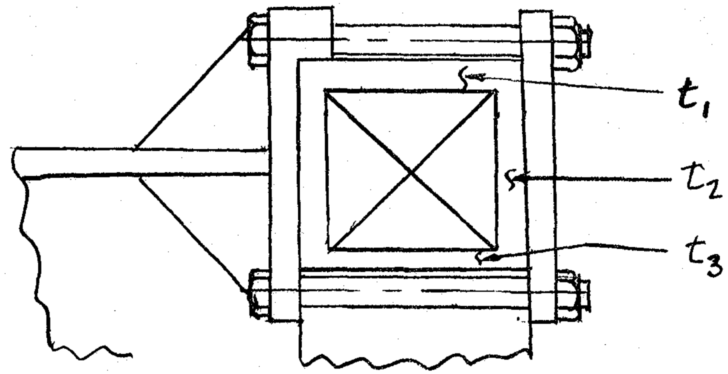

	Case 1			Case 2			Case 3		
COIL	t_1	t_2	t_3	t_1	t_2	t_3	t_1	t_2	t_3
Drag	3	2	2	2.0	1.5	1.5	1.0	.75	1.0
Mag.	3	2	2	2.0	1.5	1.5	1.0	.75	1.0
Z Grad.	2.0	1.5	1.5	1.5	1.0	1.0	NA	NA	NA
Y Grad.	2.0	1.5	1.5	1.5	1.0	1.0	NA	NA	NA
Roll	2.0	1.5	1.5	1.5	1.0	1.0	NA	NA	NA

inches

requirement. A simple finite element model was constructed using the case thicknesses shown in Figure 3.28 and a tubular member having 2 sq.in. cross section for supports. The static deflections and internal loads were calculated as well as the natural frequencies. The results indicated the truss was very highly stressed but it was stiff enough to meet the oscillation requirement. The support was iterated for a cylinder and sized to accommodate the static loads. The wall thickness for the support on the Y gradient coil is 3/4" and 1/2" for the Z gradient coil.

The support for the magnetization and drag coils is dictated by the forces shown in Figure 3.26. Coils 11 and 13 will require a tension member as well as individual structure for the modules. The initial structure was a 1-5/8" thick cylinder between coils and a cylinder having stiffeners on the down stream side of the rear drag coil. This was replaced with 160-3" dia. tie bolts on the outside and segmented 1-5/8" thick plate structure on the inside for supporting the gradient coils in order to reduce the eddy current effects. The structure between magnetization coils is subjected to a tensile load and exposed to atmospheric condition, therefore, the concept is a 3/4" thick 304L cylinder having ring flanges to accommodate the tie bolts and provide support to side wall of the coils. The structure between the front magnetization and drag coils is subjected to a compressive load. This structure was initially a 304L cylinder 7/8" thick having flanges and stiffeners to distribute the load to side walls of the coils. This was replaced with 160 1-1/2" dia. tie bolts on the outside diameter and segmented 7/8" thick structure on the inside diameter for supporting the gradient coils.

The coil system support to ground are pads bolted to a foundation, Fig. 3.30. The pads were sized for the loads shown in Figure 3.26 and are attached to ambient structure.

In general, vacuum vessels encase individual or sets of coils, Fig. 3.31. The vacuum vessel surrounding Z gradient coils 2 and 6 or coils 4 and 8 has long flat sides which are reinforced with ribs in order to reduce the unsupported length. The vacuum vessels for the remaining coils are short circular cylinders subjected to external pressure. These vessels are SS304, but, because of the eddy current losses, a non-metallic vessel is necessary. The thicknesses for the various size vessels are shown in Fig. 3.31.

The magnet concept for Case 3, Fig. 3.19, is quite different from Cases 1 and 2. In the Case 3 concept, the gradient magnet coil, thermal resistant

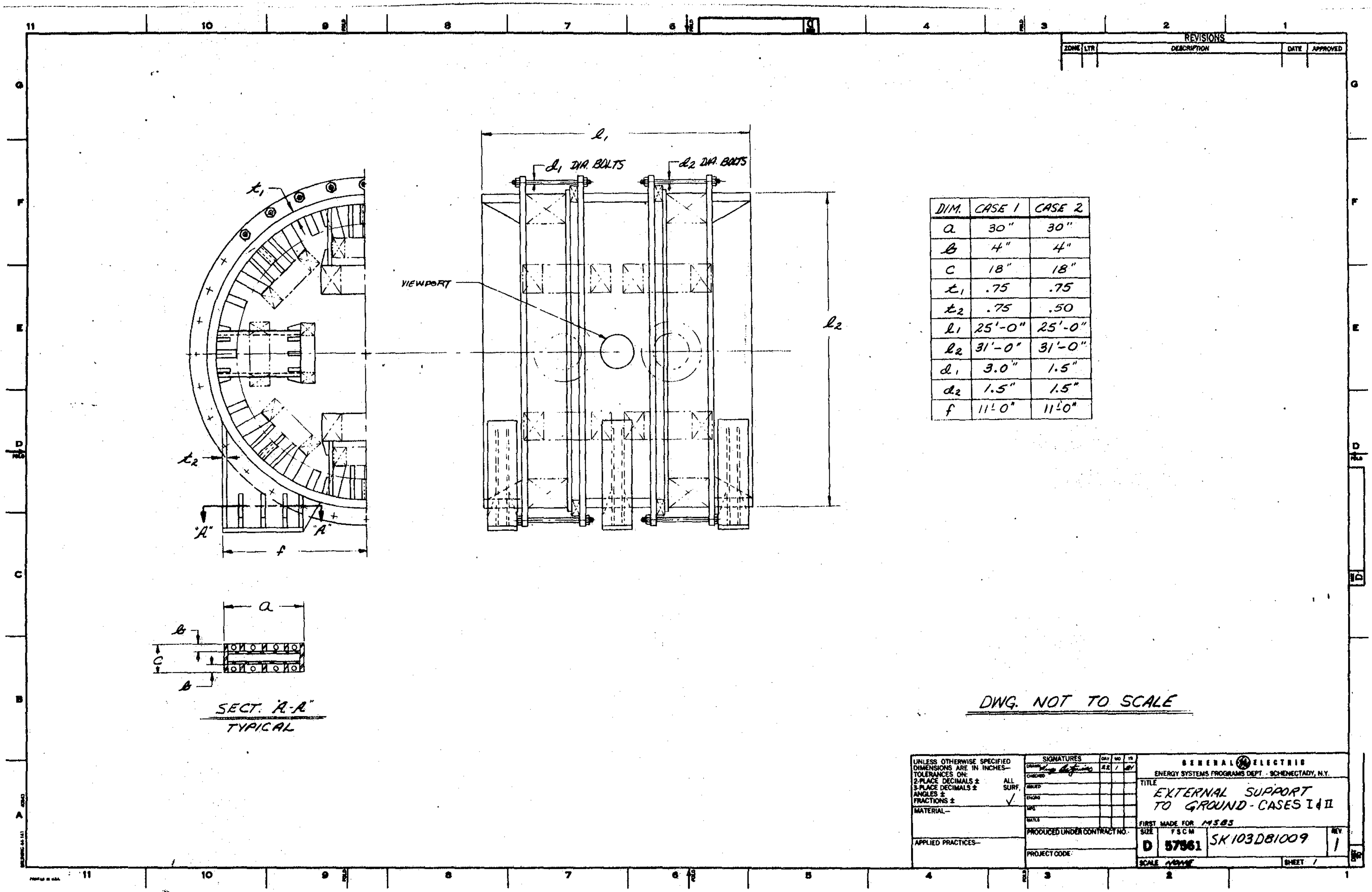

DIM.	CASE 1	CASE 2
a	30"	30"
b	4"	4"
c	18"	18"
t_1	.75	.75
t_2	.75	.50
ℓ_1	25'-0"	25'-0"
ℓ_2	31'-0"	31'-0"
d_1	3.0"	1.5"
d_2	1.5"	1.5"
f	11'-0"	11'-0"

Figure 3.30
External Support to Ground-Cases I&II

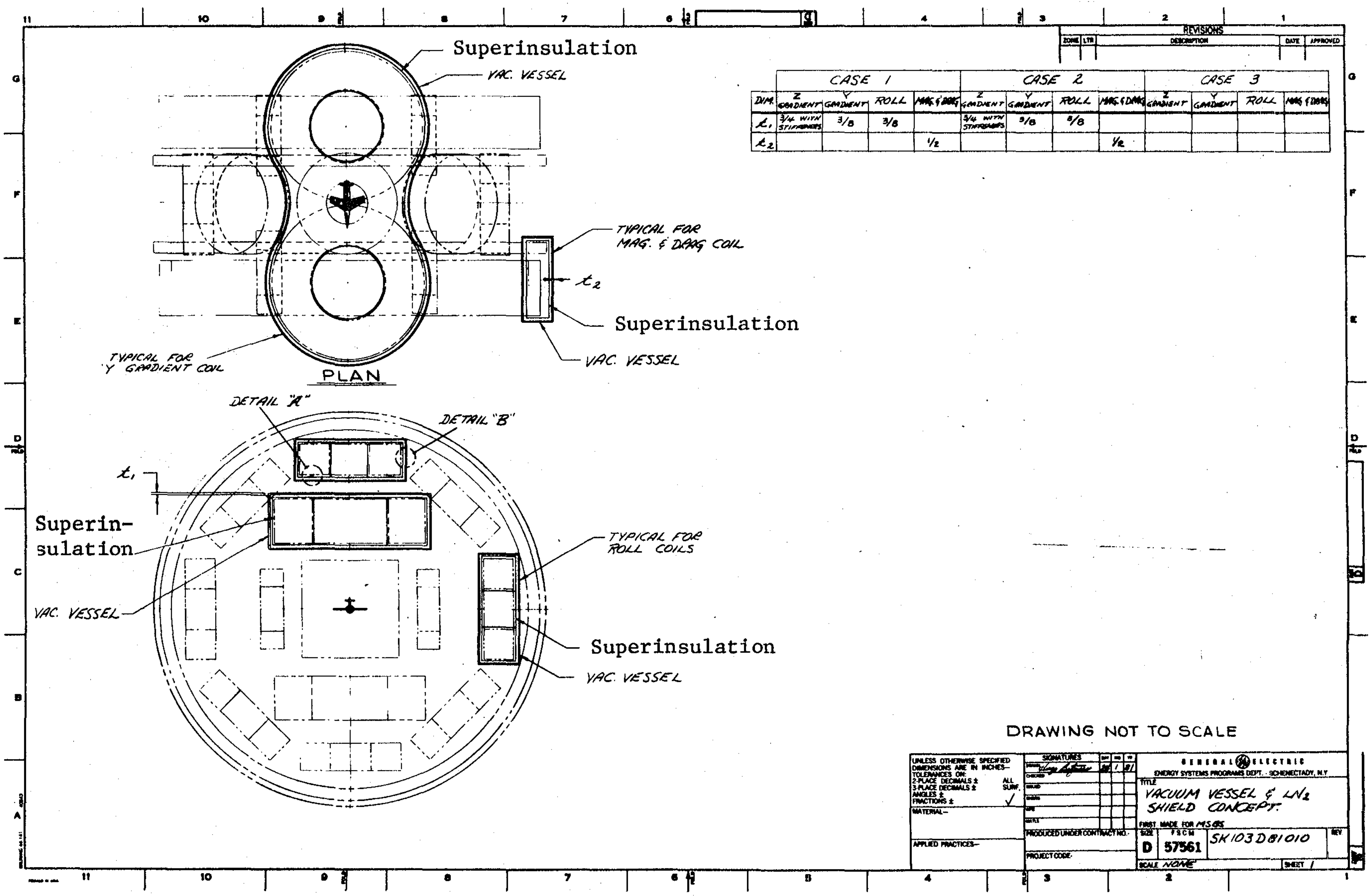

	CASE 1				CASE 2				CASE 3			
DIM.	Z GRADIENT	Y GRADIENT	ROLL	MAG & DRAG	Z GRADIENT	Y GRADIENT	ROLL	MAG & DRAG	Z GRADIENT	Y GRADIENT	ROLL	MAG & DRAG
t_1	3/4 WITH STIFFENERS	3/8	3/8		3/4 WITH STIFFENERS	3/8	3/8					
t_2				1/2				1/2				

Figure 3.31
Vacuum Vessel Concepts

path and vacuum vessel are all contained in a compact package. These coils have a mounting ring on the outside diameter which will have bolt holes for attaching at assembly. The support for the magnetization and drag coils is similar to Cases 1 and 2. There will be 100-1" dia. tie bolts on the outside and segmented 1/2" thick on the inside. The support structure for magnetization to magnetization coil support and roll coil support is an octagon having a roll coil mounted to each face and magnetization coil at each end. The analysis approach is to consider the minimum material between adjacent roll coils as being effective in carrying load and perform hand calculations to determine the required thickness. This method led to 1/2" plate with local reinforcement for the octagonal structure.

The support for the gradient coil is rectangular structure reinforced with beams and bulkheads for stiffening the corners. The analysis approach is to assume the reinforcing beams carry all the bending loads and bulkheads distribute the shear loads. The beams will be 10" deep and 5" wide and the bulkhead will be 1/4 plate with angle stiffeners.

The coil case concept for Cases 1 and 2 and Case 3 drag and magnetization coils is a two "L" shaped piece arrangement. One piece will be used to wind the conductor on and the other piece will be used to close the case. There will be two closing joints diagonally opposite each other. The closing joint concept is a torque and groove which will provide a shear transfer between the case walls. The joint will be glued and reinforced with aluminum banding around the outside. Additional stiffening is gained when the magnet is installed in its supports by the clamping action of the bar and tie rods. Non-metallic dewars will have greater H_e leakage and the vacuum pump for the magnets vacuum vessel will have a duty cycle greater than that required for metallic dewars.

The gradient and roll coil concepts for Case 3 are epoxy-impregnated coils, Fig. 3.19, supported by a cylinder attached to a mounting ring. All materials are non-metal except the conductor. The vacuum vessel and He vessel are made from cylinders and rings glued together. The vacuum vessel is made in two pieces and bolted together and sealed with an "O" ring. The short cylinder between mounting rings transfers in-plane and out-of-plane loads to the exterior mounting surface. The heavy ring around the coils will thermally insulate the coil in the radial direction. Thermal stations made of copper strips are included in ring at various radii. One end of the thermal finger will be immersed in LHe which will absorb the heat.

The concept for supporting the gradient and roll magnets for Cases 1 and 2 utilizes a segmented interface having a shear restraint and gusset attached to a cylindrical support and clamping bars and tie rods, Fig. 3.32. The segmented interface and clamping bars are used to reduce eddy current losses. The cylindrical barrel for the gradient coil is attached to the inside diameter of the drag to magnetization coil structure. The roll coils are too close to the inside diameter of the magnetization to magnetization coil structure to permit a cylindrical support, therefore, gussets are being proposed. The concept for the drag to magnetization coil and magnetization to magnetization coil support structure is similar to the gradient coil except the inside diameter connection will be segments of stiffened plate which will be used to support the gradient and roll coils. The structure at the ends of the drag coils and between the magnetization coils will have saddle support feet to mount the magnet system to a foundation.

The concept for supporting the magnets for Case 3 is shown in Fig. 3.33. There is a separate structure for the magnetization, drag and roll coils and another structure for the gradient coils. The magnetization and drag coil being made of G-10 will use tie rods similar to Cases 1 and 2. The structure between magnetization coils is an octagon having flanged ends to butt to the magnetization coils and ribbed faces for the roll coils. The Y and Z gradient coils are located in position that requires a separate structure of stiffened plate and reinforcing beams. The coils are mounted to a plate that is stiffened with bulkheads and supported by beams mounted to the end cylinders of the outer structure.

The concepts considered for the vacuum vessel for Cases 1 and 2 were either one large enclosing system or individual vacuum vessels. The large enclosing vacuum vessel concept is similar to that for GE's magnet for the Component Development and Integration Facility, which has eight individual high thermal resistant supports between the vacuum vessel and the cold mass, an inner wall surrounding the tunnel and end transition pieces. This concept was rejected for MSBS because of the need for high thermal resistant supports, the complex system of steady-state loads resisted by the thermal supports and the gravity loads. Also, accessibility and maintenance of the coils becomes more difficult. The concept proposed, Fig. 3.31, is an individual vacuum vessel for Y gradient and roll coils, a vacuum vessel for pairs of Z gradient and drag and magnetization coils. The material is non-conducting, such as G-10, because of the eddy current losses. There will be numerous joints due

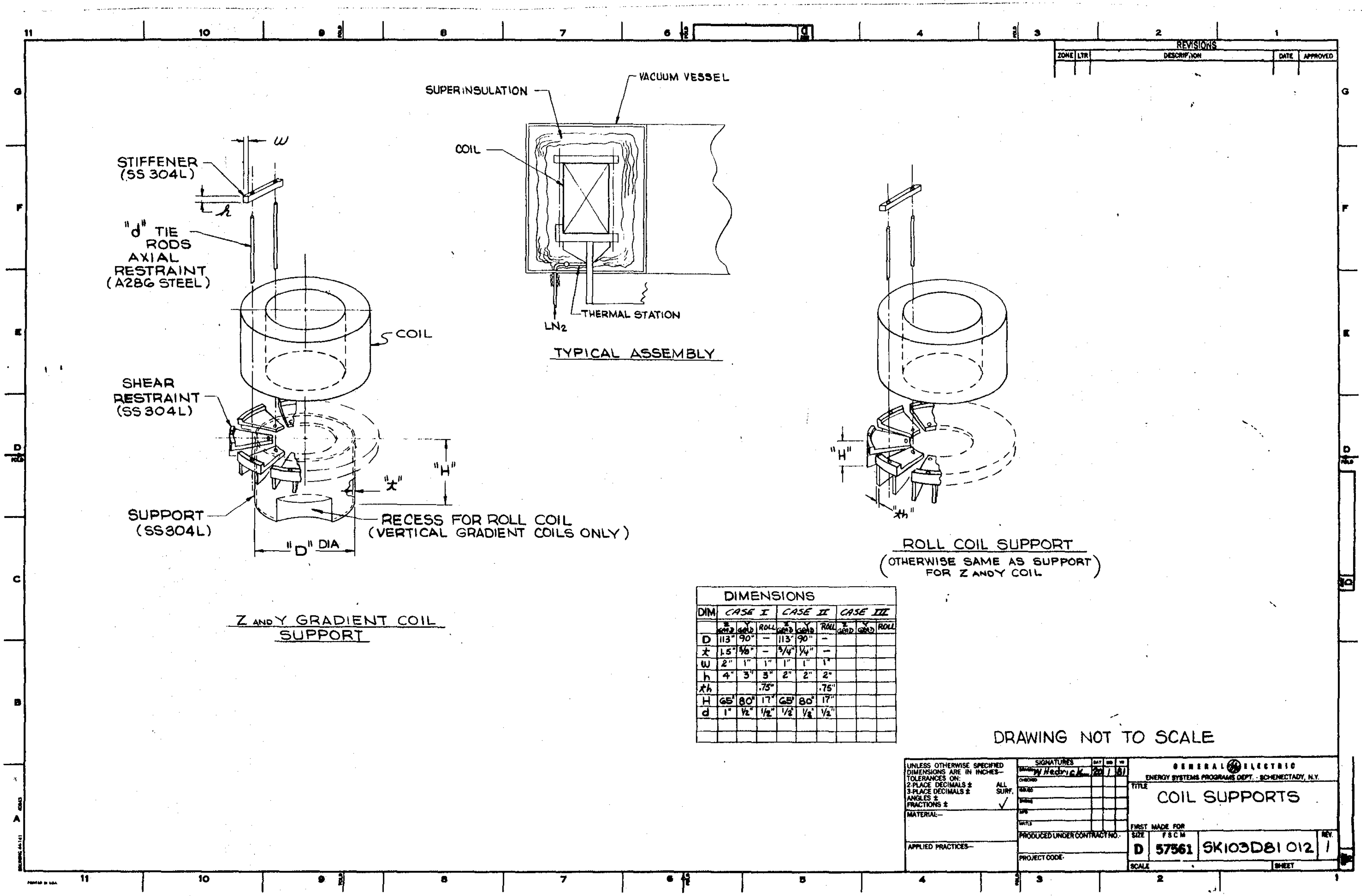

DIMENSIONS

DIM	CASE I			CASE II			CASE III		
	Z GRAD	Y GRAD	ROLL	Z GRAD	Y GRAD	ROLL	Z GRAD	Y GRAD	ROLL
D	113"	90"	—	113"	90"	—			
t	1.5"	3/8"	—	3/4"	1/4"	—			
w	2"	1"	1"	1"	1"	1"			
h	4"	3"	3"	2"	2"	2"			
th			.75"			.75"			
H	65"	80"	17"	65"	80"	17"			
d	1"	1/2"	1/2"	1/2"	1/2"	1/2"			

Figure 3.32
Coil Supports

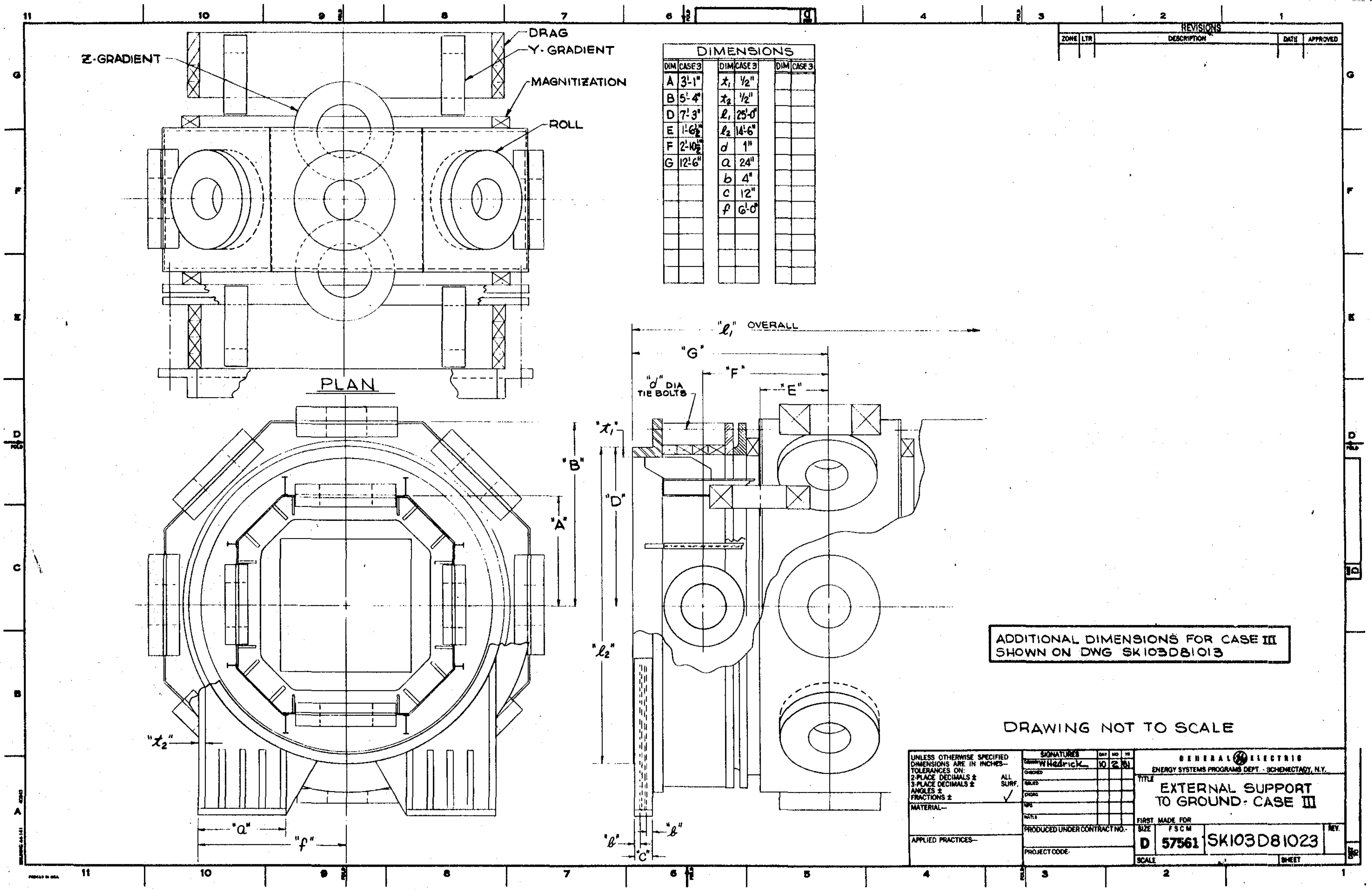

Figure 3.33
External Support to Ground-Case III

to penetrations by the gradient coil supports. The closure concept for these joints utilize bolted connections having vacuum tight seals.

The concept for reducing heat transferred into the magnet coil case for Cases 1 and 2 is a combination of superinsulation and liquid nitrogen (LN_2) shield. Superinsulation will be used on the gradient coils because their support penetrates the vacuum vessel containing the drag coils and magnetization coils, and is attached to the cold intercoil support. Roll coils will use a LN_2 shield and thermal stations to intercept the heat flow in the coil support. The drag coils and magnetization coils will also use an LN_2 shield for the same reasons as the roll coils.

3.4 TECHNICAL RISKS

The use of "state-of-the-art" technology and the imposition of reasonable design limits in all key areas combine to make the overall technical risk in the magnet system relatively low. Performance failures in previous superconducting magnets have been traced to a number of causes including:

- conductor instability
- damage due to voltage breakdown and arcing
- gross structural failures
- inability to cool down or fill with helium due to vacuum/ cryogenic failures

The third of these are relatively straightforward engineering concerns which can be dealt with effectively through careful analysis using finite element techniques and adherence to proper design standards and will not be a concern for MSBS.

The problem of conductor stability has achieved a great deal of attention because of its fundamental impact on magnet performance and cost. Although the fundamental physical mechanisms of stability are not yet completely understood, design principles have been developed based on a combination of analysis and experiments on conductors and winding sections. In the case of MSBS, the conductor has been designed to satisfy the most conservative of the existing stability criterion, full cryogenic stability, which allows recovery from virtually any disturbance. The relatively open structure of the conductor and winding assures adequate venting of helium vapor and replenishment of liquid helium to maintain heat transfer. The stability of the conductor has been demonstrated experimentally through tests of both conductor components and the full-scale conductor in the winding configuration. Finally, performance data on the 20 MJ ohmic heating coil in which the 50 kA conductor is used will be available in about two years and will serve as final verification of the conductor well in advance of the fabrication of the MSBS coils. Thus, the risk of performance failures due to conductor instability is very low.

The other two areas, voltage breakdown and vacuum/cryogenic failures, are of some concern for MSBS and will be discussed in more detail.

3.4.1 Voltage Breakdown

Superconducting magnets must be exposed to inductive voltages during discharge as a result of some malfunction. The discharge voltage tends to be driven to high levels for large magnets as a result of

- the economic incentive to design at high current densities
- the need to keep the maximum temperature during a discharge low to prevent excessive thermal stresses and damage to the winding
- the difficulty of detecting normal zones in large magnets, which can result in a normal zone reaching a temperature significantly above 4.2°K prior to the initiation of discharge.

In the MSBS coils, the use of a high operating current (50 kA for all except the Case 3 Z, Y, and roll coils) is relatively effective in limiting the discharge voltage to modest values (a few hundred volts or less) which should not be of concern.

However, the rapid changes in current required to produce the specified forced oscillation modes result in very large inductive voltages, for larger than the discharge voltage, and create the possibility of damage due to breakdown and arcing within the winding. The 20 MJ ohmic heating coil is being designed for a peak terminal voltage of 10 kV, and this value has been chosen as a design limit for MSBS as described in Section 3.1.3. The design of the 20 MJ coil is based on well-known data for the breakdown voltage of helium vapor at low temperatures and incorporates substantial factors of safety(1). These design approaches will be verified by the testing of the 20 MJ coil and will be incorporated into the MSBS coils to the maximum extent possible.

However, it is also well known that the breakdown voltage of helium, like any dielectric medium, can be substantially reduced as a result of

- pointed or irregular surfaces which cause inhomogeneous electric fields
- chemical impurities
- physical impurities such as dust, metal whiskers, etc.

It is virtually certain that the design of the MSBS coils will differ in some respects from that of the 20 MJ coil. Any departures from that design must be carefully evaluated as potential sites for voltage breakdown, and testing would be advisable to verify performance in any areas where doubt exists. Current and instrumentation leads and separations between pancakes or layers, all of which can develop high voltages over small physical distances, are of particular concern.

During manufacture of the coil, specific QC techniques must be applied to prevent any conditions which might result in reduced voltage capability. Careful inspection of conductor, insulation, and other components would be essential to prevent cracks or surface irregularities. Cleanliness during the winding process to prevent any contaminants from entering the winding would be critical, and specific high-voltage in-process tests would be needed to ensure that proper cleanliness is maintained. Finally, a thorough program of acceptance testing, including hi-pot testing and actual high-voltage operation, would be needed prior to use in the system. These measures do not represent an extension in the present state of the art in superconducting magnet design and manufacture. However, they almost certainly represent a difference in degree requiring extra care and effort.

In summary, an element of technical risk exists for the MSBS coils because of the high voltages required during forced oscillation test modes. This risk cannot be regarded as negligible because, at the present low level of design detail, the applicability of existing design approaches cannot be assured. Specific effort during the design and manufacture of the MSBS coils must be directed at reducing this risk to an acceptably low level.

3.4.2 Vacuum/Cryogenic Failures

The large current ramp rates required for forced oscillatory testing in MSBS force a departure from typical cryostat design techniques using welded or bolted/seal-welded metal vessels to ensure helium tightness. Because the eddy current losses in metal vessels would be intolerably high, the use of non-metallic vessels is necessary. Again, the 20 MJ ohmic heating coil and 30 MJ energy storage coil being developed by LASL are expected to provide basic technology which should be of use on MSBS. However, the requirements for MSBS differ from the 20 MJ requirements in two key respects which tend to limit the direct applicability of the LASL technology and inject an element of technical risk into MSBS. Specific developmental effort will be required in advance of the fabrication of MSBS in order to reduce this risk to an acceptable level.

First, the dewars for the 20 MJ and 30 MJ coils are "pot" dewars, as shown in Figure 3.33, where in the magnet is hung with its axis vertical from a top plate in a cylindrical or annular "pot" of liquid helium. The significance of this is that the seals which maintain helium and vacuum tightness can be made at the top flanges of the pot by relatively conventional techniques such as O-rings. In addition, since access to the bore of the coil is not required, the seals need be made only on the vessel OD.

Most of the coils for MSBS, by contrast, have horizontal axes, and the seals on the helium vessel, which will likely be made of two L-shaped rings joined together after winding, will be directly exposed to liquid helium. O-ring or other pressure-type or mechanical seals cannot be used, and adhesive sealing of some type will be required. This technique has been unsuccessful in the past, probably because of a combination of poor mechanical properties and incompatibility of thermal expansion in the adhesive, and will require development and testing to assure that adequate helium and vacuum tightness can be maintained. Thorough testing of the completed vessels, both at room temperature and at cryogenic temperatures, will also be required to ensure that helium tightness is achieved and maintained.

Secondly, the 20 MJ and 30 MJ coils are operated individually and the electromagnetic forces produced in the winding are reacted internally by support structure in the coil. In MSBS, on the other hand, the coil array produces large, three-dimensional forces and moments on all the coils, and these must be reacted with other coils and/or transmitted to the external support structure. This will require a thermally efficient support mechanism which has sufficient stiffness to carry these loads with acceptable stresses and is compatible with non-metallic dewar construction. A concept to satisfy these requirements through the use of an extension on the non-metallic helium vessel with integral thermal stations is shown in Section 3.3.8. However, development and testing to verify the feasibility of this or some other approach will certainly be required.

The need for non-metallic dewars for the MSBS coils involves an area of technology which has only recently been addressed in a systematic way. Difference in coil configuration and orientation and the need to support large net forces are significant departures from the non-metallic dewar technology presently under development, and significant component development and testing work will be required to reduce the risk presently associated with this problem to an acceptable level.

Section 3 References

1. Heinrich, J.P., et al, IEEE Transactions on Magnetics, MAG-17, 1, P. 634 (Jan. 1981).

2. Covert, E. E., Finston, M. Vlajinac, M., and Stevens, T., Magnetic Balance and Suspension Systems for Use with Wind Tunnels, in "Progress in Aerospace Sciences", Vol. 14 (A74-12203), Oxford and New York, Pergamon Press, 1973, pp. 27-107 (A74-12204).

3. Britcher, C.P., et al, "Preliminary Investigation of Design Philosophies and Features Applicable to Large Magnetic Suspension and Balance Systems," NASA CR-162433 (November 1979).

4. Grover, F. W., "Inductance Calculations", Van Nostrand, New York (1946).

5. Walker, M.S., et al, IEEE Transactions on Magentics, MAG-17, 1, p. 908 (January 1981).

6. Wollan, J. J., et al, IEEE Transactions on Magnetics, MAG-17, 1, p. 842 (January 1981).

7. Sydoviak, S. G., Low Temperature Physics, LT 13, Vol. 4, Plenum Press, New York, p. 607 (1973).

8. Goodyer, M.J., Aeronautical Quarterly, 18, p. 22 (February 1967).

9. Goodyer, M.J., "The Theoretical and Experimental Performance of Roll Control Elements in the Six Component Magnetic Wind Tunnel Balance," ARL 66-0135 (1966).

10. Osborn, J. A., physical Review, 67, 11 & 12, p. 351 (1945).

11. Stone, F.L. and Young, W. C., "Compressive Strength of Glass Fiber Reinforced Composites at Room Temperature, 77°K and 4.2°K, "Proceedings of the 7th Symposium on Engineering Problems of Fusion Research, IEEE Publication 77CH1267-4-NPS, October 1977.

4.0 CRYOGENIC SYSTEM CONCEPT

The cryogenic system required to cool and maintain the magnet coils at the superconducting temperature consists of the helium, nitrogen and vacuum subsystems.

In such a system liquid helium (LHe) is provided from a liquefier plant to a large storage dewar from which the liquid is transferred to the magnet coil cases by gravity feed. During operation of the magnet, when helium is being vaporized by magnet coil heat at a rate greater than the liquefier capacity, the resulting gas is stored at medium pressure for later liquefaction when the tunnel is not operating.

Liquid nitrogen (LN_2) is used in the liquefier heat exchangers to pre-cool the helium, to jacket the liquid helium transfer lines and cool the high current magnet leads where they exit the helium filled coil cases.

A vacuum is maintained in the outer casing of the dewar around the coil cases to provide insulation, which reduces the heat losses from the helium cooled coils. Vacuum jackets are also provided around transfer lines, storage dewars and the refrigerator liquefier.

4.1 REQUIREMENTS

The cryogenic system requirements are summarized in Figure 4.1 and below:

- As in the basic MSBS requirements, all cryogenic system equipment shall be standard off-the-shelf or existing technology.
- Liquid helium at 4.2°K supply temperature at 1 to 2 atm pressure is a standard for maintaining magnet coils at a maximum temperature of 4.4°K.
- Liquid nitrogen at 77°K supply temperature is used to cooldown the helium in the refrigerator/liquefier and for second stage cooling of current leads operating above 25 KA.
- The cryogenic system shall operate 2 hours at 100% of maximum load, 8 hours at 25% of maximum load, out of 24 hours; and 14 hours shall be used to replenish the liquid helium supply.
- Refrigeration and liquefier shall be sized for 24 hour operation as above with the commonly accepted 50% contingency provided in the liquid helium storage.

Figure 4.1

KEY REQUIREMENTS OF CRYOGENIC SYSTEM

- Cryogenic equipment standard and similar to existing equipment
- Liquid helium at 4.2°K
- Liquid nitrogen at 77°K
- Closed loop helium operation
- Magnet cooldown in approximately 7 days
- 24-Hour per day liquefier operation
- Dewar sized for 50% contingency
- Daily helium requirement for 2 hours at 100% operation, 8 hours at 25% operation and 14 hours standby
- Vacuum jacketed liquid and cold gas lines
- Excess gas produced at 100% operation stored for reuse at 250 psig
- Cold helium gas used to cool support structures
- Input helium is Government Grade A (maximum impurity of 50 ppm) delivered through 5 micron filter

- The cryogenic system shall provide magnet cooldown from ambient in 7 days (based on analysis of previous systems of similar size).
- For the large scale of the MSBS helium use, closed loop helium operation is logical, and liquid nitrogen shall be vaporized to atmosphere.
- Cold helium gas shall be utilized for the cold jacket on the storage dewar.
- Vacuum jacket, insulation and LN_2 jacket shall be used on liquid helium transfer lines.
- Vacuum jacket and insulation shall be used on all other liquid and cold gas lines and components.
- Thermal insulation is required on lines which could sweat inside building.
- Bayonet joints shall be used only between magnet coils and transfer lines - all other lines welded.
- Excess gas produced at 100% operation will be stored at 250 psig for use. This requirement is specified because standard liquefaction plant compressors operate at 250 psig. (During future design effort, a trade study should be performed to determine the economics of providing a high pressure compressor with storage of gas at up to 3000 psi.)
- Quality standards for the cryogenic fluids shall be as follows: Helium; Government Grade A, maximum impurity of 50 parts per million, supply tanker shall be equipped with 5 micron solid filtration at discharge. Commercial grade nitrogen with maximum oxygen impurity of 10 parts per million.

The cryogenics system heat loss, and cryogenics usage requirements are shown in Figures 4.2 through 4.10 for Cases 1, 2, and 3, Alternatives E, F, and G. Alternative G usage is very nearly that of Alternative F. Heat losses in the magnet systems studied herein result from the following sources:

- vapor cooled current leads, 2 liters/hour/kiloamp /pair LHe + .88 liters/hour/kiloamp /pair LN_2
- relief valve/burst disc and service stack, 12.5 watts/stack
- transfer line bayonet, 1 watt/penetration
- radiation, .004 watts/foot^2
- conduction from structures, 10 watts/coil
- splice I^2R losses, $R = .5 \times 10^{-8}$ ohm

FIGURE 4.2
HEAT LOSSES AND CRYOGEN USAGE REQUIREMENTS
CASE 1 ALTERNATIVE E

Usage at Maximum Load:

	Z-Gradient Magnets	Y-Gradient Magnets	Roll Magnets	Magnetization Coils	Drag Magnet	TOTAL
CURRENT LEADS, LHe (liters/hr)	1200	400	800	200	600	3200
LN_2 (liters/hr)	525	176	352	88	264	1405
RADIATION/CONDUCTION						
STACK & PIPING HEAT LOSS (watts)	54	54	108	27	27	270
DEWAR HEAT LOSS (watts)	44	42	82	26	26	220
MAGNET A/C HEATING LOSS (watts)	116000	11600	5600	0	266	133466
SPLICES HEAT LOSS (watts)	200	25	187	25	200	637

Daily Duty Cycle Usage:

	Leads	Radiation/Conduction*	A/C Losses*	Splices*	TOTAL
2 HOURS @ MAX. LOAD LHe (liters)	6400	1400	381331	1819	390950
LN_2 (liters)	2810	∿ 0	--	--	2800
8 HOURS @ 25% MAX. LOAD LHe (liters)	7680**	5600	95332	468	109080
LN_2 (liters)	3372	∿ 0	--	--	3372
14 HOURS @ STANDBY LHe (liters)	13400**	9800	0	0	23240
Total Daily Usage LHe (liters)					523270
LN_2 (liters)					6182

* Heat loss converted to liters/hr of LHe (.7 watt hr/liter)

** Minimum current heat losses are 30% of maximum

FIGURE 4.3
HEAT LOSSES AND CRYOGEN USAGE REQUIREMENTS
CASE 2 ALTERNATIVE E

Usage at Maximum Load:

	Z-Gradient Magnets	Y-Gradient Magnets	Roll Magnets	Magnetization Coils	Drag Magnet	TOTAL
CURRENT LEADS, LHe (liters/hr)	400	400	800	200	200	2000
LN_2 (liters/hr)	176	176	352	88	88	880
RADIATION/CONDUCTION STACK & PIPING HEAT LOSS (watts)	54	54	108	27	27	270
DEWAR HEAT LOSS (watts)	44	42	82	26	26	220
MAGNET A/C HEATING LOSS (watts)	48000	3760	1600	0	80	53440
SPLICES HEAT LOSS (watts)	0	0	50	25	50	125

Daily Duty Cycle Usage:

	Leads	Radiation/Conduction*	A/C Losses*	Splices*	TOTAL
2 HOURS @ MAX. LOAD LHe (liters)	4000	1400	152685	360	158445
LN_2 (liters)	1760	∿ 0	--	--	1760
8 HOURS @ 25% MAX. LOAD LHe (liters)	4800**	5600	38170	90	48660
LN_2 (liters)	2112	∿ 0	--	--	2112
14 HOURS @ STANDBY LHe (liters)	8400**	9800	0	0	18200
				Total Daily Usage LHe (liters)	225305
				LN_2 (liters)	3872

* Heat loss converted to liters/hr of LHe (.7 watt hr/liter)
** Minimum current heat losses are 30% of maximum

FIGURE 4.4
HEAT LOSSES AND CRYOGEN USAGE REQUIREMENTS
CASE 3 ALTERNATIVE E

Usage at Maximum Load:

	Z-Gradient Magnets	Y-Gradient Magnets	Roll Magnets	Magnetization Coils	Drag Magnet	TOTAL
CURRENT LEADS, LHe (liters/hr)	17	16	135	200	200	568
LN_2 (liters/hr)	--	--		88	88	176
RADIATION/CONDUCTION STACK & PIPING HEAT LOSS (watts)	54	54	108	27	27	270
DEWAR HEAT LOSS (watts)	22	21	41	13	13	110
MAGNET A/C HEATING LOSS (watts)	1000	360	4000	0	18	5378
SPLICES HEAT LOSS (watts)	.1	.1	.2	0	0	.4

Daily Duty Cycle Usage:

	Leads	Radiation/Conduction*	A/C Losses*	Splices*	TOTAL
2 HOURS @ MAX. LOAD LHe (liters)	1136	1086	15366	∼ 0	17588
LN_2 (liters)	352	∼ 0	--	--	352
8 HOURS @ 25% MAX. LOAD LHe (liters)	1363**	4344	3841	∼ 0	9548
LN_2 (liters)	422	∼ 0	--	--	422
14 HOURS @ STANDBY LHe (liters)	2386**	7602	0	0	9988
Total Daily Usage LHe (liters)					37124
LN_2 (liters)					774

* Heat loss converted to liters/hr of LHe (.7 watt hr/liter)
** Minimum current heat losses are 30% of maximum

FIGURE 4.5
HEAT LOSSES AND CRYOGEN USAGE REQUIREMENTS
CASE 1 ALTERNATIVE F

Usage at Maximum Load:

	Z-Gradient Magnets	Y-Gradient Magnets	Roll Magnets	Magnetization Coils	Drag Magnet	TOTAL
CURRENT LEADS, LHe (liters/hr)	400	400	800	200	600	2400
LN_2 (liters/hr)	176	176	352	88	264	1056
RADIATION/CONDUCTION						
STACK & PIPING HEAT LOSS (watts)	54	54	108	27	27	270
DEWAR HEAT LOSS (watts)	44	42	82	26	26	220
MAGNET A/C HEATING LOSS (watts)	4000	520	576	0	266	5362
SPLICES HEAT LOSS (watts)	200	25	187	25	200	637

Daily Duty Cycle Usage:

	Leads	Radiation/Conduction*	A/C Losses*	Splices*	TOTAL
2 HOURS @ MAX. LOAD LHe (liters)	4800	1400	15320	1820	23340
LN_2 (liters)	2112	∿ 0	--	--	2112
8 HOURS @ 25% MAX. LOAD LHe (liters)	5760**	5600	3830	455	15645
LN_2 (liters)	2534	∿ 0	--	--	2534
14 HOURS @ STANDBY LHe (liters)	10080**	9800	0	0	19880
				Total Daily Usage LHe (liters)	58865
				LN_2 (liters)	4646

* Heat loss converted to liters/hr of LHe (.7 watt hr/liter)

** Minimum current heat losses are 30% of maximum

FIGURE 4.6
HEAT LOSSES AND CRYOGEN USAGE REQUIREMENTS
CASE 2 ALTERNATIVE F

Usage at Maximum Load:

	Z-Gradient Magnets	Y-Gradient Magnets	Roll Magnets	Magnetization Coils	Drag Magnet	TOTAL
CURRENT LEADS, LHe (liters/hr)	400	400	800	200	200	2000
LN_2 (liters/hr)	176	176	352	88	88	880
RADIATION/CONDUCTION						
STACK & PIPING HEAT LOSS (watts)	54	54	108	27	27	270
DEWAR HEAT LOSS (watts)	44	42	82	26	26	220
MAGNET A/C HEATING LOSS (watts)	1600	124	160	0	80	1964
SPLICES HEAT LOSS (watts)	0	0	50	25	50	125

Daily Duty Cycle Usage:

	Leads	Radiation/Conduction*	A/C Losses*	Splices*	TOTAL
2 HOURS @ MAX. LOAD LHe (liters)	4000	1400	5611	357	11368
LN_2 (liters)	1760	∿ 0	--	--	1760
8 HOURS @ 25% MAX. LOAD LHe (liters)	4800**	5600	1403	89	11892
LN_2 (liters)	2112	∿ 0	--	--	2112
14 HOURS @ STANDBY LHe (liters)	8400**	9800	0	0	18200
				Total Daily Usage LHe (liters)	41460
				LN_2 (liters)	3872

* Heat loss converted to liters/hr of LHe (.7 watt hr/liter)
** Minimum current heat losses are 30% of maximum

FIGURE 4.7
HEAT LOSSES AND CRYOGEN USAGE REQUIREMENTS
CASE 3 ALTERNATIVE F

Usage at Maximum Load:

	Z-Gradient Magnets	Y-Gradient Magnets	Roll Magnets	Magnetization Coils	Drag Magnet	TOTAL
CURRENT LEADS, LHe (liters/hr)	34	16	34	200	200	484
LN_2 (liters/hr)	--	--	--	88	88	176
RADIATION/CONDUCTION						
STACK & PIPING HEAT LOSS (watts)	54	54	108	27	27	270
DEWAR HEAT LOSS (watts)	22	21	41	13	13	110
MAGNET A/C HEATING LOSS (watts)	6	1	40	0	18	65
SPLICES HEAT LOSS (watts)	.1	.1	.2	0	0	.4

Daily Duty Cycle Usage:

	Leads	Radiation/Conduction*	A/C Losses*	Splices*	TOTAL
2 HOURS @ MAX. LOAD LHe (liters)	968	1086	186	1	2241
LN_2 (liters)	352	∿ 0	--	--	352
8 HOURS @ 25% MAX. LOAD LHe (liters)	1162**	4344	47	1	5554
LN_2 (liters)	423	∿ 0	--	--	423
14 HOURS @ STANDBY LHe (liters)	2033**	7602	0	0	9635
Total Daily Usage LHe (liters)					17430
LN_2 (liters)					775

* Heat loss converted to liters/hr of LHe (.7 watt hr/liter)
** Minimum current heat losses are 30% of maximum

FIGURE 4.8
HEAT LOSSES AND CRYOGEN USAGE REQUIREMENTS
CASE 1 ALTERNATIVE G

Usage at Maximum Load:

	Z-Gradient Magnets	Y-Gradient Magnets	Roll Magnets	Magnetization Coils	Drag Magnet	TOTAL
CURRENT LEADS, LHe (liters/hr)	400	400	800	200	600	2400
LN_2 (liters/hr)	176	176	352	88	264	1056
RADIATION/CONDUCTION						
STACK & PIPING HEAT LOSS (watts)	54	54	108	27	27	270
DEWAR HEAT LOSS (watts)	44	42	82	26	26	220
MAGNET A/C HEATING LOSS (watts)	800	92	96	0	46	1034
SPLICES HEAT LOSS (watts)	200	25	187	25	200	637

Daily Duty Cycle Usage:

	Leads	Radiation/Conduction*	A/C Losses*	Splices*	TOTAL
2 HOURS @ MAX. LOAD LHe (liters)	4800	1400	2954	1820	10974
LN_2 (liters)	2112	∿ 0	--	--	2112
8 HOURS @ 25% MAX. LOAD LHe (liters)	5760**	5600	738	456	12554
LN_2 (liters)	2534	∿ 0	--	--	2534
14 HOURS @ STANDBY LHe (liters)	10080**	9800	0	0	19880
				Total Daily Usage LHe (liters)	43408
				LN_2 (liters)	4646

* Heat loss converted to liters/hr of LHe (.7 watt hr/liter)
** Minimum current heat losses are 30% of maximum

FIGURE 4.9
HEAT LOSSES AND CRYOGEN USAGE REQUIREMENTS
CASE 2 ALTERNATIVE G

Usage at Maximum Load:

	Z-Gradient Magnets	Y-Gradient Magnets	Roll Magnets	Magnetization Coils	Drag Magnet	TOTAL
CURRENT LEADS, LHe (liters/hr)	400	400	800	200	200	2000
LN_2 (liters/hr)	176	176	352	88	88	880
RADIATION/CONDUCTION STACK & PIPING HEAT LOSS (watts)	54	54	108	27	27	270
DEWAR HEAT LOSS (watts)	44	42	82	26	26	220
MAGNET A/C HEATING LOSS (watts)	200	20	24	0	10	254
SPLICES HEAT LOSS (watts)	0	0	50	25	50	125

Daily Duty Cycle Usage:

	Leads	Radiation/Conduction*	A/C Losses*	Splices*	TOTAL
2 HOURS @ MAX. LOAD LHe (liters)	4000	1400	726	357	6483
LN_2 (liters)	1760	∿ 0	--	--	1760
8 HOURS @ 25% MAX. LOAD LHe (liters)	4800**	5600	182	89	10671
LN_2 (liters)	2112	∿ 0	--	--	2112
14 HOURS @ STANDBY LHe (liters)	8400**	9800	0	0	18200
				Total Daily Usage LHe (liters)	35354
				LN_2 (liters)	3872

* Heat loss converted to liters/hr of LHe (.7 watt hr/liter)
** Minimum current heat losses are 30% of maximum

FIGURE 4.10
HEAT LOSSES AND CRYOGEN USAGE REQUIREMENTS
CASE 3 ALTERNATIVE G

Usage at Maximum Load:

	Z-Gradient Magnets	Y-Gradient Magnets	Roll Magnets	Magnetization Coils	Drag Magnet	TOTAL
CURRENT LEADS, LHe (liters/hr)	34	16	34	200	200	484
LN_2 (liters/hr)	--	--	--	88	88	176
RADIATION/CONDUCTION STACK & PIPING HEAT LOSS (watts)	54	54	108	27	27	270
DEWAR HEAT LOSS (watts)	22	21	41	13	13	110
MAGNET A/C HEATING LOSS (watts)	1.2	.4	6	0	2.6	10.2
SPLICES HEAT LOSS (watts)	.1	.1	.2	0	0	.4

Daily Duty Cycle Usage:

	Leads	Radiation/Conduction*	A/C Losses*	Splices*	TOTAL
2 HOURS @ MAX. LOAD LHe (liters)	968	1086	29	1	2084
LN_2 (liters)	352	∿ 0	--	--	352
8 HOURS @ 25% MAX. LOAD LHe (liters)	1162**	4344	7.3	.2	5514
LN_2 (liters)	423	∿ 0	--	--	423
14 HOURS @ STANDBY LHe (liters)	2033**	7602	0	0	9635
Total Daily Usage LHe (liters)					17233
LN_2 (liters)					775

* Heat loss converted to liters/hr of LHe (.7 watt hr/liter)
** Minimum current heat losses are 30% of maximum

- eddy current (AC) losses from heating coils, calculated for AC frequency
- overall system piping, 100 watts (estimated for nominal runs)
- storage dewars, 1/2% of volume per day

4.2 APPROACH

The concept established for cooling the MSBS magnets requires liquid helium utilized in the "pool boiling" method of cooling. Therefore, the cryogenic system does not require additional design features to provide for supercooling the helium or for forced coolant flow through the magnet windings.

The use of a helium liquefaction system, and replenishment of the magnet cryostat from a storage dewar is standard for superconducting magnets. Liquid nitrogen is used where feasible to reduce heat loss and excessive use of liquid helium. Magnet cryostat boiloff of cold gaseous helium may be used to cool the support structures of the magnet coil cases, and should be considered during design.

For multiple magnet systems, it is also common practice for the liquid helium supply to be manifolded and lines connected from the manifold to each magnet coil case. For safety and reliability, each coil assembly must have its own liquid level monitoring probes and regulating control so that refilling is automatic. Furthermore, each coil must be connected through a pressure relief valve and burst disc to a common discharge manifold, which is, in turn, connected to a low pressure gas collection reservoir.

In the planned closed loop helium system, helium is returned to the refrigerator through a cold gas (4.5°K) return line from each coil assembly, and the gas is used as a heat exchanger coolant. In addition, the use of vapor cooled current leads will boil off helium, which is returned at room temperature to the compressor suction manifold. As noted earlier, helium vapor at 4.2°K may be used as cold intercepts on the structure supports which pass from the cold coil structure to room temperature. In present superconducting magnet designs, the vapor cooled current leads and return cold gas lines exit through a service stack at the top of each coil assembly.

As an economic measure, liquid nitrogen is provided to reduce the helium heat loads in the gas cooled current leads and transfer lines. It is also used in the helium liquefier heat exchangers to improve efficiency. Gaseous nitrogen is vented to atmosphere outside the building, since closed loop liquid nitrogen systems are not economical in such applications.

A vacuum roughing pump is required to evacuate the outer container of the dewars containing the coil assemblies. The vacuum is generally established through a manifold to a moderate level, approximately 10^{-3} torr, and each coil assembly then requires its own diffusion pump to reduce the vacuum to below 10^{-6} torr. After the coils are cooled the vacuum is maintained by the cryopumping action of the helium cooled cold wall of the coil case.

In the operational approach, initial cooldown is performed by passing cold helium gas from the refrigeration units through the coil cases lowering the temperature to approximately 20°K. Then liquid helium is introduced to complete cooling of the coil and coil cases, and to start filling. While it is expected that operating requirements will define sufficient refrigeration available to cooldown the magnets in less than 7 days, detailed analysis on other magnets of similar size indicate that approximately 7 days should be planned to maintain temperature differentials below overstress conditions.

4.3 DESIGN CONCEPT

The standard closed system liquid helium plant consists of gaseous helium storage, liquefier/refrigerator, liquid helium storage and requisite piping, valving and controls.

Liquid helium consumption is plotted in Figure 4.11, showing helium drawn from the storage dewar during the time magnets are powered and replenishment of storage during standby. Use of large storage capacity has been traded-off for reduction in liquefaction to reduce costs.

Figures 4.12, 4.13 and 4.14 summarize the required capacity and size of the cryogenic system components for all study cases and alternatives. Typical available large sized cryogenic components are listed for comparison.

Cases 1 and 2, Alternative E, require large quantities of helium for removal of heat from eddy currents. Resulting liquefaction requirements are 2 to 5 times greater than the largest plant being built to date(1), although the design and hardware technology for such systems are state of the art.

Figure 4.15 is a block diagram of the cryogenic system for MSBS. The size and number of units required for each of the major components shown in the diagram is given in Figure 4.16.

---

(1) Eber, N., "Worldwide Cryogenics: Switzerland", Cryogenics, Vol. 20 Number 4, April 1980

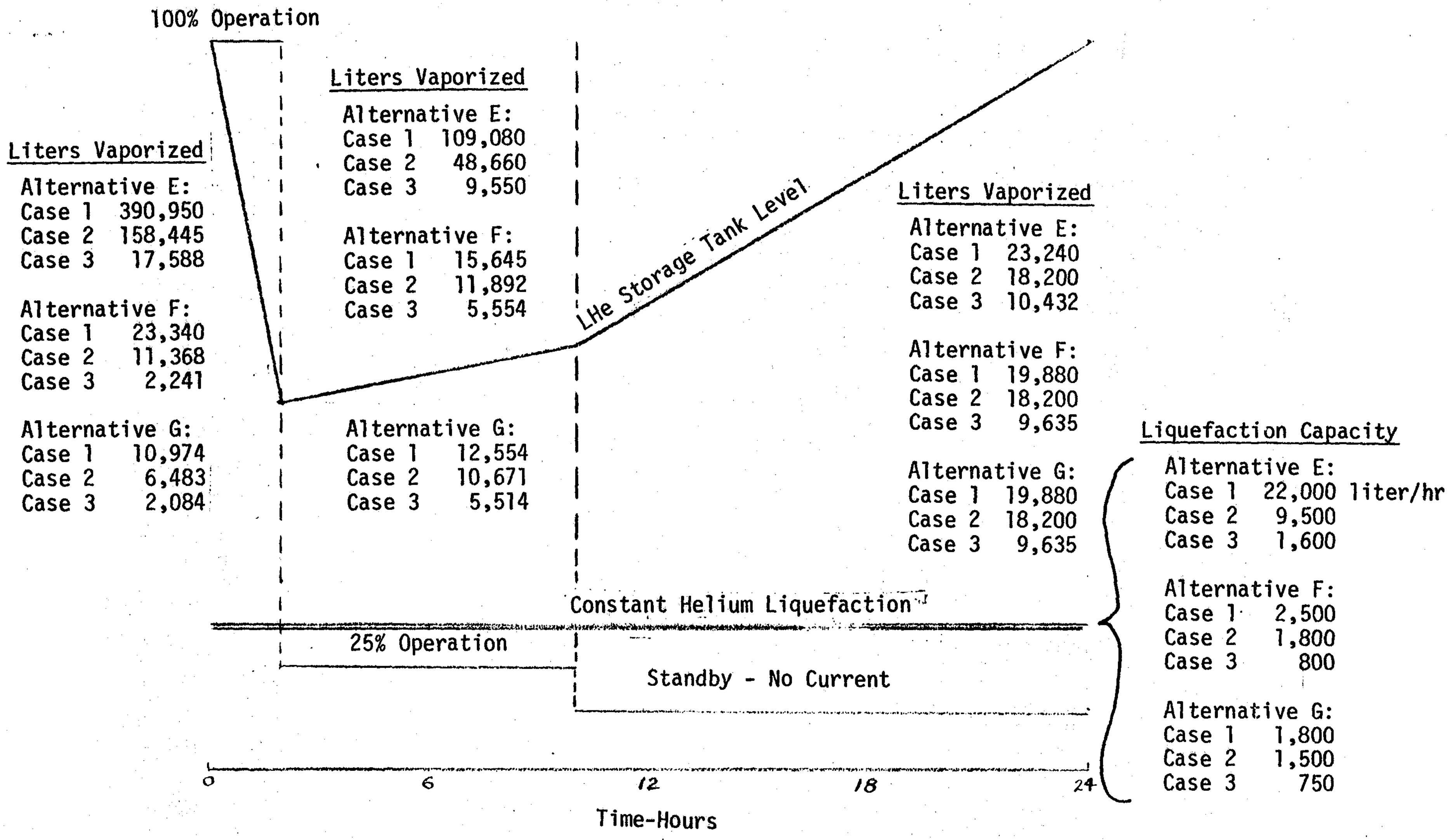

Figure 4.11 Liquid Helium Consumption During Daily Duty Cycle

Figure 4.12

CRYOGENIC SYSTEM COMPONENT SIZES - ALTERNATIVE E

	CASE		
	1	2	3
Helium Refrigerator/Liquefier Capacity (liters/hr)	22,000	9,500	1,600
Liquid Helium Storage (kiloliters)	700	300	30
Helium Gas Storage @ 250 psi (kiloliters)	18,000	7,200	800
Liquid Nitrogen Storage (liters for 1 week)	50,000	30,000	10,000

NOTE: Typical available large cryogenic components: LHe Liquefier, 5,000 liter/hr; LHe Storage Dewar, 121,120 liter; Gas Helium Tanks, 340,650 liter; LN_2 Storage Tank (Low Pressure), 50,000 liter.

Figure 4.13

CRYOGENIC SYSTEM COMPONENT SIZES - ALTERNATIVE F

	CASE		
	1	2	3
Helium Refrigerator/Liquefier Capacity (liter/hr)	2,500	1,800	800
Liquid Helium Storage (kiloliters)	35	15	10
Helium Gas Storage @ 250 psi (kiloliters)	1,000	500	100
Liquid Nitrogen Storage (liters for 1 week)	50,000	30,000	10,000

NOTE: Typical available large cryogenic components: LHe Liquefier, 5,000 liter/hr; LHe Storage Dewar, 121,120 liter; Gas Helium Tanks, 340,650 liter; LN_2 Storage Tank (Low Pressure), 50,000 liter.

Figure 4.14

CRYOGENIC SYSTEM COMPONENT SIZES - ALTERNATIVE G

	CASE		
	1	2	3
Helium Refrigerator/Liquefier Capacity (liter/hr)	1,800	1,500	750
Liquid Helium Storage (kiloliters)	15	6	5
Helium Gas Storage @ 250 psi (kiloliters)	500	300	100
Liquid Nitrogen Storage (liters for 1 week)	40,000	20,000	10,000

NOTE: Typical available large cryogenic components: LHe Liquefier, 5,000 liter/hr; LHe Storage Dewar, 121,120 liter; Gas Helium Tanks, 340,650 liter; LN_2 Storage Tank (Low Pressure), 50,000 liter.

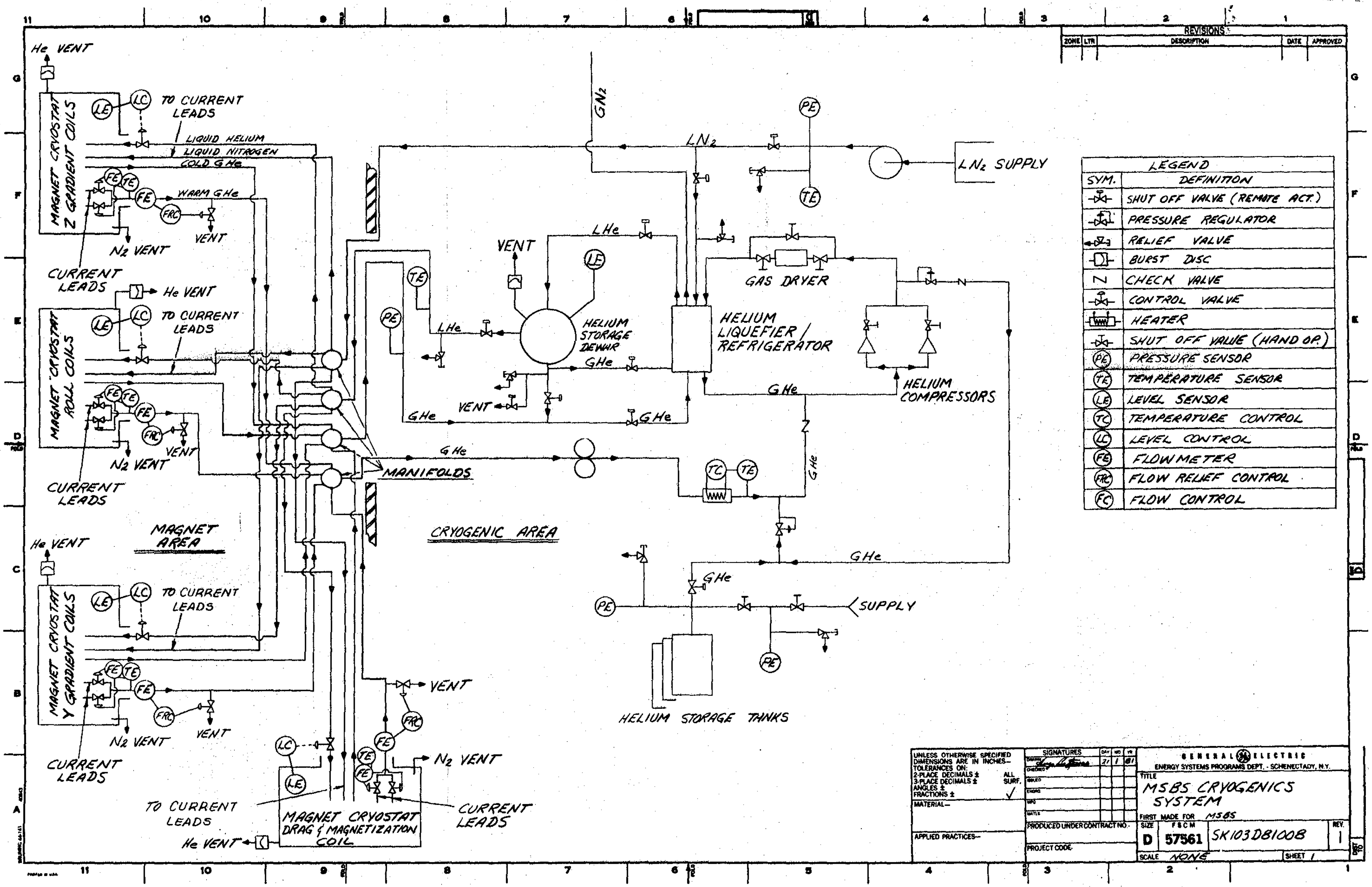

Figure 4.15 MSBS CRYOGENIC SYSTEM

Figure 4.16

REQUIRED MAJOR COMPONENTS OF THE MSBS CRYOGENIC SYSTEMS CONCEPTS
SIZE AND (NUMBER) OF UNITS REQUIRED

CASES / ALTERNATIVES / COMPONENTS	1			2			3		
	E	F	G	E	F	G	E	F	G
Helium Storage Tanks	(52) 340,650 liter	(3) 340,650 liter	(2) 340,650 liter	(20) 340,650 liter	(2) 340,650 liter	(2) 340,650 liter	(3) 340,650 liter	(2) 113,000 liter	(1) 113,000 liter
Helium Refrigerator/Liquefiers	(2) 10,000 liter/hr + (1) 2,000 liter/hr	(1) 2,500 liter/hr	(1) 1,800 liter/hr	(1) 10,000 liter/hr	(1) 1,800 liter/hr	(1) 1,500 liter/hr	(1) 1,600 liter/hr	(1) 800 liter/hr	(1) 750 liter/hr
Helium Compressors* *sized to match refrigerator/liquefiers. quoted as part of refrigerator/liquefiers.number of units is internal estimate.	(10)to(12)	(3)or(4)	(3)or(4)	(5)or(6)	(3)or(4)	(3)or(4)	(3)or(4)	(2)or(3)	(2)or(3)
Helium Storage Dewars	(6) 121,120 liter	(1) 35,000 liter	(1) 15,000 liter	(3) 100,000 liter	(1) 15,000 liter	(1) 6,000 liter	(1) 30,000 liter	(1) 10,000 liter	(1) 5,000 liter
Liquid Nitrogen Storage Tanks	(1) 50,000 liter	(1) 50,000 liter	(1) 40,000 liter	(1) 30,000 liter	(1) 30,000 liter	(1) 20,000 liter	(1) 10,000 liter	(1) 10,000 liter	(1) 10,000 liter

4.4 TECHNICAL RISKS

In all cases, the cryogenics concept utilizes components and technology within the state-of-art of cryogenic systems used on other magnet systems being built for MHD and fusion experiments. However, the extremely large amounts of helium for Cases 1 and 2, Alternative E have been met with liquefiers of 10,000 liter/hr capacity. These units, twice the capacity of units currently being built, are considered by potential vendors to be the largest plants practical based on current compressor capacity.

5.0 POWER SUPPLY, PROTECTION & MAGNET INSTRUMENTATION CONCEPTS

The power supply subsystem provides monopolar or bipolar power to the magnet coils, as required, to generate the static and/or dynamic fields that suspend, move and/or oscillate the model within the wind tunnel test section. A system using SCR converter/inverter power supplies for each coil has been selected. This approach provides the greatest versatility using available technology. Custom design will be required, particularly in the area of the maximum peak power requirements.

It is standard practice in Large Superconducting Magnet applications to include with the power supply a protection system which provides monitoring of key magnet operating characteristics to obtain an indication of impending damage to a superconducting coil and which provides mechanisms for protecting the coil in the event of such an indication. A protection subsystem similar to that used for the Component Development and Integration Facility (CDIF)(1) magnet has been selected. The CDIF system has system features unique to that application, however, its major components are available and are being used in several applications by GE and other organizations.

The functional subsystem magnet instrumentation is also covered in this section of the report. This area represents parts of several subsystems, but past experience indicates that it is best treated as an integrated area within the framework of the power supply subsystem and protection system. These utilize the majority of the instrumentation and, thus, simplify interface control. The previously designed system for CDIF provides a fairly good model for MSBS instrumentation. This system has been supplemented and complemented by sensors and techniques used on several other magnet systems, where applicable.

5.1 REQUIREMENTS

5.1.1 POWER SUPPLY REQUIREMENTS

The power supply subsystem is required to provide electrical power to each superconductor coil to obtain four types of magnetic fields dependent on the magnet's function in the MSBS function, as follows:

Magnetization Coils - These provide a uni-directional static field to magnetize the model. Power requirements are satisfied by a low voltage, high current 2-quadrant ($\pm$ voltage zero-to-plus current) power supply.

Drag Coils - These provide a uni-directional static field plus a small alternating field for control. Power Requirements are satisfied by a medium voltage, high current, 2-quadrant power supply.

Gradient and Roll Coils - These coils provide bi-directional static fields plus small alternating fields for control plus (for Alternatives E and F) large alternating fields for forced sinusoidal model oscillations. This requires 4-guadrant ($\pm$ voltage, $\pm$ current) power supplies, high voltages for Alternative E, medium voltages for Alternative E, medium voltages for Alternatives F and G, high currents for Cases 1 and 2 and medium currents for Case 3.

Figure 5.1, summarizes the driving requirements that are imposed on the power supply concepts to satsify the above needs and the overall MSBS system requirements.

The design-related requirements, such as those characterizing availability of hardware and technology, independent power supplies, by-pass circuitry, circuit protection, and control and maintenance guidelines have been adopted to meet system requirements for minimizing technical, cost and schedule risks. Reduction of technical risks so as to maximize safety, reliability and productivity have been accorded primary consideration in the power supply design concepts. In future design efforts, it is likely that Failure Modes and Effects Analysis and Reliability/Maintainability Studies will indicate changes to certain of these requirements that will enable cost reductions without significantly increasing technical risks. For example, single power supplies for multiple magnet modules may offer such an opportunity.

- Available Hardware or State-of-the-Art Technology.
- Separate Power Supply for each Magnet Module.
- Maximum Frequency of Operation - 20 Hz.
- Voltage Output - Maximum, 8.0 KV; Minimum, 10V.
- Current Output - Maximum 50 kA; Minimum .75 kA.
- Configurations 2 and 4 Quadrant.
- Output Voltage Regulation $\pm$ 1%.
- Output Current Regulation $\pm$ 1%.
- By-Pass Circuitry to Carry Maximum Operating Current in the Event of a Power Supply Fault.
- Internal Interlock & Fault Protection.
- Local Control with Provision for Operation and Indication to Trouble-Shoot and Perform Periodic Maintenance.
- Remote Control Provision, Including Alarm and Indication for Operation.
- Input Power - 440 Volt 3Ø, 13200 Volt 3Ø

Figure 5.1
DRIVING POWER SUPPLY REQUIREMENTS

The power supply band width of 20 Hz has been selected as a nominal value for this study. It represents a reasonable compromise between higher frequencies, which would call for more complex, costly power supplies, and lower frequencies which would be incompatible with the control tolerance required of MSBS Control System.

Voltage and current output requirements of the power supplies are established by the magnet conductor, magnet module configurations and the static and dynamic magnetic force requirements. For the maximum 50 kilo amp current of conductor selected for Cases 1 and 2, the magnets with maximum inductances and current rates corresponding to maximum magnetic force oscillations yield a maximum voltage output of 8.0 KV. As the inductances and current rates differ from magnet to magnet, Case to Case, and Alternative to Alternative, the required voltages also differ. Thus, the minimum power supply voltage output is 10 volts. Such differences will have a profound effect on the design and cost of the power supplies, since voltage outputs above about 1000V imply more complex equipment, and a higher order of insulation to prevent voltage breakdown.

5.1.2 PROTECTION SYSTEM REQUIREMENTS

The protection system is intended to prevent damage to the MSBS coils resulting from abnormal conditions, such as:

- a non-superconducting (normal) region generated in any coil
- loss of coolant flow in gas cooled current leads
- loss of helium coolant or vacuum in dewars
- a serious short-to-ground of a superconducting coil

In order to accomplish this purpose, the design of the protection system must solve two key technical problems:

- o Rapid (< 30 seconds) extraction of the stored energy in the magnet in an acceptable combination of maximum magnet temperature ($\sim 200^{O}K$) and voltage (< 1000V) to prevent damage from arcing, thermal stresses, or electromechanical interaction between coils.

- o Achievement of high system reliability to maintain magnet system availability and prevent coil damage due to loss of protection capability.

Past programs have identified key design requirements for solving these problems:

Sensors provided for each magnet to acquire data indicative of impending damage must be redundant, as must be the wiring to transmit the data. Such sensors must be compatible with conditions for cryogenic measurements, and must be insensitive to, and/or correctable for, high magnetic fields.

Signal conditioning requires isolation from ground and conductor, and use of hard wired circuitry. For reliability and assurance of operability, parallel self test circuitry is required, as are a standby power supply, parallel output for diagnostic test use, individual circuitry for each magnet, redundant circuitry, and status output. However, a common cabinet and/or console is acceptable for monitoring and self-testing.

Discharge switches must be redundant, and provided with self-contained logic and control circuits. They require standby power supplies and status instrumentation for monitoring and interlock. They must be resettable, manually or automatically for repeated usage without parts replacement.

Dump (Discharge) Resistors require highly reliable passive cooling by either non-pumped water or natural air convection. Status instrumentation is required for monitoring and interlock, and units must be capable of repeated usage without parts replacement.

5.1.3 INSTRUMENTATION REQUIREMENTS

A primary guideline in developing instrumentation requirements is that emphasis is to be placed on the MSBS as a functional tool, rather than a device to develop other MSBS's. Thus, instrumentation is primarily that which is required for operations rather than for acquiring MSBS developmental data. This guideline does not eliminate the need for instrumentation that assures the safe, reliable, effective performance of the MSBS.

Four areas of measurement are considered in selecting instrumentation sensors:

- Measurements during Acceptance and Performance Testing, including initial cooldown and operation of the magnet, require particular emphasis on detecting and avoiding thermal stresses. In addition, measurements are required to establish or confirm the parameters for operation and startup of the magnets.
- Measurements during operations include functions, such as tracking the He supply, that occur during normal energization, shutdown and on-line operation.
- Protect and alarm measurements must provide feedback for automatic shutdown, or for annunciation of impending problems.
- Diagnostic measurements must be made available as parallel outputs of all of the above, and measurements are required to evaluate performance of the overall system.

To meet the measurement requirements cost effectively, instrument sensors should be provided to meet more than one measurement objective, where possible, but sufficient quantities are required to assure reliability and complete measurement capability. In accordance with project guidelines, the sensors and sensor support equipment should be selected from existing state-of-the-art. Because of the rigorous cryogenic/magnetic environment to which instrumentation is exposed, support equipment, such as leadouts must be included in selection of each sensor. Subsequently, installation designs must be provided to assure that sensors and leadouts will be installed without degradation to the coil.

5.2 APPROACH

5.2.1 POWER SUPPLIES APPROACH

Several available types of power supplies were evaluated to meet the requirements for MSBS. Figure 5-2 illustrates key requirements and/ or impact areas versus three basic types of power supplies. Following are brief descriptions of the basic types.

- SCR-Rectifier - This type is an outgrowth of rectifier technology using up-to-date Silicon Controlled Rectifier (SCR) equipment. A typical model is the CDIF 2-quadrant power supply illustrated in Figure 5-3. In addition to converting AC to DC current, the power supply is capable of inverting the DC to AC for return to the power grid source. Although this model is 2-quadrant, a circuit design using additional switching and reactance will allow 4-quadrant operation wherein current can reverse direction in order to reverse the magnetic field of the magnet being charged.

- Rotating DC Machines - Two available types were explored and evaluated, motor/generator (M/G) and Homopolar generator. The MG's have longstanding usage and experience as a source of DC power. However, it is of note that most users have converted to SCR-Rectifier systems in preference to MG's over the past years to reduce costs and installation space. Homopolar generators are capable of extremely high current but are limited to quite low voltages, and have yet to achieve widespread use.

- Energy Storage Devices - Mechanical devices utilizing flywheels to store very high kinetic energy are available, and are used most effectively with an AC generator. Several examples were explored, particularly those at Los Alamos and at Princeton, where TFTR is currently installing two very large units supplied by GE. These

ITEM	SCR/RECTIFIER	DC ROTATING MACHINES (MOTOR/ GENERATOR) HOLOPOLAR GENERATOR	ENERGY STORAGE (MECHANICAL) (ELECT. CAPAC.) SUPERCOND. MAGNET)
AVAILABLE TECHNOLOGY (STATE-OF-THE-ART)	VERY GOOD	GOOD	FAIR - MAINLY CONCEPTUAL
AVAILABLE SUPPLY SOURCES	VERY GOOD	VERY GOOD	QUESTIONABLE
COST	HIGH BUT KNOWN	HIGH BUT UNKNOWN	UNKNOWN
DELIVERY	VERY GOOD	UNKNOWN	UNKNOWN
SYSTEM INTEGRATION	VERY GOOD	STEADY STATE - GOOD DYNAMICS WILL NEED EXTRA EQUIPMENT	WILL NEED ADDED EQUIP-MENT POSSIBLY AS MUCH AS SCR SYSTEM
STEADY STATE OPERATION	YES	YES	YES
DYNAMIC OPERATION	YES	NO	NO
DEVELOPMENT REQUIRED FOR THIS APPLICATION	MINIMAL	STEADY STATE - NO DYNAMICS - YES	YES - MAXIMUM
POWER REQUIRED (COMMENTS)	VERY HIGH DURING PEAK DYNAMIC OPERATION	MG CAN ALSO BE USED FOR ENERGY STORAGE AS AN AC GENERATOR	LIMITS PEAK POWER INPUTS DURING DYNAMIC OPERATION
PROBLEM AREAS	PEAK POWER REQUIREMENTS	-SIZE COST -COMMUTATOR PROBLEMS -PEAK POWER REQUIREMENTS -NEED FOR SCR'S FOR DYNAMIC OPERATION -DYNAMIC RESPONSE	-SIZE COST -STATE-OF-THE-ART -STATE-OF-THE-ART -NEED FOR SCR'S FOR DYNAMIC OPERATION -DYNAMIC RESPONSE

Figure 5.2

COMPARISON OF DC POWER SUPPLY FOR MSBS S/C MAGNETS

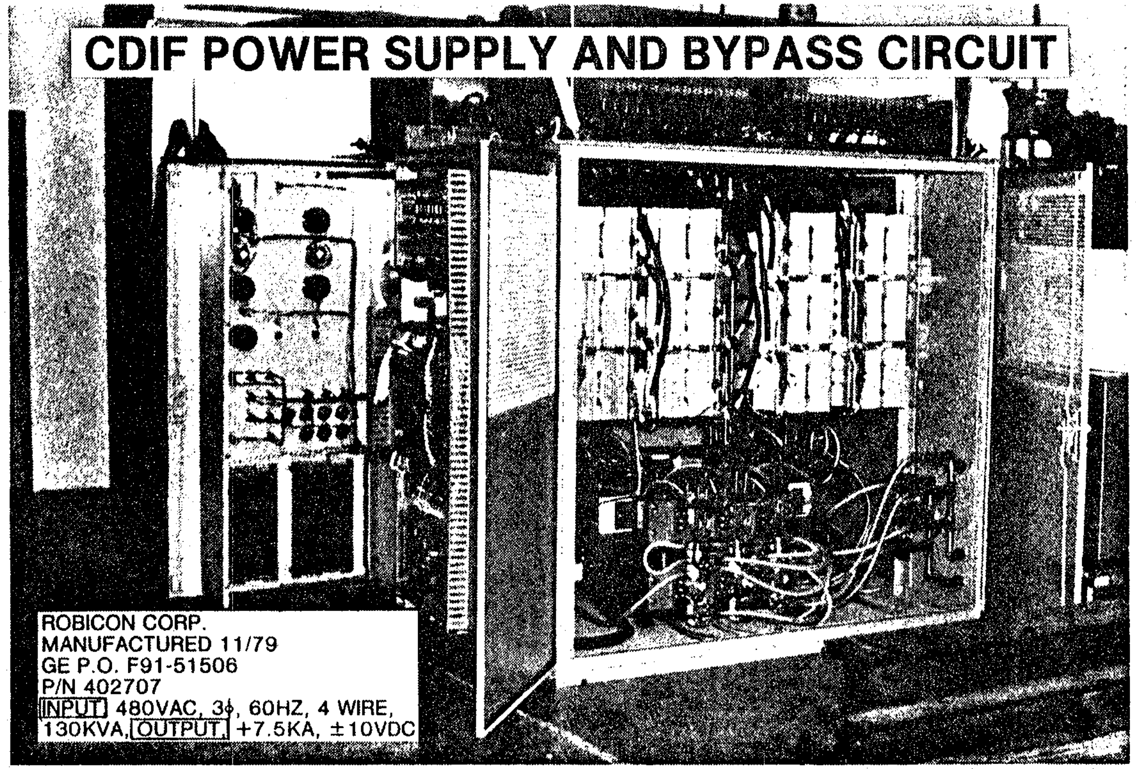
CDIF POWER SUPPLY AND BYPASS CIRCUIT
ROBICON CORP.
MANUFACTURED 11/79
GE P.O. F91-51506
P/N 402707
INPUT 480VAC, 3ϕ, 60HZ, 4 WIRE,
130KVA, OUTPUT, +7.5KA, ±10VDC

Figure 5.3

devices have an advantage over other methods in the role of a power line buffer for peak power rather than a continuous power supply for an individual magnet. Capacitive storage was also evaluated, but it appears that the required massive size and the available state-of-the-art would be limiting at this time.

Superconducting magnet energy storage was also evaluated. Of particular interest was the use of other magnets in the MSBS system, such as physically opposite gradient coils. There are both conceptual technology for large-scale units and some examples of small (laboratory) size models available. However, the MSBS requirement for cyclic operation at frequencies higher than current systems imposes major penalties. Preliminary analysis of operations in which energy was transferred between magnet coils at 5 Hz for example, indicates a need for an additional one to two more quantities of converter/inverter circuitry than that required for a basic SCR/Rectifier system.

5.2.2 PROTECTION APPROACH

The GE approach is based on past superconducting magnet design adapted to the requirements of the MSBS work statement. To remove the stored energy in the event of potential magnet damage, each coil is isolated with switches and discharged into an individual resistor. Each system includes instrumentation and control circuitry to provide sensing, signal conditioning, and protect commands. Commands are also provided to the power supply to ramp the system to zero current in response to less serious conditions such as low He level, marginal dewar vacuum, or low current lead coolant flow.

Several approaches have been adopted to ensure system reliability:

- o The design, although a custom assembly integrates state-of-the-art components in a configuration very similar to GE designs for other multiple magnet systems. Available specifications and costs from the CDIF provide a good design and cost model.

- o Circuits for rapid discharge will be hard-wired to the protection circuit to eliminate potential signal failures associated with data interfaces.
- o A self-testing microprocessor circuit which periodically checks for proper operation of all sensors and circuits in the protection system is proposed. System status will be supplies to the MSBS computer, and protective action will be initiated if an unacceptable loss of protection capability occurs, such as failure of several sensors in a single coil. This microprocessor approach has been used on the Component Development and Integration Facility (CDIF) Magnet Protection System and is expected to contribute significantly to system reliability.

5.2.3 INSTRUMENTATION APPROACH

Figure 5-4, summarizes key instrumentation trade-off issues and selection criteria. Two issues have major impact on the overall instrumentation package:

1. Quantities - Since the MSBS emphasis is toward a functional rather than a test device, the quantities of instrumentation selected are based on provision of the minimum to operate and protect a magnet, plus a moderate addition to monitor temperature, liquid level and pressure during acceptance testing and cooldown, as well as limited on-line diagnostic monitoring, especially during initial operation of a new coil design.
2. Location - For magnet development programs, the major location impact is involved in putting sensors and wiring within the windings of the coil, such as on the conductor. Such activity involves large qunatities of coil assembly time and also requires careful design and precision assembly to avoid mechanical and electrical degradation of the coil. Since for MSBS, the emphasis is on operational systems, it is not necessary to install

KEY DESIGN ITEM	TRADEOFF OPTIONS			SELECTION
Quantity of Sensors	1 HIGH - Maximum data - Diagnostic data - High cost - Objective is testing - Minimizes initial operating risks	2 MODERATE - Provides data for startup and also for cooldown and magnet charging - Cost can be controlled with prudent design - Provides data for initial operation	3 LOW - Minimum data - Operating data only - Low cost - Objective is operating - Maximum initial operating risks	2 The MSBS magnets are operating components and need the minimum of 3. However, since the final design will be the 1st of this configuration, a moderate quantity of sensors is considered necessary to monitor cooldown, acceptance testing, and operation. Cost does not appear prohibitive.
Sensor Location	1 THROUGHOUT MAGNET - INCLUDING WINDINGS	2 RESTRICTED FROM WINDINGS		2
	- Allows sensor location on conductor - Provides conductor diagnostics - Requires insulation rework and possibly conductor rework - Has serious interference with winding assemblies - High cost impact due to winding delays - Affects reliability of coil due to rework of insulation and lead-out within windings - Reliability of sensor installation is decreased	- Restricts sensor location to outer perimeter of the coil substructure - Requires analysis to predict cooldown and startup for the conductor and windings - Requires a few added precautions during initial acceptance and operation - Keeps rework of coil to a minimum		- The loss of time to install sensors during assembly has a very high cost impact which more than offsets the design and analysis time to predict winding stresses during cooldown and startup - A more deliberate procedure using sensors on the perimeter of the windings will be adequate for cooldown - The MSBS coils are essentially operating coils, not test coils coils

Figure 5.4

TRADE-OFFS CONSIDERED IN THE SELECTION OF SENSOR TYPES sensors within the MSBS coils. It is planned that design and operational considerations will be predicated on the basis that no measurements will be available within the coil windings.

5.3 CONCEPT

5.3.1 POWER SUPPLY CONCEPT

The SCR/Rectifier concept has been chosen as the most effective design concept for the MSBS Power and Protection Systems shown in Figure 5.5. This is a system that will meet all of the requirements of Paragraph 5.1, and which has a clear advantage over other types of power supplies considered in Figure 5.2. However, it would likely be necessary to use an AC/Rotating Generator similar to the units at Princeton TFTR as a buffer between the MSBS test facility and the power utility if performance at the dynamic level originally specified in the MSBS work statement were to be confirmed, and if the utility were to find the resulting "power swings" unacceptable.

The specific characteristics and quantities of power supply components required to implement the Power Supply concept of Figure 5.5 for Cases 1,2, and 3, Alternatives E,F, and G are shown in Figure 5.6, 5.7 and 5.8.

SCR power supplies have been fabricated by several vendors using the components shown in Figures 5.6, 5.7 and 5.8 for the lower power cases ($\leq$ 1000V). Technology and equipment for the larger power supplies is available but custom design costs will be encountered.

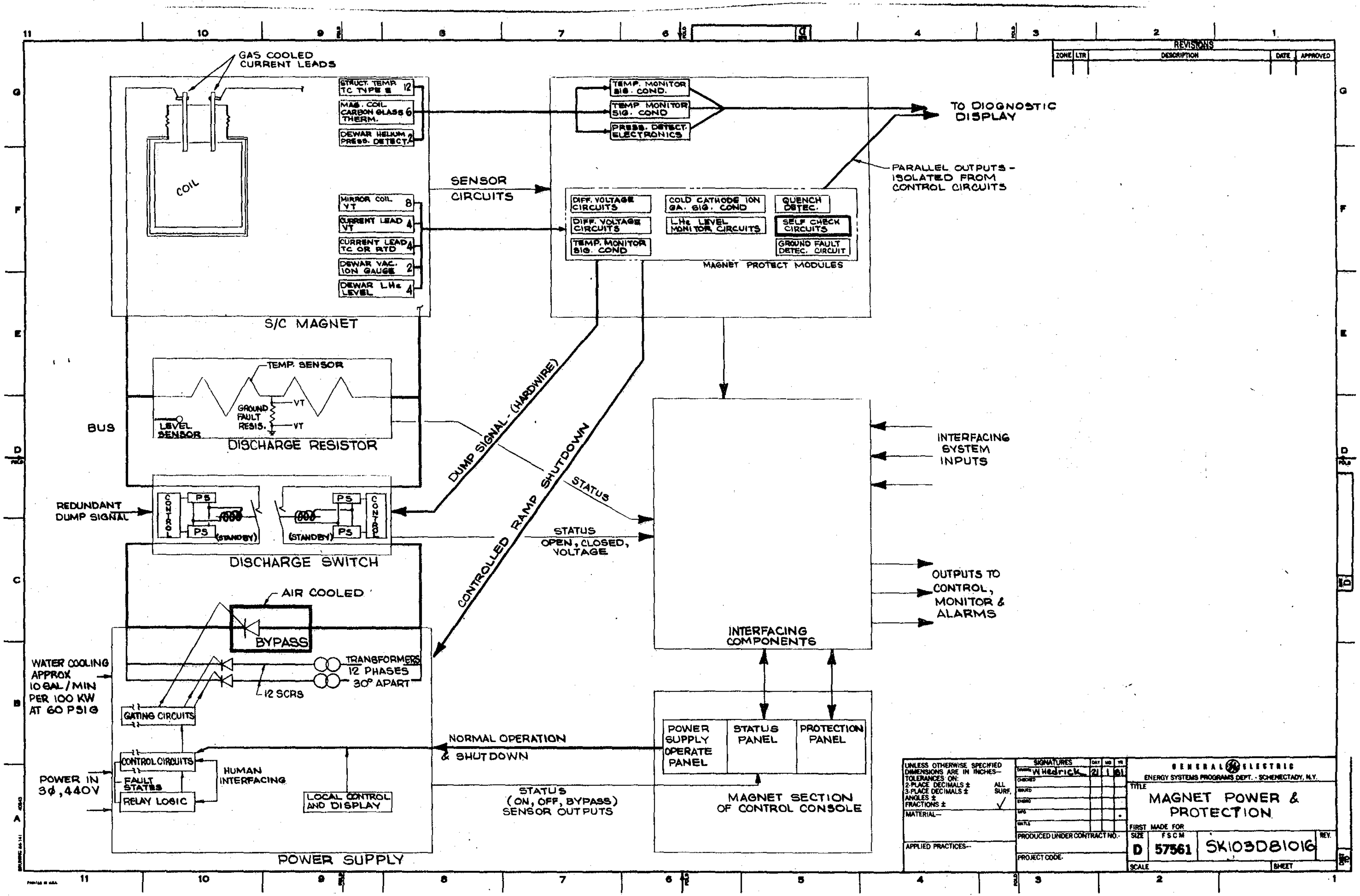

Figure 5.5

MAGNET POWER & PROTECTION

5.3.1.1 Power Factor

An SCR/Converter Power Supply will typically run at a 0.8-0.9 power factor when delivering rated current and voltage.

In the typical MSBS application, the load is highly inductive with a very small resistive component. The load voltage induced by changes in load current to control the model, will vary between 0 and plus and minus the maximum voltage shown in Figures 5.6, 5.7 and 5.8. The load current will vary between 0 and plus and minus the maximum current. Since the Power Supply Power Factor depends on the instantaneous product of voltage and current, the power factor is expected to vary between 0 and 0.8-0.9. Actually, the power factor never goes exactly to zero because the grid must supply the resistive losses in busses, power supply components, periferals and magnets. However, in the MSBS application these resistive losses are @ 5% or lower of the reactive power.

A 67% Power Factor has been selected to establish peak demand at the INPUT of the Power Supplies. The number is considered as a rough order of magnitude, but sufficient to establish requirements at a feasibility level of work. The study of Power Factor and efficiency should be addressed early in the system analysis and preliminary design effort of any future MSBS work.

5.3.1.2 Maximum Total Power Demand

The total power required to the magnets from the power supply varies from a very high level of Case 1, Alternative E, in Figure 5.6 to a relatively low level for steady state operation shown in Figure 5.8 for Case 3, Alternative G. The range is from 5360 MVA to 15 MVA.

Inquiries to power supply vendors within[(2)*] and outside[(3)*] GE were made in the process of determining that a power factor of 67% is nominal as described in the above paragraph. This requires that the utility provide a peak input of 50% above the magnet input for each particular case and alternative being evaluated.

* See total list of Reference Sources in Section 5.8.

Magnet Type	Z Gradient			Y Gradient			Roll			Magnetiz.			Drag		
Case No.	I	II	III	I	II	III	I	II	III	I	II	III	I	II	III
Power Supplies															
Type	← SCR Converter/Inverter →														
Quantity	12	4	8	4	4	4	8	8	64	2	2	2	2	2	2
Configuration	← 4 Quad. →									← 2 Quad. →					
Max. Current (KA)	50	50	.75	50	50	1.4	50	50	.75	50	50	50	50	50	50
Max. Voltage (KV)	8.0	4.8	2.25	1.2	.22	.66	.575	.82	2.0	.02	.02	.02	.9	.063	.012
Dump (Discharge) Resistors															
Time Constant	← 30 Seconds →														
Resistance	$4x10^{-3}$	$3.2x10^{-4}$	.16	$3.6x10^{-4}$	$3.6x10^{-5}$	$2.4x10^{-2}$	$8x10^{-4}$	$7x10^{-5}$	.16	$6.8x10^{-4}$	$6.8x10^{-4}$	$1.6x10^{-5}$	10^{-2}	$6.8x10^{4}$	$1.3x10^{-4}$
Type (W-Water Cooled) (A-Air Cooled) (W/A-Either)	W	W/A	A	W/A	A	A	W/A	A	A	W/A	W/A	A	W	W/A	A
Quantity	16	44	16	4	4	4	8	8	8	2	2	2	6	2	2
Rating (MJ)	148	24	1.4	14	2.7	.7	31	5.25	8.0	26	26	.6	379	52.2	5.1
Dump (Discharge) Switches															
Circuit Breaker	← GE Model GEH-1803B/MC6B (12 KA Max.) →														
Quantity Each -	16	16	2	8	8	2	16	8	2	8	8	8	8	8	8
Quantity Total -	192	64	32	32	32	8	128	64	128	16	16	16	16	16	16
Configuration (S-Series) (P-Parallel)	S-P	S-P	S	S	S	S	S-P	S	S	S-P	S-P	S-P	S-P	S-P	S-P

TOTAL POWER REQUIRED

Case I	5,360 MVA
Case II	1,340 MVA
Case III	220 MVA

Figure 5.7

POWER CIRCUITRY COMPONENTS - ALTERNATIVE F

Magnet Type	Z Gradient			Y Gradient			Roll			Magnetiz.			Drag		
Case No.	I	II	III	I	II	III	I	II	III	I	II	III	I	II	III
Power Supplies															
Type	SCR Converter/Inverter														
Quantity	4	4	4	4	4	4	8	8	8	2	2	2	2	2	2
Configuration	4 Quad.									2 Quad.					
Max. Current (KA)	50	50	.75	50	50	1.4	50	50	.75	50	50	50	50	50	50
Max. Voltage (KV)	.38	.033	.24	.035	.01	.063	.078	.01	.72	.02	.02	.02	.9	.063	.12
Dump (Discharge) Resistors															
Time Constant	30 Seconds														
Resistance	4×10^{-3}	3.2×10^{-4}	.16	3.6×10^{-4}	3.6×10^{-5}	2.4×10^{-2}	8×10^{-4}	7×10^{-5}	.16	6.8×10^{-4}	6.8×10^{-4}	1.6×10^{-5}	10^{-2}	6.8×10^{4}	1.3×10^{-4}
Type (W-Water Cooled) (A-Air Cooled) (W/A-Either)	W	W/A	A	W/A	A	A	W/A	A	A	W/A	W/A	A	W	W/A	A
Quantity	16	44	16	4	4	4	8	8	8	2	2	2	6	2	2
Rating (MJ)	148	23.8	1.4	14	2.75	.7	31	5.25	8.0	26	26	.6	379	52.2	5.1
Dump (Discharge) Switches															
Circuit Breaker	GE Model GEH-1803B/MC6B (12 KA Max.)														
Quantity Each -	8	8	2	8	8	2	8	8	2	8	8	8	8	8	8
Quantity Total -	32	64	8	32	32	8	64	64	16	16	32	16	16	16	16
Configuration (S-Series) (P-Parallel)	S-P	S-P	S	S	S	S	S-P	S	S	S-P	S-P	S-P	S-P	S-P	S-P

TOTAL POWER REQUIRED

Case I	206 MVA
Case II	21 MVA
Case III	16 MVA

POWER CIRCUITRY COMPONENTS - ALTERNATIVE G

Magnet Type	Z Gradient			Y Gradient			Roll			Magnetiz.			Drag		
Case No.	I	II	III	I	II	III	I	II	III	I	II	III	I	II	III
Power Supplies															
Type	SCR Converter/Inverter														
Quantity	4	4	4	4	4	4	8	8	8	2	2	2	2	2	2
Configuration	4 Quad.									2 Quad.					
Max. Current (KA)	50	50	.75	50	50	1.4	50	50	.75	50	50	50	50	50	50
Max. Voltage (KV)	.36	.03	.22	.033	.01	.060	.075	.01	.72	.02	.02	.02	.9	.06	.12
Dump (Discharge) Resistors															
Time Constant	30 Seconds														
Resistance	$4x10^{-3}$	$8.2x10^{-4}$	.16	$3.6x10^{-4}$	$3.6x10^{-5}$	$2.4x10^{-2}$	$8x10^{-4}$	$7x10^{-5}$	.16	$6.8x10^{-4}$	$6.8x10^{-4}$	$1.6x10^{-5}$	10^{-2}	$6.8x10^{4}$	$1.3x10^{-4}$
Type (W-Water Cooled) (A-Air Cooled) (W/A-Either)	W	W/A	A	W/A	A	A	W/A	A	A	W/A	W/A	A	W	W/A	A
Quantity	16	44	16	4	4	4	8	8	8	2	2	2	6	2	2
Rating (MJ)	148	23.8	1.4	14	2.75	.7	31	5.25	8.0	26	26	.6	379	52.2	5.1
Dump (Discharge) Switches															
Circuit Breaker	GE Model GEH-1803B/MC6B (12 KA Max.)														
Quantity Each -	8	16	2	8	8	2	8	8	2	8	16	8	8	8	8
Quantity Total -	32	64	8	32	32	8	64		16	16	32	16	16	16	16
Configuration (S-Series) (P-Parallel)	S-P	S-P	S	S-P	S-P	S	S-P	S	S	S-P	S-P	S-P	S-P	S-P	S-P

TOTAL POWER REQUIRED

Case I	196 MVA
Case II	20 MVA
Case III	15 MVA

It should be noted that the factor increases as the power increases, particularly when the power supplies are operating at maximum design voltage. It may be feasible to achieve more favorable factor with sufficient controls and design consideration. Further study on this subject is warranted.

5.3.2 PROTECTION SYSTEM CONCEPT

The protection system is shown in the diagram, Figure 5.5. The concept is similar to that used for the CDIF equipment presently being manufactured by GE.

Reference (1) provides a description of instrumentation and control concepts which can be applied for each magnet in the MSBS program. Since this paper was published, GE has evaluated several applications which effectively apply this concept to multiple magnet systems, such as MSBS, and has determined that optimization of circuitry, packaging and monitoring equipment for applications other than CDIF is well within the state-of-the-art.

The power switching for each magnet has been evaluated using available power breaker switches manufactured by the GE Switchgear Department. The switch has a long service listing, particularly in steel mill applications. This switch, Model MC-6B, has a maximum rating of 12,000 amps and 2000 volts which would not meet all requirements with a single switch. However, a series/parallel network of switches is feasible, as shown in Figure 5.9. Note that every magnet would normally have 2 switches in series for control redundancy. Figure 5.6, 5.7 and 5.8 list the quantity of switches required.

A search for larger switches for this type of application has been in progress prior to the MSBS project, but the MC-6B is the only switch readily available at this time. Costs and schedules for this switch are available which enables ready estimates for use of this switch for series/parallel applications. In addition, a brief analysis of costs and time to develop larger switches indicate at least a comparable cost.

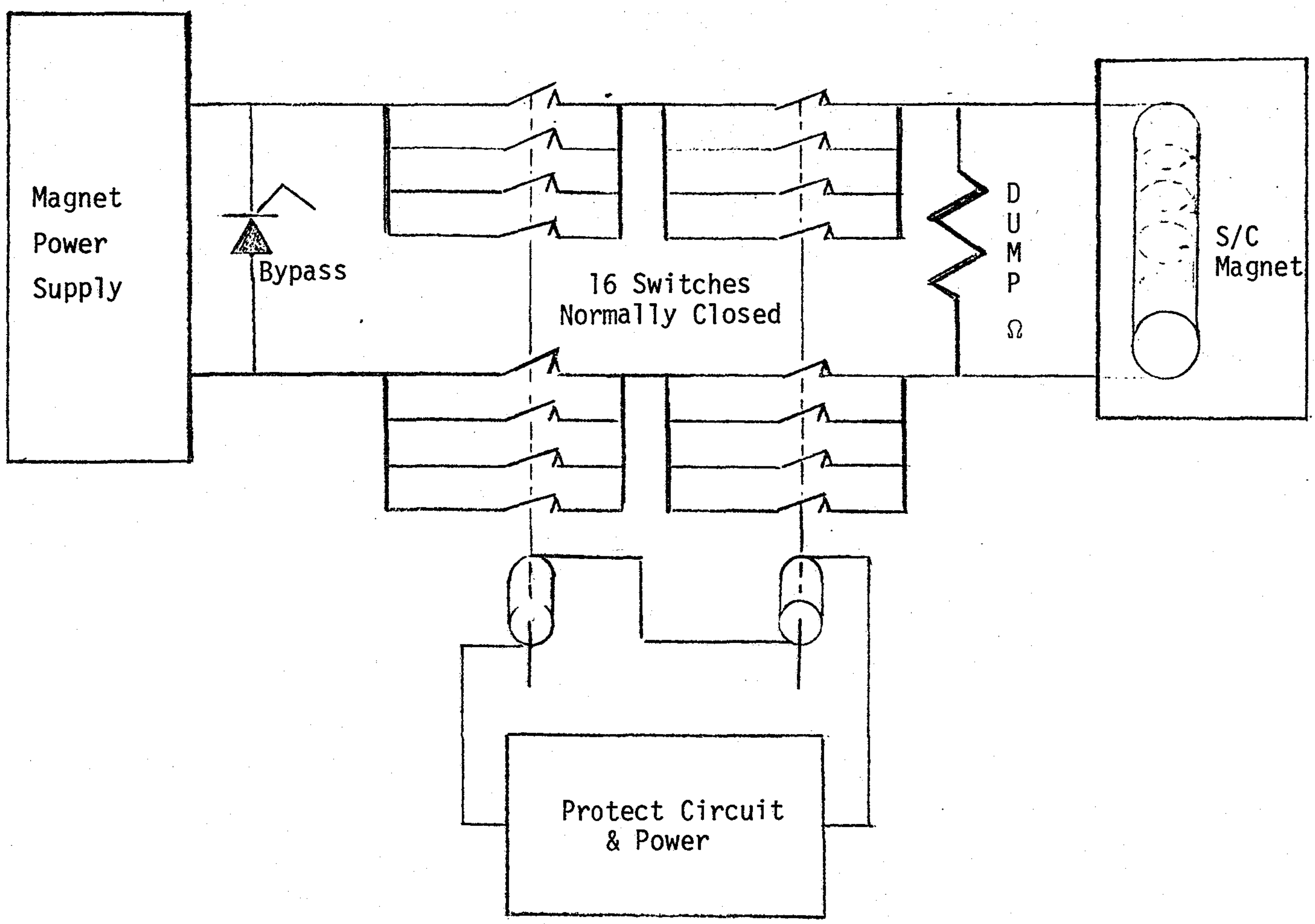

Fig. 5-9. Multiple Discharge Switch Circuit
for 50 KA/8 KV Circuit
(Series/Parallel)

NOTE: Switches in parallel are required for high current. Switches in series, they are required for high voltage.

Another type of switching was evaluated for MSBS employing SCR's. There are applications in S/C magnet circuitry at Los Alamos and Oak Ridge National Labs which use SCR's, particularly for multiple magnet systems. However, with the immediate availability of switches compared to an evaluation of high current SCR circuitry, it seemed prudent to go with the switches at this point in the MSBS program. Future work should consider both types. A typical SCR circuit is shown in Figure 5.10.

5.3.2.1 Dump (Discharge) Resistor

Several types of dump resistors have been used in past S/C magnet applications and an absolute selection for MSBS doesn't appear necessary at this time. However, several features in the dump resistors concept should be established at this time. A long dump time constant should be employed if possible, so that the magnet involved will provide a field as long as possible to allow the system control time to initiate corrective action. Also, the cooling concept should not be dependent on plant or building services that would shut down the cooling system during a service failure. Figures 5.6, 5.7 and 5.8 provides a tabulation of the various dump resistor features. Note that the larger energy dissipation requirements call for water that is not pump dependent and the smaller energy dissipation requirements call for convection cooling. The intermediate ratings will require detailed design study. For comparison, Figure 5.11 is a drawing of the CDIF water cooled 186MJ dump resistor. It is expected that costs and delivery would be comparable for either air or water cooling.

5.3.3 INSTRUMENTATION CONCEPTS

Figure 5.12, Measurement Requirements, is a table of proposed instrumentation for all components in each superconducting magnet. As indicated in the approach presented in Para. 5.2.3, this list presents minimum quantities to operate and protect a magnet plus a moderate addition for use during acceptance tests, cooldown, and diagnostic mounting.

A brief discussion is presented of sources and installation.

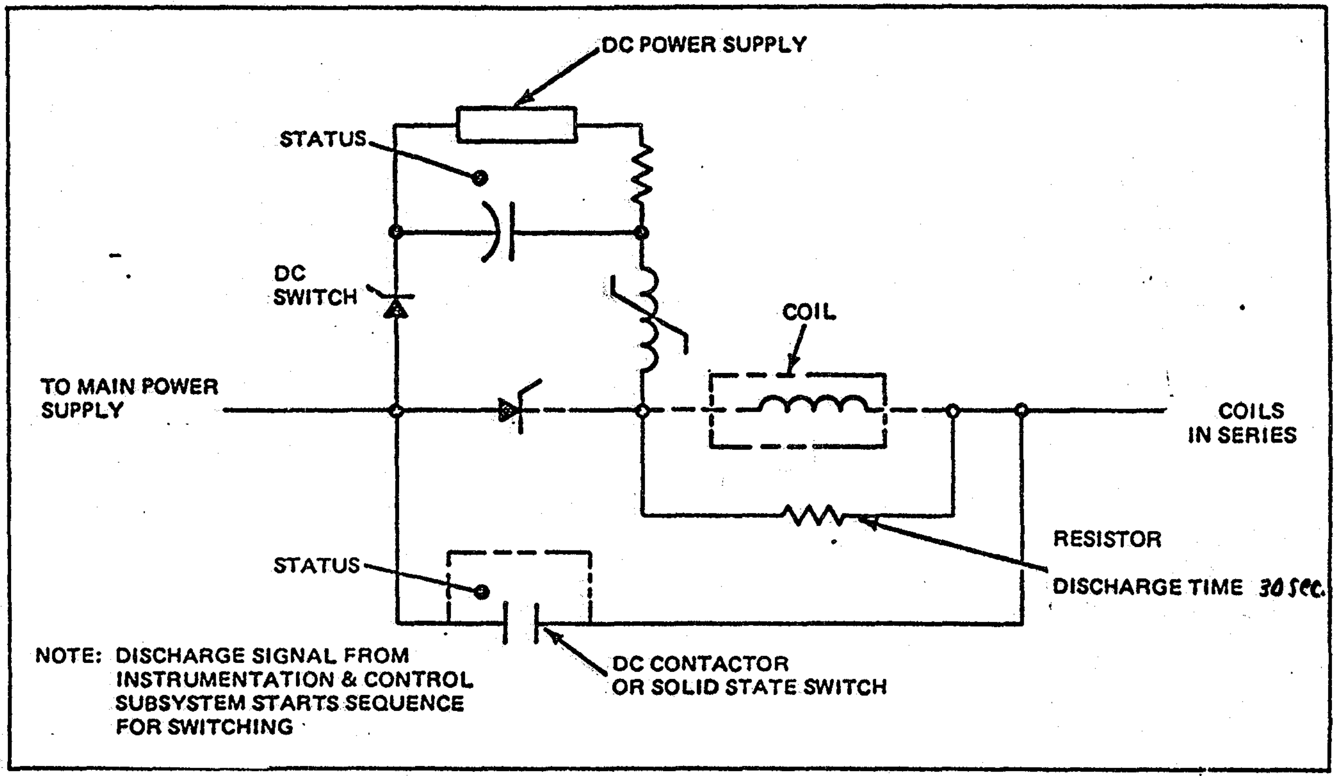

Figure 5.10
COIL PROTECTION CIRCUIT

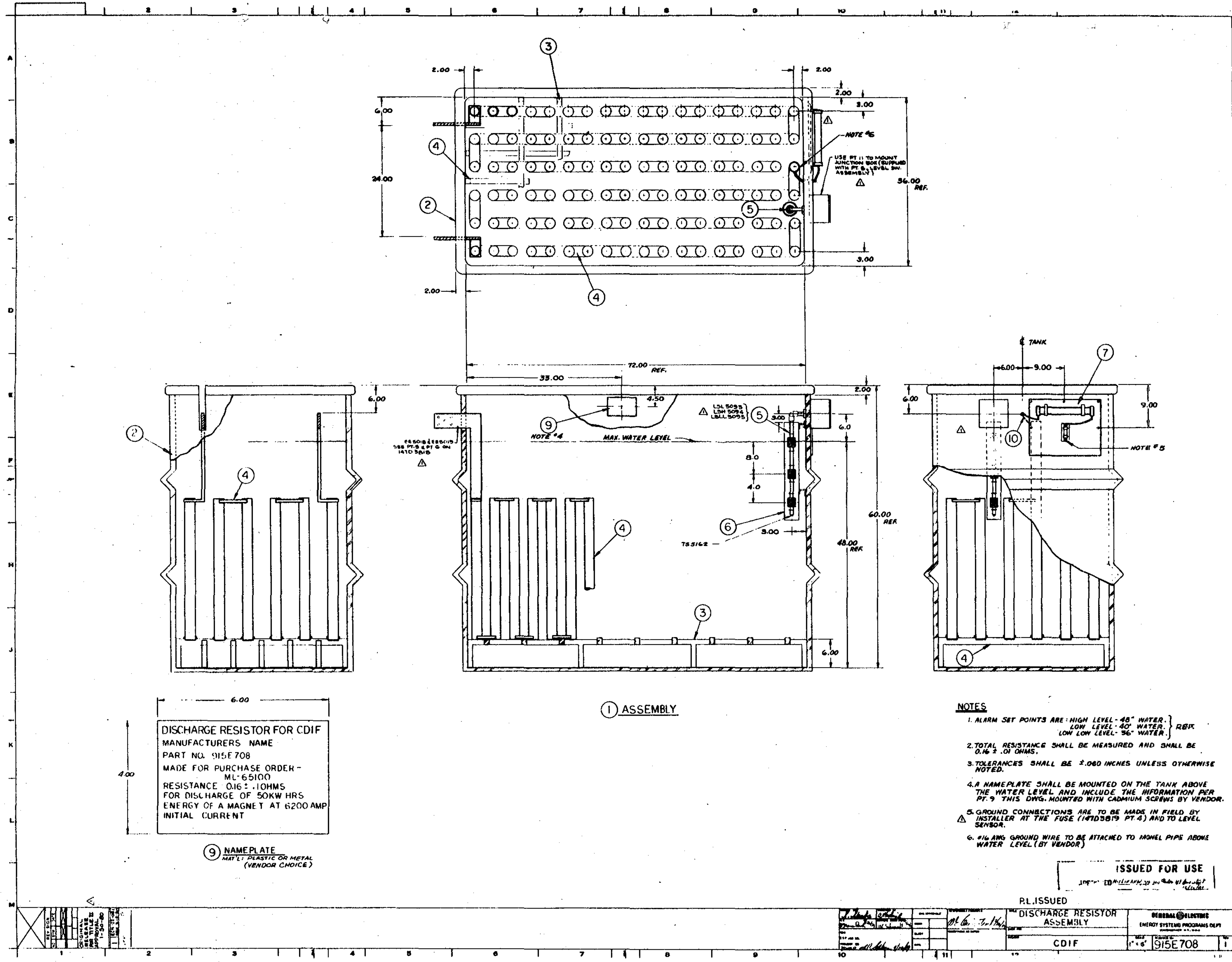
2.00
6.00
24.00
36.00 REF.
3.00
NOTE #6
USE PT. 11 TO MOUNT JUNCTION BOX (SUPPLIED WITH PT. 6, LEVEL SW. ASSEMBLY)
72.00 REF.
33.00
4.50
MAX. WATER LEVEL
NOTE #4
60.00 REF
48.00 REF.
NOTE #5
9.00
6.00
€ TANK
ASSEMBLY
DISCHARGE RESISTOR FOR CDIF
MANUFACTURERS NAME
PART NO. 915E708
MADE FOR PURCHASE ORDER - ML-65100
RESISTANCE 0.16 ± .1OHMS
FOR DISCHARGE OF 50KW HRS
ENERGY OF A MAGNET AT 6200 AMP
INITIAL CURRENT
NAMEPLATE
MAT'L: PLASTIC OR METAL (VENDOR CHOICE)
NOTES
1. ALARM SET POINTS ARE: HIGH LEVEL - 48" WATER. LOW LEVEL - 40" WATER. LOW LOW LEVEL - 36" WATER. } REF.
2. TOTAL RESISTANCE SHALL BE MEASURED AND SHALL BE 0.16 ± .01 OHMS.
3. TOLERANCES SHALL BE ±.060 INCHES UNLESS OTHERWISE NOTED.
4. A NAMEPLATE SHALL BE MOUNTED ON THE TANK ABOVE THE WATER LEVEL AND INCLUDE THE INFORMATION PER PT. 9 THIS DWG. MOUNTED WITH CADMIUM SCREWS BY VENDOR.
5. GROUND CONNECTIONS ARE TO BE MADE IN FIELD BY INSTALLER AT THE FUSE (141D5819 PT. 4) AND TO LEVEL SENSOR.
6. #16 AWG GROUND WIRE TO BE ATTACHED TO MONEL PIPE ABOVE WATER LEVEL (BY VENDOR)
ISSUED FOR USE
P.L. ISSUED
DISCHARGE RESISTOR ASSEMBLY
GENERAL ELECTRIC
ENERGY SYSTEMS PROGRAMS DEPT
CDIF
915E708

Figure 5.11

Figure 5.12

MEASUREMENT REQUIREMENT

	Type & (Sensor)	Qty	Protect	Control	Alarm	Diagnostic
Magnet	Quench Voltage (Voltage Taps)	8	X		X	X
	Current Lead Voltage (Voltage Taps)	4	X		X	X
	Current Lead Temp. (T/C's)	4	X		X	X
	Continuous LH_e Level (S/C Wire)	4		X(2)	X(2)	X
	Vacuum (ion gauge)	2	X		X	X
	Pressure (Strain Gage Xducer)	1				X
	Structure Temp. (T/C's)	12				X
	LH_e Temp. (Carbon Glass Sensors)	6				X
Power Supply	AC Voltage (Voltage Taps)	1				X
	AC Current (Hall Xducer)	1				X
	DC Voltage (Voltage Taps)	1		X		X
	DC Current (Shunt Xducer)	1		X		X
	Temperature (Thermal Switches)	3			X	X
	Status: ON (Switches &/or Relays as required)	1		X		X
	Status: OFF (Switches &/or Relays as required)	1		X		X
	Status: BYPASS (Switches &/or Relays as required)	1			X	X
	Status: Internal Problem (Switches &/or Relays as required)	1			X	X
Dump Resistor	Temperature (T/C)	1				X
	Water Level (Float)	1			X	X
	Ground Fault (Voltage Taps)	1	X		X	X
Dump Switch	Open (Switch &/or Relays)	1			X	X
	Closed (Switch &/or Relays)	1		X		X
	Power Available (Voltage Taps)	1			X	X

Coil Quench Detection - Quench detection will be carried out with voltage taps that are attached to eight approximately equal sections of the coil. Each voltage tap connection will be accomplished by bolting a wire to the interpancake connection at the top of the coil. The bolted connection provides mechanical integrity and is impregnated with indium solder for good electrical continuity. Each voltage tap will have provision for multiple connection and wiring so that a three level redundant circuit hookup to the coil protection system is available.

Current Lead Voltage - Voltage taps similar to quench detector will be used for measuring voltage across the gas-cooled current leads to detect an unexpected lead heatup. Double wiring is employed to provide redundant measurements for the protection system.

Temperature - Two types of temperature sensors will be employed. Sensors calibrated in the 100-300K range will be installed inside and outside the coil case for measurement of cooldown and warmup. Sensors will be matched to meet required accuracy and to be interchangeable on readout. Sensors for operation will be carbon glass, which will double in use as point level sensors during initial helium fill. Calibration of the carbon glass will take into account the operation in liquid and gas.

Liquid Helium Level - Level sensors made from superconducting cable will be installed in each coil stack. These sensors are capable of single point or continuous level output based on available readout circuitry. Two probes will be installed in each stack to provide operational redundancy.

Pressure - Each stack has provision for measuring pressure in the coil case and each coil will be provided with a pressure transducer. This is considered to be a valuable measurement for use in diagnostic testing, operation of cryogenic supply system, and for overpressure alarm.

Other Sensors - Other sensors and/or measurements are coil voltage and current, dump switch position, ground fault indication, dump resistor cooling, power supply configuration and others involved with magnet operation.

Verification and Testing - All instrumentation equipment proposed has been previously used by GE in the CDIF, LCP, or other superconducting designs. Verification of the measurement method or sensors is not considered to be necessary beyond this history. However, each sensor installation design includes qualification and/or acceptance tests. Testing of "as-installed" sensors is included in verification testing.

Instrumentation Leads - Leads and cabling for MSBS will be stranded silver-plated copper conductor with Kapton/FEP teflon insulation. Shielding will be provided where required by tape wrapped aluminum/Kapton with a silver-plated copper drain wire. Requirement will be based on existing military specification MIL-W-81381 and MIL-C-27500. All cable insulation will be rated for 1000 volts dc minimum. Special insulation will be added where higher voltages used to power or dump the coil are encountered.

Cable Routing - Cable for all sensors will be routed to minimize interference with coil components. Routing design will make effective use of cabling and bundling techniques. Exit from the helium space will be through the stack directly to air. Heat inputs will be minimized by use of small wire and cable and a deliberately long lead length in the gas space prior to exit. The feedthru connectors will have a pipe extension above the stack to insure operation at room temperature air to avoid icing of the electrical connections.

Measurement Accuracy - There are no known problem areas in measurement accuracy, with the possible exception of DC current to the magnet coils, where .01% may be required. In the present concept, this measurement will be made using a current shunt which has commercially available accuracy in the .1 to .2% range. A special design using a temperature controlled environment around the shunt will be required to obtain the .01% accuracy.

5.4 TECHNICAL RISKS

The concepts for power supplies, protection and instrumentation are within the state-of-the-art of superconducting magnet technology. However, Case 1 and Case 2 provide a design challenge to meet the peak reactive power requirements.

All components listed in Figures 5.6, 5.7 and 5.8, but power supplies, are in, or approaching off-the-shelf status. Furthermore, power supplies for the steady state and low reactive power requirements have been built and are readily available. However, difficult packaging and interfacing design problems will be encountered to meet the high reactive power requirements.

Consideration of using MSBS in a test duty cycle during off peak power usage time has been evaluated, but the peak power demand still appears too high for most commercial power companies to supply. The use of an energy storage system to allenate this problem will involve design of equipment beyond the scope of the present MSBS statement of work.

The single design parameter that has most impact in the risk and complexity of the power supply and protection is peak voltage. This, in turn, is dependent on reactive power required, which is tied to dynamic current rate-of-change requirements of the MSBS.

5.8 SECTION 5 REFERENCE SOURCES

The following tabulation includes, but is not the limit, of sources which were called upon to establish design feasibility, cost & schedule data for the MSBS power supply, protection and instrumentation effort. Past experience and contact with project and personnel at Lawrence Livermore National Laboratory, Argonne National Laboratory, Oak Ridge National Laboratory, MIT/FBNML and several other components within GE were called upon for data utilized in the MSBS study.

Subjects	Sources
Power Supply Concepts & SCR Design Feasibility	GE - Electric Utility System Equipment Department, Schenectady, New York. R. Pohl - Consulting Engineer
Power Supply Availability and Cost	GE - Drive Systems Department Salem, Virginia. Wm. O'Brien - Product Planning Engineer
Energy Storage & Wind Tunnel Design TFTR AC Storage Generator	GE - Marine & Defense Facilities Schenectady, New York. Malcolm Houton - Systems Design Engineer
Power Supply Availability, Cost and Energy Storage	GE - Energy Systems Programs Department ETF/Fusion DOE Design Team Oak Ridge National Lab, Oak Ridge, Tennessee. George E. Gorker - Project Engineer
Discharge Switching	GE - Switchgear Department Philadelphia, PA. Charles Titus - Senior Design Eng.
Protection Electronics	GE - Materials & Processes Laboratory Schenectady, New York. J.M. Reschovsky - Mgr. Advanced Design
Power Supply Availability and Cost Estimate	- Robicon Corporation Pittsburgh, PA
Power Supplies	- Sabon Electric Warner, NH
Power Supplies	- Trancnex/Bulton Ind. Carson, California
Power Supplies	- PRW Inc. Westfield, Indiana

FOOTNOTES

(1) Protection Instrumentation for a Large Superconducting Magnet J.M. Reschovsky, P.C. Bronw, W.R. Court, and W.E. Overstreet, General Electric Company, Eighth Symposium on Engineering Problems of Fusion Research, Nov. 1979.

(2) a) R. Pohl - Consulting Engineer, Electronics Utility System Equipment Department - GE - Schenectady, New York.

b) W. O'Brien - Product Planning Engineer, Drive Systems Department - GE - Salem, Virginia.

(3) Robicon Corporation, Pittsburgh, PA - Keith Sueker - Manager, Engineering

6.0 CONTROL SYSTEM CONCEPTS

6.1 INTRODUCTION

The purpose of the control system is to provide the following functions:

- Suspension of the model with specified position and attitude accuracies
- Forced model sinusoidal oscillations for dynamic tests
- Limits on the maximum position and orientation errors to insure safe and reliable operation
- Inputs to the aerodynamic data acquisition, computation and display subsystems

The control system for the MSBS as shown in Figure 6.1 is a position servo by which the suspended model with six degrees of freedom is required to follow given static or dynamic input commands. The position and orientation of the model is measured by position sensors. The difference between the command inputs and the measured model position and orientation signals are modified by a dynamic compensator. The outputs of the control compensator are corrected for the static model attitudes, then amplified and applied to the suspension system magnet coils. The magnetic fields produce magnetic forces and movements defined in a wind tunnel coordinate system. The magnetic forces and torques added to the aerodynamic and gravity forces and torques, act through the model inertia to cause changes in the position and attitude of the model. These changes are measured by the position sensor system and the feedback loop is closed. The function of the feedback loop is to minimize the integral of the absolute position error by continuously counteracting the aerodynamic and gravity loads. The magnet currents are measured to determine the aerodynamic forces and movements acting on the model with appropriate calibrations.

The purpose of the compensator is to provide the control system stability and good dynamic response characteristics. A major consideration in the compensator design is to minimize the effects of aerodynamic and magnetic cross couplings such that each control loop operates with minimum interaction. The compensator design is based on the multivariable control theory that treats all inputs and outputs in a matrix fashion. The basic approach is to determine a matrix compensator to decouple the system at an appropriate high frequency and then design a dynamic compensation to stabilize each control loop.

TOP LEVEL SCHEMATIC OF CONTROL SYSTEM

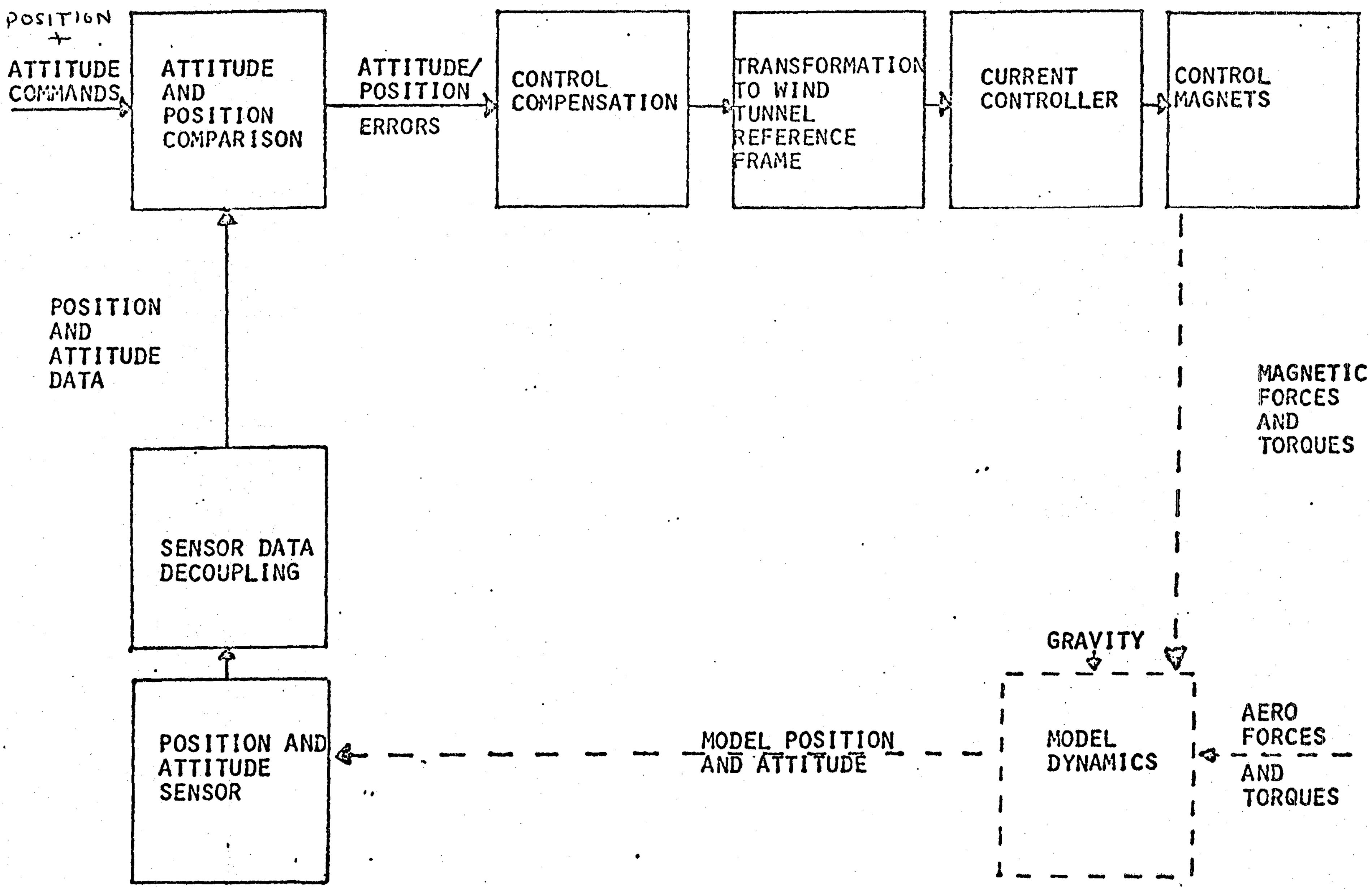

Figure 6.1

The organization of the section is as follows. In section 6.2, the static and dynamic model position and attitude accuracy requirements for the control system are given. In section 6.3, mathematical models to represent the dynamics of the suspended model, the aerodynamic and the magnetic cross couplings are developed. These relations are used to design the control compensator in section 6.4. The control system response for step, sinusoidal and random input commands is simulated in section 6.5. The computer selection, hardware and software modules required to implement the control system are presented in section 6.6.

6.2 PERFORMANCE REQUIREMENTS

The RFQ indicates a performance requirement for establishing and holding the position and attitude of the model with within $\pm$ 0.01 inches and $\pm$ 0.02° respectively of a commanded value. A tentative error budget is proposed which allocate maximum position and attitude measurement errors one half this (i.e., $\pm$ .005 in. and 0.01° respectively). During the course of the investigation, it was agreed that this requirement applied primarily to the static case and not to the case of forced oscillations.

6.3 PRELIMINARY MATHEMATICAL DYNAMIC MODEL DEVELOPMENT

Identification and modeling the system characteristics for the suspended model, gradient magnets and the power supply is presented in the following.

Let x, y, z denote the wind tunnel axis coordinate system, with the x axis against the direction of the wind, the z axis in the direction of gravity, and the y axis orthogonal to form a right-handed coordinate system. In the analytical development, the model displacement is assumed small, about a static model attitude. The aerodynamic and magnetic cross couplings of smaller magnitude are omitted to simplify the analysis.

6.3.1 Aerodynamic and Inertial Coupling

The aerodynamic and inertial response are best described in "stability axes" which are defined as being aligned with the relative wind for steady state flight conditions. Hence, "stability axes" are coincident with wind tunnel axes. Since, in the wind tunnel there are no steady state translational or rotational velocities of the model relative to an inertial frame, most of the inertial coupling terms which would otherwise occur do not exist.

The aerodynamic and inertial models which have been used in the control system development follow the common convention of separation into longitudinal and lateral response. (However, an extension to fully coupled 5 or even 6 degrees of freedom as might be required in any future free flight tunnel application could be readily implemented, if so desired.)

The response equations expressed in wind tunnel axes employed in the control system development are shown for the longitudinal and lateral mode, respectively, in Figures 6.2 and 6.3.

6.3.2 Magnetic Coupling

The cross-coupling of magnetic forces and torques will occur whenever the core of the model is oriented away from its "initial" orientation along the "x" axis. This has been developed elsewhere[1] and will be adopted here for the presently proposed configuration of magnets.

Force Response

Consider first the force response. Magnetic force is proportional to the product of the magnetic field gradient and the magnetization vector and is given by equation (6.1). But the magnetization vector for a soft iron core is best defined in a model frame of reference as being proportional to the product of the magnetic field and a demagnetization matrix. For an ellipsoidally shaped ideal core, the off-diagonal demagnetization terms are equal to zero. For a highly elongated ellipsoid, a single term on the diagonal will dominate, here defined as $1/D_A$ where D_A is the non-dimensional demagnetization along the core axis. The present core is sufficiently close to an elongated ellipsoid to justify this approximation given by equation (6.2). Hence, the magnetic force in the wind tunnel is obtained by making suitable linear transformations of the magnetic field vector and the magnetization vector, respectively, to and from the model frame of reference as shown in equation (6.3). M is defined as the transformation from the wind tunnel frame of reference to the model frame of reference as expressed in the needed Euler angles and M^{-1} is its inverse (and being an orthogonal transformation, its transpose). For 3 angular degrees of freedom, M is expressed in equation (6.4).

Attitude is derived here by Euler angles defined in a non-commutative sequence of yaw (Φ), pitch (θ) and roll (ϕ).

1. See, for example, a similar development in: Gilliam, G., "Data Reduction Techniques for Use with a Wind Tunnel Magnetic Suspension and Balance System, MIT Aerophysics Lab Tech Report 167, June 1970.

FIGURE 6.2

LONGITUDINAL MODE WITH THREE

DEGREES OF FREEDOM

Drag $\ddot{x} = X_\alpha \alpha + X_u \dot{x} + \frac{F_x}{m}$

Heave $\ddot{z} = Z_\alpha \alpha + \frac{F_z}{m}$

Pitch $\ddot{\theta} = M_\alpha \alpha + M_{\dot{\alpha}} \dot{\alpha} + M_q \dot{\theta} + \frac{T_y}{I_{yy}}$

Angle of Attack $\alpha = \theta - \frac{\dot{z}}{V}$

where $Z_\alpha = \frac{\partial \ddot{z}}{\partial \alpha}$; $M_\alpha = \frac{\partial \ddot{\theta}}{\partial \alpha}$ etc. are the linearized dimensional aerodynamic parameters.

V = Free stream wind velocity

F_x = Magnetic force in the x direction

F_z = Magnetic force in the z direction

T_y = Magnetic torque about the y axis

m = Mass of the model

I_{yy} = Moment of inertia about pitch axis

FIGURE 6.3

LATERAL MODE WITH THREE

DEGREES OF FREEDOM

Roll

$$\dot{p} = \dot{r}\frac{I_{xz}}{I_{xx}} + L_r r + L_{\dot{r}}\dot{r} + L_p p + L_{\dot{p}}\dot{p} + L_\beta \beta + L_{\dot{\beta}}\dot{\beta} + \frac{T_x}{I_{xx}}$$

Yaw

$$\dot{r} = \dot{p}\frac{I_{xz}}{I_{zz}} + N_r r + N_{\dot{r}}\dot{r} + N_p p + N_{\dot{p}}\dot{p} + N_\beta \beta + N_{\dot{\beta}}\dot{\beta} + \frac{T_z}{I_{zz}}$$

Side

$$\ddot{y} = Y_\beta \beta + Y_{\dot{\beta}}\dot{\beta} + Y_r r + Y_{\dot{r}}\dot{r} + Y_{\dot{p}}\dot{p} + \frac{F_y}{m}$$

Sideslip

$$\beta = \Psi - \frac{\dot{y}}{V} \qquad p \sim \dot{\phi} \qquad r \sim \dot{\Psi}$$

F_y = Magnetic side force
T_z = Magnetic yaw torque
T_x = Magnetic roll torque
Ψ = Yaw angle
r = Yaw rate
p = Roll rate

I_{xz} = Cross product of inertia (results in inertial coupling due to non-symmetry of model about z axis)

Other terms defined in analogous manner.

FORCE RESPONSE

$$\begin{bmatrix} F_x \\ F_y \\ F_z \end{bmatrix} = \begin{bmatrix} \frac{\partial H_x}{\partial x} & \frac{\partial H_x}{\partial y} & \frac{\partial H_x}{\partial z} \\ \frac{\partial H_y}{\partial x} & \frac{\partial H_y}{\partial y} & \frac{\partial H_y}{\partial z} \\ \frac{\partial H_z}{\partial x} & \frac{\partial H_z}{\partial y} & \frac{\partial H_z}{\partial z} \end{bmatrix} \begin{bmatrix} M_x \\ M_y \\ M_z \end{bmatrix}$$

Eq. (6.1)

$$\begin{bmatrix} M_A \\ M_B \\ M_C \end{bmatrix} = \begin{bmatrix} \frac{1}{D_A} & 0 & 0 \\ 0 & 0 & 0 \\ 0 & 0 & 0 \end{bmatrix} \begin{bmatrix} H_A \\ H_B \\ H_C \end{bmatrix}$$

Eq. (6.2)

$$\begin{bmatrix} F_x \\ F_y \\ F_z \end{bmatrix} = \begin{bmatrix} \frac{\partial H_x}{\partial x} & \frac{\partial H_x}{\partial y} & \frac{\partial H_x}{\partial z} \\ \frac{\partial H_y}{\partial x} & \frac{\partial H_y}{\partial y} & \frac{\partial H_y}{\partial z} \\ \frac{\partial H_z}{\partial x} & \frac{\partial H_z}{\partial y} & \frac{\partial H_z}{\partial z} \end{bmatrix} [M]^T \begin{bmatrix} \frac{1}{D_A} & 0 & 0 \\ 0 & 0 & 0 \\ 0 & 0 & 0 \end{bmatrix} [M] \begin{bmatrix} H_x \\ H_y \\ H_z \end{bmatrix}$$

Eq. (6.3)

$$[M] = \begin{bmatrix} \cos\theta\cos\psi & \sin\psi\cos\theta & -\sin\theta \\ -\sin\psi\cos\phi + \sin\phi\cos\psi\sin\theta & \cos\psi\cos\phi + \sin\phi\sin\psi\sin\theta & \sin\phi\cos\theta \\ \sin\psi\sin\phi + \cos\phi\cos\psi\sin\theta & -\sin\phi\cos\psi + \cos\phi\sin\psi\sin\theta & \cos\phi\cos\theta \end{bmatrix}$$

Eq. (6.4)

Carrying out this complete multiplication (not shown in detail here) leads to a force vector having many terms each of which is product of a field, a field gradient and sinusoidal functions of Euler angles.

But, in an idealized model each field component and each field gradient component is proportional to a current. Hence, each component of force is made up of a series of terms which are the product of two currents and sinusoidal functions of the Euler angles. Consider the simple case where the only non-zero Euler angle is pitch angle. Then, the force relationship is shown in equation (6.5). The relationship between field and field gradient and current is shown in equation (6.6).

Making the substitution and using appropriate constants of proportionality results in the forces as a function of current (equations 6.7 and 6.8). The heave force (F_z) and the drag force (F_x) are used in the response equations for the longitudinal mode.

Following a similar approach, the side forces can be written as functions of currents and sinusoidal functions of Euler angles for the small angle approximation of the lateral mode (i.e., $\Theta = 0$ and Ψ and ϕ are small). (Equation 6.9) This is used in the response equations for the lateral mode.

6.3.3 Torque Response

The torque response can be developed in a similar way. The torque on the core is proportional to the vector cross product of the magnetization vector and the magnetic field. As before, the core magnetization vector must be transformed from the model frame of reference. The torque response can then be expressed by equation 6.10. Each component of torque is then expressed as a summation of terms each of which is proportional to a product of magnetic field components and sinusoidal functions of Euler angles.

For the case where pitch angle is the only non-zero Euler angle, then the torque response reduces to that of equation 6.11. Expressing the torque component about the pitch axis (y) in terms of magnet currents and neglecting the field due to roll coils results in equation 6.12. This is the equation used in the longitudinal mode to express the magnetic torque about the pitch axis.

In a similar manner, the magnetic torque about the yaw and roll axes can be developed for the lateral mode. (Equations 6.13 and 6.14). In these equations, only a simplified non-coupled response of the roll torque coils is included. This is adequate for small angle response. Further development of

$$\begin{bmatrix} F_x \\ F_y \\ F_z \end{bmatrix} = \begin{bmatrix} \frac{\partial H_x}{\partial x}\left(H_x\cos^2\theta - H_z\sin\theta\cos\theta\right) + \frac{\partial H_x}{\partial z}\left(-H_x\cos\theta\sin\theta + H_z\sin^2\theta\right) \\ \frac{\partial H_y}{\partial x}\left(H_x\cos^2\theta - H_z\sin\theta\cos\theta\right) + \frac{\partial H_y}{\partial z}\left(-H_x\cos\theta\sin\theta + H_z\sin^2\theta\right) \\ \frac{\partial H_z}{\partial x}\left(H_x\cos^2\theta - H_z\sin\theta\cos\theta\right) + \frac{\partial H_z}{\partial z}\left(-H_x\cos\theta\sin\theta + H_z\sin^2\theta\right) \end{bmatrix}$$

Eq. (6.5)

BUT

$$\frac{\partial H_x}{\partial x} = K_D I_D$$

$$\frac{\partial H_y}{\partial x} = K_{F1}(I_3 + I_4)$$

$$\frac{\partial H_z}{\partial x} = \frac{\partial H_x}{\partial z} = K_{F2}(I_1 + I_2)$$

$$\frac{\partial H_y}{\partial z} = \frac{\partial H_z}{\partial z} = 0$$

Eq. (6.6)

$$H_x = K_M i_M$$

$$H_y = K_{T2}(I_3 - I_4)$$

$$H_z = K_{T1}(I_1 - I_2)$$

Where

I_M	Magnetization Coil Current
I_D	Drag Coil current.
I_1, I_2	vertical gradient coil currents
I_3, I_4	Side gradient coil currents

The heave force is given by

$$F_Z = K_{F_1} K_M I_M (I_1 + I_2) \cos^2\theta$$

$$- K_{F_1} K_{T_1} (I_1 + I_2)(I_1 - I_2) \sin\theta \cos\theta$$

Eq. (6.7)

Drag Force is given by

$$F_x = K_D K_M I_D I_M \cos^2\theta - K_D K_{T1} i_D (I_1 - I_2)\cos\theta\sin\theta$$
$$- K_m K_{F1} i_m (I_1 + I_2)\cos\theta\sin\theta + K_{T1} K_{F1} (I_1 + I_2)(I_1 - I_2)\sin^2\theta$$

Eq. (6.8)

Force Lateral Mode is given by

$$F_y = K_M K_{F2} (I_3 + I_4) I_m + K_{F2} K_{T2} (I_3 + I_4)(I_3 - I_4)\sin\psi$$

Eq. (6.9)

<u>Torque Response</u>

$$\begin{bmatrix} T_x \\ T_y \\ T_z \end{bmatrix} = [M]^T \begin{bmatrix} \frac{1}{D_A} & 0 & 0 \\ 0 & 0 & 0 \\ 0 & 0 & 0 \end{bmatrix} [M] \begin{bmatrix} H_x \\ H_y \\ H_z \end{bmatrix} \times \begin{bmatrix} H_x \\ H_y \\ H_z \end{bmatrix}$$

Eq. (6.10)

For $\psi = 0 \quad \phi = 0$:

$$\begin{bmatrix} T_x \\ T_y \\ T_z \end{bmatrix} = \frac{1}{D_A} \begin{bmatrix} H_y H_x \cos\theta\sin\theta - H_y H_z \sin^2\theta \\ H_z H_x \cos^2\theta - H_z^2 \sin\theta\cos\theta + H_x^2 \cos\theta\sin\theta - H_x H_z \sin^2\theta \\ H_x H_y \cos^2\theta - H_y H_z \sin\theta\cos\theta \end{bmatrix}$$

Eq. (6.11)

Pitch Torque is given by

$$T_y = k_M k_{T_1} I_m (I_1 - I_2)(\cos^2\theta - \sin^2\theta) + k_M^2 I_m^2 \cos\theta \sin\theta - k_{T_1}^2 (I_1 - I_2)^2 \sin\theta \cos\theta \qquad \text{Eq. (6.12)}$$

Yaw Torque (for $\theta = 0$, ψ and ϕ small) is given by

$$T_z = k_M k_{T2} (I_3 - I_4) I_M + k_{T2}^2 (I_3 - I_4)^2 \sin\psi - k_M^2 I_M^2 \sin\psi \qquad \text{Eq. (6.13)}$$

Roll Torque is given by

$$T_x = k_{R1} k_{R2} I_R \qquad \text{Eq. (6.14)}$$

where I_R is the roll magnet current.

the response of the roll coils for large angles including cross coupling effect will be required in the future control system design effort.

6.3.4 Power Supply and Magnet Coils

For the preliminary design, it is assumed that each gradient magnet has a separate power supply with 20 Hz bandwidth. The transfer function of the power supply and the magnet can be represented by

$$\frac{I(s)}{V(s)} = \frac{10^5}{L(1 + 0.008s)s} \tag{6.15}$$

Where L is the self inductance of the gradient coil. I(s) and V(s) are the Laplace transforms of the coil current and the power supply input voltage respectively. The mutual inductances between the magnet coils are small and can be neglected in the control design.

6.4 CONCEPTUAL DESIGN OF THE CONTROL SYSTEM

This section describes the design of a control system to provide the stability and response characteristics of the magnetic suspension system. The analytical models developed in the previous section with a representative aerodynamic and magnetic parameters are used to simulate the cross couplings in the control system. A matrix compensator is designed such that each control loop operates with minimum interaction. The control system stability is achieved with velocity and position feedback loops.

6.4.1 Aerodynamic and Magnetic Couplings

A state variable representation is used to study the aerodynamic and magnetic cross couplings in the MSBS system. The response of the system with no feedback is simulated for step changes in the applied forces and torques.

6.4.1.1 Longitudinal Mode

A state variable model for the longitudinal mode (heave, pitch and drag) defined in Table 6.1 is given by

$$\frac{d}{dt}\begin{bmatrix}\dot{z}\\ \theta\\ \dot{\theta}\\ \dot{x}\end{bmatrix} = \begin{bmatrix}-\frac{Z_\alpha}{V} & Z_\alpha & 0 & 0\\ 0 & 0 & 1 & 0\\ -\frac{M_\alpha}{V} & M_\alpha & M_{\dot{\alpha}}+M_q & 0\\ -\frac{X_\alpha}{V} & X_\alpha & 0 & X_u\end{bmatrix}\begin{bmatrix}\dot{z}\\ \theta\\ \dot{\theta}\\ \dot{x}\end{bmatrix} + \begin{bmatrix}\frac{1}{m} & 0 & 0\\ 0 & 0 & 0\\ 0 & \frac{1}{I_{yy}} & 0\\ 0 & 0 & \frac{1}{m}\end{bmatrix}\begin{bmatrix}F_z\\ T_y\\ F_x\end{bmatrix}$$

Eq. (6.16)

A block diagram of the system transfer function is given in Figure 6.4. The parameters used for the control design are given in Figure 6.5. The longitudinal mode response is simulated for 1 lb-ft torque step input as seen in Figure 6.6. It is seen that a major coupling exists between the heave and pitch axis. The response to a 10 lb. force step input is shown in Figure 6.7.

The magnetic forces and torque in the longitudinal mode are given by equations (6.7), (6.8) and (6.12). The parameters obtained from the magnet design are given in Figure 6.8. A linearized relation for a static pitch angle θ_0 between the forces, torque and the currents is given by

$$\begin{bmatrix}F_z\\ T_y\\ F_x\end{bmatrix} = \begin{bmatrix}\cos^2\theta_0 & 0 & 0\\ 0 & (\cos^2\theta_0 - \sin^2\theta_0) & 0\\ 0 & 0 & \cos^2\theta_0\end{bmatrix} \cdot \quad *$$

Eq. (6.17)

*Equation continued on page 189.

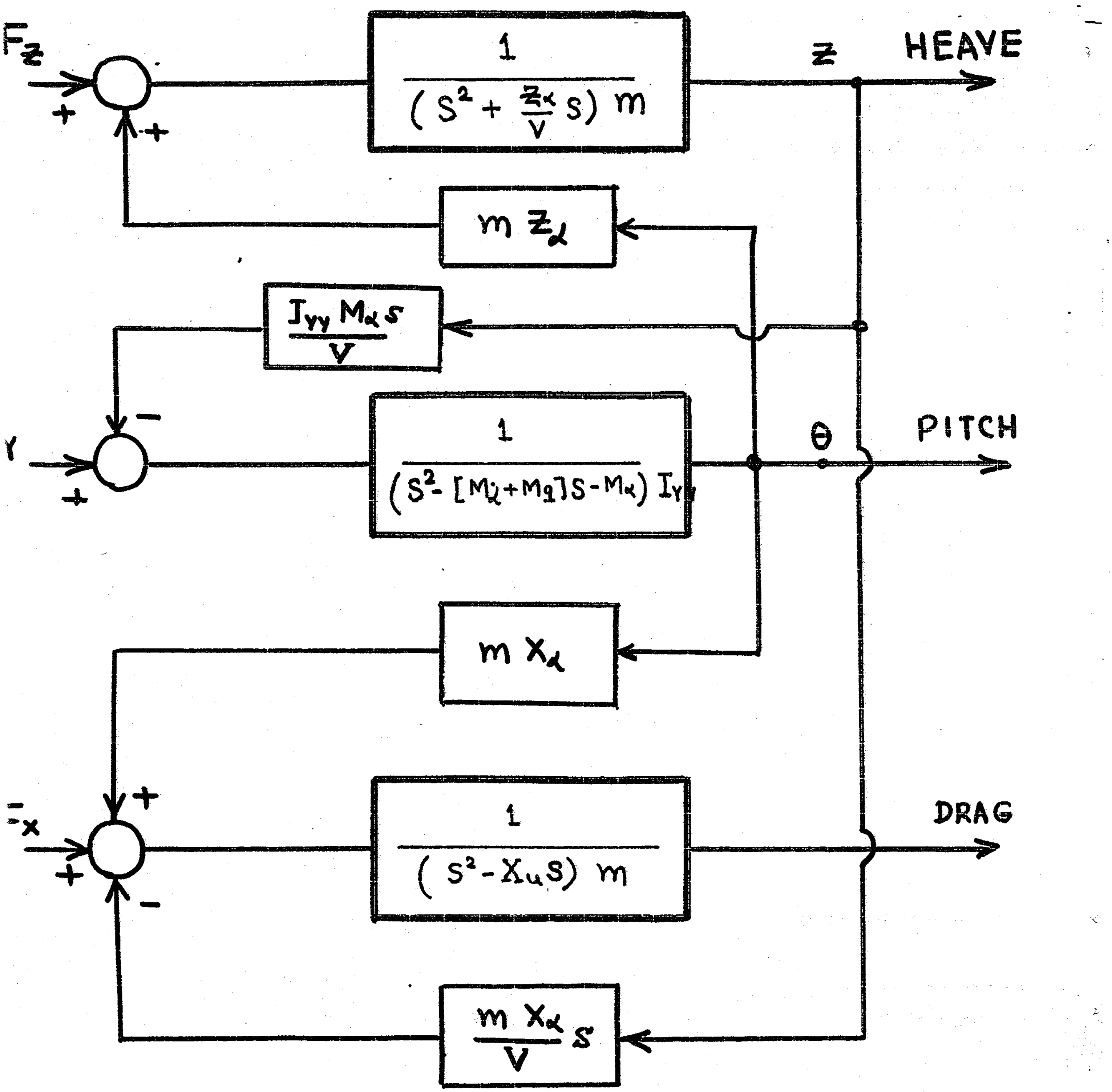

AERODYNAMIC COUPLING (LONGITUDINAL MODE)

Figure 6.4

FIGURE 6.5

PARAMETERS USED FOR LONGITUDINAL MODE

PARAMETERS	UNITS	EXPECTED RANGE			VALUES USI
		CASE 1	CASE 2	CASE 3	(CASE 1)
Z_α	Ft / SEC^2	500 TO 2000	40 TO 200	1000 TO 4000	1000
M_α	1/ SEC^2	-200 TO 200	-10 TO 10	-200 TO 200	-40
$M_{\dot\alpha}$	1/ SEC	-5 TO -1	-1.0 TO -0.2	-20 TO -4	-1
M_q	1/SEC	-10 TO -3	-2.0 TO -0.5	-30 TO -6	-3
X_α	Ft/SEC^2	-100 TO -10			-30
X_u	1/ SEC	-0.1 TO -0.01			- 0.03
V	Ft/SEC				1000
m	SLUGS	6.2	6.2	0.75	6.2
I_{yy}	SLUG-FT^2	2.98	2.98	0.0931	2.98

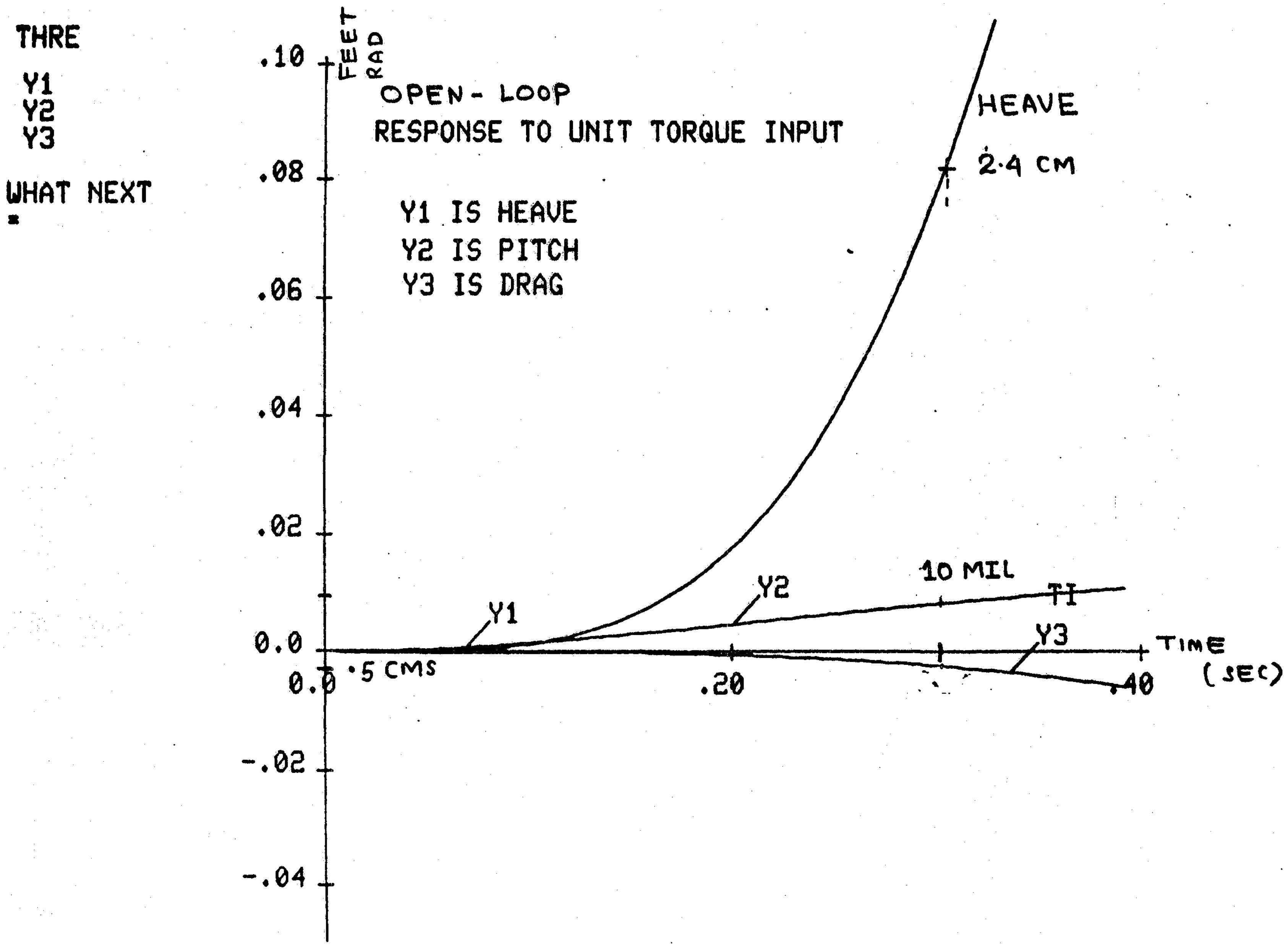

THRE
Y1
Y2
Y3
WHAT NEXT
*
FEET
RAD
OPEN-LOOP
RESPONSE TO UNIT TORQUE INPUT
Y1 IS HEAVE
Y2 IS PITCH
Y3 IS DRAG
HEAVE
2.4 CM
10 MIL
.5 CMS
Y1
Y2
Y3
.10
.08
.06
.04
.02
0.0
-.02
-.04
0.0
.20
.40
TIME
(SEC)

FIGURE 6.6

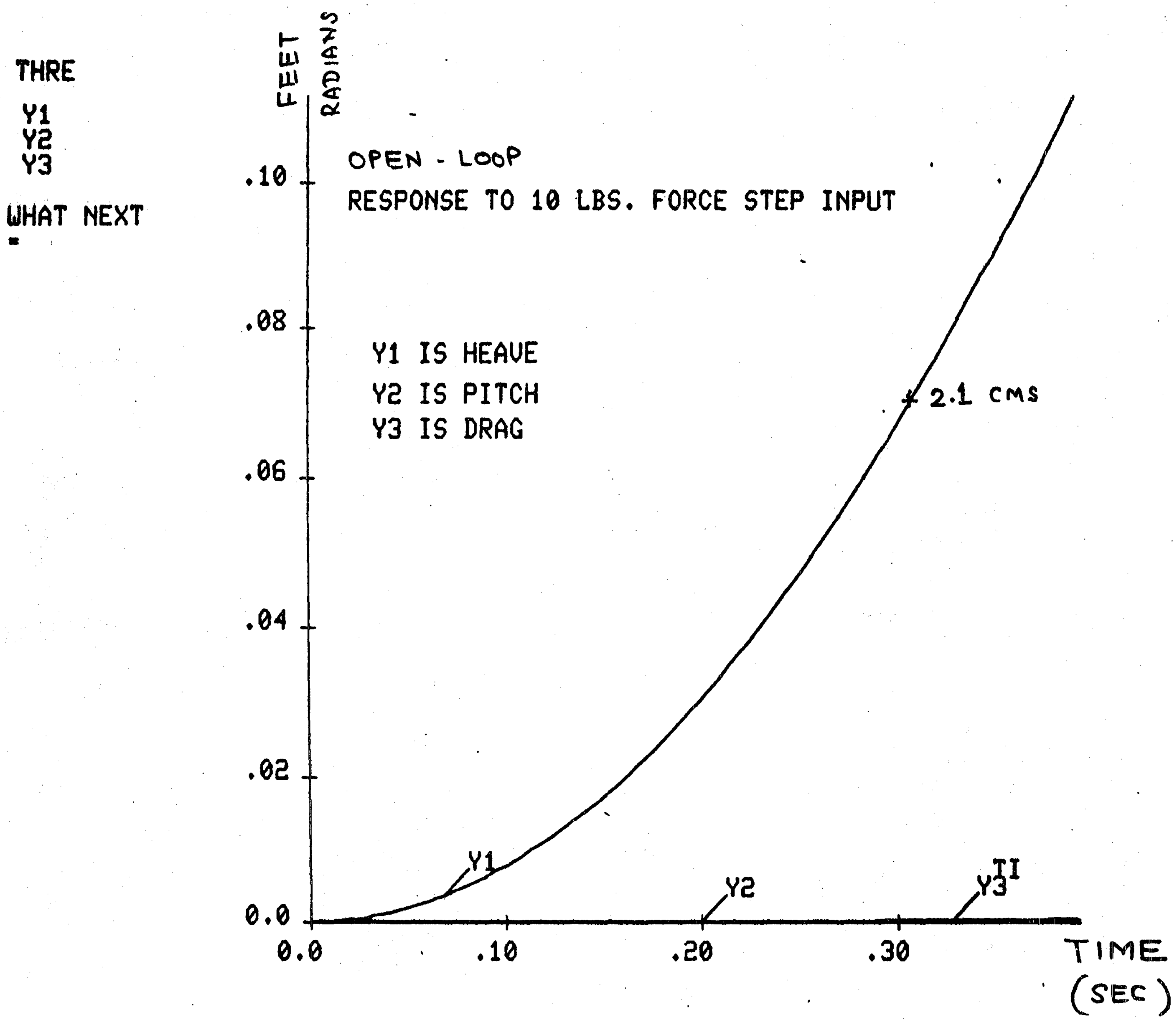

THRE
Y1
Y2
Y3
WHAT NEXT
FEET
RADIANS
OPEN - LOOP
RESPONSE TO 10 LBS. FORCE STEP INPUT
Y1 IS HEAVE
Y2 IS PITCH
Y3 IS DRAG
2.1 CMS
.10
.08
.06
.04
.02
0.0
0.0
.10
.20
.30
TIME (SEC)
Y1
Y2
Y3
TI

FIGURE 6.7

FIGURE 6.8

GRADIENT MAGNET PARAMETERS

FOR LONGITUDINAL MODE

PARAMETER	UNITS		VALUE
K_D	Drag	$\frac{1}{Amp}(\frac{N}{M})^{1/2}$	7×10^{-3}
K_m	Magnetization	$\frac{(M \cdot N)^{1/2}}{Amp}$	5.23×10^{-4}
K_{F_1}	Heave	$\frac{1}{Amp}(\frac{N}{M})^{1/2}$	47×10^{-4}
K_{T_1}	Pitch	$\frac{(M \cdot N)^{1/2}}{Amp}$	8.09×10^{-4}
I_m	Magnetization Coil	Amps	50,000
L	Vertical Coil	H	0.12
L_D	Drag Coil	H	0.3

$$
* \begin{bmatrix} 0.0275 & 0.0275 & 0 \\ 0.0156 & -0.0156 & 0 \\ 0 & 0 & 0.0188 \end{bmatrix} \begin{bmatrix} I_1 \\ I_2 \\ I_D \end{bmatrix} + \begin{bmatrix} 0 \\ 501 \cos\theta_0 \\ 0 \end{bmatrix} \begin{bmatrix} \theta \end{bmatrix}
$$

Eq. (6.17) continued

Where I_1, I_2 are the two vertical gradient magnet currents; I_D is the drag magnet current and θ is the deviation in the pitch angle from the static angle θ_0.

6.4.1.2 Lateral Mode

A state variable model for the lateral mode (side position, yaw angle and roll angle) defined in Figure 6.3 is given by

$$
\frac{d}{dt}\begin{bmatrix} \dot{y} \\ \psi \\ \dot{\psi} \\ \dot{\phi} \end{bmatrix} = \begin{bmatrix} -\frac{Y_\beta}{V} & Y_\beta & 0 & Y_p \\ 0 & 0 & 1 & 0 \\ -\frac{N_\beta}{V} & N_\beta & N_r & N_p \\ -\frac{L_\beta}{V} & L_\beta & L_r & L_p \end{bmatrix} \begin{bmatrix} \dot{y} \\ \psi \\ \dot{\psi} \\ \dot{\phi} \end{bmatrix} + \begin{bmatrix} \frac{1}{m} & 0 & 0 \\ 0 & 0 & 0 \\ 0 & \frac{1}{I_{zz}} & 0 \\ 0 & 0 & \frac{1}{I_{xx}} \end{bmatrix} \begin{bmatrix} F_y \\ T_z \\ T_x \end{bmatrix}
$$

*Equation continued from page 183.

A block diagram of the system transfer function is given in Figure 6.9. The parameters used for the control design are given in Figure 6.10. To study the effects of the aerodynamic coupling, the open-loop system response is simulated for step inputs. The response for a step input of one ft-lb torque in the yaw axis is shown in Figure 6.11. The force input in the side axis and the torque input in the roll axis are zero. Next, the open-loop response of the system for a unit torque in the roll axis is shown in Figure 6.12. The system response to a step force input in the side axis is shown in Figure 6.13.

The magnetic force and torques in the lateral mode are given by equations (6.9), (6.12) and (6.13).

Let I_3 and I_4 represent the side magnet currents and I_R represent the roll magnet current. Based on the magnet design, it is seen that 310 lbs of force is developed with $I_3 = I_4 = 29{,}000$ amps. A torque of 1250 in-lb is developed with $I_3 = I_4 = 22{,}000$ amps. A roll magnet current of 50,000 amps is required to develop 1250 in-lb roll torque.

A linearized relation between the force, torques and the magnet currents for a static yaw angle Ψ_o can be represented by

$$\begin{bmatrix} F_y \\ T_z \\ T_x \end{bmatrix} = \begin{bmatrix} .0054 & .0054 & 0 \\ .00238 & -.00238 & 0 \\ 0 & 0 & .0021 \end{bmatrix} \begin{bmatrix} I_3 \\ I_4 \\ I_R \end{bmatrix} + \begin{bmatrix} 0 \\ 501 \cos\psi_o \\ 0 \end{bmatrix} \psi$$

where Ψ is the deviation of the side angle from the static angle Ψ_o.

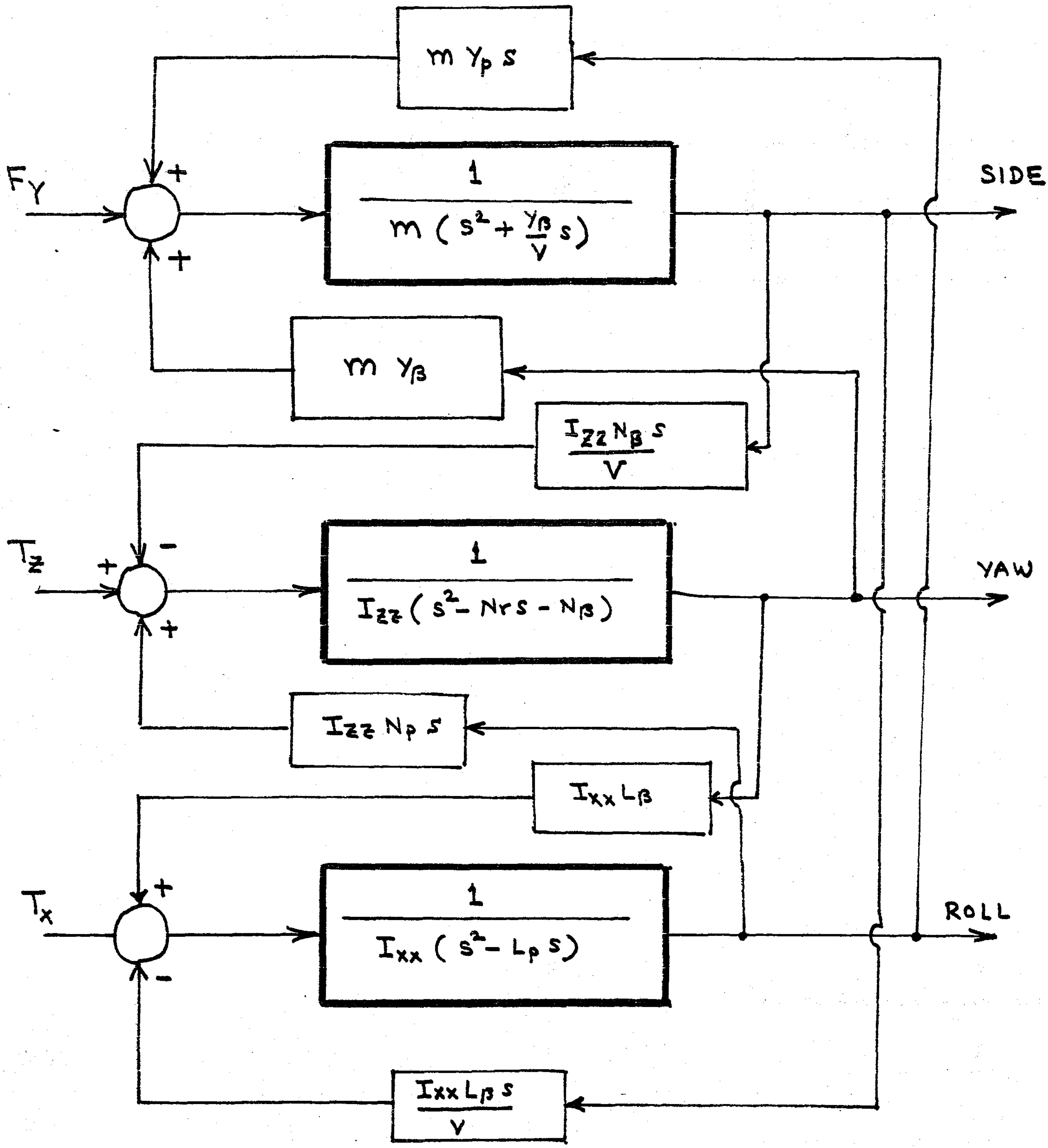

AERODYNAMIC COUPLING (LATERAL MODE)

FIGURE 6.9

FIGURE 6.10

PARAMETERS USED FOR LATERAL MODE

PARAMETER	UNITS	EXPECTED RANGE	VALUES USED
Y_β	Ft/SEC^2	100 TO 200	100
Y_p	Ft/SEC	−10 TO 10	−10
N_r	1/SEC	−5 TO −2	−3
N_p	1/SEC	−0.5 TO 0	−0.2
N_β	$1/SEC^2$	−5 TO 5	−3
L_r	1/SEC	−1 TO 1	−0.5
L_p	1/SEC	−5 TO −2	−3
L_β	$1/SEC^2$	−10 TO 0	−5
I_{zz}	$SLUG\text{-}Ft^2$		3.05
I_{xx}	$SLUG\text{-}FT^2$		0.17

OTHER PARAMETERS ASSUMED ZERO

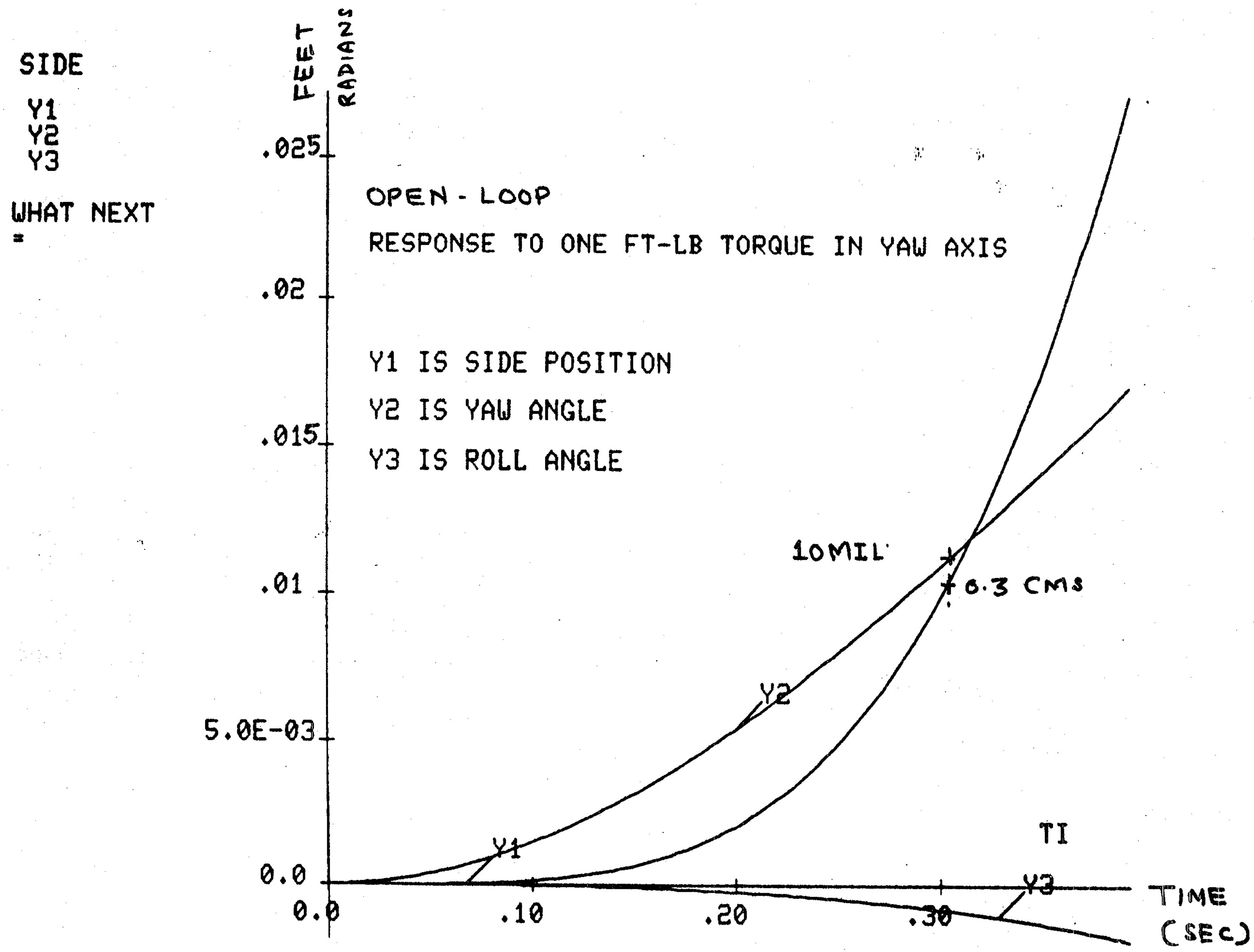
SIDE
Y1
Y2
Y3
WHAT NEXT
=
FEET
RADIANS
.025
.02
.015
.01
5.0E-03
0.0
OPEN - LOOP
RESPONSE TO ONE FT-LB TORQUE IN YAW AXIS
Y1 IS SIDE POSITION
Y2 IS YAW ANGLE
Y3 IS ROLL ANGLE
10MIL
0.3 CMS
Y2
Y1
TI
Y3
0.0
.10
.20
.30
TIME
(SEC)

FIGURE 6.11

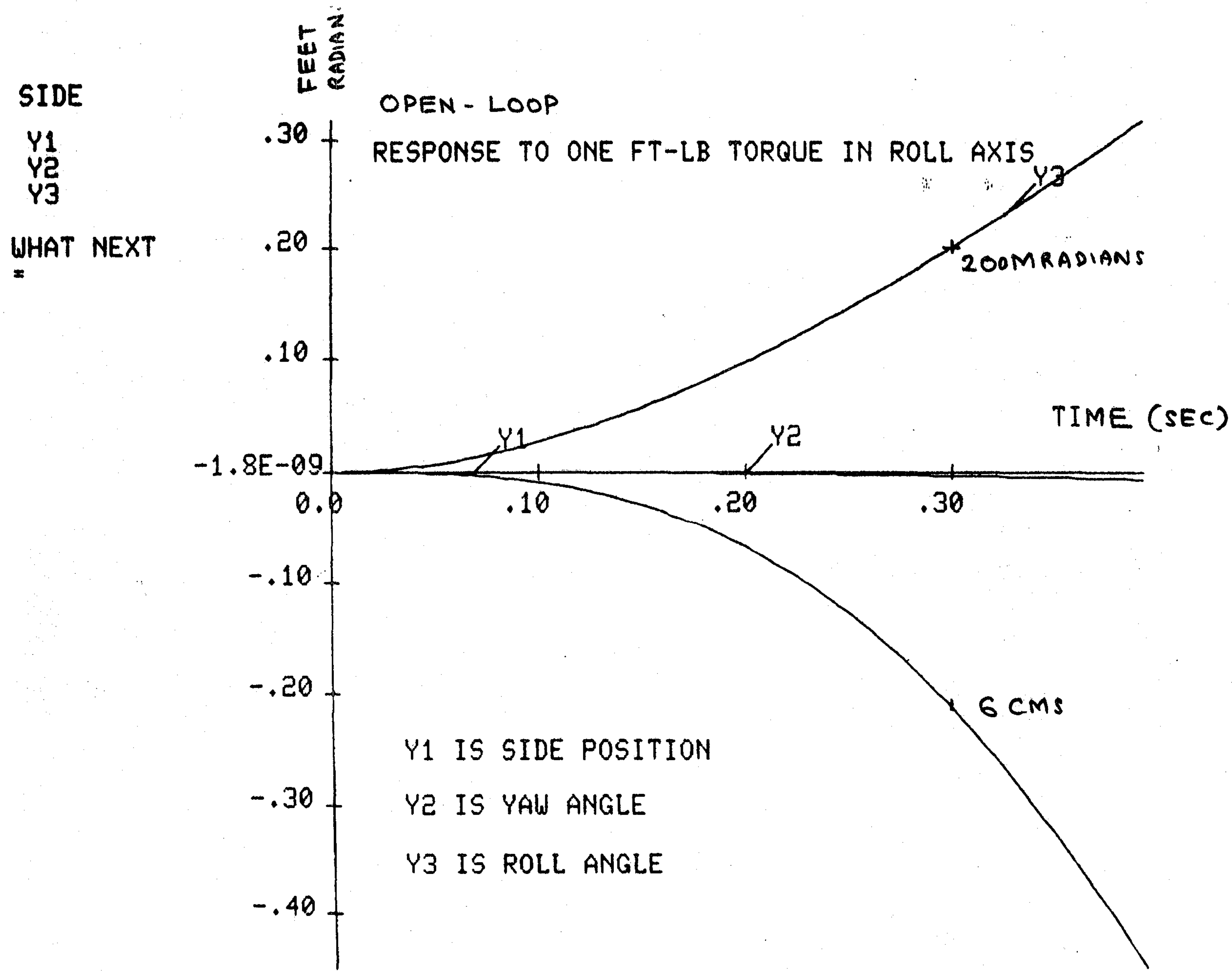
SIDE
Y1
Y2
Y3
WHAT NEXT
FEET
RADIANS
OPEN - LOOP
RESPONSE TO ONE FT-LB TORQUE IN ROLL AXIS
.30
.20
.10
-1.8E-09
0.0
.10
.20
.30
-.10
-.20
-.30
-.40
TIME (SEC)
Y1
Y2
Y3
200MRADIANS
6 CMS
Y1 IS SIDE POSITION
Y2 IS YAW ANGLE
Y3 IS ROLL ANGLE

FIGURE 6.12

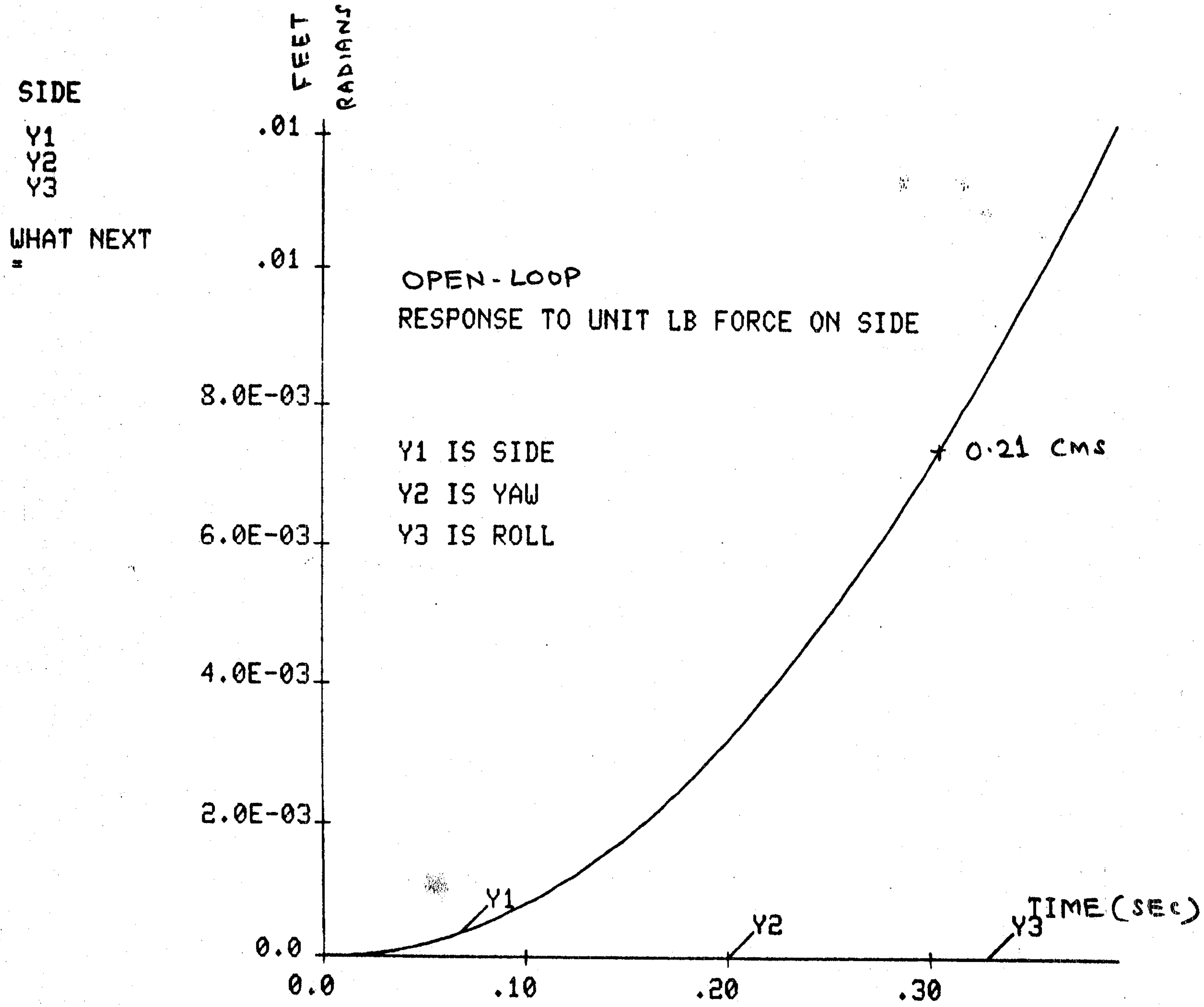
SIDE
Y1
Y2
Y3
WHAT NEXT
=
FEET
RADIANS
.01
.01
8.0E-03
6.0E-03
4.0E-03
2.0E-03
0.0
0.0
.10
.20
.30
TIME (SEC)
OPEN-LOOP
RESPONSE TO UNIT LB FORCE ON SIDE
Y1 IS SIDE
Y2 IS YAW
Y3 IS ROLL
0.21 CMS
Y1
Y2
Y3

FIGURE 6.13

The dynamics of the power supply and the magnet coils is represented by

$$\begin{bmatrix} I_3(s) \\ I_4(s) \\ I_R(s) \end{bmatrix} = \begin{bmatrix} \frac{10^5}{L_3(1+.008s)s} & 0 & 0 \\ 0 & \frac{10^5}{L_4(1+.008s)s} & 0 \\ 0 & 0 & \frac{10^5}{L_R(1+.008s)s} \end{bmatrix} \begin{bmatrix} E_3(s) \\ E_4(s) \\ E_R(s) \end{bmatrix}$$

where $E_3(s)$, $E_4(s)$, $E_R(s)$ represent the Laplace transform of the input signals to the power supply and $I_3(s)$, $I_4(s)$, $I_R(s)$ represent the Laplace transform of the currents in the two side magnet coils and roll coil respectively. The inductances are $L_3 = L_4 = 0.011$ H and $L_R = 0.025$ H. The power supply bandwidth is assumed 20 Hz.

6.4.1.3 Design of Compensation System

A block diagram of the multi-axis control system is shown in Figure 6.14. The input and output are 3x1 vectors representing heave, pitch, and drag axes in the longitudinal mode and yaw, side and roll in the lateral mode. The "SYSTEM" block represents the aerodynamic couplings between the forces and torques and the corresponding model motion. The "FEEDBACK" block is the feedback due to the magnetization coil and produces a restoring torque proportional to the model attitude. The "MAGNET COUPLING" is an algebraic relation between the gradient magnet currents and the forces and the torques. The block "P.S. + COILS" is a diagonal matrix consisting of the dynamics of the power supply and the self inductances of the magnet coils. The "FILTER" block is a state estimator (Kalman Filter) to recursively estimate the model velocity based on the position and attitude measurements.

The compensators "PRE1 - PRE4" are in software modules with the following functions.

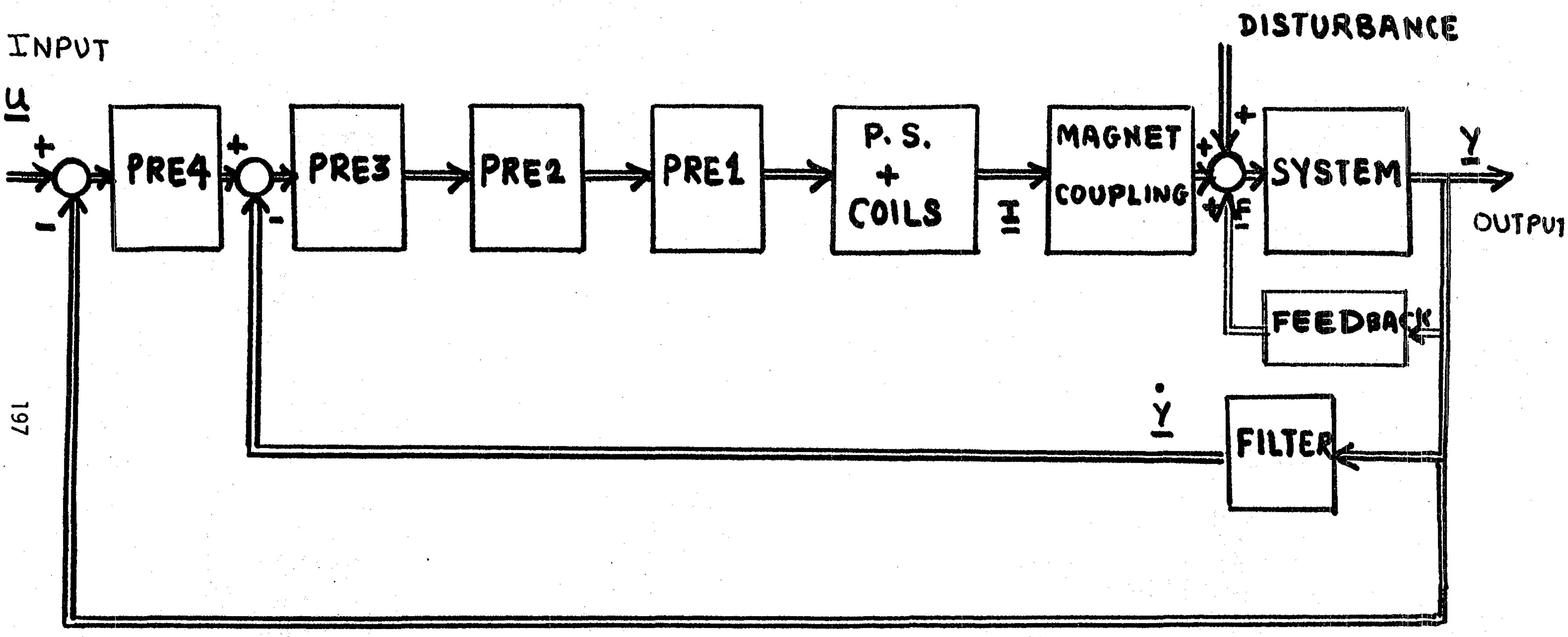

BLOCK DIAGRAM FOR MULTI-AXIS CONTROL SYSTEM

FIGURE 6.14

PRE1- A diagonal matrix to account for the model orientation at an operating point.

PRE2- A matrix to minimize the magnetic and aerodynamic couplings.

PRE3- A diagonal matrix with dynamic elements to achieve the closed-loop control system stability and the dynamic performance.

PRE4- A constant matrix to achieve the control system bandwidth.

The compensators designed for the longitudinal and lateral modes are given in the following.

6.4.1.4 Compensator for Longitudinal Mode

$$\mathbf{PRE1} = \begin{bmatrix} \frac{1}{\cos^2\theta_0} & 0 & 0 \\ 0 & \frac{1}{\cos^2\theta_0 - \sin^2\theta_0} & 0 \\ 0 & 0 & \frac{1}{\cos^2\theta_0} \end{bmatrix}$$

where Θ_0 is the desired pitch angle in the steady state.

$$\text{PRE2} = \begin{bmatrix} 1.1043 & 1.95 & 0 \\ 0.139 & -0.244 & 0 \\ 0 & 0 & 8.05 \end{bmatrix}$$

The compensator PRE2 is selected such that the system is decoupled at 100 radians frequency.

PRE3 is a diagonal matrix with

$$\text{PRE3 }(1,1) = \frac{(1 + .01s)(1 + .02s)}{(1 + .001s)(1 + .002s)}$$

$$\text{PRE3 }(2,2) = \frac{1 + .02s)(1 + .035s)(s^2 + 1.98s + 9)}{(1 + .002s)(1 + .0035s)(s^2 + 11.92s + 9)}$$

$$\text{PRE3 }(3,3) = \frac{(1 + .01s)(1 + .02s)}{(1 + .001s)(1 + .002s)}$$

The function of PRE3 is to provide a phase lead to compensate the phase-lag due to the model inertia and coil inductance.

PRE4 is a diagonal matrix given by

$$PRE4 = \begin{bmatrix} 50 & 0 & 0 \\ 0 & 80 & 0 \\ 0 & 0 & 60 \end{bmatrix}$$

A plot of the frequency response characteristics of the control system with the no position feedback is given in Figure 6.15. The frequency calibration is in radians. From reference, based on the multivariable Nyquist stability criteria, the system for the longitudinal mode is closed-loop stable. It is seen that the characteristic loci do not encircle the critical point (-1+j0). The velocity loop was designed using the same criteria. Bode diagrams for the open-loop control system (with no position feedback) and closed-loop system (with the position feedback) are shown in Figures 6.16 and 6.17.

6.4.1.5 Compensator for Lateral Mode

The compensator matrix PRE1 to account for the model orientation in the lateral mode is an identity matrix under the assumption that $\theta_0 = 0$, Ψ and ϕ are small.

$$PRE1 = \begin{bmatrix} 1 & 0 & 0 \\ 0 & 1 & 0 \\ 0 & 0 & 1 \end{bmatrix}$$

The matrix PRE2 is selected such that the system, along with the compensator, is decoupled at 100 radians frequency.

$$PRE2 = \begin{bmatrix} .1703 & .0264 & .002 \\ .1703 & -.0116 & .002 \\ 0 & 0 & .0538 \end{bmatrix}$$

1. A. G. J. MacFarlane and and B. Kouvaritakis, "A design technique for linear multivariable feedback system", International Journal of Control, 1977, Vol. 25, No. 6, pp. 837-874.

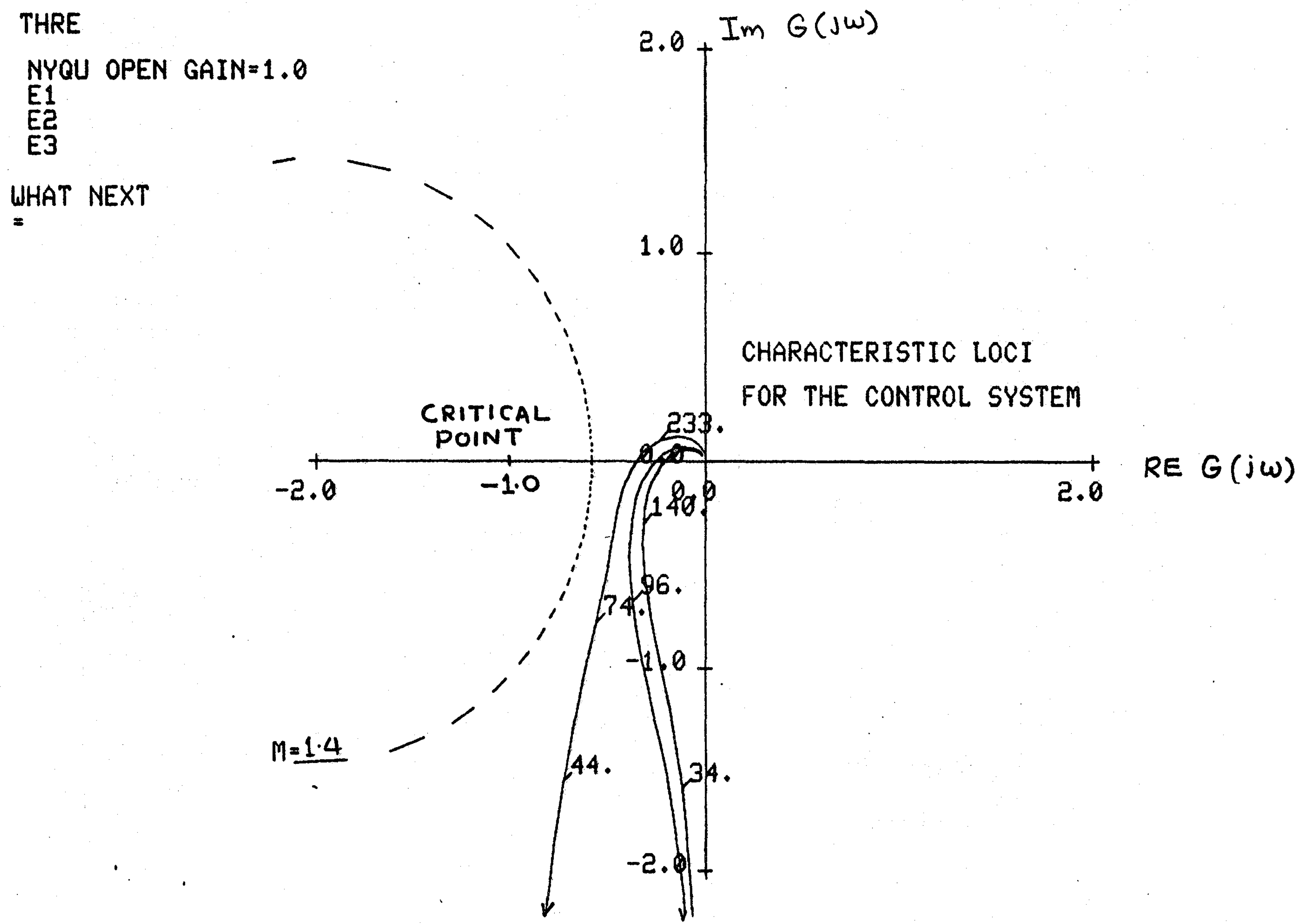

THRE
NYQU OPEN GAIN=1.0
E1
E2
E3
WHAT NEXT
=
Im G(jω)
2.0
1.0
-1.0
-2.0
CHARACTERISTIC LOCI
FOR THE CONTROL SYSTEM
CRITICAL POINT
233.
0.0
-2.0
-1.0
0.0
2.0
RE G(jω)
140.
96.
74.
44.
34.
M=1.4

FIGURE 6.15

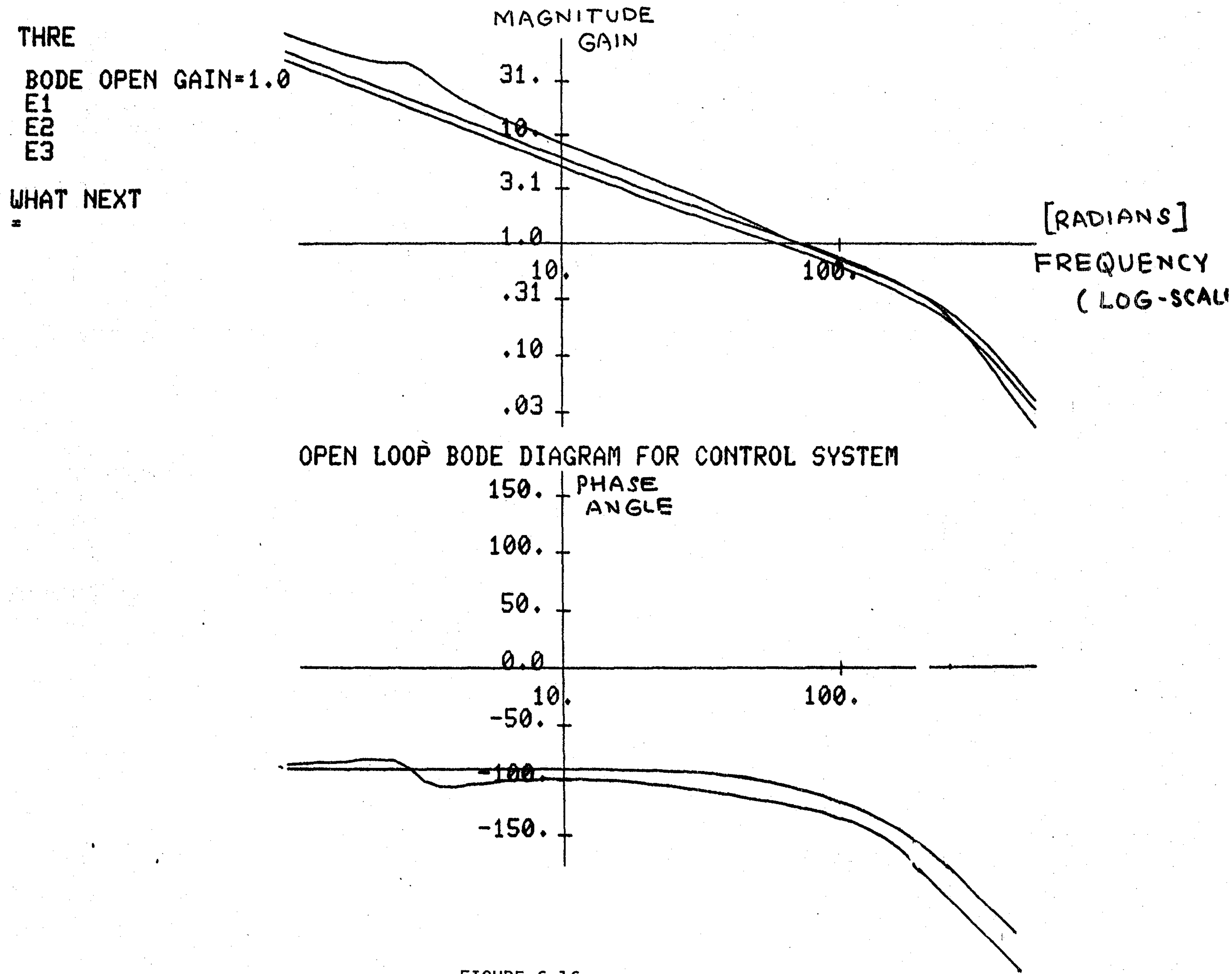
THRE
BODE OPEN GAIN=1.0
E1
E2
E3
WHAT NEXT
=
MAGNITUDE
GAIN
31.
10.
3.1
1.0
10.
100.
.31
.10
.03
[RADIANS]
FREQUENCY
(LOG-SCAL
OPEN LOOP BODE DIAGRAM FOR CONTROL SYSTEM
150.
PHASE
ANGLE
100.
50.
0.0
10.
100.
-50.
-100.
-150.

FIGURE 6.16

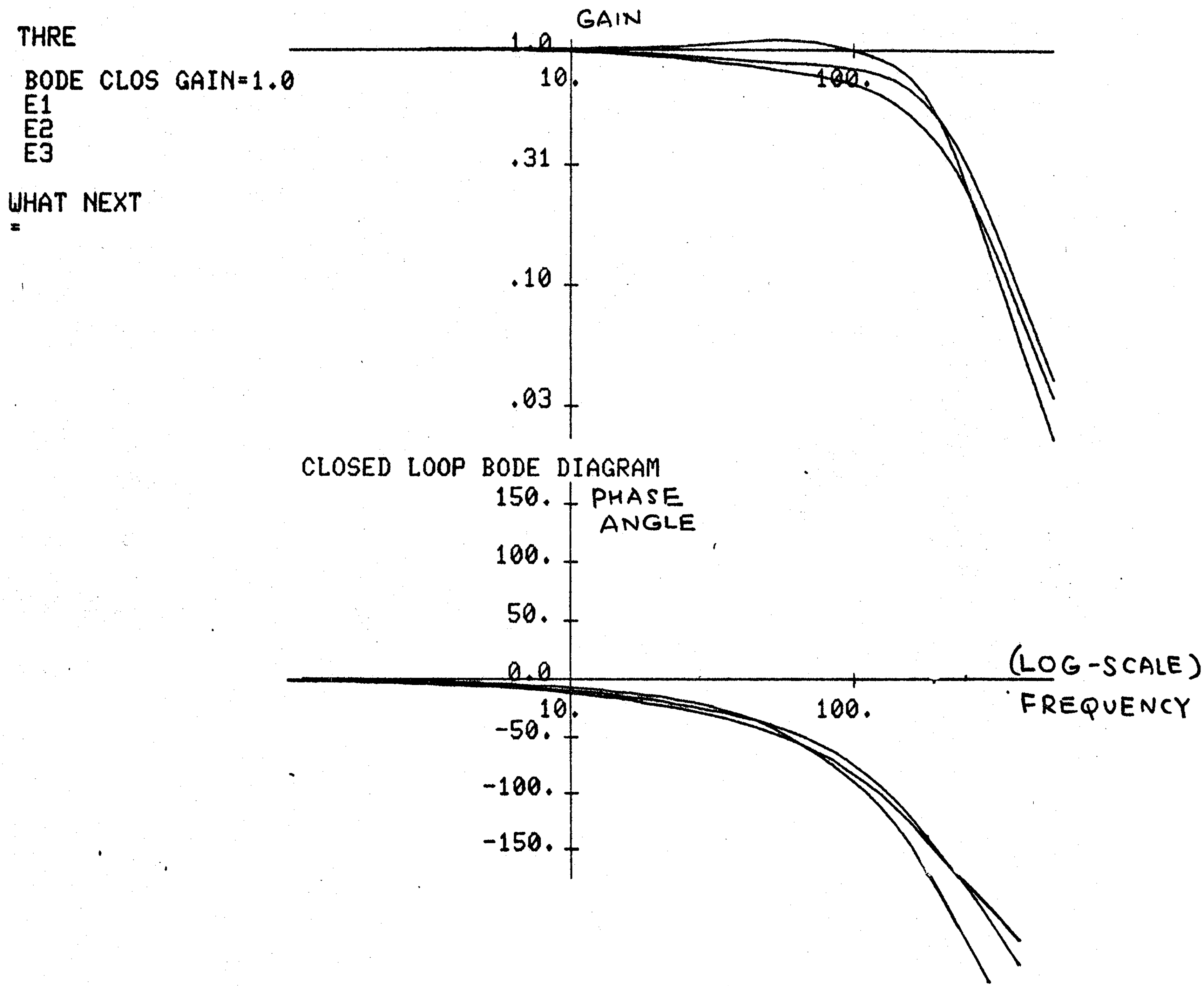
THRE
BODE CLOS GAIN=1.0
E1
E2
E3
WHAT NEXT
=
GAIN
1.0
10.
100.
.31
.10
.03
CLOSED LOOP BODE DIAGRAM
150.
PHASE ANGLE
100.
50.
0.0
-50.
-100.
-150.
(LOG-SCALE)
FREQUENCY

FIGURE 6.17

PRE3 is a diagonal matrix with

$$PRE3(1,1) = \frac{(1+.01s)(1+.02s)}{(1+.001s)(1+.002s)}$$

$$PRE3(2,2) = \frac{(1+.01s)(1+.035s)}{(1+.001s)(1+.0035s)}$$

$$PRE3(3,3) = \frac{(1+.01s)(1+.02s)}{(1+.001s)(1+.002s)}$$

The compensator PRE3 introduces a phase advance to correct the phase lag due to the model inertia and coil inductances.

PRE4 is a constant matrix in the outer loop to further decouple the control system at 50 radians frequency and to achieve a control system bandwidth.

$$PRE4 = \begin{bmatrix} 33.5 & -0.05 & 6.45 \\ 0 & 42.1 & 0.1 \\ 0 & 0.32 & 36.0 \end{bmatrix}$$

The open-loop (with no position feedback and the velocity loop closed) frequency response characteristics of the lateral mode control system is shown in Figure 6.18. Based on the multivariable Nyquist stability criteria, the system is closed-loop stable. The characteristic loci do not encircle the critical point $(-1 + j_0)$. Bode diagrams for the open-loop control system (with no position feedback) and the closed-loop control system (with position feedback shown in Figure 6.9) are given in Figures 6.19 and 6.20.

6.5 TIME RESPONSE OF THE CONTROL SYSTEM

The response of the MSBS control system for step, sinusoidal and random inputs is presented in the following. It is assumed that the system is linear with time invariant parameters. The saturation effects of the gradient magnet currents are not considered in the simulation mode. It is assumed that inputs are perturbations about steady-state, model position and attitude.

6.5.1 Longitudinal Mode

The input is a 3x1 vector with heave, pitch and drag position commands respectively. All the inputs are applied at time zero and the corresponding model positions and attitude are plotted.

In Figure 6.21, a step input is applied to the pitch axis with other two inputs zero. The pitch response tracks the command input with a very small overshoot. A perturbation less than 0.025 cms is observed in the heave axis.

In Figure 6.22, a sinusoidal input of 0.5 Hz frequency is applied to the pitch axis. The model response is given.

In Figure 6.23, the heave force F_z on the model is sinusoidal with amplitude 110 lbs. This force is applied by the vertical gradient magnets to counteract the aerodynamic coupling in the heave and pitch axis.

In Figure 6.24, the torque T_y has a maximum amplitude of 2 lbs-ft. The maximum drag force F_x is 3.5 lbs. The input command is 1 deg. sinusoidal in pitch axis.

In Figure 6.25, the gradient magnet currents I_1, I_2, and the drag magnet current I_D are plotted for 1 deg sinusoidal input command in the pitch axis.

In Figures 6.26 and 6.27, the tracking performance of the control system is demonstrated with command inputs applied simultaneously.

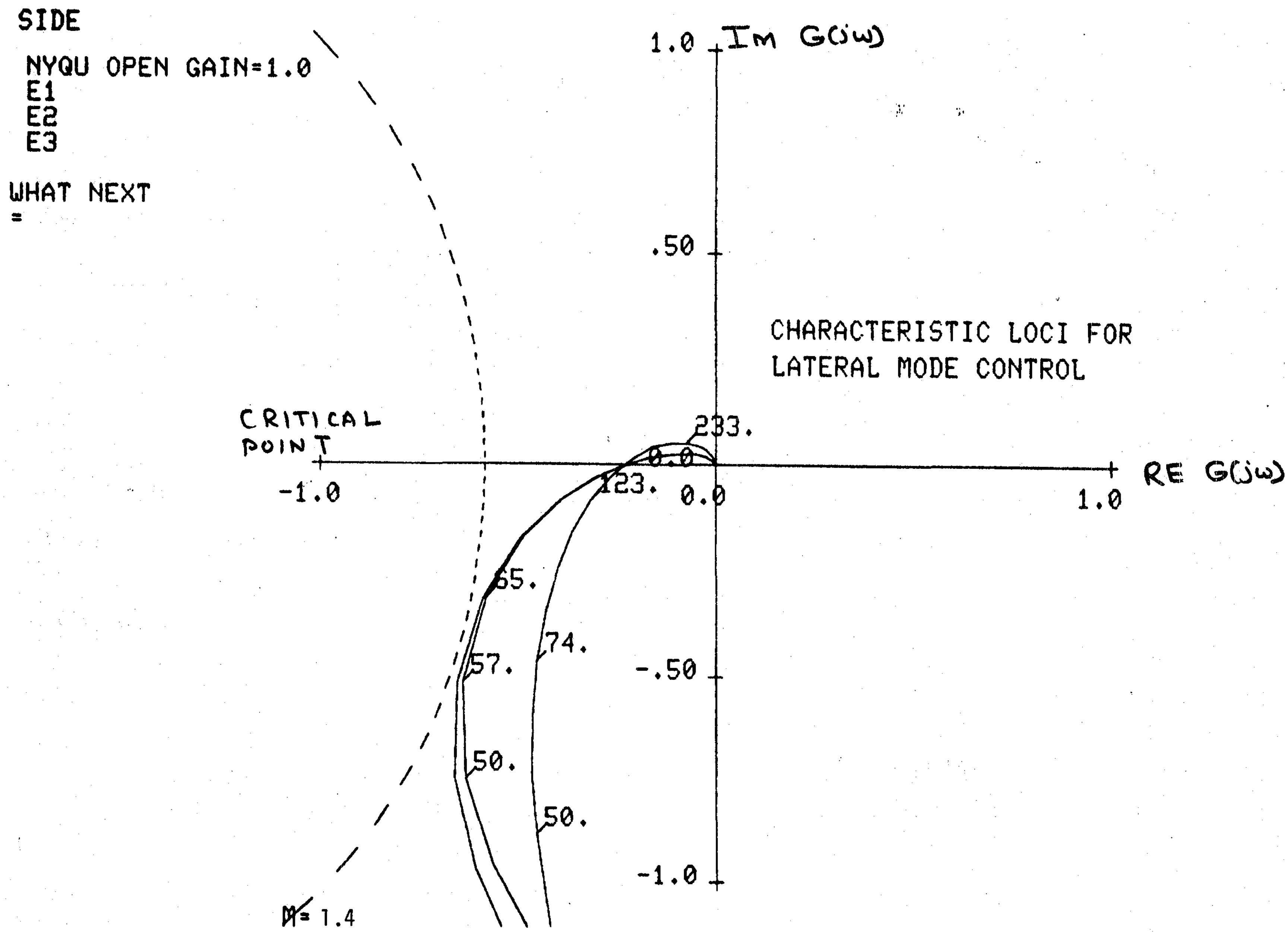
SIDE
NYQU OPEN GAIN=1.0
E1
E2
E3
WHAT NEXT
=
1.0
Im G(jω)
.50
CHARACTERISTIC LOCI FOR
LATERAL MODE CONTROL
CRITICAL
POINT
233.
0.0
123.
-1.0
0.0
1.0
RE G(jω)
65.
74.
57.
-.50
50.
50.
-1.0
M= 1.4

FIGURE 6.18

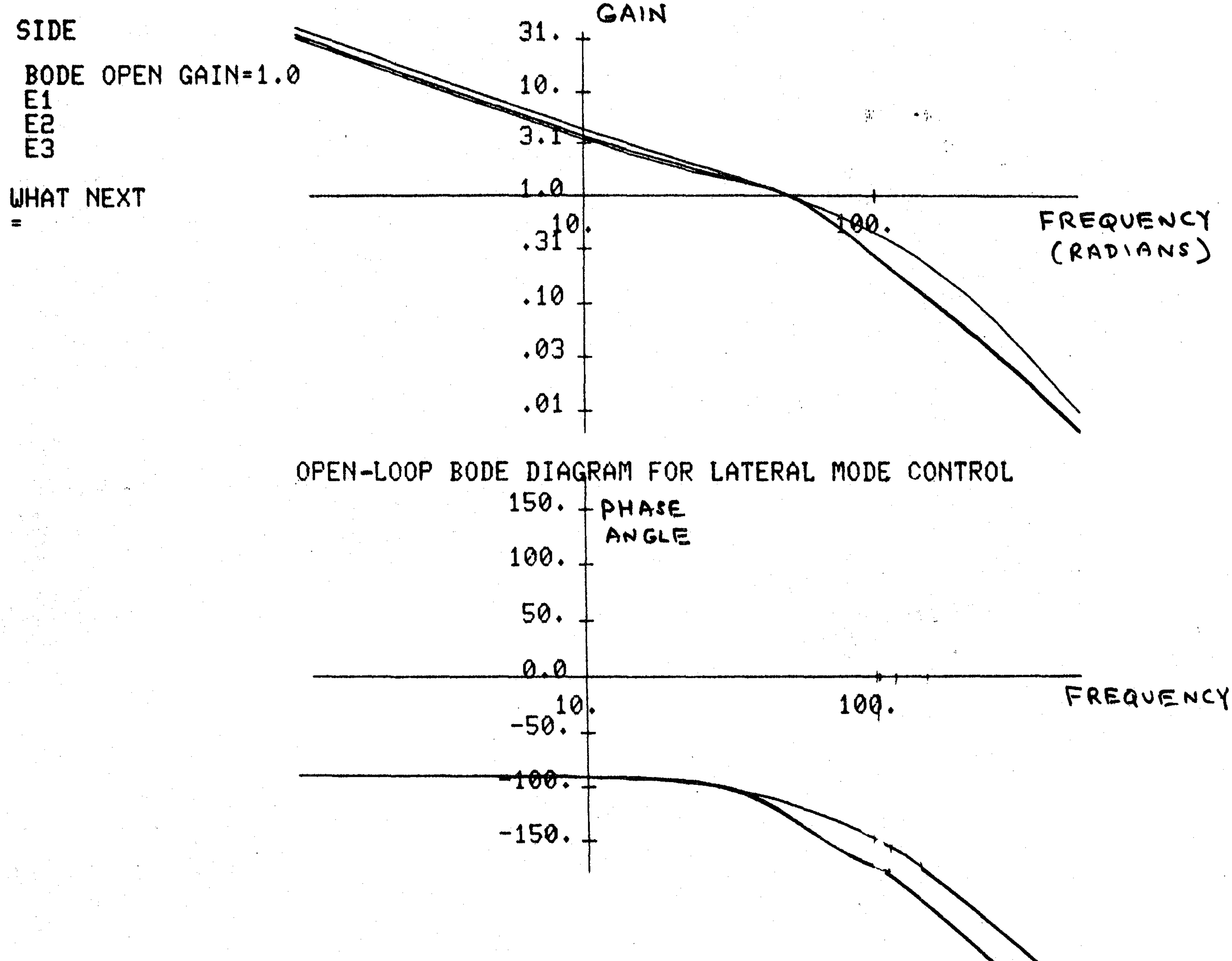
SIDE
BODE OPEN GAIN=1.0
E1
E2
E3
WHAT NEXT
=
GAIN
31.
10.
3.1
1.0
.31
.10
.03
.01
10.
100.
FREQUENCY
(RADIANS)
OPEN-LOOP BODE DIAGRAM FOR LATERAL MODE CONTROL
PHASE
ANGLE
150.
100.
50.
0.0
-50.
-100.
-150.
10.
100.
FREQUENCY

FIGURE 6.19

SIDE

BODE CLOS GAIN=1.0
E1
E2
E3

WHAT NEXT
=

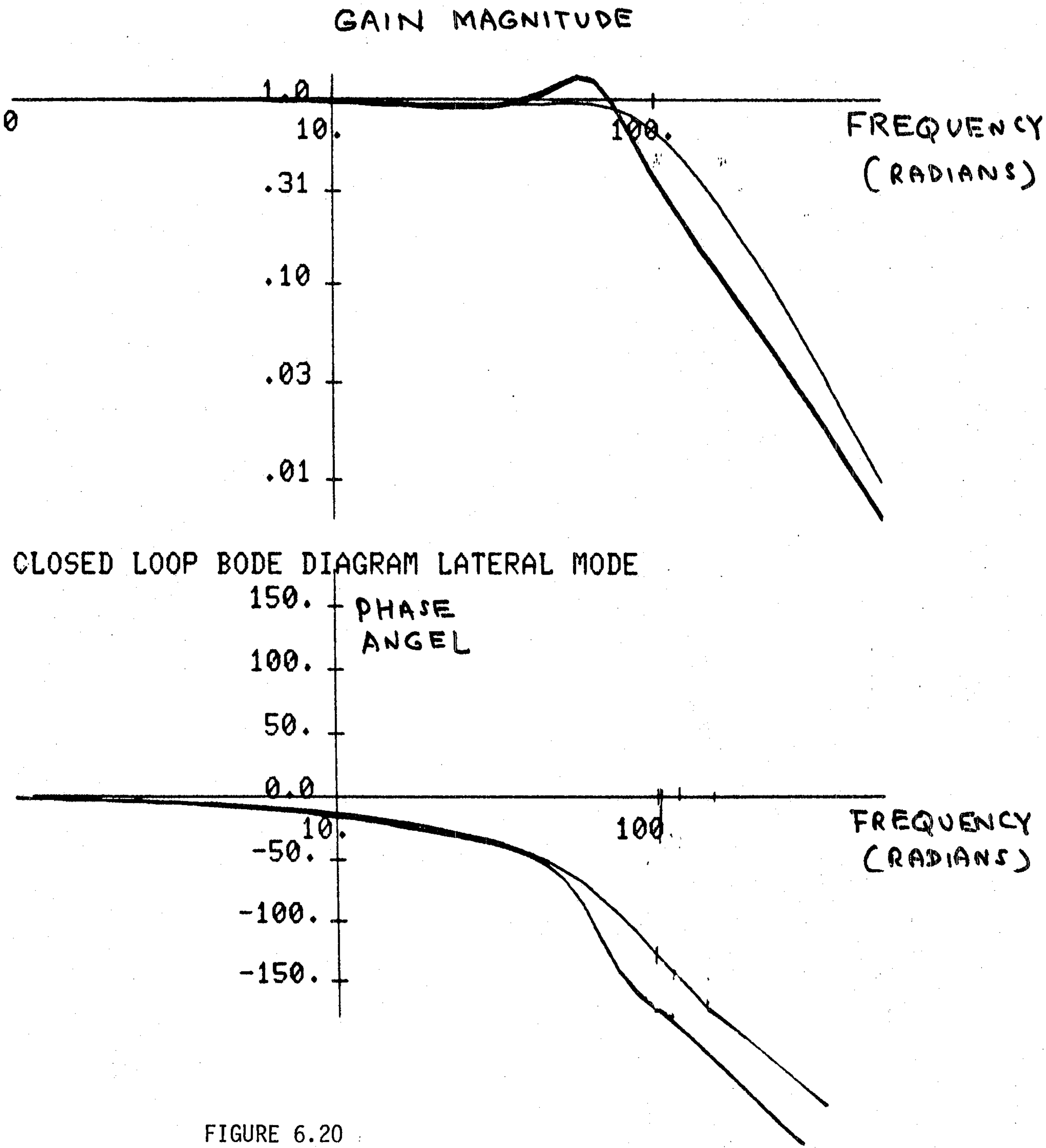

FIGURE 6.20

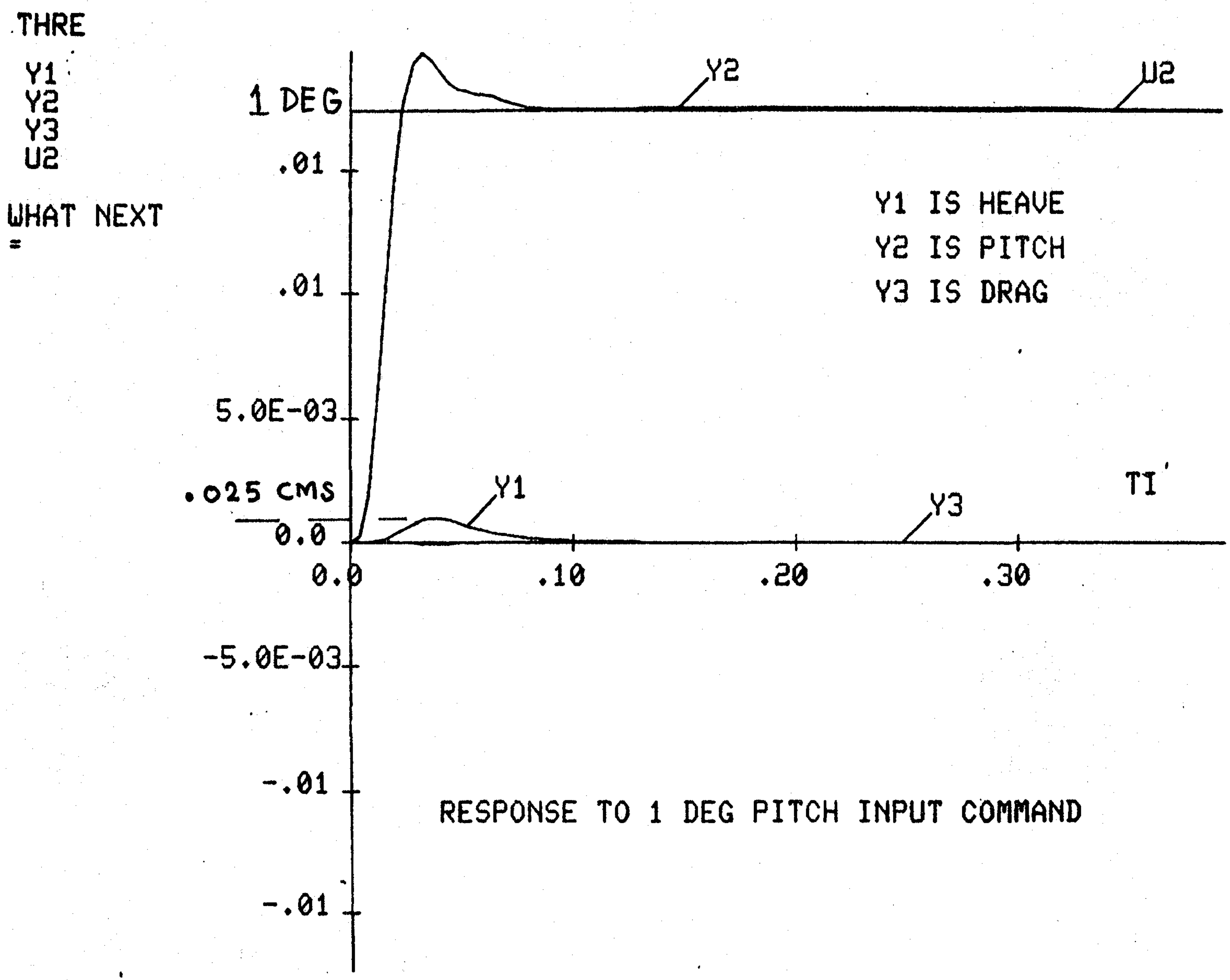
THRE
Y1
Y2
Y3
U2
WHAT NEXT
=
1 DEG
.01
.01
5.0E-03
.025 CMS
0.0
-5.0E-03
-.01
-.01
0.0
.10
.20
.30
TI
Y1
Y2
Y3
U2
Y1 IS HEAVE
Y2 IS PITCH
Y3 IS DRAG
RESPONSE TO 1 DEG PITCH INPUT COMMAND

FIGURE 6.21

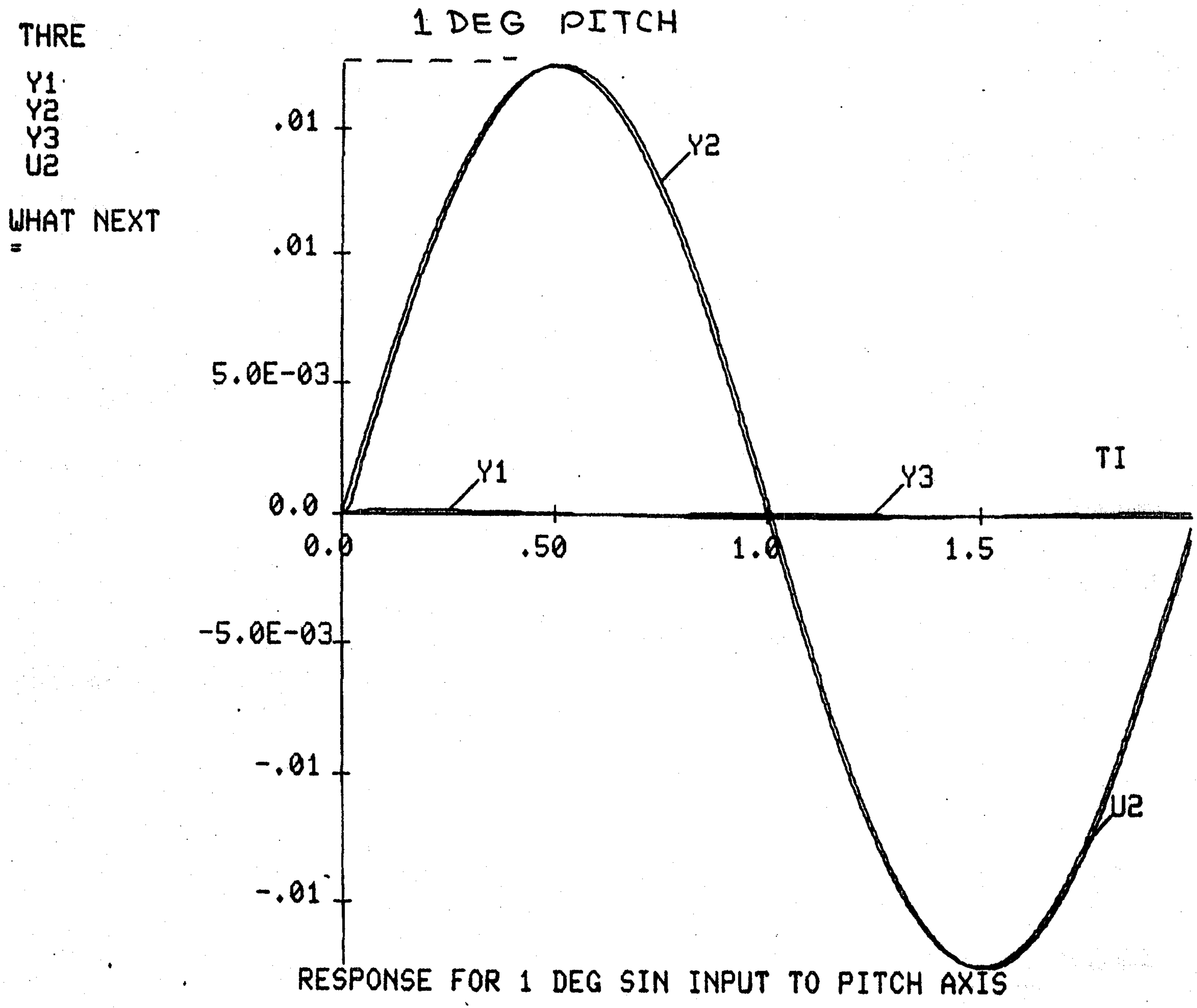
1 DEG PITCH
THRE
Y1
Y2
Y3
U2
WHAT NEXT
=
.01
.01
5.0E-03
0.0
-5.0E-03
-.01
-.01
0.0
.50
1.0
1.5
TI
Y1
Y2
Y3
U2
RESPONSE FOR 1 DEG SIN INPUT TO PITCH AXIS

FIGURE 6.22

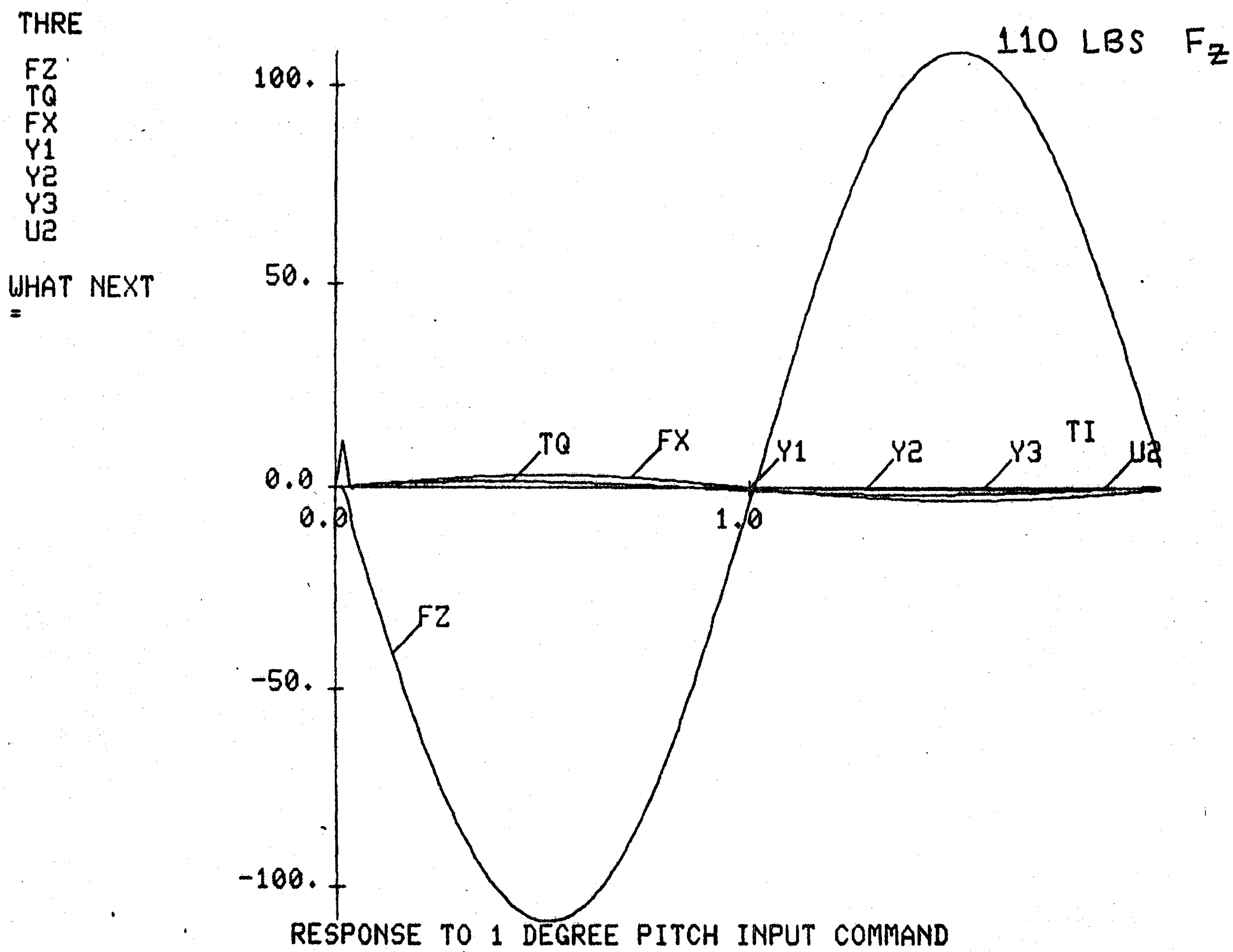
THRE
FZ
TQ
FX
Y1
Y2
Y3
U2
WHAT NEXT
=
110 LBS F_Z
100.
50.
0.0
-50.
-100.
0.0
1.0
TQ
FX
Y1
Y2
Y3
TI
U2
FZ
RESPONSE TO 1 DEGREE PITCH INPUT COMMAND

FIGURE 6.23

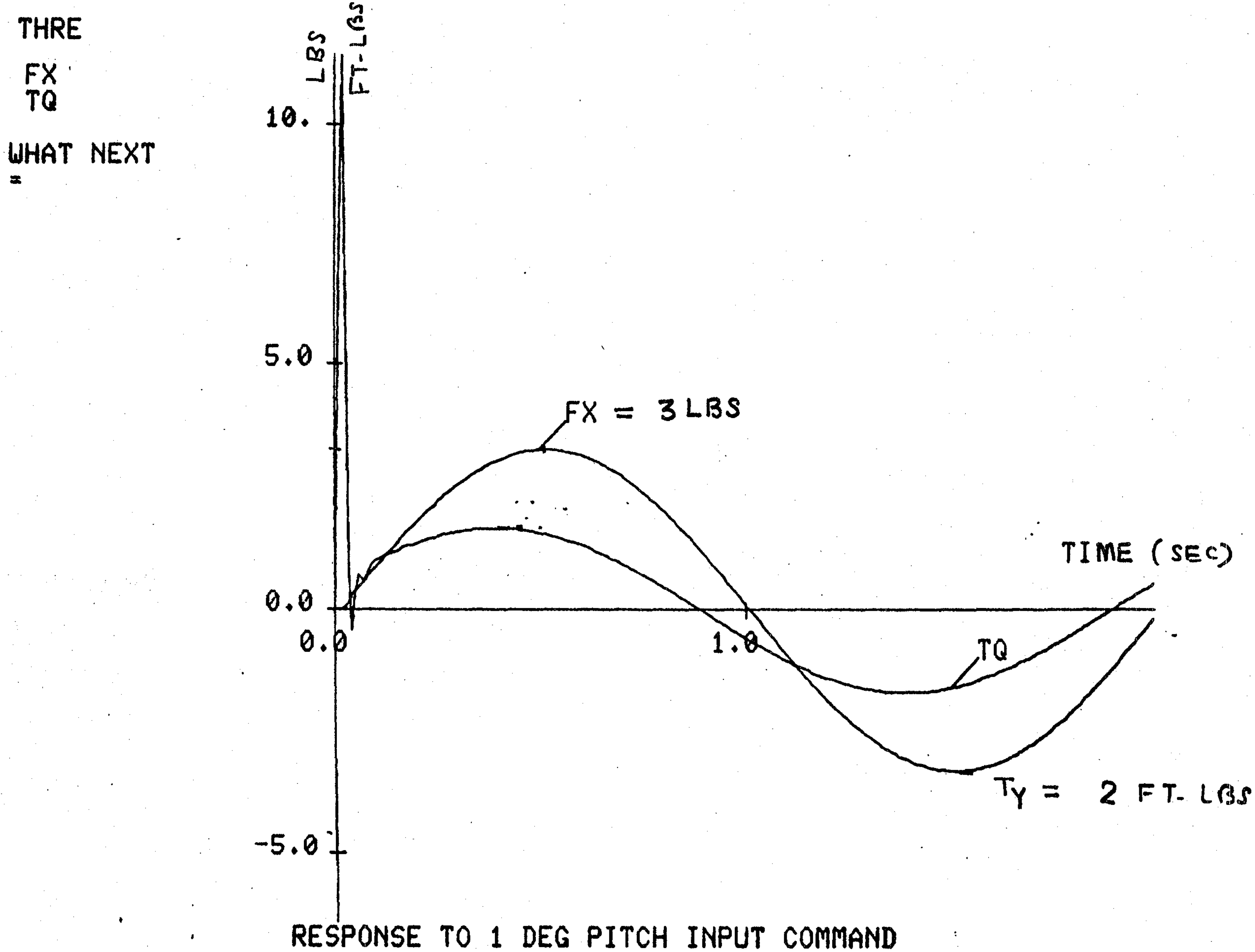
THRE
FX
TQ
WHAT NEXT
LBS
FT-LBS
10.
5.0
0.0
-5.0
0.0
1.0
FX = 3 LBS
TIME (SEC)
TQ
TY = 2 FT-LBS
RESPONSE TO 1 DEG PITCH INPUT COMMAND

FIGURE 6.24

THRE
I1
I2
ID

WHAT NEXT
=

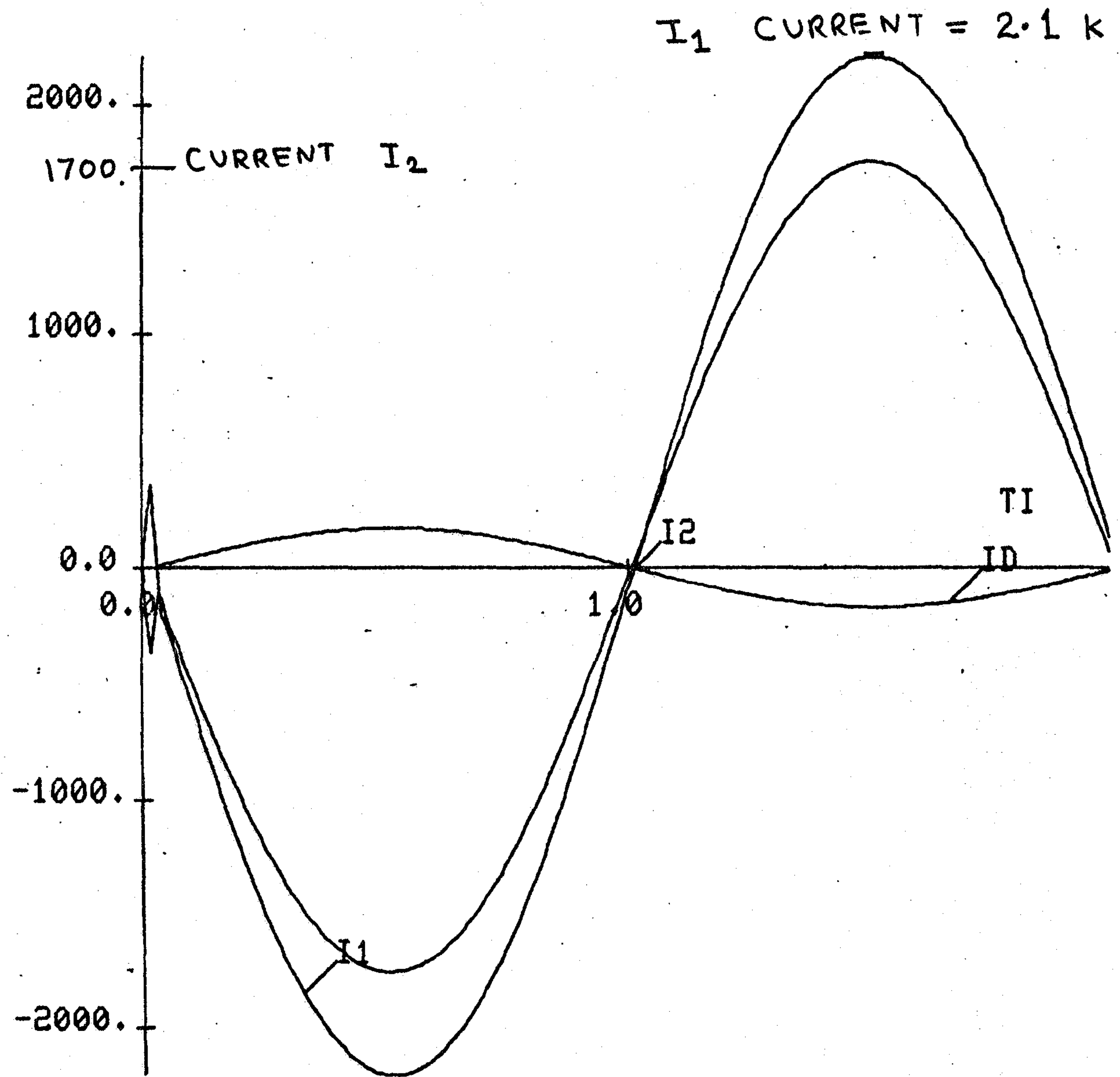

CURRENTS FOR 1 DEG SIN PITCH INPUT

FIGURE 6.25

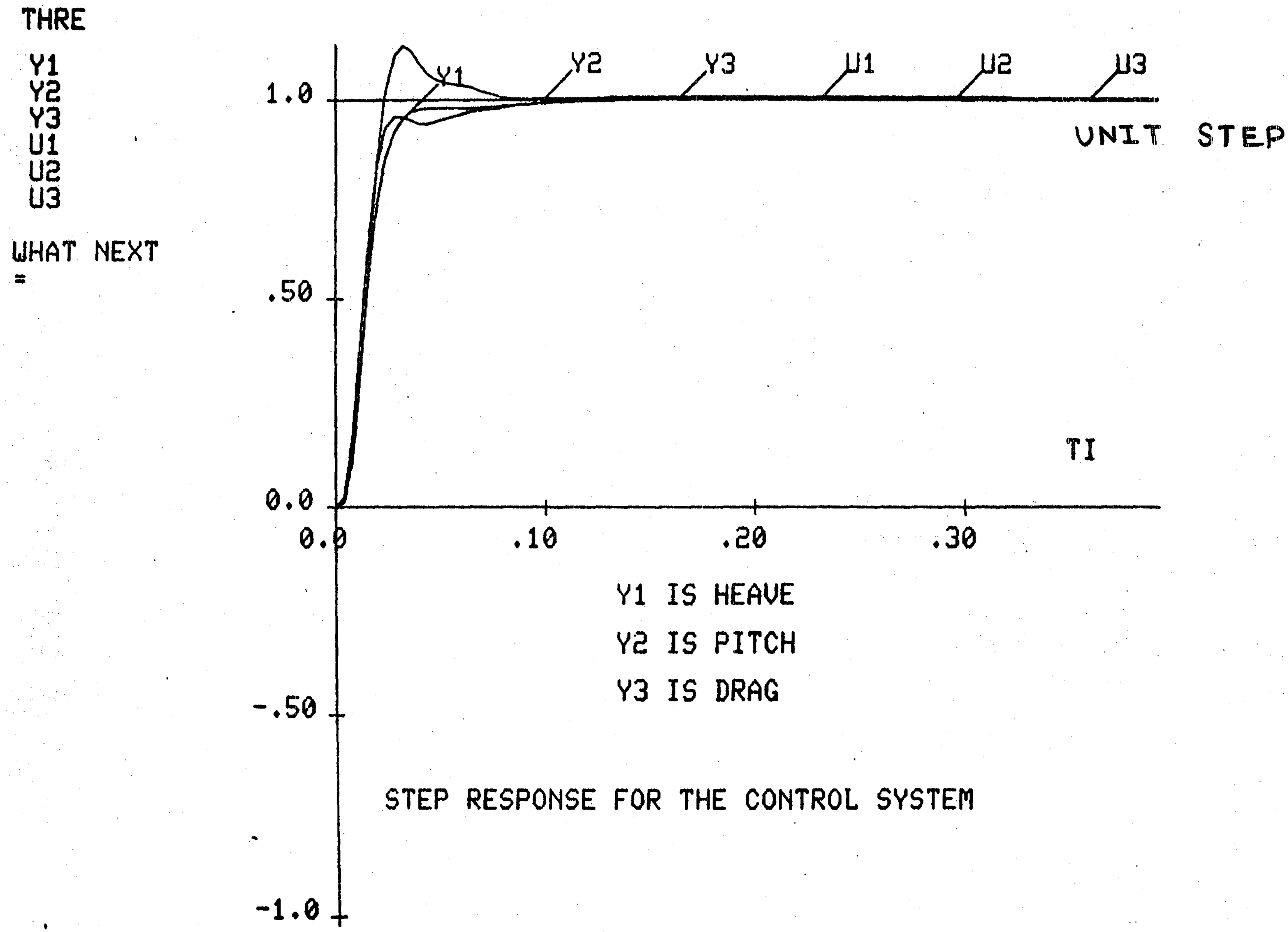
THRE
Y1
Y2
Y3
U1
U2
U3
WHAT NEXT
=
1.0
.50
0.0
-.50
-1.0
0.0
.10
.20
.30
Y1
Y2
Y3
U1
U2
U3
UNIT STEP
TI
Y1 IS HEAVE
Y2 IS PITCH
Y3 IS DRAG
STEP RESPONSE FOR THE CONTROL SYSTEM

FIGURE 6.26

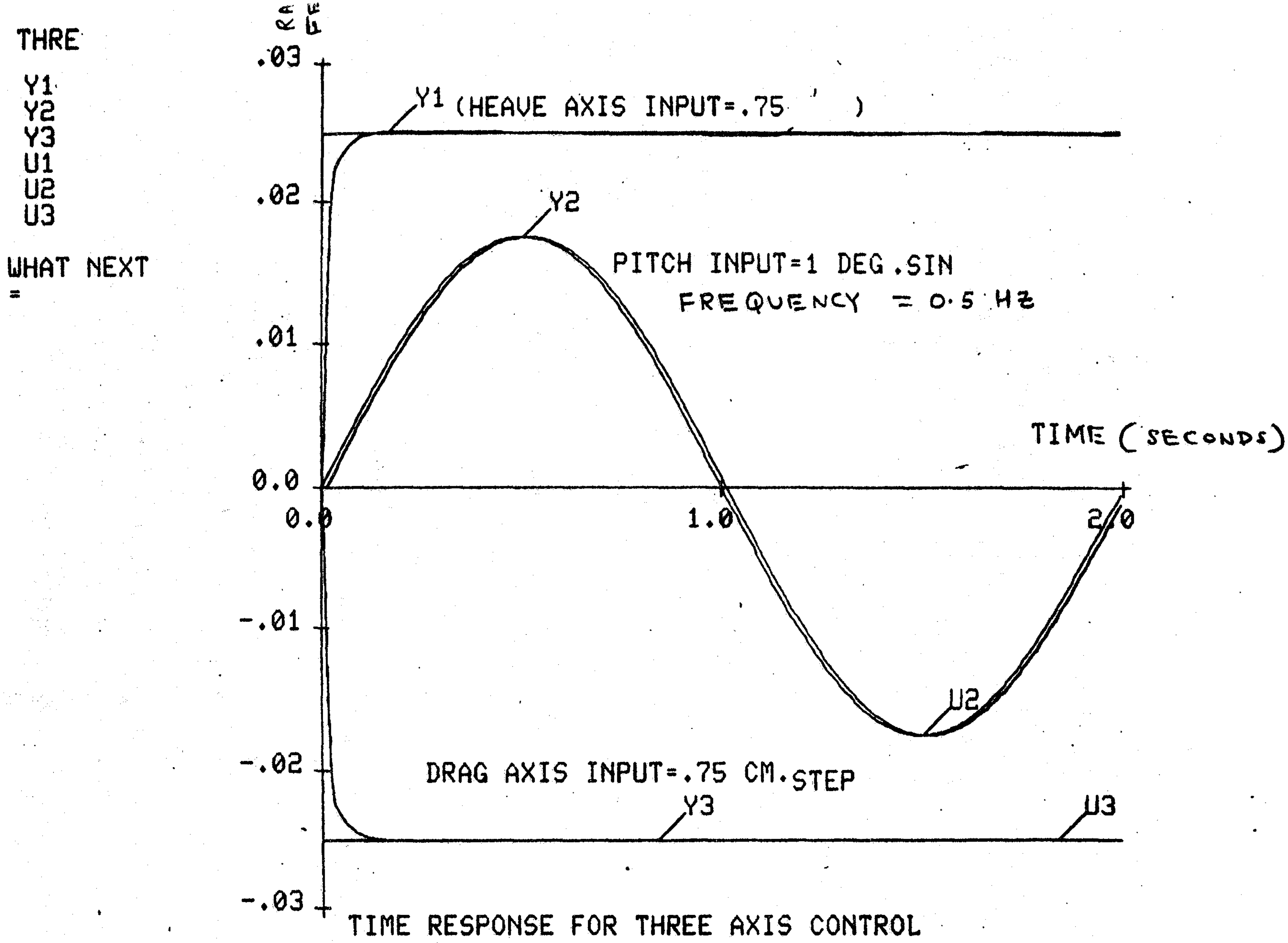
THRE
Y1
Y2
Y3
U1
U2
U3
WHAT NEXT
=
.03
.02
.01
0.0
-.01
-.02
-.03
0.0
1.0
2.0
Y1 (HEAVE AXIS INPUT=.75)
Y2
PITCH INPUT=1 DEG.SIN
FREQUENCY = 0.5 HZ
TIME (SECONDS)
U2
DRAG AXIS INPUT=.75 CM.STEP
Y3
U3
TIME RESPONSE FOR THREE AXIS CONTROL

FIGURE 6.27

6.5.2 Response to Unstable Aerodynamic Coupling

The robustness of the control system is demonstrated by considering parameter values such that the system model has poles in the right half of the complex S-plane. For example, with $M_\alpha = 200$ in the longitudinal mode system model, the unstable pole is on the positive real axis at S=11. The time response of the control system for a step input is shown in Figure 6.28. The tracking performance of the control system for sinusoidal input of 0.5 Hz in the pitch axis is shown in Figure 6.29. The closed-loop bandwidth of the control system is shown in Figure 6.30.

6.5.3 Nonlinear System Simulation

In the simulation results presented in the previous sections, a linearized force-current relation given by equation 6.17 is used. To study the effects of nonlinear term, the algebraic relations given by equations (6.7), (6.8), and (6.12) are programmed in the simulation model. The controller is based on the linear design presented in the previous sections. The time response in the heave and pitch axes are given in Figures 6.31 and 6.32 respectively. It has been observed that the difference between the time response of the linearized model and the nonlinear model is very small.

6.5.4 Lateral Mode

The input is a 3 x 1 vector with side position, roll angle and yaw angle commands respectively. The model position and attitude response as a function of time is simulated in the following:

In Figure 6.33, to test the stability of the control system, unit step inputs are simultaneously applied in the side, yaw and roll axes. It is seen that the response tracks the command inputs within 0.2 seconds.

In Figure 6.34, to study the couplings with the compensators in the lateral mode control system, a step of 1 degree is applied in the yaw axis. The response in the yaw and the roll axis are zero.

In Figure 6.35, a step of 1 degree is applied to the roll axis. The response in the yaw axis is zero. The maximum response in the side position is 0.025 cms.

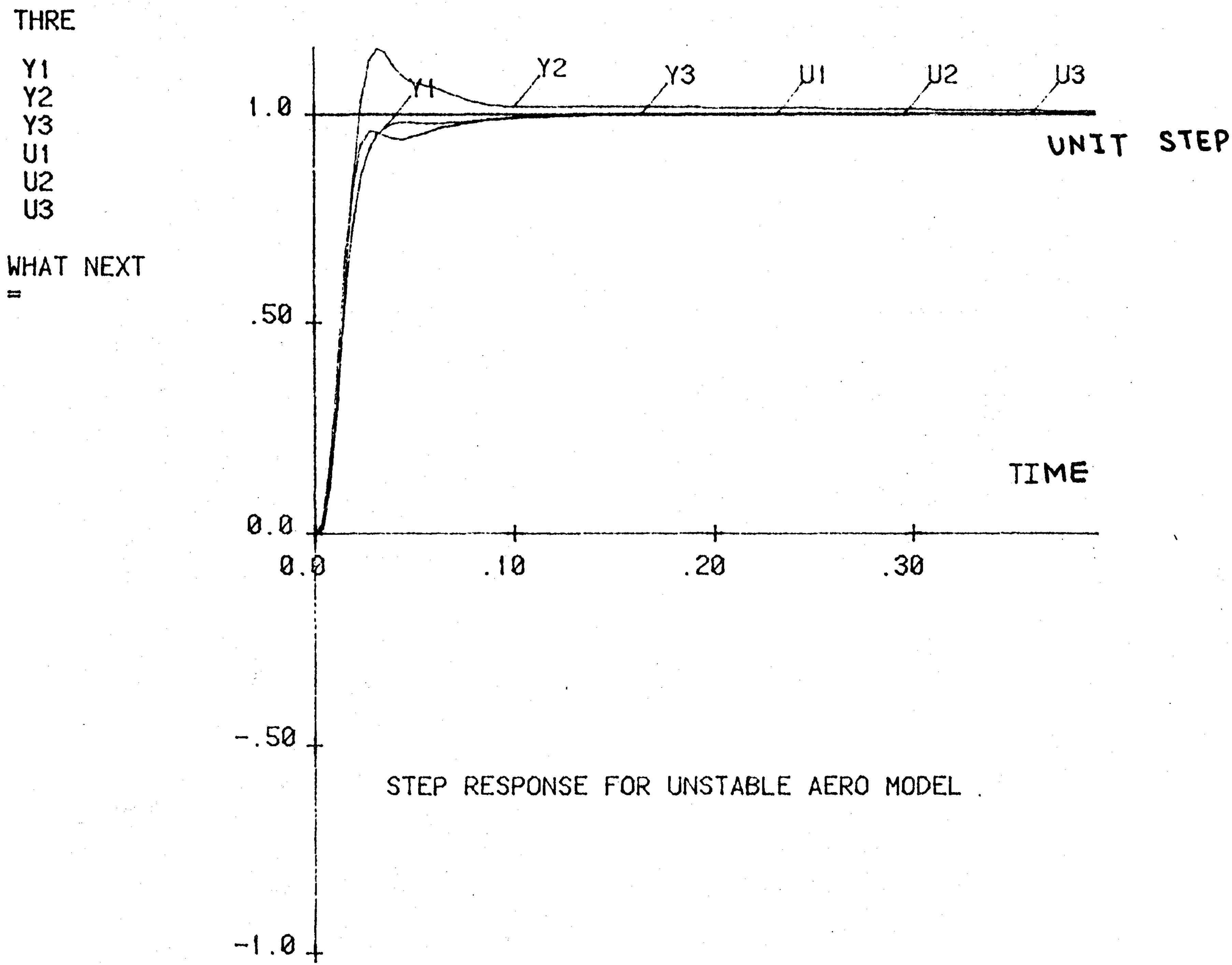
THRE
Y1
Y2
Y3
U1
U2
U3
WHAT NEXT
=
Y1
Y2
Y3
U1
U2
U3
1.0
.50
0.0
-.50
-1.0
0.0
.10
.20
.30
UNIT STEP
TIME
STEP RESPONSE FOR UNSTABLE AERO MODEL .

FIGURE 6.28

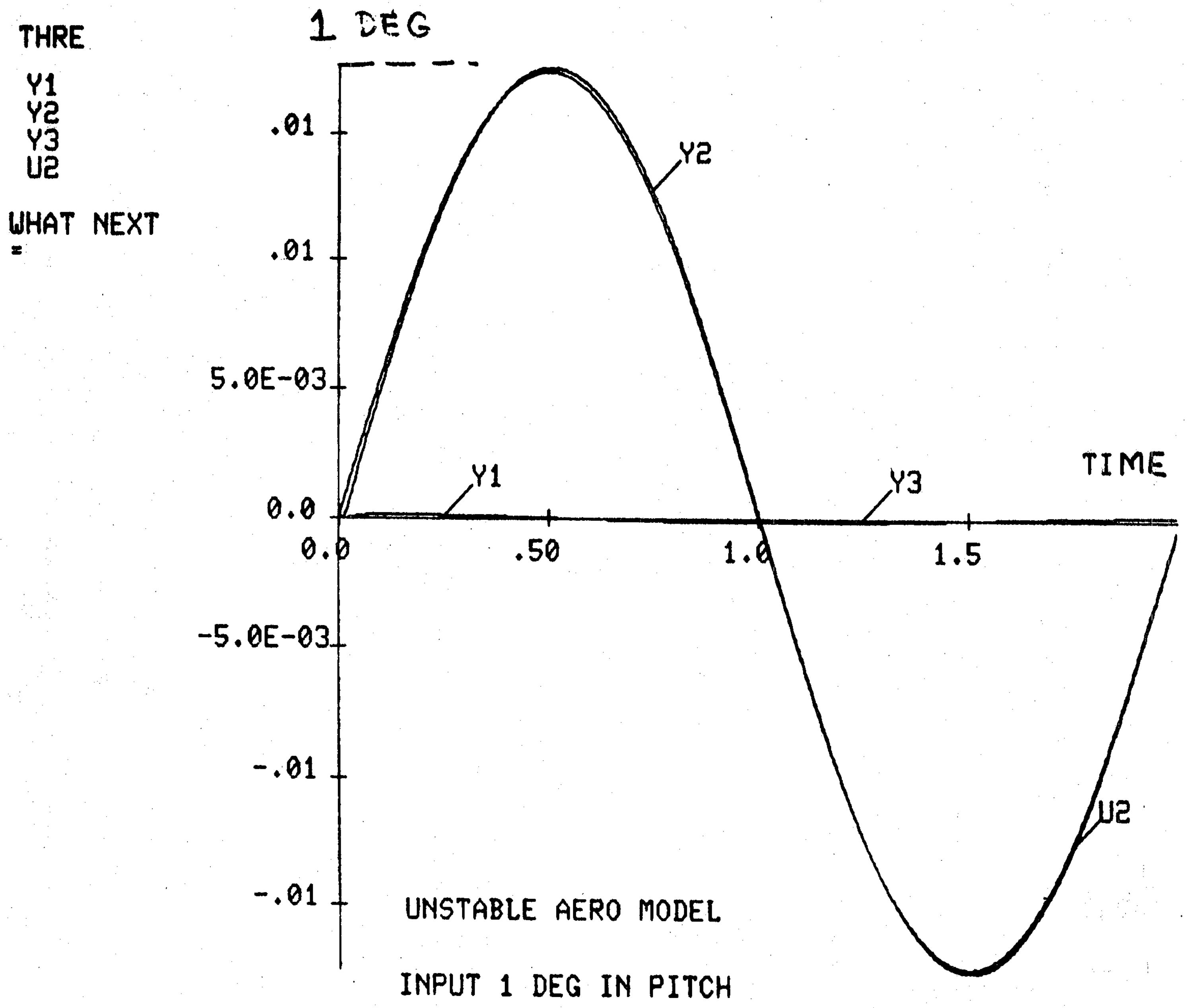
THRE
Y1
Y2
Y3
U2
WHAT NEXT
=
1 DEG
.01
.01
5.0E-03
0.0
-5.0E-03
-.01
-.01
0.0
.50
1.0
1.5
TIME
Y1
Y2
Y3
U2
UNSTABLE AERO MODEL
INPUT 1 DEG IN PITCH

FIGURE 6.29

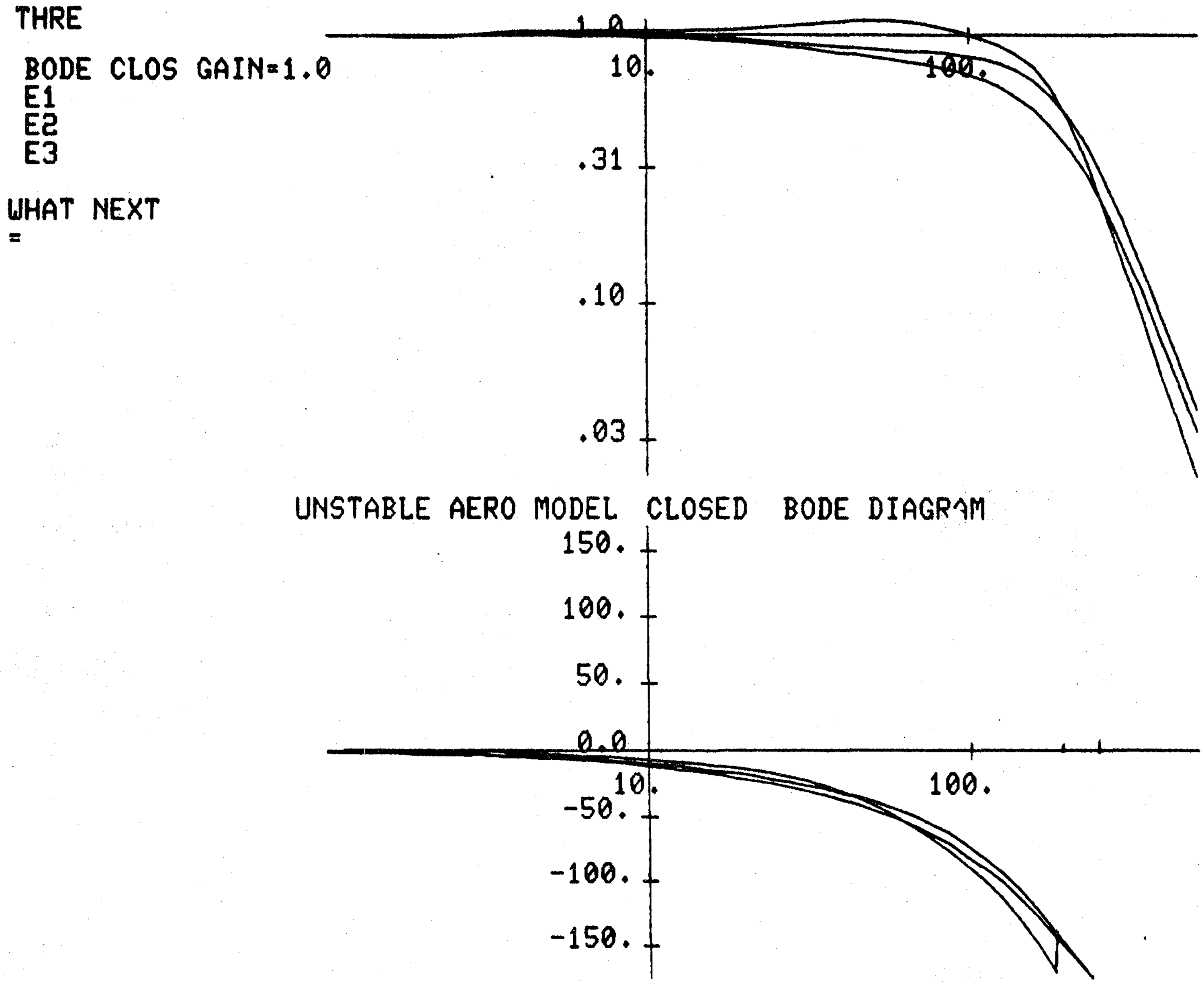
THRE
BODE CLOS GAIN=1.0
E1
E2
E3
WHAT NEXT
=
1.0
10.
100.
.31
.10
.03
UNSTABLE AERO MODEL CLOSED BODE DIAGRAM
150.
100.
50.
0.0
10.
100.
-50.
-100.
-150.

FIGURE 6.30

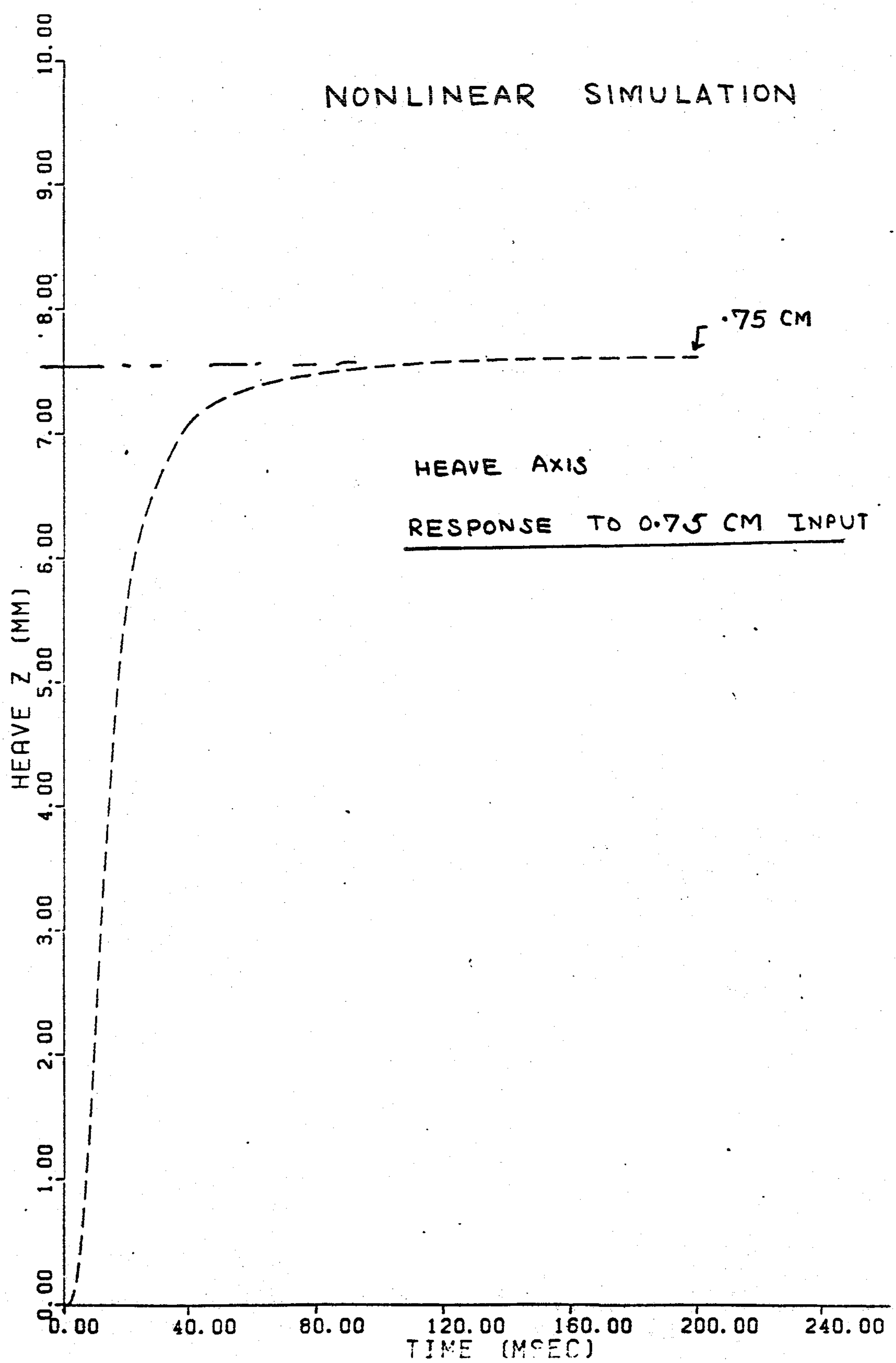
NONLINEAR SIMULATION
·75 CM
HEAVE AXIS
RESPONSE TO 0·75 CM INPUT
HEAVE Z (MM)
0.00
1.00
2.00
3.00
4.00
5.00
6.00
7.00
8.00
9.00
10.00
0.00
40.00
80.00
120.00
160.00
200.00
240.00

FIGURE 6.31

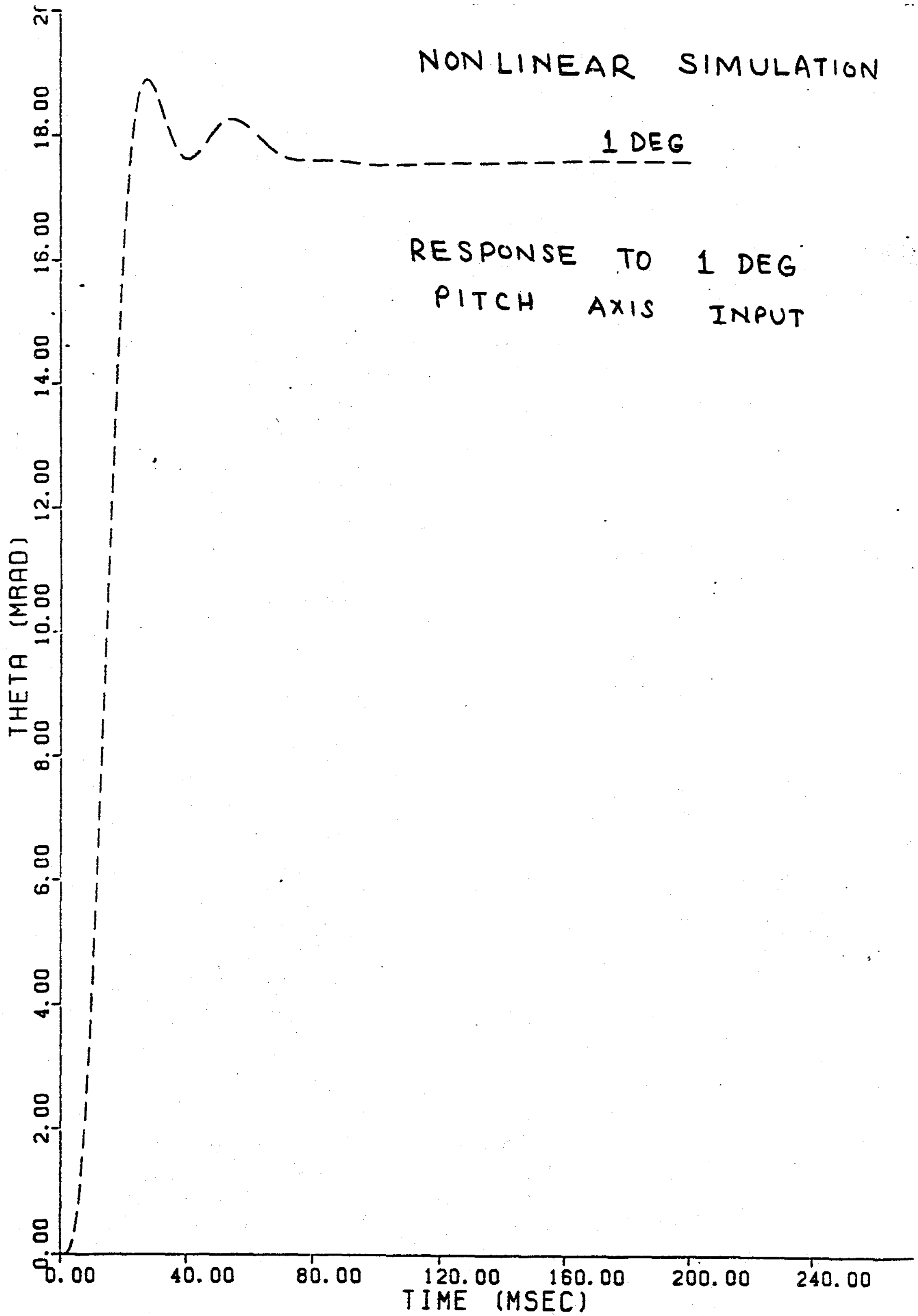
NON LINEAR SIMULATION
1 DEG
RESPONSE TO 1 DEG
PITCH AXIS INPUT
THETA (MRAD)
0.00
2.00
4.00
6.00
8.00
10.00
12.00
14.00
16.00
18.00
0.00
40.00
80.00
120.00
160.00
200.00
240.00
TIME (MSEC)

FIGURE 6.32

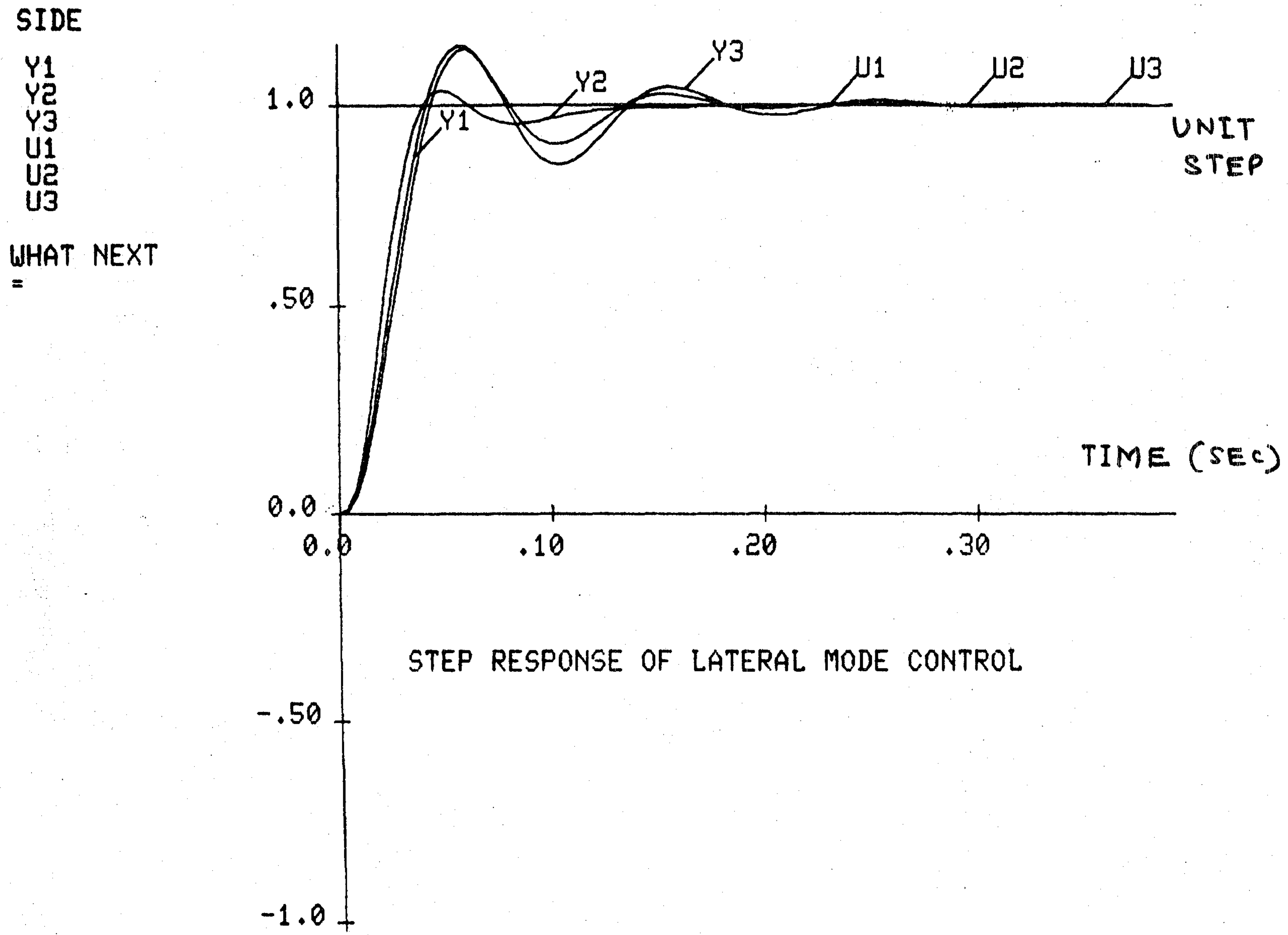
SIDE
Y1
Y2
Y3
U1
U2
U3
WHAT NEXT
=
1.0
.50
0.0
-.50
-1.0
0.0
.10
.20
.30
Y1
Y2
Y3
U1
U2
U3
UNIT STEP
TIME (SEC)
STEP RESPONSE OF LATERAL MODE CONTROL

FIGURE 6.33

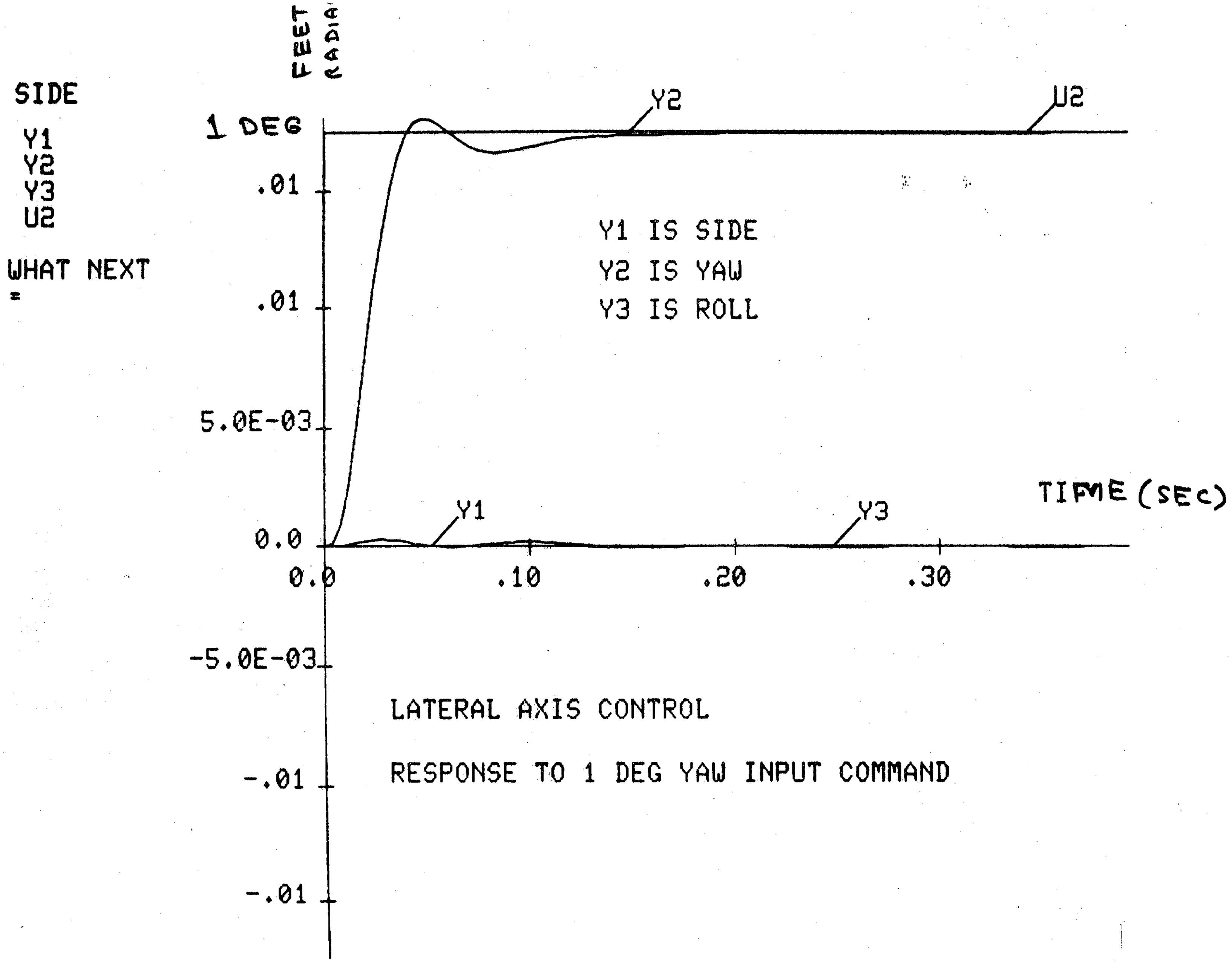
SIDE
Y1
Y2
Y3
U2
WHAT NEXT
=
FEET
RADIA
1 DEG
.01
.01
5.0E-03
0.0
-5.0E-03
-.01
-.01
0.0
.10
.20
.30
TIME (SEC)
Y1
Y2
Y3
U2
Y1 IS SIDE
Y2 IS YAW
Y3 IS ROLL
LATERAL AXIS CONTROL
RESPONSE TO 1 DEG YAW INPUT COMMAND

FIGURE 6.34

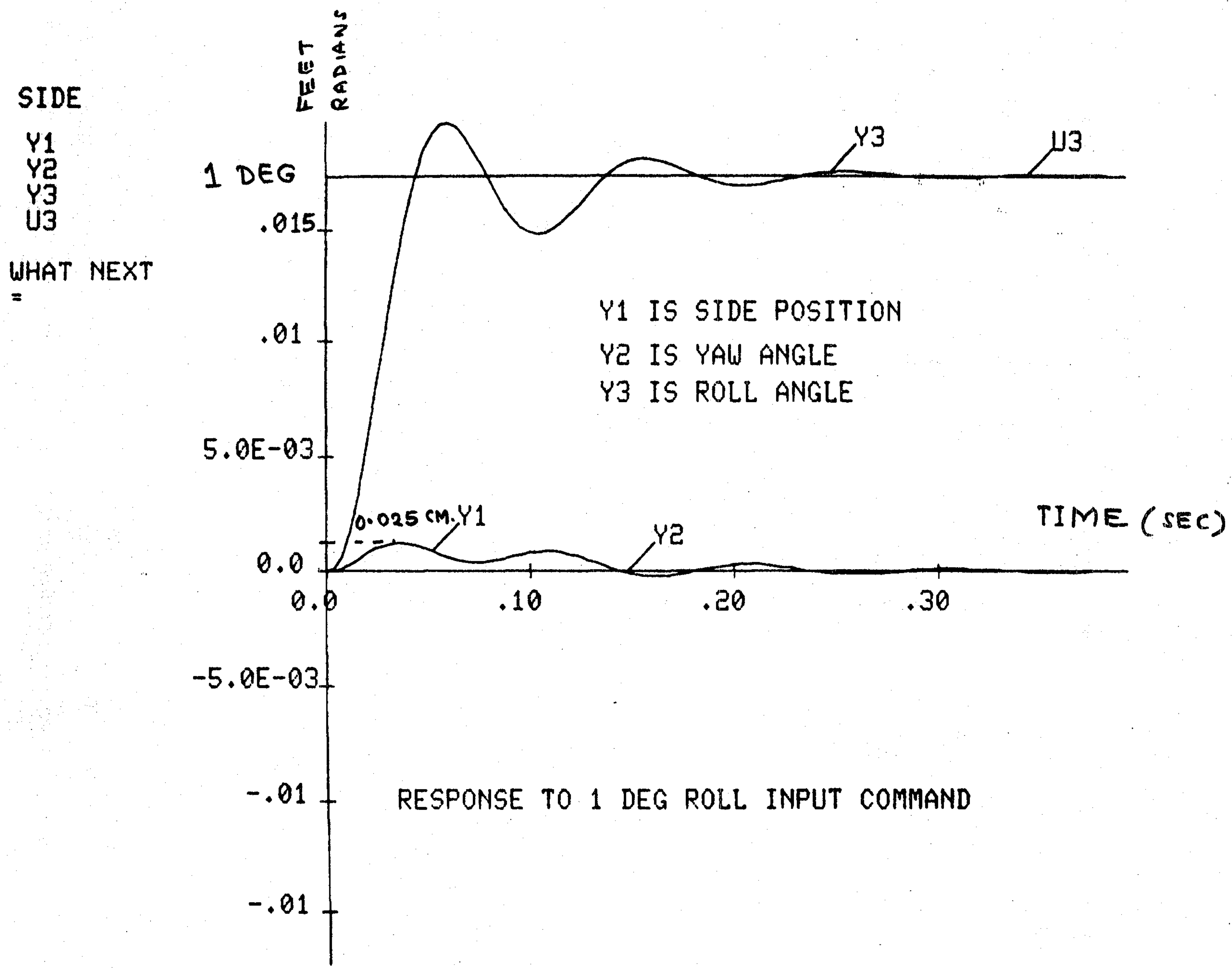
SIDE
Y1
Y2
Y3
U3
WHAT NEXT
=
FEET
RADIANS
1 DEG
.015
.01
5.0E-03
0.0
-5.0E-03
-.01
-.01
0.0
.10
.20
.30
TIME (SEC)
Y1 IS SIDE POSITION
Y2 IS YAW ANGLE
Y3 IS ROLL ANGLE
0.025 CM.
Y1
Y2
Y3
U3
RESPONSE TO 1 DEG ROLL INPUT COMMAND

FIGURE 6.35

6.6 MSBS COMPUTER SELECTION

The primary function of the control computer is to provide control signals to a 6 degree of freedom magnetic suspension system for a model suspended in a wind tunnel. In addition to the primary control system, the control computer will also furnish:

1. Data storage of critical parameters
2. Graphics display
3. Communications to a host computer
4. Communication to magnet sequence controller
5. Interface to operator CRT and keyboard

The control function can be further subdivided into two separate tasks: the primary control related to stabilizing the aerodynamic model, and a control dedicated to the start up and monitor of the magnet system. The dynamic model control algorithm will reside in the control computer where as the magnet monitor and start up will be implemented with individual programmable logic controller.

In order to size the control computer, several factors have to be considered:

1. The number of inputs and outputs
2. The peripheral computer hardware
3. The data storage requirements
4. The bandpass requirements of the control algorithm

As shown in Figure 6.36, the anticipated computer peripheral equipment is presented above the system bus and the input/output devices are shown below.

The dynamic control requires that the position of the model be determined. Several different types of sensors have been considered, such as electromagnetic and optical. In each case, several inputs to the computer are demanded. For the electromagnetic sensor, 12 are required for resolving the 6 axes of motion. The position sensors represent the dynamic feedback signals for the control algorithm. If the sensor outputs are digital, the inputs to the computer would be accomplished as logic ins. For the application investigated, it was assumed that the sensor inputs are analog and an analog to digital converter is required for interfacing with the computer. If electro-optical sensor is used, the analog to digital converter is replaced by a digital interface logic.

MSBS COMPUTER CONTROL

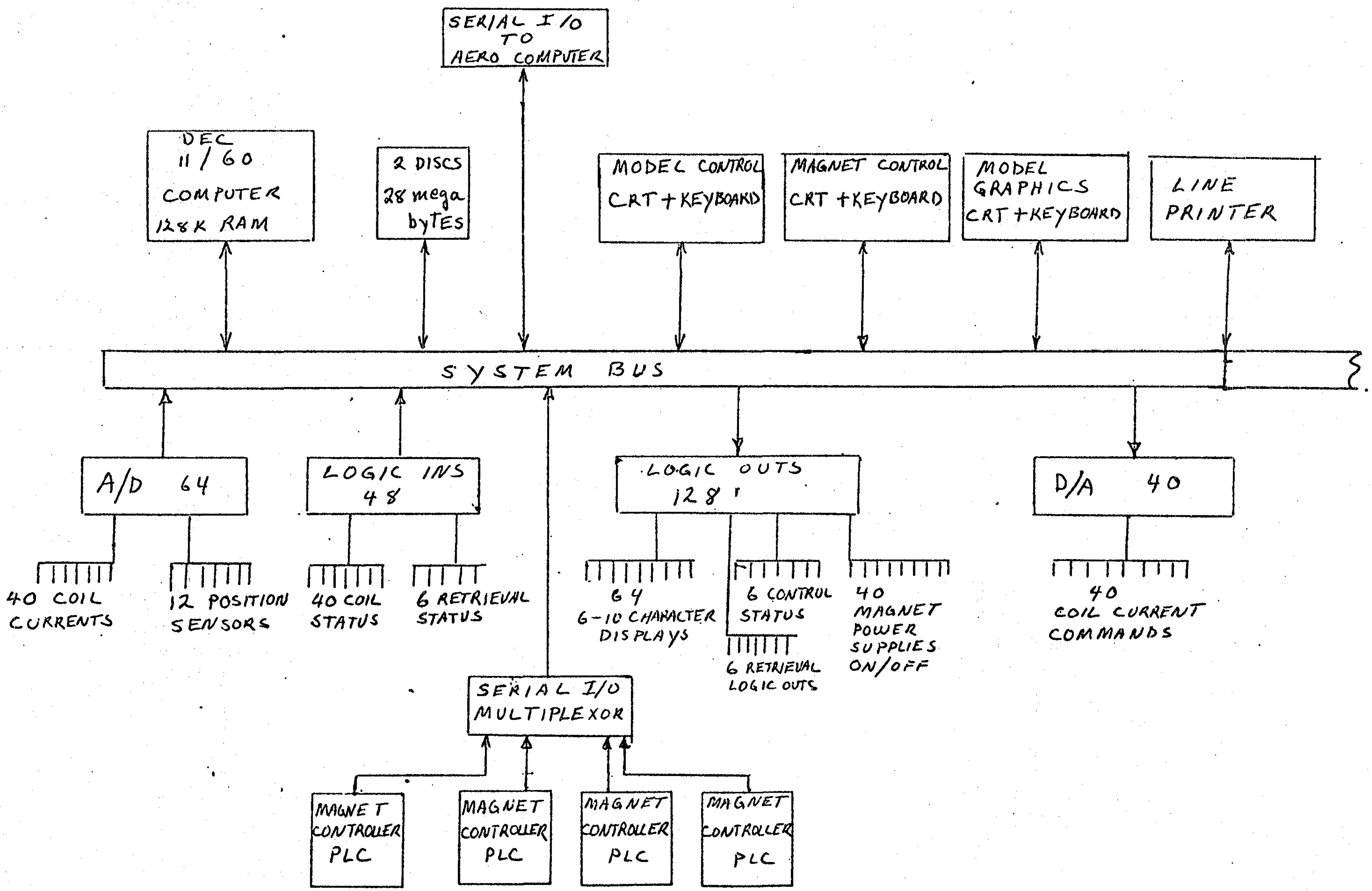

FIGURE 6.36

Additional analog inputs are also required for monitor and display of the magnet coil currents. The coil currents will be used for calculating the dynamic force loads on the model during wind tunnel tests.

As outputs from the control computer, 40 coil current commands are needed for regulating the magnet power supplies. The conversion interface from the computer to the power supply will be accomplished with 40 digital to analog interface devices.

Logic in signals are also required for monitoring the magnet coil and retrieval device status. Logic outs are needed for turning external devices on and off such as the magnet power supplies, driving digital displays for on line coil current presentation and providing status outputs for other control devices. It is estimated that a total of 48 logic ins and 128 logic outs will be required for the MSBS installation.

A communication interface with the logic controllers will be accomplished via a serial input/output multiplexer. The serial communication interface will provide the main control computer with a means of monitoring the status inputs from the individual magnet sequence controllers.

The main computer will consist of the computer processor unit and random access memory. As peripheral devices, a hard disc will be required for data storage and a second disc for program development and back up.

A cathode ray tubes (CRT) plus keyboards will provide the interface with the operator. One CRT plus keyboard will be dedicated to controlling the model movement. A second CRT terminal will provide access to the magnet monitor and control. In each case, only ASCII character presentation of the data will be presented to the operator.

A third graphic CRT plus keyboard is included in order to provide a means of presenting time plots of dynamic control outputs. More CRT displays can be added to see TV images made available by CID or other TV cameras when operating in the TV scan mode.

The line printer is necessary for providing hardcopy of any data or software development.

An additional communication interface will be furnished for transmitting data to a host aero computer which will process the aero data.

The size of the data storage was approximated by assuming that 24 variables will be stored at a rate of 50 samples/sec. A smaller set of variables can be stored at a higher data rate to extract the aerodynamic parameters. This requires that for each hour of data a 10 megabyte capability is needed. Therefore, in order to fulfill both the support software development and the on line data storage for two hours, two 28-megabyte discs were selected.

The PDP 11/60 computer was selected based on the bandpass of 20 Hz needed for the control algorithm. In order to achieve a 20 Hz bandpass, it will be necessary to sample the data input, perform the control algorithm calculation and output the commands to the magnets in a time interval not more than 10 milliseconds. It is anticipated that the data acquisition and data output will be implemented using an additional intelligent microcomputer controller which performs the task of scanning the A/D and outputting to the D/A using direct memory access for transfers to and from the main CPU memory. The data interface controller minimizes the time required for data acquisition and data output from the main computer. With the number of control ins and outs it is estimated that all the data acquisition and outputs for a single control update can be completed in less than a millisecond.

The control algorithm involves a maximum of 600 multiplies and 600 additions which makes up the major portion of the time required for a control iteration.

The following table shows a comparison of the multiply times for various Digital Equipment Corp. computers with a floating point processor (32 bit word length).

Computer	Single Precision	Double Precision
11/34	16.2 microsec	25.4 microsec
11/60	1.5 microsec	3.74 microsec
11/70	3.27 microsec	5.43 microsec
11/44	16.2 microsec	25.4 microsec

Based on the add and multiply times, it appears that the 11/60 computer can accomplish the control computation in 4 to 5 milliseconds which will impose a 50% demand on the CPU computation time for a 10 millisec control update rate.

Computer Redundancy

In order to provide for a backup to the main computer, a bus switch and an additional computer is recommended (Figure 6.37). This backup system is a stripped down version of the main 11/60 computer system and furnishes a real time redundant means of controlling the model in the event the main CPU becomes inoperative. The backup computer is programmed to perform the control algorithm and only those control functions necessary for insuring a failsafe retrieval of the aero model.

The bus switch which can be activated in less than a microsecond, is a device which monitors the main CPU operation and switches the main system bus to the backup computer in the event of a main CPU failure. The backup computer then picks up the main memory and all the critical input/output devices and continues to provide a minimal control of the aero model. During the backup operation, all non-critical functions such as data storage, graphics, and communications to the aero computer are eliminated.

The main bus with the memory will be housed in a separate chassis with its own power supply, thus insuring complete independence from the main CPU frame. Both the main bus and the backup computer will be provided with uninterruptable power supplies (UPS) to insure continuous computer operation during short power interruptions.

Software

The software will be developed using the RSX 11 operating system and a higher level language such as FORTRAN. For faster computation times, macro level software will be used for input/output buffering and other functions which are not efficient when using FORTRAN.

The software modules identified for the control computer are shown in Figure 6.38.

A control system executive will be necessary for coordinating all of the operating software modules in the computer. This executive is in addition to the operating system provided by the computer manufacturer.

The control loop is comprised of four software modules which include data acquisition, position sensor decoupling, the main computation algorithm, and the data command output.

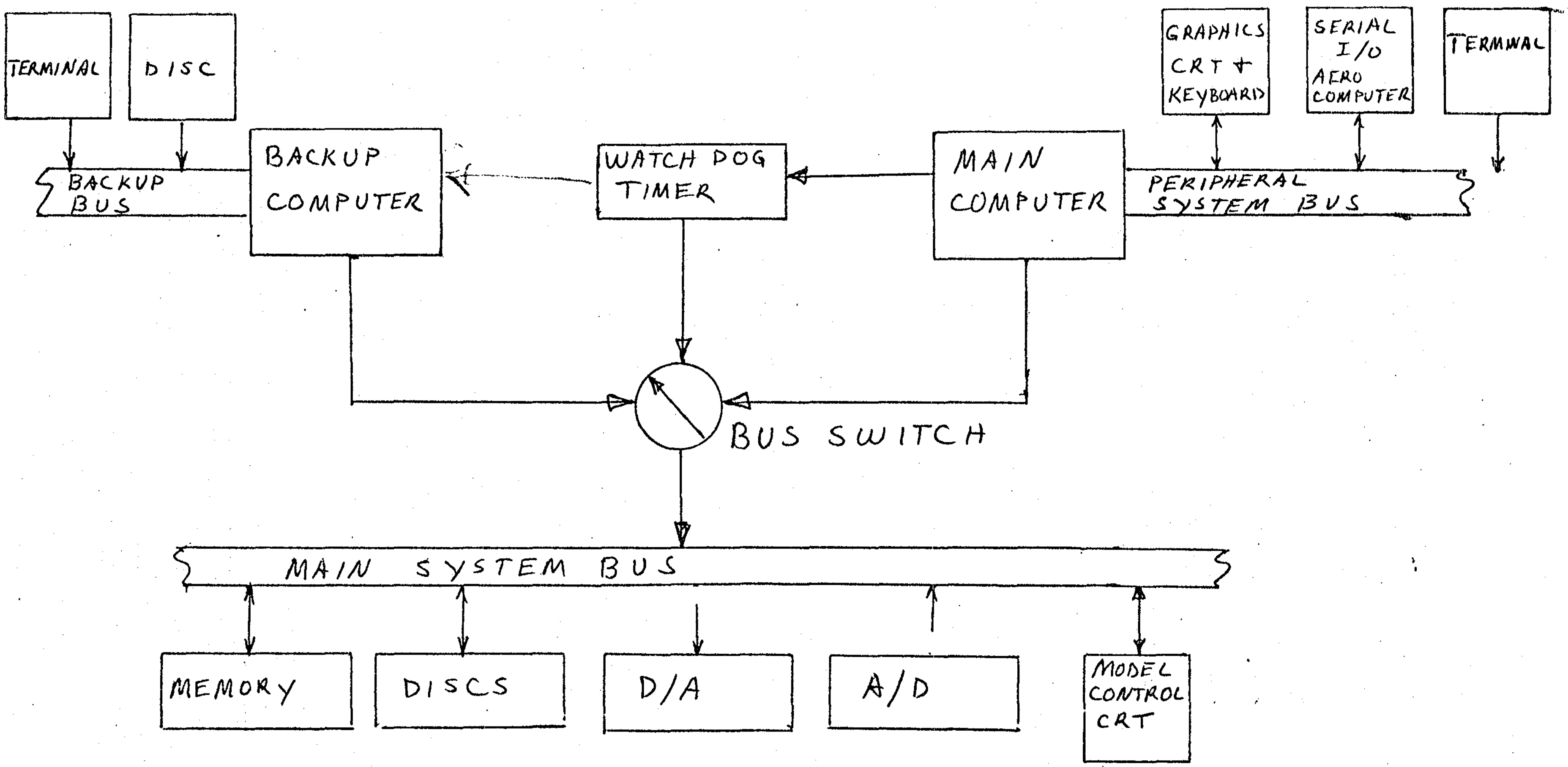

BACKUP COMPUTER
FOR
MSBS

FIGURE 6.37

MSBS SOFTWARE MODULES

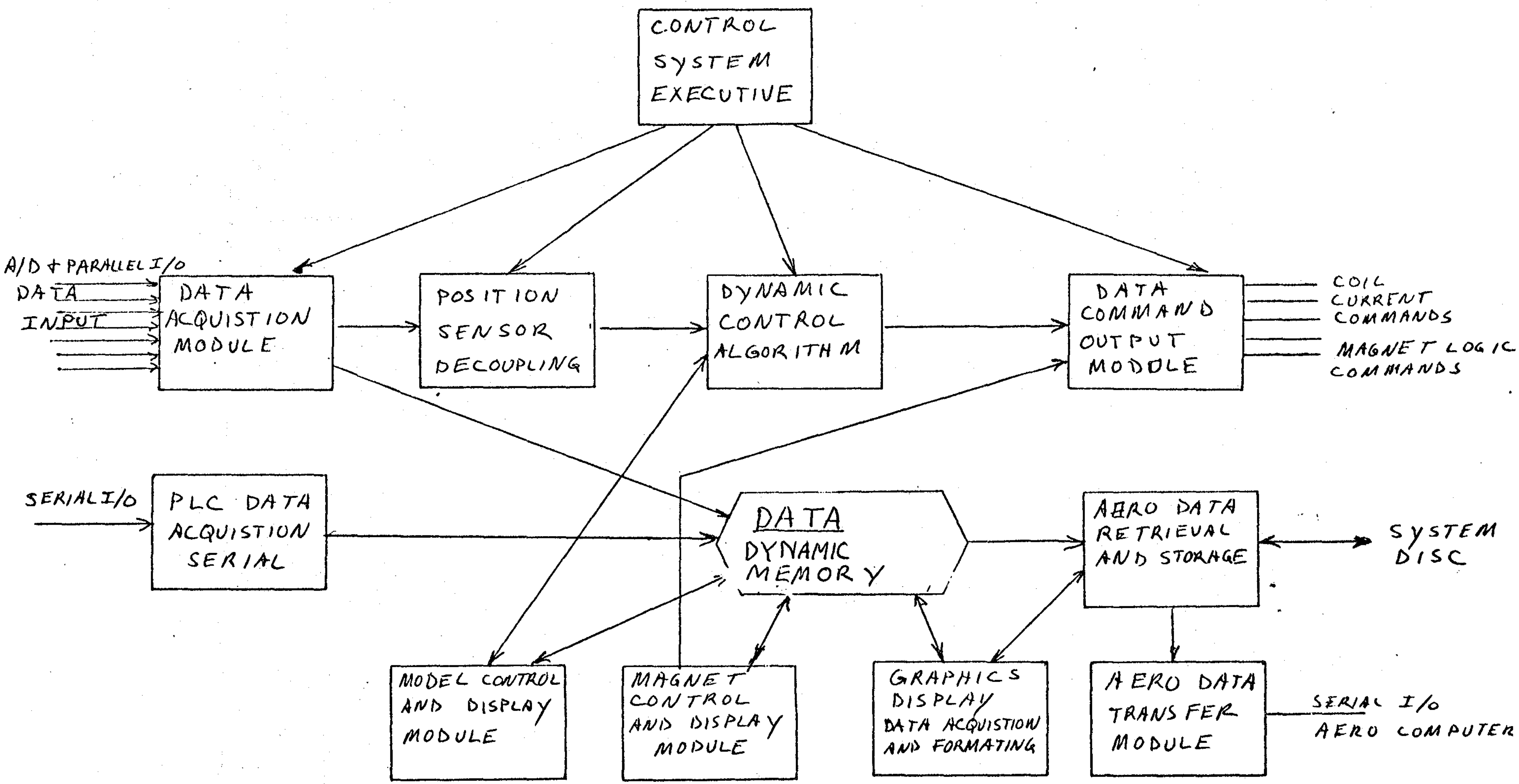

FIGURE 6.38

The data acquisition module acquires the data from memory and scales it for computation in the computer.

Decoupling of the EPS sensor inputs is required in order to resolve the respective coordinate axes motions from the sensor inputs.

The dynamic control algorithm encompasses the filtering of the sensors signals, the frequency compensation networks and the command outputs to the magnet coils. The control algorithm is formulated as a multivariable system which is designed with 6 error multi-inputs and 10 multi-output magnet commands. The control algorithm also derives inputs from the control CRT which specifies the position and angle commands for the aero model.

The data output command module interfaces with the control algorithm and performs the necessary conversions for directly controlling the magnets. For redundancy, a total of 40 output magnet commands are required for the system. Logic is performed which monitors the status of the magnet electronics and in the event of a failure, eliminates pairs of magnets from the control in order to keep the system balanced. The output module also provides the control logic outputs for the magnet electronics.

The program logic controllers (PLC) are used primarily to sequence the start up and shutdown of the magnet and cryogenic power supplies. In addition, various sensors are monitored relative to temperature, vacuum, and liquid level which are critical to the overall system performance. The PLC data acquisition module acquires and formats this data on a periodic interval and stores it in dynamic memory for display and for transfer to long term storage.

Software is required for each of the CRT controls and graphics terminals which are used for operator interface.

The aero data retrieval and storage module will perform the task of formating the data and transferring it to the disc long term memory. When data is transferred to the aero computer, this module will also transfer the data from the disc to the aero data output module.

Each of the software modules, briefly described, will be implemented on the control computer. It is anticipated that the CPU time not allocated to the control algorithm will be adequate for servicing the remaining tasks.

6.7 TECHNICAL RISKS

The requirements for the control and computer system is well within the current state-of-the-art technology. The PDP 11/60 minicomputer with 1.5 μsec multiply time can compute the control signals to gradient magnets in real time. The backup computer provides necessary control functions to insure a failsafe retrieval of the aeroplane model.

We have used PDP 11/60 minicomputer for real time computer control of 24 directional solidification furnaces. Based on our experience, the technical risk associated with the MSBS computer control is very minimal.

7.0 POSITION SENSOR CONCEPTS

The MSBS Statement of Work calls for two different approaches to be utilized in defining design concepts for the MSBS Position Sensors:

1. "a scaled up version of the electromagnetic (non-optical) position sensing system (EPS) as developed and used at MIT. For redundancy, a second EPS system identical to the primary EPS except for operating frequency shall be used."
2. "A third system using visible light and photo-sensors shall be the reference system used for initial alignment as well as potentially being used as third redundant system during operation of the MSBS."

In pursuing approach #1, frequent interaction was carried out with MIT personnel, who not only furnished appropriate drawings and reports, but gave their own time for consultation. Using such invaluable data and scale-up approximations, this portion of the study has developed significant insights into the capabilities and limitations of the EPS.

Should such limitations prove unacceptable, the optical approach assumes more significance than implied by the Statement of Work. In pursuing the optical approach, #2, reports and discussion by University of Southampton personnel provided stimulating ideas, as did current work on star trackers being carried on within GE.

7.1 ELECTROMAGNETIC POSITION SENSOR

The MIT Aerophysics Laboratory has designed, installed and operated an Electromagnetic Position Sensor (EPS) on their 5 inch diameter wind tunnel which has normal coil magnetic suspension for the test model. This sensor system evolved from some basic design analysis and the applications of available hardware components which could be obtained in a timely and relatively inexpensive manner. No serious attempt has been made to optimize the coils, shielding or electronic circuits used for identifying and amplifying the voltage signals from the sensor coils which are proportional to the deviation of a magnetic material core in the model from some fixed reference position at which the EPS system was calibrated. Nevertheless this position sensing system has worked sufficiently well to be considered for use in larger magnetic suspension and balance systems. There is, of course, no inherent reason why its application must be limited to magnetic suspension systems since it would work equally well in other wind tunnels using a non-magnetic mechanical sting for the model suspension. The MIT EPS has been discussed in several technical papers and reports, of which three are listed here as references 1, 2 and 3.

7.1.1 Requirements

It is not required of this study to design an EPS system that will meet all the requirements for position sensors in the MSBS facility. It is required that the feasibility of scaling up the MIT small model EPS be considered. This task therefore has been defined as one of applying reasonable scaling laws to the characteristic parameters of the MIT model and then commenting on the feasibility of the resulting voltage signals from the scaled up coil sizes being useful as input to the electronic circuitry which identifies, amplifies, and converts the pick-up coil voltages into position sensor output voltages. These have a known, independent and stable relationship to the three orthogonal distances and three Euler angles which completely characterize the position and attitude of the model relative to a fixed reference frame. The electronic circuitry which does this will need to be different from the MIT model only to the extent that the coil signals are different or the model amplifiers and processors can be improved to better serve the needs of a large scale operating MSBS.

7.1.2 Approach

The approach used in this feasibility study is to consider linear scaling of all dimensions of the energizing and pick-up coils and to show parametrically how the resulting output signal voltage to input energizing voltage ratio should scale to larger sizes, and to consider how these values would be expected to be affected by noise, stray capacitance and coil circuit resonance. For a first order approximation this linear scaling can be done from either the more basic magnetic field equations or from the familiar voltage relationships for inductively coupled circuit elements.

7.1.3 Concept

The EPS MIT model operates as a linear voltage differential transformer consisting of two circular excitation coils with one at each end of the suspended model; two circular axial position coils a small distance axially from the excitation coils; and 12 horizontal and vertical position coils located in three axial bands of four coils each in a transducer coil form surrounding the model as shown as Figure 7.1, extracted from Reference 1. The magnetic core material located in the aerodynamic model serves as the differential coupler between the stationary coils described.

The excitation coils are driven by a 20 kHz power supply chosen partially for convenience and somewhat intuitively to be above the major harmonics of the coils of the suspension system and below the higher frequency resonances of the RLC circuits comprising the EPS system. This frequency worked well at MIT but would be selected based on circuit analysis for other larger systems for MSBS. There exists a significant coupling between the excitation coils and the position coils even with no magnetic core material present; but this coupling is a function of coil positions and the electrical and magnetic properties of the surrounding medium. The coil form should be sufficiently rigid and stable to maintain the same coil positions under all operating conditions for which the EPS has been calibrated. The insertion of a magnetic material inside this coil cage changes the coupling between the energizing coils and the position detecting coils proportional to the distances involved. The system is calibrated by measuring the voltage induced in the 14 pick-up coils for various positions of the core. The electronic circuit detects, amplifies and identifies these coil voltages and converts them into three output signals proportional to the three orthogonal positions and three signals proportional to three Euler angles completely describing the position of the magnetic core material. If the core is also fixed relative to the aerodynamic model being tested, then the model position and attitude is also described. (Signal output in other forms could be obtained if it were appropriate for the control system.)

7.1.3.1 Coil Form

The scaled-up coil form concept is shown in Figure 7.2. It is anticipated that all materials would be non-magnetic and probably non-metallic similar to G-10 or some other dimensionally and electrically and magnetically stable epoxy fiberglass. The coils would be wound on forms similar to window frames and inserted in openings in the coil form structure. This type of structure could be assembled and checked out in the factory before partial disassembly for shipment and re-assembly around the wind tunnel. Non-symmetric dimensional changes must be minimized since the induced voltage cannot distinguish between

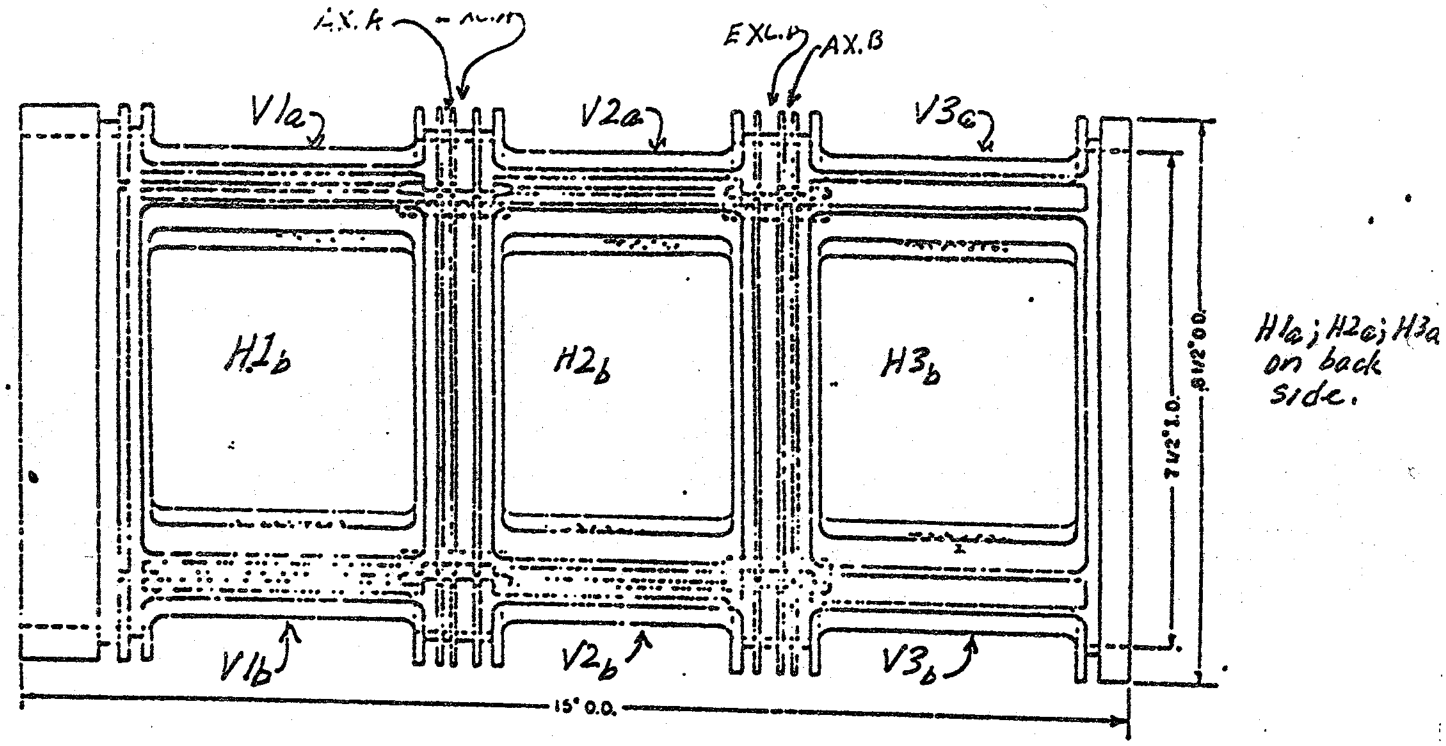

Figure B.1. E.P.S. transducer coil form for Cylindrical Wind Tunnel

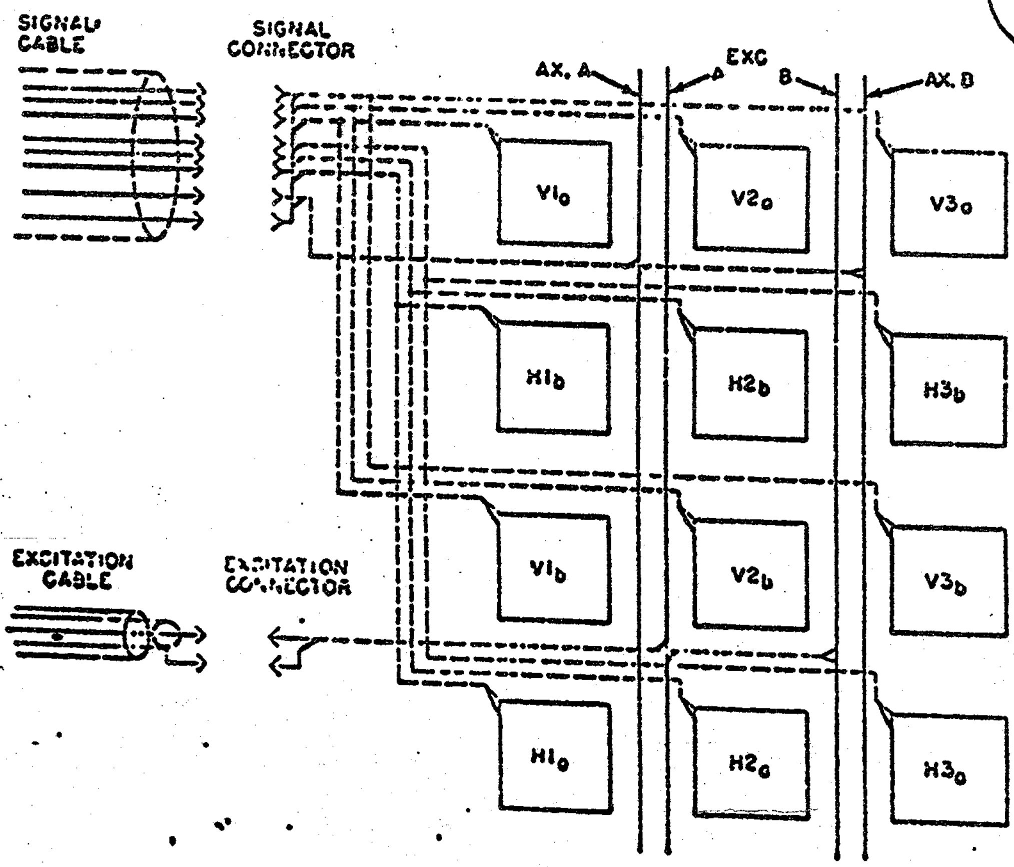

Figure B.2. E.P.S. transducer coil windings: developed view showing wire routing

Figure 7.1
FIGURES EXTRACTED FROM REFERENCE 1

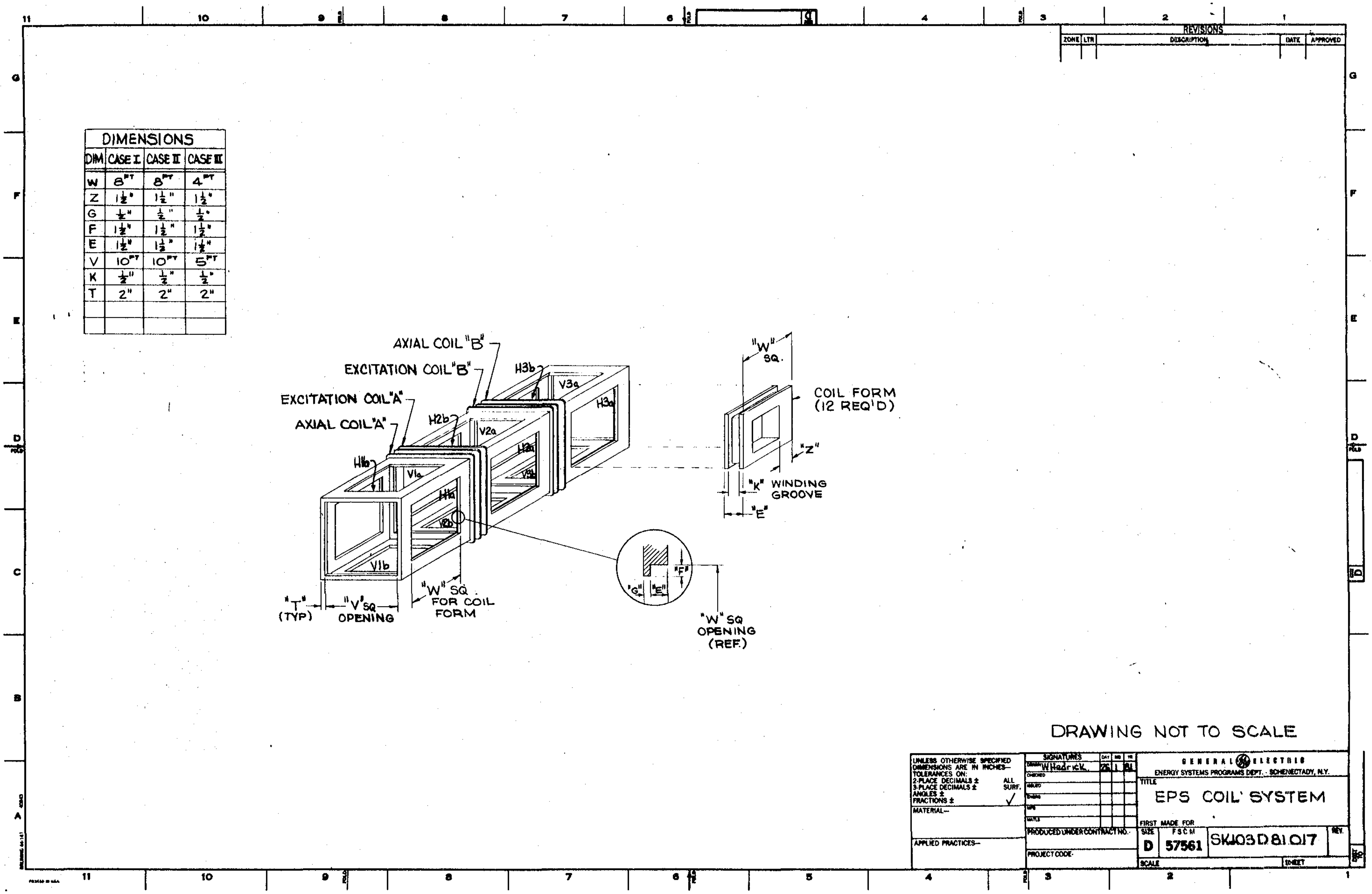

DIMENSIONS			
DIM	CASE I	CASE II	CASE III
W	8FT	8FT	4FT
Z	1½"	1½"	1½"
G	½"	½"	½"
F	1½"	1½"	1½"
E	1½"	1½"	1½"
V	10FT	10FT	5FT
K	½"	½"	½"
T	2"	2"	2"

Figure 7.2
EPS COIL SYSTEM

a movement of a coil toward the core or of core toward the coil. For the voltage analysis of this concept all dimensions are assumed to have been scaled linearly and this assumption fits well with this coil form structure while maintaining maximum window space. For redundant back-up two coils could be wound on each form. During normal operation they may be connected in series for maximum sensitivity when the whole facility is being used as an aerodynamic measuring instrument. If a circuit or coil should fail then the two coils could be electrically separated and still retain sufficient sensor capability for gross control of the model.

7.1.3.2 Coil Voltage

From the magnetic field equations in the cited reference it is shown that the core displacement voltages are directly proportional to magnetization of the core (M), volume of the core (a^3), area of the pick-up coil (R^2) and number of turns on the coil (N) and inversely proportional to the core to coil distance cubed (R^3). The scaled up voltage may then be written as:

$$V_s = \frac{N_s}{N_m} \frac{M_s}{M_m} \frac{a_s^3}{a_m^3} \frac{R_s^2}{R_m^2} \frac{R_m^3}{R_s^3} V_m$$

$$= \frac{N_s}{N_m} \frac{M_s}{M_m} \frac{a_s^3}{a_m^3} \frac{R_m}{R_s} V_m \qquad (1)$$

where: subscript s refers to scale-up
subscript m refers to MIT model

The magnetization in the above relationship is, of course, that differential magnetization produced by the 20 kHz excitation coil current and is proportional to the slope of the B-H curve at the point of operation due to the large magnetizing coils. High core saturation decreases the EPS sensitivity about in the ratio of $\frac{\mu-1}{\mu+2}$ which is in the order of 3% for μ as low as 100.

Assuming a constant number of turns and core magnetization then the sensor voltage from the above equation can be seen to vary with the ratio of core volume to core to coil distance cubed and for the model and MSBS dimensions given the ratio of V_s to V_m will vary as shown in Figure 7.3 and is seen to increase due to core volume increasing more than distance.

Figure 7.3

SCALE-UP VOLTAGE DUE TO CORE SIZE

	MIT (5")	4'x4'	8'x8'
$\frac{a^3}{R}$	0.6	2	8
$\frac{V_s}{V_m}$	1.0	3.3	13.3

7.1.3.3 Output to Input Voltage Scaling

a) Magnetic Field View

Using the voltage relationships from equation (1) it is interesting to consider the ratio of output to input voltage which is obtained by linear scaling. If the excitation coil is assumed to be as shown below, with the core located in the center of a coil of radius R, then some simple relationships can be deduced.

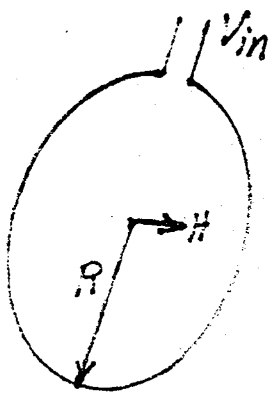

$H \propto \frac{NI}{R}$ $\qquad\qquad L \propto R$

Excitation Coil Voltage$=V_{in} = L\,\frac{dNI}{dt} \propto R\frac{dNi}{dt}$

or $\frac{dNi}{dt} \propto \frac{V_{in}}{R}$

and $\frac{dH}{dt} \propto \frac{I}{R}\,\frac{dNI}{dt} \propto \frac{V_{in}^2}{R}$

A.C. Magnetization of the Core$=M \propto \frac{dH}{dt} \propto \frac{V_{in}}{R^2}$

If the scaled up magnetization is equal to the model magnetization then:

$$\frac{M_s}{M_m} = 1 \quad \text{and} \quad \frac{V_{s(in)}}{V_{m(in)}} = \frac{R_s^{\,2}}{R_m^{\,2}}$$

From equation (1)

$$\frac{V_s(out)}{V_m(out)} = \frac{N_s}{N_m} \frac{M_s}{M_m} \frac{a_s^3}{a_m^3} \frac{R_m}{R_s}$$

for $\frac{M_s}{M_m} = 1$ $\frac{N_s}{N_m} = 1$ and linear core scaling $\frac{a_s^3}{a_m^3} = \frac{R_s^3}{R_m^3}$

$$\frac{V_s(out)}{V_m(out)} = (1)(1) \frac{R_s^3}{R_m^3} \frac{R_m}{R_s} = \frac{R_s^2}{R_m^2} = \frac{V_{s(in)}}{V_{m(in)}}$$

or $\frac{V_s(out)}{V_s(in)} = \frac{V_m(out)}{V_m(in)}$ = same output to input voltage ratio

b) Circuit Element View

Another approach to voltage scaling relationships more often used by those who regularly work with circuit elements, such as those in a Low Voltage Differential Transformer (LVDT) is to consider a simple inductively coupled circuit, shown below.

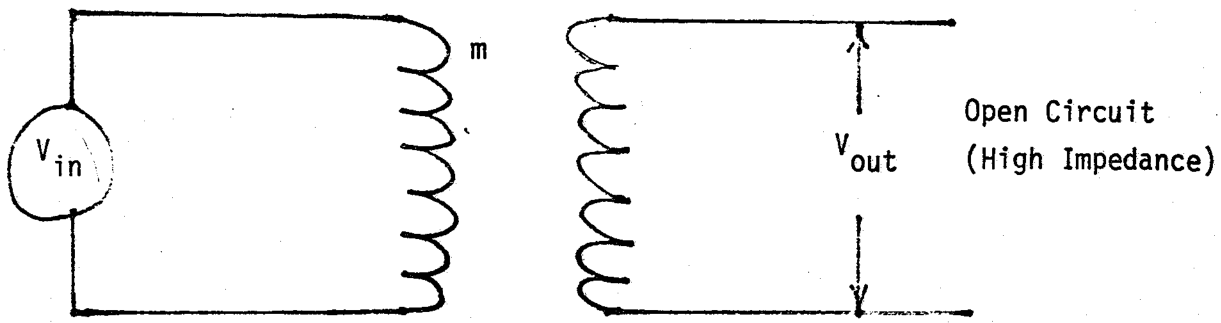

$$V_{in} = L_{in} \frac{dIin}{dt} \qquad V_{out} = m \frac{dIin}{dt}$$

$\frac{V_{out}}{V_{in}} = \frac{m}{L_{in}}$ = constant for linear scaling

Thus confirming the previous result that for linear scaling the same ratio of displacement voltage to excitation voltage can be obtained and that the same conclusions are reached from circuit element or magnetic field equation approaches. Qualitative and approximate quantitative scale-up values can be obtained from either, and both confirm that the displacement voltage to excitation voltage ratio can be similar for the large and small size. Therefore similar signal processing circuits may be used.

7.1.3.4 Position Resolution

In Reference 2 the MIT model is shown to measure to ± 0.0008 inch and 0.1 degree in all components. If the larger size system were to have the same sensitivity in terms of $\Delta X/R$ then the measurement resolution would be shown in Figure 7.4.

Figure 7.4

SENSOR RESOLUTION SCALED AS $\Delta X/R$

	MIT (5")	4'x4' (25")	8'x8' (50")
Distance (in)	0.0008	0.004	0.08
Degree	0.1	0.25	0.5

The requirements of the work statement are for positional accuracy of 0.01 inch and angular accuracy of 0.02 degrees. The distance measurement in the scaled-up system has a high probability of meeting these requirements by taking advantage of the increased voltage signal (which with linear scaling increases as R^2) to increase the sensitivity. The angular measurement capability however of the present MIT model does not appear to meet the requirements and this should be considered further in future work.

In Reference 3, the applicability of using digital rather than analog signals was considered with the results shown in Figure 7.5 (Table 4 of the Reference).

Figure 7.5

RESOLUTION FOR DIFFERENT A/D CONVERTORS

No. of Bit of A/D	mv per Bit	Corresponding Movement: Lift (in)	Drag (in)	Pitch (deg)	Yaw (deg)
8	7.81	2.32×10^{-2}	1.45×10^{-2}	4.67×10^{-1}	2.81×10^{-1}
10	1.95	5.79×10^{-3}	3.61×10^{-3}	1.19×10^{-1}	7.03×10^{-2}
12	4.88×10^{-1}	1.45×10^{-3}	9.03×10^{-4}	2.78×10^{-2}	1.76×10^{-2}
16	3.05×10^{-2}	9.05×10^{-5}	5.65×10^{-5}	1.86×10^{-3}	1.10×10^{-3}

The conclusion of the Reference that the system sensitivity using digital signals would be limited by the EPS and not by the A to D conversion capability should also hold true for the scale-up.

The major limitation to the utilization of the EPS for MSBS is the shielding of the EPS signal from the model core, if metallic test section walls are utilized. This problem is discussed in Section 2.2.1 of this report. Essentially, the characteristic time for the 20 KHz EPS signal is so substantially smaller than the time constant for field diffusion through typical metallic walls that the EPS signal would be completely shielded. Since sufficiently low frequency EPS signals to alleviate this problem would interfere with magnet controls, the alternative approach is to use non-metallic or composite material walls. G-10 glass fiber/epoxy is a potentially feasible material that combines the electrical resistance, strength, and tolerance of cryogenic temperatures for possible development for test section walls.

7.1.3.5 Shielding

The MIT model EPS has an electrostatic (Faraday) shield completely surrounding the sensor coils except for windows cut out for access. This would also be incorporated in the scaled-up system. However, the large copper electromagnetic shields over the pole faces of the iron core saddle magnets would not be expected to be used with the superconducting coils of the larger system. Twenty kiloHertz (20 kHz) parallel resonant traps with a Q of 760 were used in the roll coil power supply circuits on the MIT model. Similar traps may also be required as part of, or in addition to, the larger power supplies for the superconducting magnets. Noise density, primarily expected to come from the magnet coil power supplies, may be a constant and thus scale as R^2. Power supplies with low noise levels in the EPS operating frequency range are required.

7.1.3.6 Sensor Coil Resonant Frequencies

The resistance, inductance and capacitance of the MIT EPS coils were recently measured with the values shown in Figure 7.6.

Figure 7.6

NASA PROTOTYPE BALANCE
EPS COIL PARAMETERS

EPS Coil Circuit	DC Resistance[1] ohms	Inductance[2] millihenrys	Self-capacitance[3] microfarads
Axial	14.76	.919	.00141
Lateral I	7.57	.468	.00156
Lateral II	10.41	.517	.00143
Lateral III	7.18	.416	.00126
Vertical I	12.42	.509	.00144
Vertical II	9.49	.502	.00146
Vertical III	12.47	.488	.00152

(1) Measured with fluke digital VOM.

(2) Calculated from resonance frequency with .25 μf mica transmitting capacitor.

(3) Calculated from self-resonant frequency.

The resonant frequencies can easily be calculated by the simple relationship:

$$f = \frac{1}{2\pi}\sqrt{\frac{1}{LC}}$$

and expected frequencies for a linear MSBS scale-up can be found.

$$\frac{f_s}{f_m} = \sqrt{\frac{L_m C_m}{L_s C_s}}$$

Both L and C scale as R so LC goes as R^2

$$f_s = f_m \sqrt{\frac{R_m^{\ 2}}{R_s^{\ 2}}} = f_m \frac{R_m}{R_s}$$

The resonant frequencies would then be as shown in Figure 7.7.

Figure 7.7

RESONANT FREQUENCIES WITH LINEAR SCALING
(kHz)

EPS Coil Circuit	MIT R=5"	4'x4' R=25"	8'x8' R=50"
Axial	140	28	14
Lateral I	186	37.2	18.6
Lateral II	185	37	18.5
Lateral III	219	43.8	21.9
Vertical I	186	37.2	18.6
Vertical II	186	37.2	18.6
Vertical III	181	36.2	18.1

The 10 to 1 separation between resonant frequency and operating frequency of 20 kHz achieved on the MIT model cannot be maintained on the MSBS with simple linear scaling. The EPS operating frequency, the number of turns per coil and the size wire used in the coils would all be modified to achieve a non-resonant operating frequency. This may be the criterion which determines that the two independent EPS systems desired for the MSBS should operate at the same frequency, and be physically constructed as previously considered in the last two sentences of paragraph 7.1.3.1. Ample voltage levels are predicted by the linear scaling laws to justify consideration of these parametric changes during EPS scale-up design.

7.1.4 Technical Risks

The electronic circuits and A to D converters, if used, are typical of many sensor installations for which the components should be considered state-of-the-art. For maximum sensitivity and stability with a minimum of cross-coupling effects, high quality elements and circuit design is required. Since the larger coils in a scaled-up EPS may inherently produce higher voltages, some voltage isolation may be used between the sensor coil signal and the circuit elements.

The size of the sensor coils and separation from the core is very large compared to any other known application of LVDT's. This must be considered as a technical risk requiring further investigation. Mechanical, electrical and magnetic stability of these large diameter coils are all suspect when considered as measurement devices for movements in the order of a few mils. Fortunately, however, early verification of their capabilities is feasible, since they appear to be suitable for some simple single (or two) coil tests in simulated environments.

During unusual conditions in which the suspension magnet coils are driven to maximum output to hold the model, it is conceivable that the core saturation could increase sufficiently to change the calibration of the sensor coil coupling. Linearity of the sensor system would then be lost, but the sense should be retained and the model controlled as in other fault scenarios.

Overall, it has been shown that the appropriate scaling laws indicate that a displacement signal from the EPS coils in the same range as that obtained on the MIT model should be achievable from the scaled up system, It is concluded that the EPS has the inherent capability for application on MSBS.

7.2 AN ELECTRO-OPTICAL APPROACH TO MEASURING POSITION AND ATTITUDE

This section considers the conceptual design of non-tactile position and attitude sensing system which would be independent of any measurement system depending on use of magnetic fields. Such a system should be passive in the sense of not requiring any radiation source on the model. However, the use of target patterns on the model which do not affect either the aerodynamic or the magnetic characteristics of the model are considered to be acceptable.

The basic schemes to be considered then involve the illumination of the model by sources located flush with the tunnel walls and detecting reflections of the model (or, preferably, targets mounted there-on) by sensors also mounted fixed relative to the tunnel. The approach, then, generally can be considered a type of target(s) tracking. The use of standardized targets is favored because it avoids the more difficult problem of pattern recognition when tracking a model not having such targets.

Sources and sensors operating in the visible spectrum are favored due to their high resolution, low noise characteristics, their advanced state of development and their high degree of de-coupling from the aero-thermodynamic response of the model. IR sensing, for example, would be subject to interference by aerodynamically induced heating of the model.

Sensors to be considered might include "point detectors" as well as area or linear imaging detectors. Point detectors (e.g. conventional photodiodes) are rejected since their use would involve mechanically rotatable mounts for the sensor and/or its optical elements in order to accurately measure position and attitude over the required range of displacements and angles. Being analog devices they are also subject to errors due to viewing degradations (e.g. smoke in tunnel). Imaging sensors include more conventional vacuum tube types such as vidicons and image orthicons as well as the more recently developed solid-state array types. The former types are judged as being inappropriate for the present application due to their inherent read-out non-linearities and especially due to their sensitivity to operation in the expected high magnetic field.

Hence, we converge on application of solid state detector arrays. These can be classified generally as linear or area arrays. The linear array will generally be suitable, in tracking, for constraining a single degree of freedom of the model.[4] Typically such tracking might be accomplished by application of some type of "linear" target mounted on the model. Intersection of the image of such a target on the linear detector array would constitute the tracking information. Hence, a minimum of six such linear array cameras each having the requisite degree of relative orthogonality would be required to constrain the six degrees of freedom of the model. This approach may be somewhat complicated by the model surface curvature where the targets are located. If such curvature were significant then it would be necessary to model such curvature as part of the calibration procedure for each model. Even if such curvature were not significant, however, "self-calibration" of targets on the model tends to be somewhat complex since the location and orientation of each linear target represents 5 degrees of freedom. By "self-calibration" is meant the very attractive use of the sensors themselves in an initial mode to precisely define location and orientation of targets on the model. Self-calibration by linear detector arrays would then involve five independent combinations of precision calibration positions of the model and/or multiple simultaneously viewing linear detector array cameras (e.g. one such camera observing the target at each of 5 precisely determined orientations or five such cameras with overlapping fields of view observing the target at one such precisely determined orientations, or some other combination of these).

Because of these complications involved in self-calibration and because of the larger number of sensors required, the linear array solid state sensors are not favored for the present application.

The use of area array type of solid state imager can minimize most of the problems associated with the various sensors discussed above. They are highly linear, insensitive to high magnetic fields, can be used to implement self-calibration very readily and, since they have 2 degrees of freedom measurement capability a minimum of only 3 such sensors having adequate relative orthogonality is required. Since they operate in a digital mode they are relatively insensitive to viewing degradations. For these reasons the area array type of solid-state camera is recommended for the present application.

Area array solid state detectors can be classified as to their read-out mode. Most of them, and most typically the Charge Coupled Device (CCD) are by the very nature of their readout, constrained to a normal TV raster scan type of readout. Another type, most notably the Charge Injection Device (CID) has random access (i.e. "matrix addressable") readout. As discussed subsequently this type of area array detector can also be implemented to directly read certain sums and differences of sensed picture cell ("pixel") outputs corresponding to image tracking algorithms. This provides much greater flexibility in read-out and is ideally suited for tracking operations. They are in use and/or development, for example, for star trackers. The CID can operate in a conventional TV scan mode in an initial target (e.g. star) "acquisition mode". Then in the subsequent "track mode" the readout can be concentrated on the localized area of the target to provide higher tracking accuracy with lower bandwidth and consequent reduced Johnson noise in the video amplifier.

The remainder of this section of this report will consider a position and attitude measurement system based on application of area array solid state detector arrays of the CID type. As such it will be an adaptation of CID star tracking technology developed by General Electric and funded, in part, under contract to NASA (NAS8-32801)(cf. Ref. 5).

7.2.1 The Sensing Problem

7.2.1.1 General Target Considerations

The sensing problem can be most effectively implemented by application of artificial "targets" applied to the model. Such targets may be in the form of "decals" attached on the model at suitable locations. These "decals" must be designed so as to have no affect on the aerodynamic or magnetic characteristics of the model and be sufficiently sturdy so as to be not affected by the aero-thermodynamic conditions prevailing on the model and in the tunnel. Each "decal" should have three distinct types of patterns:

- A "small angle" precision tracking target
- A "wide angle" acquisition/verification pattern
- A distinctive decal identification pattern

7.2.1.2 Tracking Target

A two-dimensional sensing array can most effectively operate with a tracking target having a high degree of rotational symmetry. A star-like image which, in a limit approaches a two-dimensional Dirac Delta spatial function, is a common example. (In a practical case a star image as viewed with realistic optics will exhibit a symmetrical intensity distribution described by an Airy Function.) Because CID's have been applied to star tracking and computerized interpolation algorithms have been developed for such star tracking, a "star-like" fine tracking image will be considered here in most of the discussions to follow.

It should be recognized, however, that such a star-like image may not be an optimum one for fine tracking. Alternatives could be an extended cruciform image, a small "plus" sign image or concentric circular images or some other type of rotationally symmetric target. Such targets may require modified interpolation algorithms. A more extensive investigation than is now possible would be needed to determine the optimum fine tracking target shape for the present application. Some potential patterns are shown in Figure 7.8.

By a "star-like" target here we will mean a small uniformly reflective* circular disk. As stated, each such target detected by a CID type sensor will constrain two degrees of freedom of the model. Hence a minimum of 3 such sensors and 3 such targets on the model will be required. This presumes adequate orthogonality in orienting the sensors to the wind tunnel and afixing the target decals to the model. (As discussed subsequently more than this minimum is desirable).

The diameter of the target will depend upon the CID camera field of view and the accuracy requirements. The field of view, in turn, will depend on the maximum expected displacement of the target due to rectilinear and rotational motions of the target and also on the location of the camera relative to the model. Consider what is probably the maximum required field of view: Assume for the 8x8 tunnel case a target decal located 2 feet in the roll axis direction from the center of rotation of a 4 foot long model. Then a pitch rotation from -45° to +45° would correspond to a target displacement of 2x2 ft = 2.8 ft. If we assume a possible 1.2 ft simultaneous additive rectilinear excursion (which seems reasonable in a 8'x8' tunnel) then a total rectilinear excursion of a target could be as much as 4 ft. But the accuracy of maintaining rectilinear and angular position in the static case is required to be ± 0.01 in. and ± 0.02 respectively. Here we will tentatively assume that the corresponding measurement accuracy must be better than that by a factor of two: ± 0.005 in.

---

*Note this assumes a "white" target on a "black" background. This reverse pattern of a "black" target on a "white" background will work equally well with the CID type of tracker.

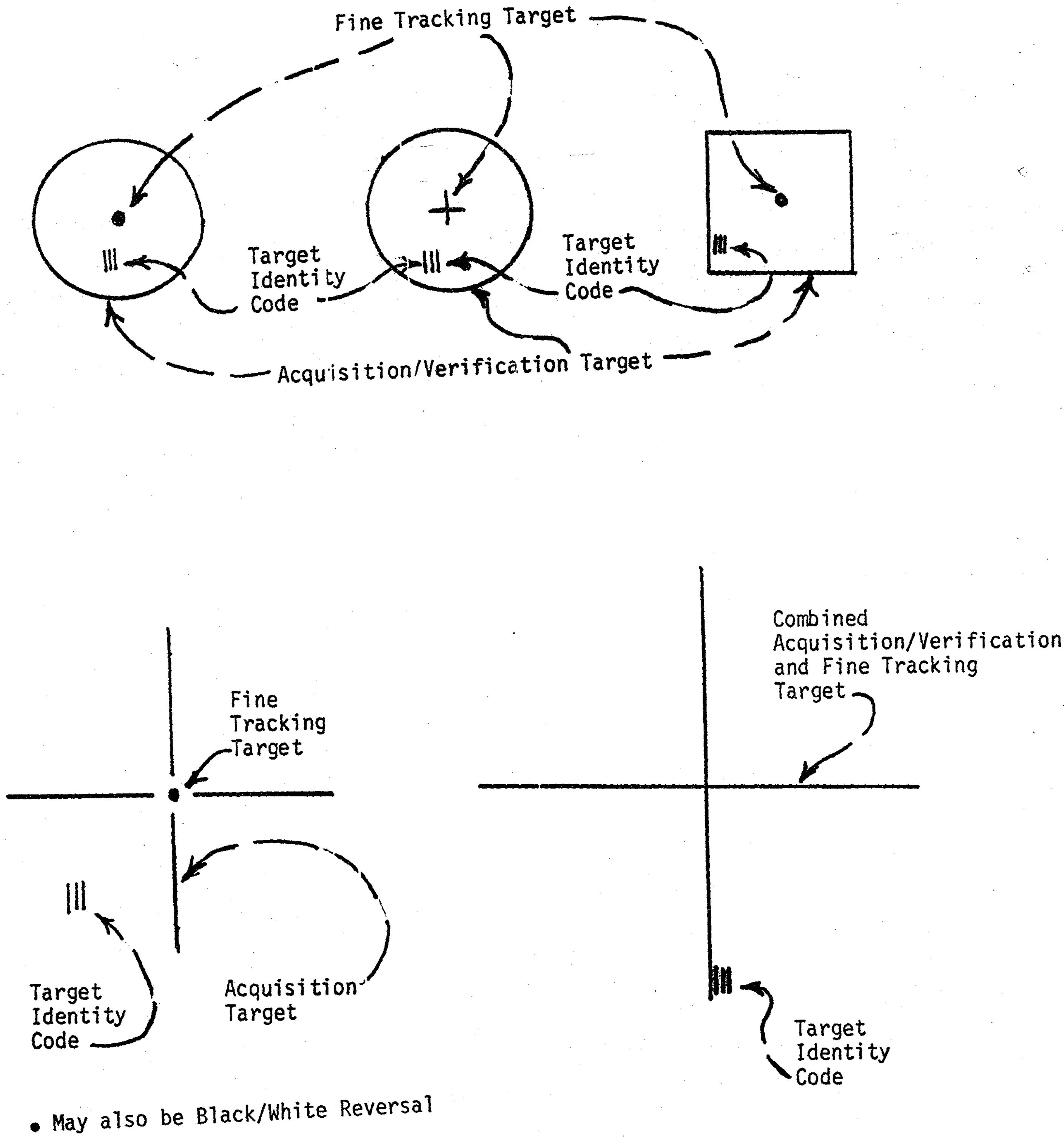

Figure 7.8
SEVERAL ALTERNATIVE TARGET PATTERNS

and ± 0.01° respectively. Note that for the above example a ± 0.01° angular excursion corresponds to a rectilinear displacement of the target of ± 0.004 in. To be conservative a need to measure the rectilinear displacement to within 0.005 inches. This implies a relative tracking resolution of $\frac{0.005}{48} = 10^{-4}$.

To provide this tracking capability with a single camera will require a solid state sensing array having NxN sensing cells where $N = \frac{10^{-4}}{K}$, where K is an "interpolation factor" (discussed below). For operation on star images with CID's values of K from a conservative low of 10 to as high as 100 have been reported. An assumption of K=40 can be made. This means that array sizes should be* at least as large as 250x250. This compares favorably with an available tracking camera having 256x256 elements. Based on assumptions discussed each sensing cell will correspond to area at the target (as a minimum) of about 0.2 inches. For interpolation purposes the fine tracking target should have a diameter of 2 to 4 times this. Hence, we assume fine tracking target diameter should have a diameter of somewhere about 0.4 to 0.8 inch. To account for increased distances from camera to target due to translational and rotational motions, a fine tracking target diameter of about 0.5 inch will be tentatively selected for the 8x8 tunnel case.

Because of the smaller size model and the smaller dimensions involved a fine tracking target diameter of about 0.3 inch is tentatively selected for the 4x4 tunnel case.

Note that in tracking of target at any given model position and attitude, any given CID camera may view only one target, or several targets or none at all. The model position and attitude are, nontheless, constrained at any given time if a minimum of three such targets are tracked in such a way as to provide independent tracking data. Any tracking data obtained beyond that minimum will be used in a data smoothing operation to reduce errors in position and attitude determination.

Fine tracking of such a target for the present application will be different from star tracking in one important aspect. Whereas the size and shape of a given star image formed by a given optical system will remain invariable, the target image for the present application will change in size as a function of viewing range and in shape as a function of viewing obliquity

*This assumes a single camera to cover a needed field of view. Adding additional cameras, of course, could reduce needed size arrays and/or improve sensing resolution.

(the image shape developing an elipticity for non-zero obliquity angles). Further investigation is needed to determine the effect of these image variations on the interpolation algorithms. It is expected that, at most, additional redundant CID cameras may be required to limit, for example, maximum obliquity angle to some limited value, perhaps about 30°.

A further difference from star tracking is the much higher optical energies which can be available from the targets as compared to stars.

7.2.1.3 Acquisition/Verification

The purpose of this operation mode is to assist in acquiring the fine tracking target and to verify that it is a true target and not, for example, a small bright (or dark) spot at some highly curved surface area of the model outside of the "decal" area. The determination of the optimum size and shape of an acquisition/verification target will require further investigation. However, it can be expected to have a high degree of rotational symmetry centered about the "fine tracking target." It may be one or more concentric circles or some combination of radial line segment or some other regular geometry shape surrounding the fine tracking target. The height, width or diameter of the acquisition/verification target should be large enough to insure rapid acquisition/verification with a high degree of confidence and yet not so large as to introduce significant distortions due to model surfaces curvature. A dimension in the neighborhood of 1 to 2 inches is tentatively selected. Possible target configurations are shown in Figure 7.8.

7.2.1.4 "Decal" Identification Label

It is expected that there will also be a simple identification bar label of some kind which can be read by the CID array. The function of this label would be to uniquely identify each of the target decals and also, if desired, to identify the model.

7.2.1.5 Representative Decals

Figure 7.8 shows sketches of some possible candidate tracking decals. Furthermore, detailed investigation is needed to select an optimum design.

7.2.1.6 Location and Quantity of Targets and CID Cameras

As stated three targets suitably located on the model and three cameras suitably mounted on the wall of the wind tunnel could provide a constrained system. However, more than this minimum is recommended for these reasons:

- So as to provide overlapping images in an initial calibration procedure (as discussed in Section 7.2.2)
- So as to permit wide angle excursions of the model without excessive obliquity in the target viewing angle (not greater than, say, 30° to 45°)
- So as to insure adequate tracking data not determined by "optical cross-talk"
- So as to reduce position and angle fixing data by statistical processing (e.g. Kalman filtering) of redundant sensed data.

Determination of the optimum number of targets and sensors will require more thorough investigation. Tentatively it is suggested that about 9 targets be mounted on the model and that about 10 CID cameras be mounted on the tunnel for both the 8x8 and the 4x4 tunnel cases. A possible configuration of targets on a model is shown in the sketch of Figure 7.9.

7.2.1.7 Illumination

Suitable diffuse illumination sources will be required to be mounted on the tunnel walls. The optimum number, type, intensity and locations are TBD. In order to avoid optical cross-talk (direct detection of an illumination source by a CID camera) it may be desireable or necessary to turn off automatically one or more such sources when using certain CID cameras. This would be easy to implement as a function of CID camera operation. One such possible approach would be to use flash lamps for illumination with operation of only those lamps which are required at any given time by a specific CID camera.

7.2.2 Operational Modes

At least three distinct modes of operation can be defined:

- Alignment of the sensors and their optical systems relative to the wind tunnel
- Alignment of the model or, more specifically, the targets relative to the model
- Normal use of the system to determine model position and attitude during static and dynamic tunnel experiments

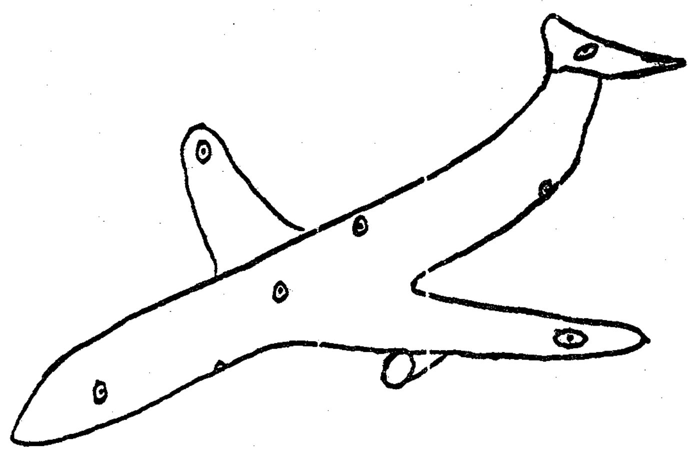

Figure 7.9

TYPICALLY EXPECTED LOCATION OF
TARGET "DECALS" ON MODEL

7.2.2.1 Sensor Alignment Relative to Tunnel

This is a "one time only" alignment of a newly constructed tunnel which should need repetition only if the CID cameras or their optics are moved or modified. It is an alignment intended to define the viewing geometry of each CID camera with respect to a fixed wind tunnel frame of reference.

The recommended procedure is to mount the cameras in their approximate desired location and orientation. No precision mechanical alignment is required. An alignment matrix is then generated for each camera by use of that camera in a self-alignment mode. An "alignment fixture" is precisely located in the working volume of the tunnel and oriented relative to a fixed wind tunnel frame. The alignment fixture consists of a frame on which a multiplicity of targets can be precisely affixed and oriented. Precision tracking data obtained from each camera when tracking these targets provides the basic data for the alignment matrix. The alignment fixture will be designed so as to provide precision placement and orientation of a sufficient number of targets to adequately provide the alignment data.

This procedure will not be as extensive as it may sound. The CID matrix geometry is well controlled, uniform and well known. The primary alignment need is to determine orientation of the optics and, possibly, also to determine some uncertainties in the optical geometry. Recall also that this alignment procedure is a "one time only" one and need be repeated only infrequently if some significant changes are made to the tunnel or to the CID cameras.

7.2.2.2 Alignment of the Targets on the Model

In order to provide high utilization of the tunnel, it is desired to be able to introduce new models into the tunnel with the minimum of time spent in positioning the targets on the model. Any kind of precision mechanical type of placement or measurement of the targets on the model should be avoided. The procedure recommended here involves use of the CID cameras in a precision target alignment mode.

In this procedure the desired number (e.g. 9) target "decals" are affixed to the model in approximately the desired positions as needed to insure adequate orthogonality of measurement for all angle and position viewing without unacceptable obscuration of targets. Since there is no need to precisely locate or orient the decals and no need to precisely measure their location or orientation by mechanical means, this procedure of affixing decals can be very rapid. The model is then introduced into the tunnel and held by a precision holding device. This device provides a precisely known reference position and orientation of the model in 6 degrees of freedom. Given an adequate number of targets and CID cameras, only one* such reference position should be required. In this procedure with one alignment position it is necessary that each target be viewable from 2 or more angularly separated (say, by ∿ 30° or more) CID cameras. A total of ∿ 10 such cameras with adequate fields of view and ∿ 9 targets should readily permit such multiple viewing. When viewed from 2 sufficiently separated cameras each point target is constrained in three axes relative to the geometry of the cameras optics. Since the cameras alignment matrices have already been determined as previously discussed the point targets have been therefore constrained relative to a wind tunnel frame of reference. Since, during this alignment operation, the model is rigidly fixed in a precisely known location and orientation relative to the wind tunnel frame of reference, then each point target is constrained relative to the model. This is the result needed. Tracking data thus obtained can then be used to define the vector locating the point targets relative to the model's coordinate system.

Note here we consider the fine tracking targets as points, thus having no rotational degrees of freedom. Since we previously said such fine tracking targets are not actually points but disks having a typical diameter of ∿ 0.1 inch this is not entirely correct. However, the approximation should be good enough if we limit target viewing maximum obliquity angle to some value, say about 30°. With respect to the acquisition/verification tracking there should be no problem in devising a pattern recognition system which can tolerate such obliquities (e.g. resulting in an elliptic distortion of an acquisition circle).

7.2.2.3 Wind Tunnel Operation

In this operational mode the electro-optical measuring system will be employed to determine the 6 degrees of freedom response during static conditions and also during dynamic maneuvers of a model in the wind tunnel.

Target acquisition logic will be employed so as to detect each acquisition target in the field of view of each CID camera. The acquisition target data

---

*In an alternative procedure, which might reduce the required number of CID cameras, more than one precisely controlled alignment position/orientation could be employed.

will also provide the location data for the corresponding fine tracking target and for the target identification. It is anticipated that the acquisition/verification target as well as the target identification code will be read with the CID camera operating in the normal orthogonal TV scan mode. The target identification code will be read so as to provide the needed unique identification of each target which is tracked.

The location of the acquisition target will provide the information required for locating and tracking the fine tracking target. Logic will provide signals to direct a search and track for the fine tracking target in the fine tracking interpolation mode of operation. Fine tracking mode data will provide the data needed to precisely determine the location and attitude of the model. This mode is described briefly in the next section.

7.2.2.4 Interpolation of Fine Tracking Target Image

Interpolation logic has been developed[(5)] which permit tracking of stars with a CID tracker with accuracies much better than that of the sensing site (i.e. much better than 1 pixel). Accuracies as good as 1/20 to 1/10 of a pixel are realistic and claims have been made as good as 0.01 pixel.

In this mode, which is employed in the alignment modes and also in the operational mode, the scan is narrowed down to a small region near the "point" target. Typically a 4 pixel x 4 pixel area is detected. Since the point target will typically extend over parts of a 3 pixel x 3 pixel array, an interpolation logic (or "centroid location calculation") is performed on the response of those 9 pixels (see Figure 7.10).

In addition to having x-y addressable random readout accessibility, as previously discussed, the CID can also have the capability for directly reading out certain combinations and sums and/or differences of pixel readings. These functions, such as the above described centroid location function, can be performed directly on the sensing chip as an integral read-out function. This represents a further advantage of the CID type of camera over other solid state types such as the CCD.

The predominant noise at high readout rates is Johnson noise in resistors, transistors, etc. Because the entire CID array need not be readout in the fine track mode this noise (proportional to the square root of the bandwidth) can be greatly reduced. At very low readout rates excess noise and leakage current can be significant. However this effect can be reduced by using multiple non-destructive readout of the images and external signal summation to further reduce the effective noise bandwidth. Because signals sum coherently and uncorrelated noise non-coherently, noise is reduced in proportion to the square root of the number of non-destructive readout operations.

A centroid calculation can be performed on a 3x3 pixel matrix shown in Figure 7.10.

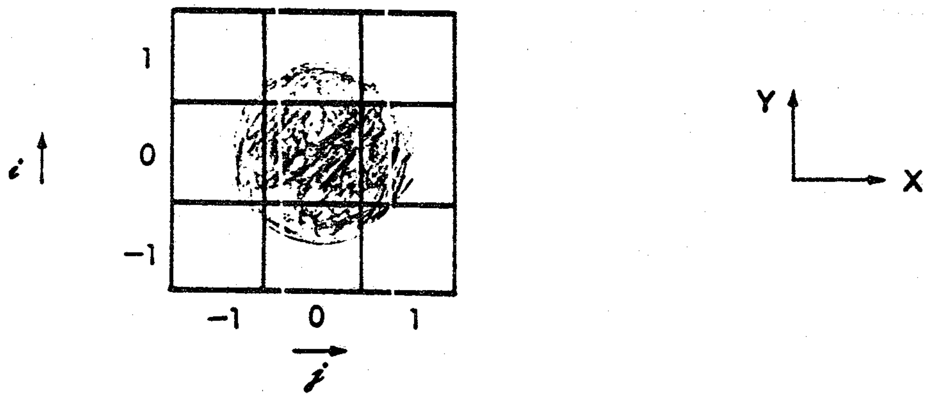

Figure 7.10. 3x3 Pixel Sub-array

The equations used to calculate the centroid position are:

$$X = \frac{1}{T} \sum_{i=-1}^{+1} \sum_{j=-1}^{+1} j \, V_{ij}$$

and

$$Y = \frac{1}{T} \sum_{i=-1}^{+1} \sum_{j=-1}^{+1} i \, V_{ij}$$

where V_{ij} is the signal at pixel location (i,j) and

$$T = \sum_{i=-1}^{+1} \sum_{j=-1}^{+1} V_{ij}$$

is the total signal falling on the 3x3 array.

Note that this is only one of several alternative algorithms which can be used for interpolation in target tracking.

7.2.3 Design Concept of Electro-Optical Position Sensor Integrated with Total System

Figure 7.11 shows a schematic of the electro-optical system integrated into the entire wind tunnel system. CID cameras which view the model from various locations and viewing angles receive their operational commands from a video command generator. These commands specify the mode of operation, such as:

- search for acquisition target
- read identification code
- automatic fine tracking
- TV viewing for optional viewing monitors

These commands are generated by a pre-designed operational sequence and as may be modified by real time system input commands and by feedback from existing tracking data especially that indicating a successful target acquisition.

The video data is processed so as to sort out the various kinds of tracking, identification and imaging data. The fine tracking data together with the "decal" identification data become the primary inputs to the geometric conversion and data smoothing function. The geometric conversion from target tracking data to six degree of freedom position and attitude data depends on the calibration data obtained in the wind tunnel calibration operation and also in the model target calibration data. This calibration data is stored in the form of calibration and alignment matrices. The geometric conversion function also incorporates smoothing of redundant sensed data as needed to meet the position and attitude measurement performance requirements.

The position and attitude data resulting from these computations are made available to the control system and also to the aerodynamic data extraction function as shown. Aerodynamic data extraction depends on this data plus data extracted from magnet currents which are related to forces and torques as shown in Figure 7.11.

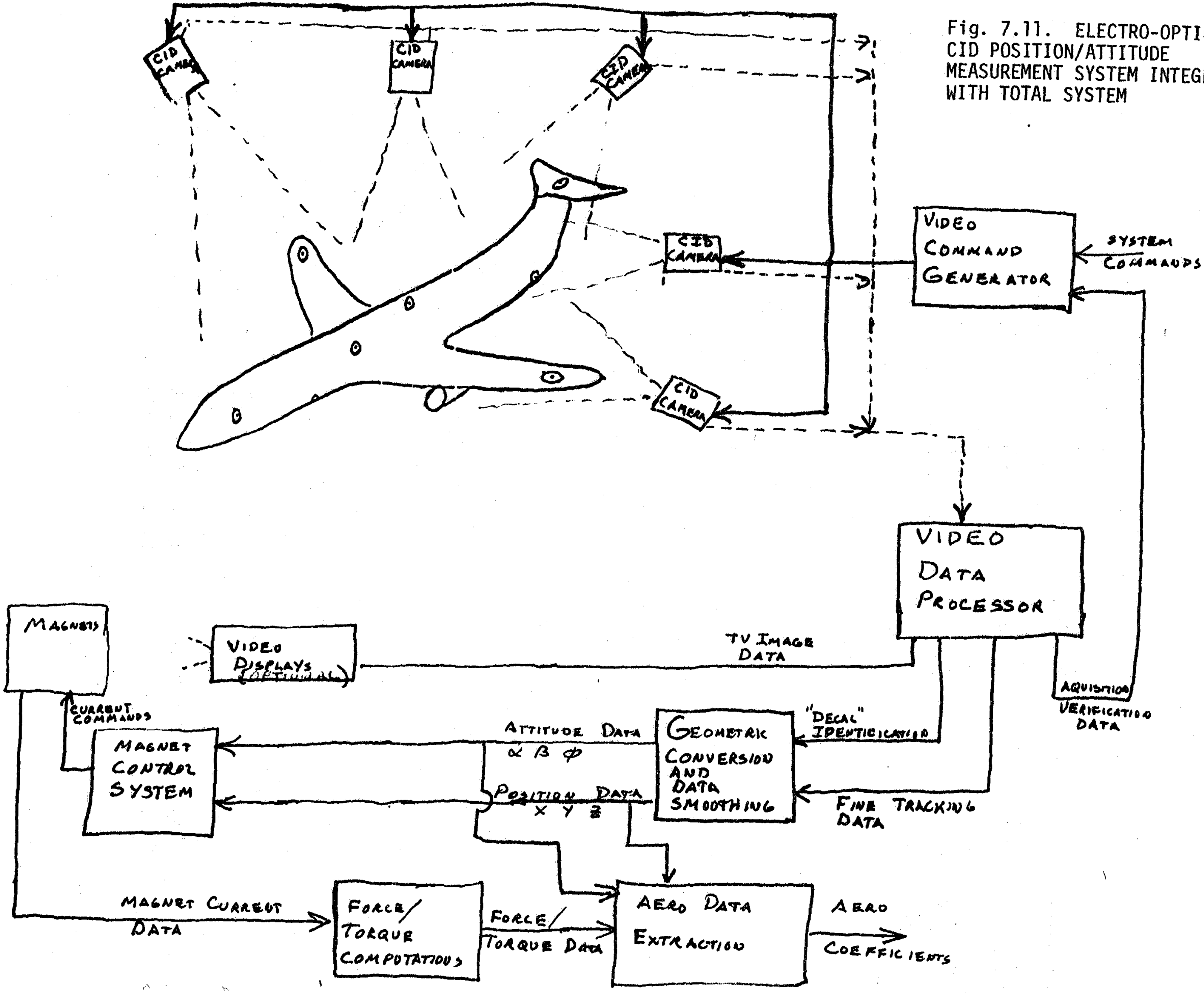

Fig. 7.11. ELECTRO-OPTICAL CID POSITION/ATTITUDE MEASUREMENT SYSTEM INTEGRATED WITH TOTAL SYSTEM

7.2.3.1 Summary of Hardware

- CID Solid State Cameras
  - Number of Cameras Mounted in Wind Tunnel: ∿ 10
  - Array Size: 256 x 256 pixels
  - Pixel Shape: Square
  - Pixel Size: 20 x 20 micrometers
  - Total CID Active Area: 5mm x 5mm
  - Optical Field of View (FOV): ∿ 35°
  - Fine Tracking Accuracy: 10^{-4} (FOV)
  - Fine Tracking Accuracy (angle): (7×10^{-3}) degree = ∿ 25 arc sec
  - Range* of Target "Single Fix" Accuracy (Depending on Range and Viewing Angle) : 0.004 to 0.008 in.
  - Focal Length of Camera Optics : 100 mm
  - f/number of Optics : f/8
  - Overall Size of Each Camera including Optics : 20 cm x 5 cm x 5 cm
- Data Processor
  - Type
    - 1 Microprocessor per camera, or
    - 1 Microprocessor shared by all cameras, or
    - Central processor shared by measurement system, control logic, etc.
    - Memory (per camera) : 2,000 to 4,000 words RAM
2,000 to 4,000 words PROM
    - Word Length : ∿ 16 bits
    - Computational Capacity and Rates : TBD (expected to be modest)

*Assumes cameras located ∿ 5 feet from center axis of 8x8 tunnel and ∿ 3 feet from center axis of 4x4 tunnel.

Section 7.0 References

1. Stephens, T., "Design, Construction and Evaluation of a Magnetic Suspension and Balance System for Wind Tunnels", MIT Aerophysics Lab TR 136, NAS1-4421, November 1969.

2. Covert, E.E., M. Finston, M. Vlajinac and T. Stephens, "Magnetic Balance and Suspension Systems for Use with Wind Tunnels", Progress in Aerospace Science, Vol. 14, Pergamon Press, 1973, pp 27-107.

3. Luh, P.B., Covert, E.E., Whitaker, H.P. and Haldeman, C.W., "Application of Digital Control to a Magnetic Model Suspension and Balance Model", NASA Contractor Report 145316, MIT to NASA Langley, January 1978.

4. Britcher, C.P. et al, "Preliminary Investigations of Design Philosophies and Features Applicable to Large Magnetic Suspension and Balance System", Dept. of Aeronautics and Astronautics, Univ. of Southampton, England under NASA Grant NSG-7523, NASA - CR-162433, November 1979

5. Burke, H.K. et al, "Design, Fabrication and Delivery of Charge Injection Device as a Stellar Tracking Device", Final Technical Report NASA Contract NAS8-32801, April 1979, General Electric Company for NASA, Marshall Space Flight Center, NASA-CR-161226

8.0 AERODYNAMIC DATA EXTRACTION AND DISPLAY

In accordance with the MSBS Statement of Work, NASA will evaluate and select techniques for aerodynamic data acquisition and display and will also define the separate data extraction and display computer with the capacity to extract the aerodynamic forces and moments acting on the model and also the standard wind tunnel parameters.

The purpose of this task is to identify the raw data parameters available from the MSBS magnet system instrumentation to support this aerodynamic data extraction and display so as to enable NASA to carry out an error analysis of the measurement system. A further purpose is to define a method of system independent calibration to support the data extraction process.

8.1 FORCE AND TORQUE DATA AVAILABLE FROM MSBS SYSTEM

The primary data available from the MSBS system is the measurement of current in each magnet coil and the measurement of model position and attitude available from the position and attitude sensing systems. The predicted magnetic forces and torques on the model are related to current in the various magnets according to the relationships summarized in Section 3.0.

The analytically predicted relationships will be refined by actual force and torque calibration data obtained experimentally as discussed in more detail below. Such data will be used in data extraction as a relationship of forces and torques to current which is more accurate than the predicted analytical relationships.

The forces and torques are generally non-linear functions of currents and model orientation angles. However, each "component" of force and torque will generally be a product of two currents (or square of one current). Hence, in a worst case situation, a given uncertainty on all currents would result in about double that uncertainty in forces or torques. For example, an uncertainty of $\pm 0.1\%$ (i.e. from 0.999 to 1.001) in all currents would result in an uncertainty range of 0.998 to 1.002 (i.e. $\pm 0.2\%$) in all forces and torques.

As discussed in Section 5.0 on Instrumentation, two alternative tolerance levels for current measurement have been considered. These correspond to two alternative levels of investment in equipment designed to measure magnet current levels.

The relationship between uncertainty in current measumement and uncertainty in aerodynamic coefficients determination for these two levels of current measuring accuracy is as follows:

• Accuracy of Current Measurement	• Corresponding Uncertainty in Current Measurement	• Corresponding "Worst Case" Uncertainty in Determination of Aerodynamic Coefficients
Moderate	0.1%	0.2%
High	0.01%	0.02%

It should be recognized, however, that in any system budgeting of errors, accommodation must be made for all sources of errors. It is expected that current measurement errors may be one of the more significant error sources. Hence, an allocation of uncertainty in aerodynamic coefficient determination due to errors in current measurements should probably be allocated to be, on an uncorrelated basis, about 50% to 60% of the total error in aerodynamic coefficient determination (this needs further resolution after more thorough consideration of all error sources including all measurement errors, modeling errors, calculation errors, etc.).

8.2 POSITION AND ATTITUDE DATA AVAILABLE FROM MSBS SYSTEM

As discussed in Section 7.0, with proper design both the electronic position sensing system and the electro-optical sensing system are likely to be capable of providing the needed position and attitude data. These measurement systems incorporate the data processing needed to convert the raw sensed data into position displacements and Eulerian angles as required by the control system and by the aerodynamic data extraction system.

The MSBS Work Statement specifies levels of accuracy within which the position and attitude must be held. A tentative judgement is made that measurement accuracies must be better than those values by a factor of two. Hence, requirements are:

		Position and Attitude Holding Accuracy Requirements	Position and Attitude Measurement Accuracy Requirements
POSITION	X, Y, Z	± 0.01 in.	± 0.005 in.
ATTITUDE	α, B, ϕ	$\pm 0.02^{\circ}$	$\pm 0.01^{\circ}$

It is expected that both the EPS and the Electro-Optical Position Sensing System will be able to meet or exceed these requirements for the static case and, where required, for the case where the model is experiencing forced oscillations. Because of the considerable latitude available in selecting the number of CID cameras, the optical fields of view etc., the electro-optical system has the greatest potential for exceeding the measurement requirements in the event that it should be so desired.

8.3 FORCE AND TORQUE CALIBRATION

Magnetic forces and torques on a given core are complex non-linear functions of magnet currents, core attitude and, to a lesser extent, core position. Because the magnetic field, field gradient and core magnetization characteristics may not be perfectly described by an ideal analytic model, there is need to provide an experimentally derived magnetic force and torque calibration. Because such a calibration procedure may be rather complex, it is fortunate that a complete calibration should be required only once for each soft iron core or only whenever significant changes are made to the wind tunnel magnet configuration. (This may not be true for a permanent magnet core, however.) It is expected that the same core would be used as an insert in several different models.

Two general approaches to force and torque calibration can be conceived as compared in Figure 8.1. In the "classical" approach combinations of forces and torques are added by means of masses subject to gravity forces and suspended by cables and, in some cases, low friction pulleys. The magnet currents required to balance these torques and forces are measured. The results obtained are a measure of current required to produce given forces and torques. Since it is the inverse of this relationship (i.e. a measure of force and/or torque produced by a given current) which is required, a matrix inversion is required. But because the force and torque relationship are non-linear functions of current, an iterative procedure is required. Because the relationship is also a non-linear function of attitude angles, it is necessary to repeat the procedure over the range of angles of interest. Computational programs for performing this function have been developed at NASA (Langley) and can be used within some restrictions in attitude angles.

An "inverse" procedure has been developed(1) at MIT in order to avoid the above described inversion procedures. It makes use of a pneumatic servo which automatically produces and measures forces and torques required to balance the forces and torques produced by the magnets and operating on the core. It is designed to provide direct high resolution force and moment readout resolved in an orthogonal coordinate system in six degrees of freedom. It is the only known hardware which has been developed thus far to implement the "inverse" approach.

There appear to be significant advantages to each general approach. There also appears to be significant opportunity for improving the equipment and methodology for each approach. Hence, it is recommended that both approaches be considered for the present application until such time as a very superior case is made for one or the other.

(1)Vlatinac, M., "A Pneumatic Calibration Rig for Use with a Magnetic Suspension and Balance System," MIT Aerospace Research Laboratories, Cambridge, Mass., ARL Report 70-0016, January 1970.

Figure 8.1

TWO GENERAL APPROACHES TO TORQUE AND FORCE CALIBTATION

Approach	Method	Equipment Used	Characteristics
"Classical Approach"	• Fix Force or Torque and Measure Required Equilibrium Currents	• Mass Balance System Using Weights, Cables and Possibly Low Friction Pulleys	• Inversion of Non-Linear Equations requires complex computerized iterations. (However, NASA-Langely Program exists for this if angles are not too large)
"Inverse Approach"	• Fix Current and Measure Resulting Torques and Forces	• Force Measuring Position Servo such as Pneumatic Calibration Rig (only known applicable hardware)	• Provides required relationship directly without inversion. • Easier to change independent variable. • Initial set-up of Pneumatic Servo may be difficult.

8.4 CALIBRATION OF POSITION AND ATTITUDE MEASURING SYSTEMS

A position and attitude calibration procedure is required for both the EPS and electro-optical position and attitude measuring systems so as to provide a more accurate relationship between output data and the needed geometric position and attitude data than is possible by pure analytical modeling. By terms of the MSBS Work Statement, the calibration procedure is to be provided by the optically-based system. This is discussed in Section 7.2.2. It is noted, however, that calibration in the case of the electro-optical position sensors is in reality self-calibration and requires no precision mechanical positioning or measuring of sensing components or tracking targets.

9.0 INTERFACE REQUIREMENTS

The MSBS is a part of a larger complex, within which the MSBS supports, and is supported by, other systems. The equipment, accommodations and utilities by which such support is provided constitute the interfaces between MSBS and the other systems.

This task has reviewed the interfaces required by the MSBS concepts to meet the installation and operation conditions of the Cases and Alternatives studied during this project.

The major interface requirements, which this study assumed would be the responsibility of the Site Manager, can be categorized according to the primary MSBS "subsystem" involved in the interface: Power Supply, Magnets, Control System, Cryogenics, Position Sensors. Figures 9.1, 9.2, 9.3 and 9.4 tabulate the principal interface requirements, and quantify them, where applicable.

9.1 POWER SUPPLIES INTERFACES

The top line in Figure 9.1 lists the peak power demands, from Section 5.0, which must be provided by the utility (or an on-site source) as input to the MSBS power supplies for energizing the magnets. Both 440V and 13,800V power are listed, since either is commonly available at an industrial site.

The listed 110V power is required to support the remaining power supply functions (power for signal conditioning, controls, etc.).

The large amounts of energy dissipated in the power supplies establish the demand shown in the figure for pressurized cooling water, while the need for an uninterruptible coolant supply for the discharge resistors establishes the tabulated needs for large tanks of water in which the resistors are immersed. For Alternative G, as shown on the figure, the resistors are air cooled by natural convection.

The site must provide the tabulated space for installation of the power supplies, preferably within a building. The figure also notes that, where power distribution or signal distribution for MSBS are constrained to using existing cabling and/or wiring, such wiring, cabling and wall penetrations must be provided (under appropriate standards and safeguards such as grounding).

Figure 9.1
INTERFACE REQUIREMENTS

Cases / Alternatives	1 E	1 F	1 G	2 E	2 F	2 G	3 E	3 F	3 G
Power Supply									
440V or 13,800V, 3 Ø Electricity-MVA	8000	310	300	2000	32	40	330	25	23
110V, 1 Electricity-KW	80	50	50	50	40	40	50	40	40
Cooling Water, Pressurized @ 60psig-GPM	50000	2000	2000	20000	200	200	2000	200	200
Cooling Water, Atmospheric, No Forced Flow-Gal	2400	440		2400	440		2400	440	
+ Cooling Air, Atmospheric, No Forced Flow			A			A			A
Interface Cabling & Wiring for Power*									
Interface Wiring (with Shielding) for Instrumentation*									
Separation Distance or Shielding for EMI-Sensitive Equipment									
Bulkhead Penetrations and Protection-Earth Ground									

*Where MSBS must Utilize Existing Cabling/Wiring
A = Aircooled by Natural Convection

The figure also notes that sensitive equipment, which is not part of the MSBS, will either require appropriate shielding or be located sufficiently distant from the power supplies to avoid Electromagnetic Interference problems.

9.2 MAGNET INTERFACE REQUIREMENTS

Since the MSBS magnets must not utilize the Test Section for support, Figure 9.2 lists the size and arrangement of mounting pads that must be provided for their installation.

The overall dimensions of the magnet installations (surrounding the Case 1, 2 and 3 test sections) are also given.

The figure also lists "Magnetic Field Exposure of Personnel" as an interface. There is a dearth of data on the human effects of high magnetic fields, but current efforts to quantify such requirements, as part of the Fusion Energy Program, provide the interim criteria of allowable field strength vs duration of exposure vs portion of body shown in Reference 4 of Section 3.0. For the present, based on the fields plotted in Figure 3.5 it is a conservative assumption that, during operation of the magnets, personnel activities no closer than 10 meters of the model should be of minimized duration, say little more than 1 hour. The figure also references the statements of Section 3.1.2.1 as to the shielding of electronic equipment and the precaution to avoid potential damage from magnetically susceptible tools in the vicinity of the operating MSBS.

9.3 CONTROL SYSTEM INTERFACES

Figure 9.2 also notes the power and installation interface requirements of the MSBS Control System as well as the need for wiring the MSBS magnet instrumentation into the Data Extraction and Display Computer.

9.4 CRYOGENICS INTERFACES

The Cryogenics systems interface requirements in Figure 9.3 list both the outdoor, gas storage installation space and the indoor areas for Compressors and Dewars that must be made available for MSBS.

The gas storage installation also requires access by tank trucks.

The recommended maximum lengths of liquid helium piping are listed so that planning of the total MSBS installation can provide for effective piping layout.

Figure 9.2

INTERFACE REQUIREMENTS

MAGNETS	CASE 1	CASE 2	CASE 3
Mounting Pads for Magnet System	3 Foundation Pads 24" x 11' each 21' - 4" Apart	3 Foundation Pads 24" x 11' each 21' - 4" Apart	2 Foundation Pads 12" x 6' each 24' Apart
Installation Dimensions	30' Wide x 32' High x 25' Long	30' Wide x 32' High x 25' Long	12' Wide x 13' High x 25' Long
Maximum Allowable Exposure of Personnel to Magnetic Field	8 hours>>Duration>1 Hour @ 10 Meters from Model →		
Location of Electronic Equipment and Tools	(See Section 3.1.2.1 of this report) →		
CONTROL SYSTEMS, DISPLAYS, COMPUTER			
110V, 10 Electricity	25.5 KVA →		
Installation Dimensions	15' x 25' x 8' →		
Interface Wiring for Data Extraction and Display Computer			

Figure 9.3

INTERFACE REQUIREMENTS

Cases	1			2			3		
Alternatives	E	F	G	E	F	G	E	F	G
Cryogenics									
Installation Dimensions for Gas Storage - Outdoors, Acres	3	1	1	2	1/2	1/2	1	1/2	1/2
Installation Dimensions, Refrigeration/ Liquefaction Compressors and Dewar - Building, 10^3 ft^2	20	3	3	12	1.5	1.5	3	1.5	1.5
Recommended Maximum Length of Run (He Piping)	50 Ft. (best) to 500 Ft. (max.)								
Power for Compressors/Refrigerators, KW	5000 to 250								
+									
Bulkhead Penetrations & Protection (Insulation, Guard Structure)									
Available Interconnecting Piping*									

*Where MSBS must use existing piping

In addition to previously noted power requirements, the cryogenic system requires power to operate liquefaction/refrigeration equipment, the two values on the figure represent the two extremes of Cases 1 and 3, Alternatives E and G respectively.

Figure 9.3 also notes the need for providing cryogenic piping access to buildings and rooms, and the need to isolate penetrations from surrounding superstructure and protect such access from damage.

As before, where MSBS cryogenics are constrained to utilize existing piping, as may be the case for the nitrogen subsystem, such piping is a required interface.

9.5 POSITION SENSORS INTERFACES

Figure 9.4 indicates that the interface requirements of the Electromagnetic Position Sensors (EPS) are considerably more severe than for the Electro-Optical Sensor.

Operation of at least one EPS in the 20KHz range calls for suppression or elimination of RFI from other sources during MSBS operations.

A more severe EPS interface discussed in Section 3.1.2.1 is the need for nonmetallic test section walls. To avoid shielding the EPS signal from the model, the wall between the EPS and the model can be fabricated from such glass-fiber/epoxy composites as G-10, which is not only a high strength material, but also is compatible with cryogenic environments.

As noted in the figure, the Electro-Optical Position Sensor requires only what has been specified as "visual access" in the MSBS Statement of Work. Ten moderate size ports or two large ports, and sufficient model lighting for "naked eye" observation will suffice.

Figure 9.4

INTERFACE REQUIREMENTS

POSITION SENSORS

- Electronic Position Sensor
  - Minimal RFI in 5-20 KHz Range
  - Nonmetallic Test Section Walls
- Electro-Optical Position Sensor

Visual Access to Model	Ten 5cm x 5cm Ports
Illumination of Model	Equivalent to "Eyeball Viewing"

10.0 MSBS CONCEPTS

The major effort during this study has been in developing the definitions and concepts of the MSBS subsystems (Sections 3.0, 4.0, 5.0, 6.0, and 7.0 of this report) to meet the evolving requirements as the study progressed.

Many of the decisions regarding requirement changes, additions and deletions stemmed from subsystem impacts rather than total MSBS impacts. Thus, for example, the decisions to pursue Alternatives F and G, which, respectively, reduced and eliminated the requirements for forced model oscillations were based on power supply impacts. As such evolutionary changes took place, however, the total system was reviewed, and the requirements imposed on subsystems were modified, as required, to accommodate the changes.

The resulting MSBS concepts for Cases 1, 2 and 3, Alternatives E, F and G, thus, represent the latest versions of the MSBS requirements as of the date of this report. During the course of the study, reasonably complete concepts were also generated for several predecessor combinations of requirements that were discarded as the requirements were modified. The study has, therefore, generated more than a dozen MSBS concepts during its performance, rather than the three (Case 1, Case 2, Case 3) anticipated at the study inception.

10.1 MSBS MAGNET CONFIGURATIONS

Figure 10.1 represents the generic configuration of the magnet portions of all nine (Cases 1,2,3; Alternatives E,F,G) final MSBS concepts. Dimensions are tabulated in the figure for Cases 1, 2, and 3. Since the sizes of the 20 magnets are essentially determined by the static forces and moments specified in the MSBS Statement of Work, the differences in forced oscillation requirements represented by Alternatives E, F and G do not result in corresponding differences in magnet sizes within a given Case.

It should be noted that the configurations represented by Figure 10.1 cannot be construed as an "optimized" concept. While many tradeoffs were carried out in such areas as "+" vs "x" arrangement of gradient magnets, degree and type of magnet modularization, coil shape, monopolar vs bipolar coils and power supplies, and others discussed in Sections 3.0, 4.0, 5.0, 6.0, and 7.0, the task of evolving design concepts also identified areas for which additional or alternative approaches might be beneficial. In several cases, such areas could not be pursued due to lack of time. For example, the requirements

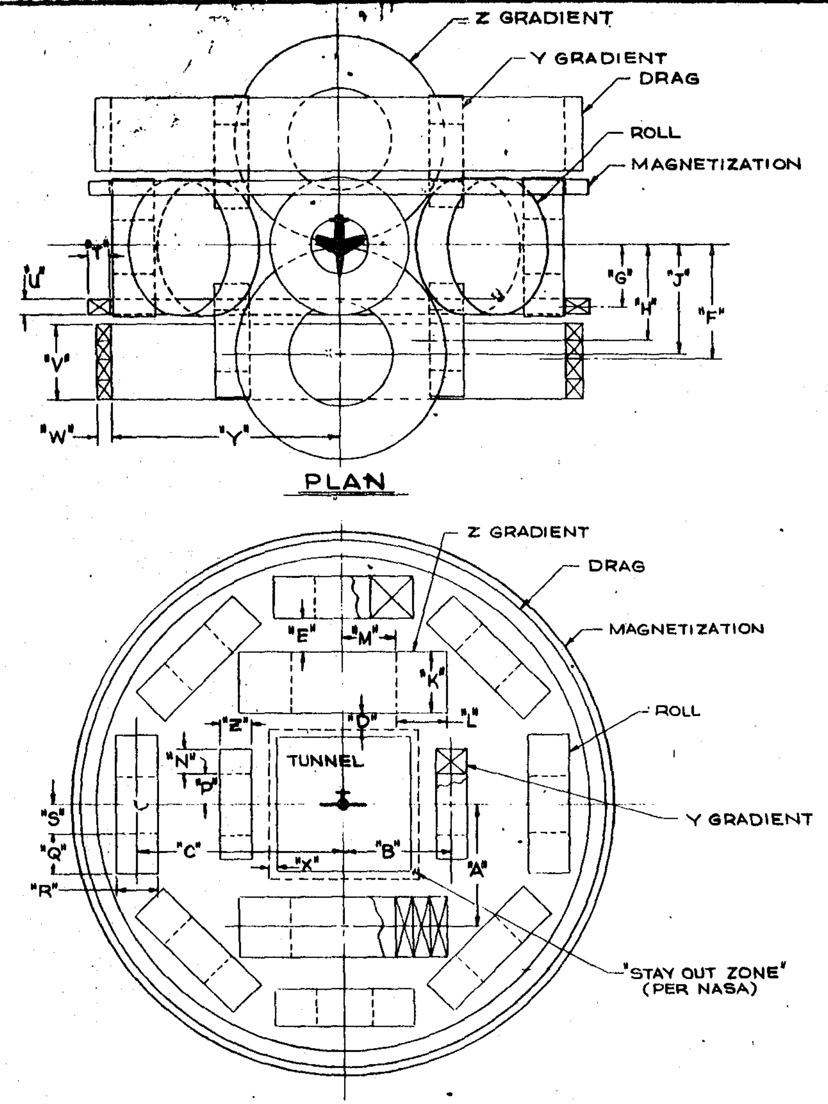

DIMENSIONS (m)			
DIM	CASE I	CASE II	CASE III
A	2.26	2.26	.94
B	2.08	2.08	.94
C	3.6	3.6	1.6 △1
D	.30	.30	.07
E	.60	.60	.15
F	2.04	2.04	1.17
G	1.03	1.03	.57
H	1.53	1.53	.88
J	1.80	1.80	.47
K	.89	.89	.20
L	.79	.22	.09
M	.94	.94	.30
N	.37	.12	.04
P	.56	.56	.24
Q	.53	.53	.09
R	.53	.53	.80 △1
S	.50	.50	.30
T	.27	.27	.08
U	.26	.26	.13
V	1.61	1.61	.53
W	.25	.07	.07
X	.30	.30	.15
Y	4.50	4.50	1.30
Z	.53	.53	.20

DRAWING NOT TO SCALE

GENERAL ELECTRIC
ENERGY SYSTEMS PROGRAMS DEPT. - SCHENECTADY, N.Y.

MSBS LAYOUT

D 57561 SK103D81013 REV. 1

Figure 10.1
MSBS LAYOUT

for forced model oscillations (Alternatives E and F) led, after considerable analysis, to the selection of non-metallic dewars for the magnets (see Section 3.2.4). As the end of the study approached, elimination of the forced model oscillation requirement (Alternative G) was considered. Although power, cooling and control effects of this change were determined, no attempt was made to modify the dewar design concept. It is likely, however, that the changed requirement would allow the dewar to be fabricated of the more conventional stainless steel. While it is estimated that the cost and schedule effects of using the steel rather than nonmetallic dewar are minor, the conventional steel dewar does reduce the technical risk, since non-metallic dewars are in initial stages of utilization.

As another example, in the "non-optimized" MSBS concept, the relative positions/configurations of the Drag/Magnetization/Roll Coils have been subjected to preliminary tradeoffs to arrive at a Design Concept. Yet the Drag and Magnetization Coils are of very large diameter (too large for land transport) and the Roll Coils do not provide sufficient torque. More detailed tradeoffs are required to ascertain the total system performance and cost effects of varying the relative positions/configurations of these coils. The aim would be to establish an optimized MSBS in which the Drag and Magnetization Coil diameters become more manageable, and the Roll Magnet torques achieve acceptable levels, at the lowest system cost.

10.2 MSBS POWER SUPPLY AND CRYOGENICS INSTALLATIONS

Figures 10.2 a, b, c and d depict the typical indoor installation of the major Power Supply and Cryogenics of the MSBS concept, Case 1, Alternative F. The MSBS installations for all cases and alternatives are predicated on a three-story building, approximately 50 feet tall, at least partially surrounding the test section. For Case 1, Alternative F, the required area is approximately 100 feet x 80 feet on each floor. Since Alternative G exhibits small difference in power supply and cryogenic requirements from Case F, the same size building is required for Case 1, Alternative G. Similarly, Case 2, Alternatives F and G will occupy approximately 7000 square foot floors, and Case 3, Alternatives F and G will also require floors of approximately 7000 square feet. Alternative E for all cases, must provide space for considerably larger power supplies and cryogenic equipment, thus requires approximately two to three times the floor space of Alternative F in Cases 1 and 2, and approximately 15% more floor space in Case 3.

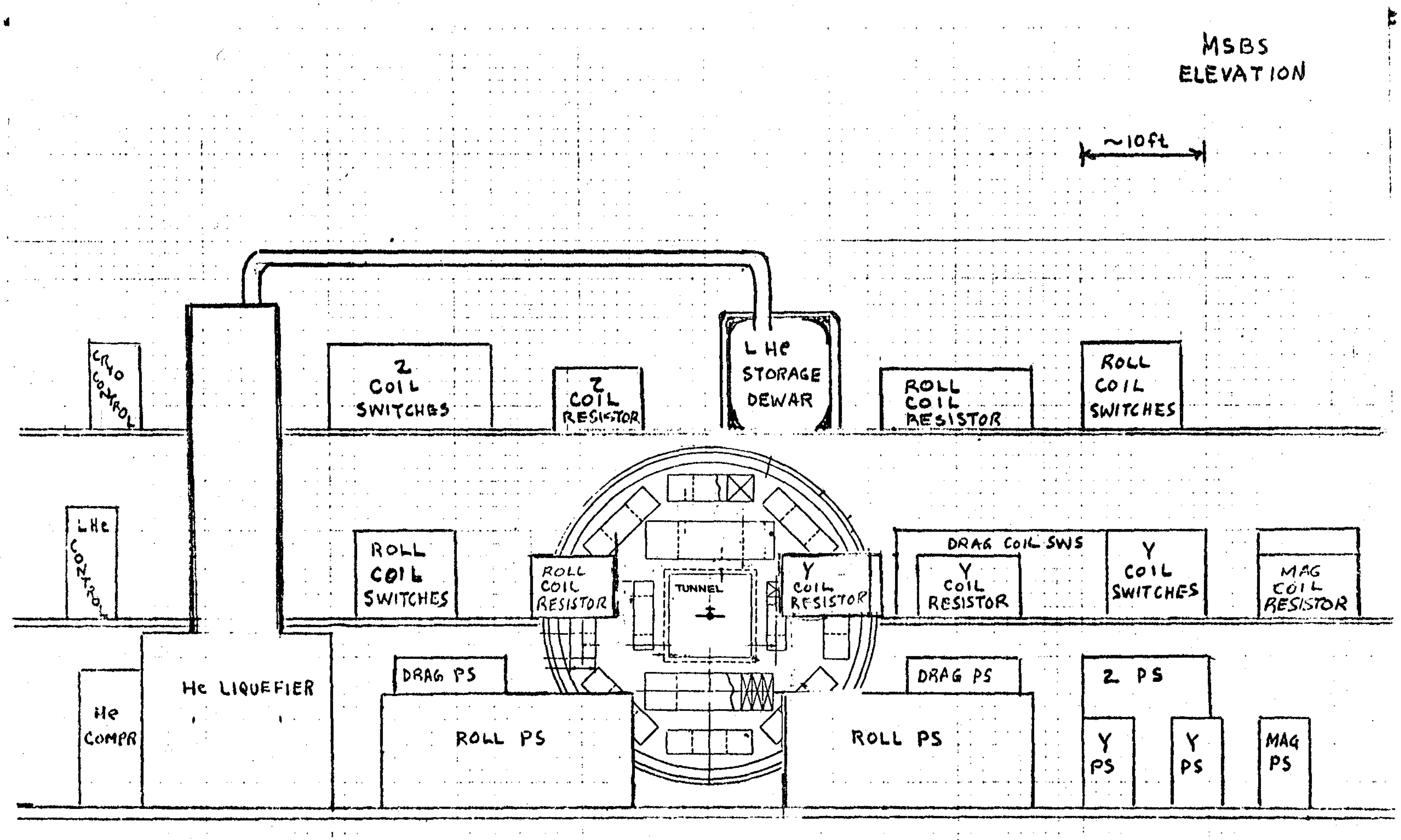

Figure 10.2a

MSBS INSTALLATION CONCEPT - CASE 1, ALTERNATIVE F

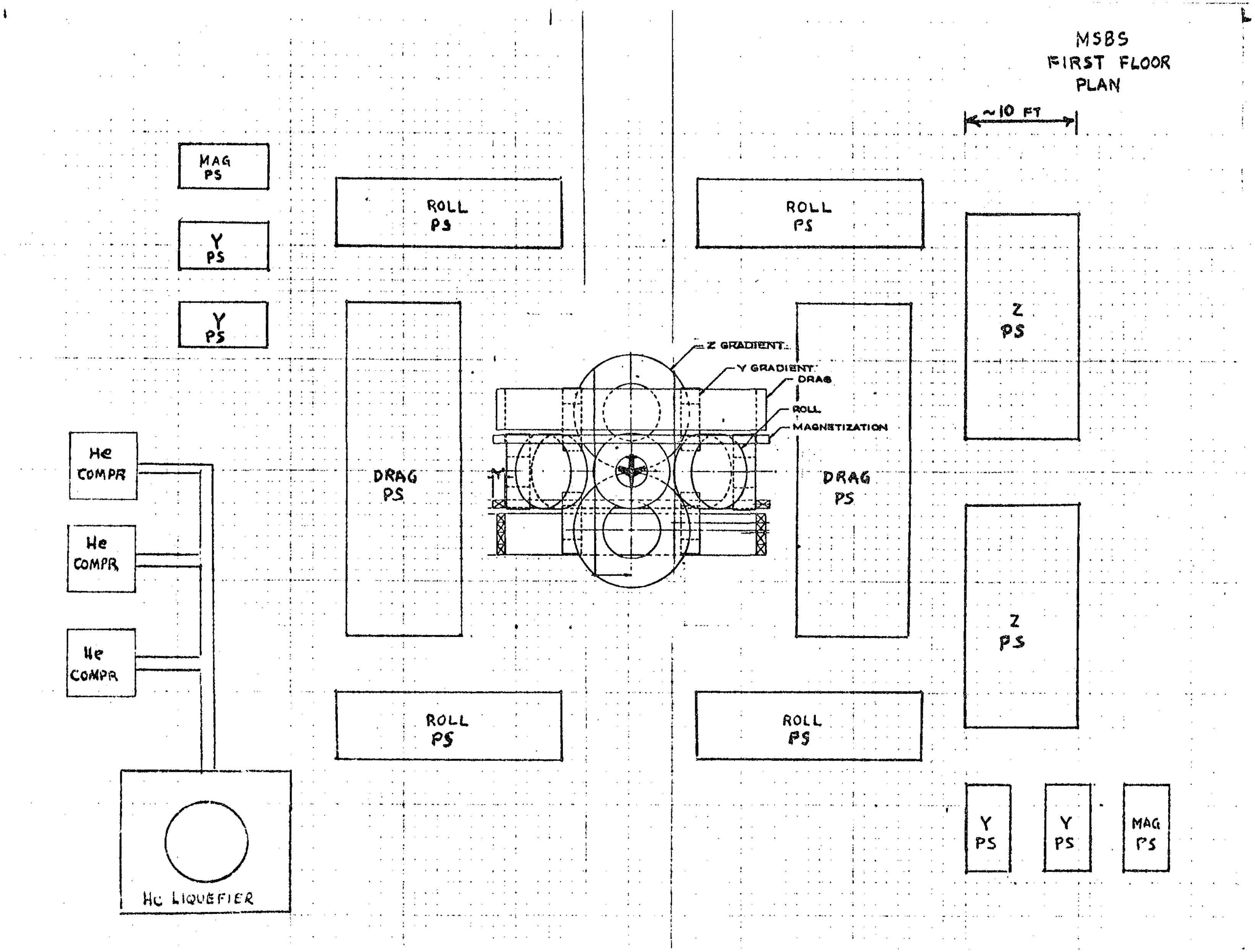

Figure 10.2b

MSBS INSTALLATION CONCEPT - CASE 1, ALTERNATIVE F

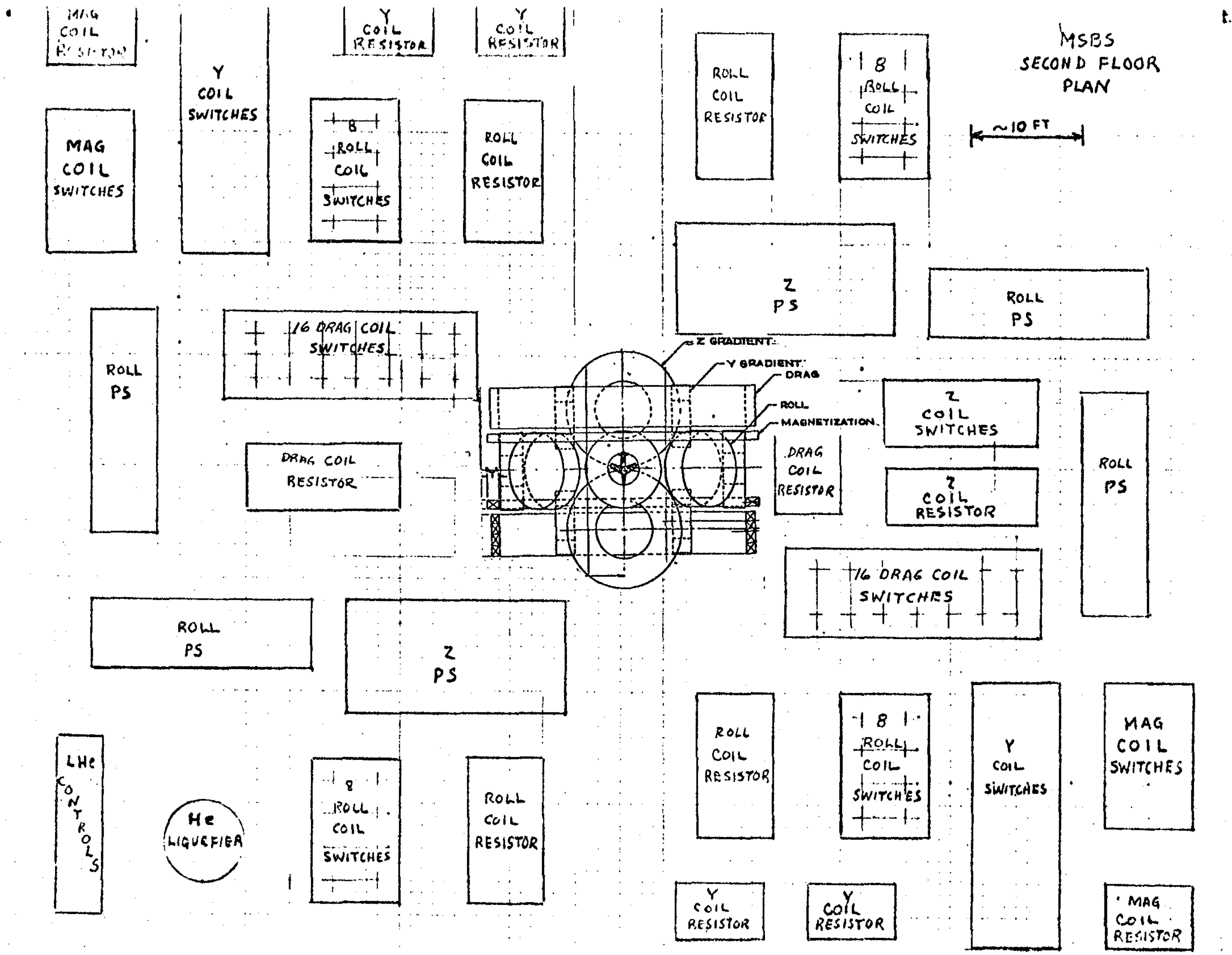

Figure 10.2c

MSBS INSTALLATION CONCEPT - CASE 1, ALTERNATIVE F

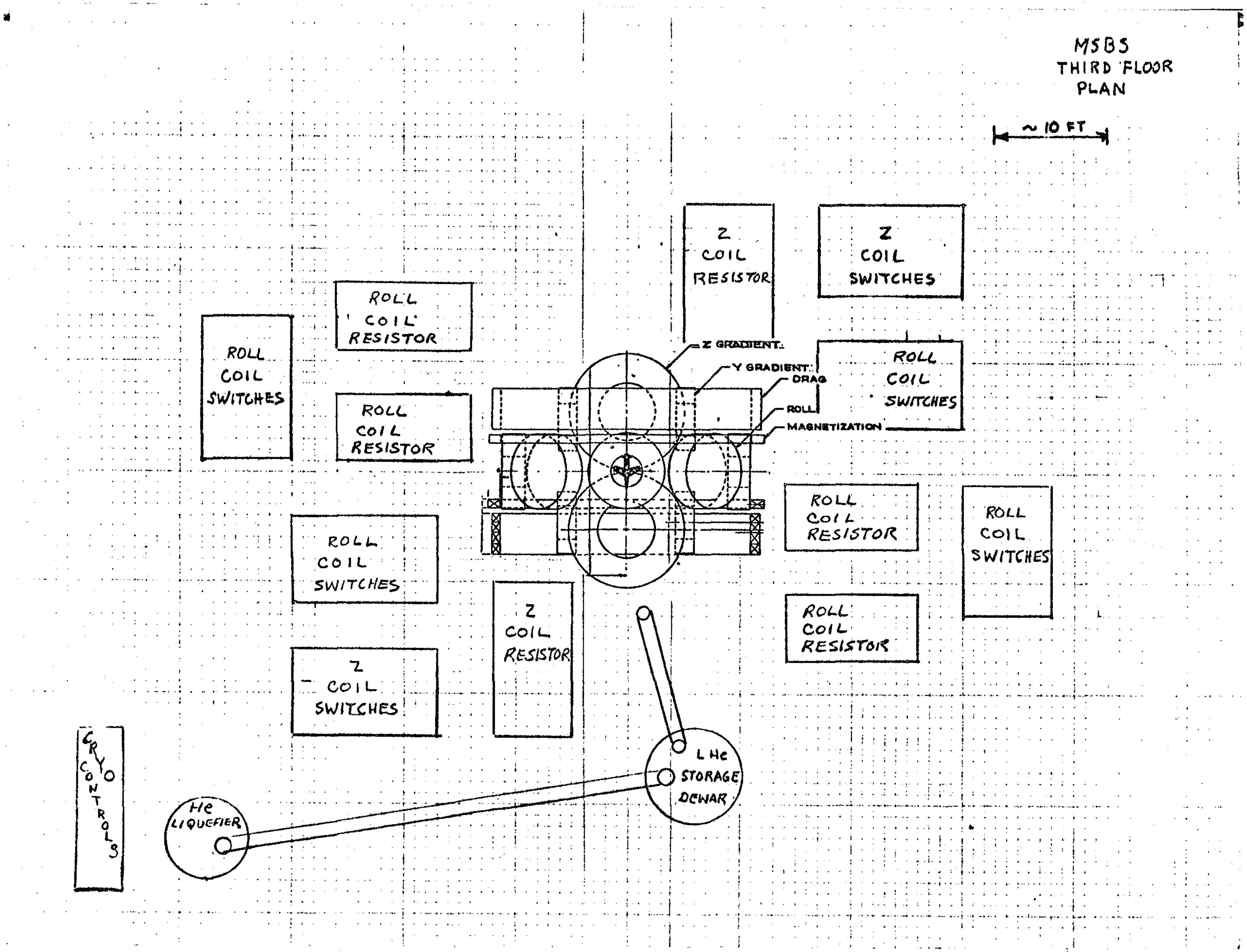

Figure 10.2d

MSBS INSTALLATION CONCEPT - CASE 1, ALTERNATIVE F

The cost of the buildings have not been included in the cost estimates of Section 12.0

While piping runs, maintenance and repair stations, and a control room (should it be located in the same building) are not shown in the Figures, allowance has been made for such requirements in sizing the buildings.

10.3 MSBS TANK FARMS

Although the MSBS helium systems are closed-loop systems, part of the loop includes the outdoor storage of the Helium charge and Helium boiloff.

Outdoor storage is also required for the liquid nitrogen.

The sizes of tank farms required to support the various MSBS concepts reported herein are tabulated in Figure 9.3, and vary from the 3 acres (accommodating the 52 300,000 liter helium tanks and the 50,000 liter nitrogen tank) of Case 1, Alternative E to the 1/2 acre of Case 3, Alternative G (which accommodates the 113,000 liter helium tank and the 10,000 liter nitrogen tank).

11.0 MSBS PROGRAM SCHEDULE

In structuring a program for carrying the MSBS to its logical conclusion of installation at a wind tunnel, it has been assumed that the Program would next schedule a Preliminary Design Phase. Implicit in that assumption is that the Conceptual Design has been established - e.g. one of the study Cases selected, one of the Alternatives selected, and outstanding questions on type of core,utility limitations, scope of contractors work, and project duration have been settled. This would support a six-month Preliminary Design Phase for transition to Final Design.

11.1 SCHEDULE

A schedule developed for Case 1, Alternative E, is shown in Figure 11.1a. Line items are listed by Work Breakdown Structure (WBS) number (see Appendix B), and the numbered milestones are listed in Figure 11.1b. Cases 2 and 3, and Alternatives F and G are expected to engender only small differences in this schedule, which are discussed below.

The total elapsed time of 60 months for preliminary design, final design, fabrication, testing, shipping, installation, and checkout is consistent with other superconducting magnet system programs with which GE has been involved. The six month Preliminary Design and 18 month Final Design phases are also consistent with previous programs.

As in many superconducting magnet programs, the MSBS program must deal with the tradeoff between advance procurement of long lead items and extending the duration of a program. In the schedule of Figure 11.1, Magnets Manufacturing, Power Supplies Manufacturing and Cryogenics Manufacturing all contain long lead items requiring advanced procurement approximately one year prior to completion of Final Design. In the Magnet area, the conductor is the long lead item. For the Power Supplies and Cryogenics equipment, which are mainly purchased, custom-designed components from specialty vendors, the long lead time has proved necessary in previous programs. It is needed to carry out the vendor solicitation, review, analysis and evaluation process, to enable initiation of the custom design process prior to later production of the large number and variety of units for MSBS.

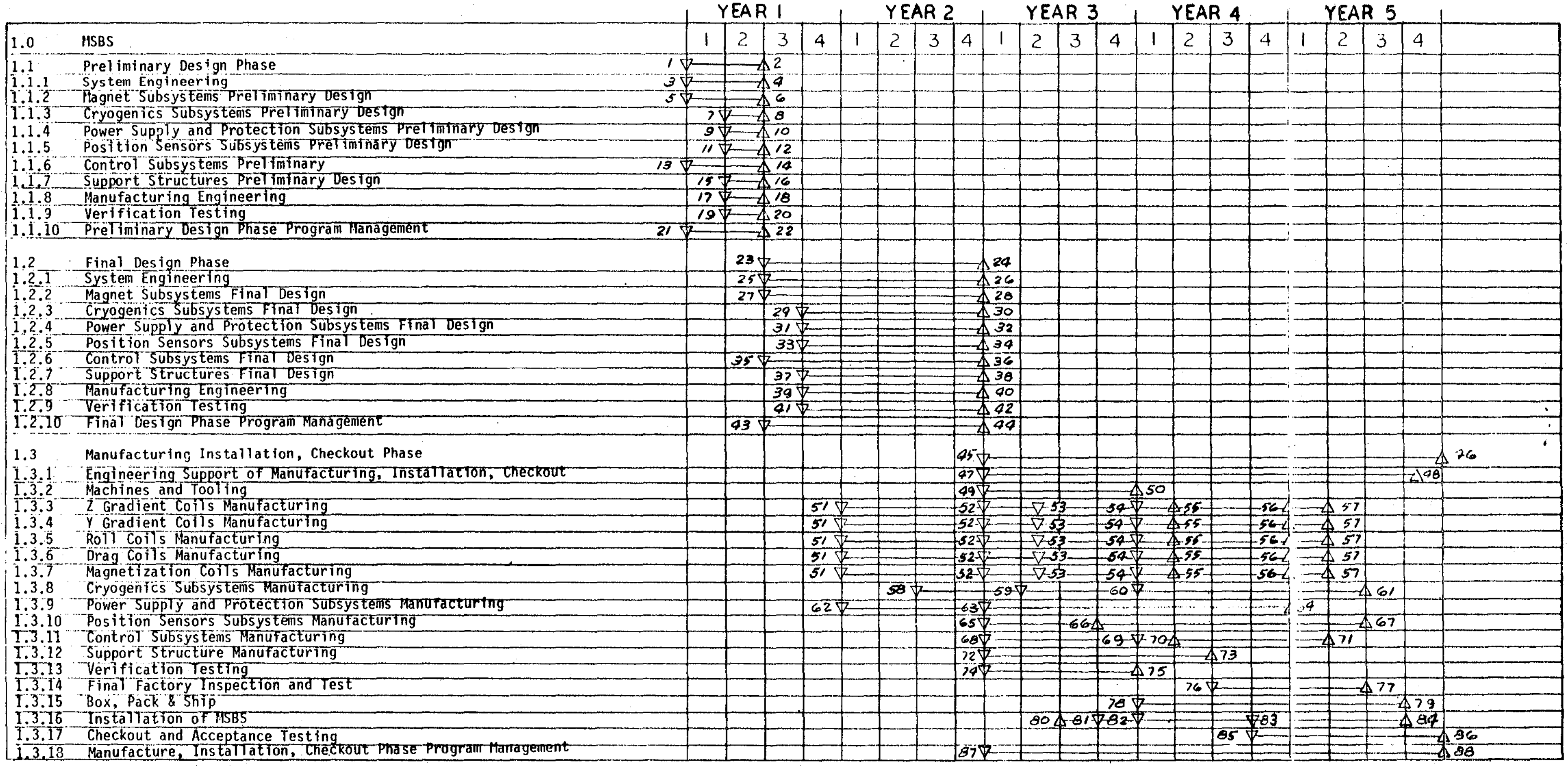

Figure 11.1a

MSBS SCHEDULE ESTIMATE (NOMINAL)

Figure 11.1b

SCHEDULE MILESTONES

1-START OF PRELIMINARY DESIGN
2-COMPLETION PRELIMINARY DESIGN
3-START OF P.D. SYST. ENG.
4-COMPLETION OF P.D. SYST. ENG.
5-START OF MAGNET S/S PRELIM. DES.
6-COMPLETION OF MAGNET S/S PRELIM. DES.
7-START OF CRYOGENICS S/S PRELIM. DES.
8-COMPLETION OF CRYOGENICS S/S PRELIM. DES.
9-START OF POW. SUPP. & PROT. S/S PRELIM. DES.
10-COMPLETION OF POW. SUPP. & PROT. S/S PRELIM. DES.
11-START OF POSITION SENSORS S/S PRELIM. DES.
12-COMPLETION OF POSITION SENSORS S/S PRELIM. DES.
13-START OF CONTROLS S/S PRELIM. DES.
14-COMPLETION OF CONTROLS S/S PRELIM. DES.
15-START OF SUPPORT STRUCT. S/S PRELIM. DES.
16-COMPLETION OF SUPPORT STRUCT. S/S PRELIM. DES.
17-START OF MANUFACT. ENG. PRELIM. DES.
18-COMPLETION OF MANUFACT. ENG. PRELIM. DES.
19-START OF VERIF. TESTING IN PRELIM. DES.
20-COMPLETION OF VERIF. TESTING IN PRELIM. DES.
21-START OF P.D. PHASE PROG. MANAGEMENT
22-COMPLETION OF P.D. PHASE PROG. MANAGEMENT
23-START OF FINAL DESIGN
24-COMPLETION OF FINAL DESIGN
25-START OF F.D. SYST. ENG.
26-COMPLETION OF F.D. SYST. ENG.
27-START OF MAGNET S/S FINAL DES.
28-COMPLETION OF MAGNET S/S FINAL DES.
29-START OF CRYOGENICS S/S FINAL DES.
30-COMPLETION OF CRYOGENICS S/S FINAL DES.
31-START OF POW. SUPP. & PROTECT. S/S FINAL DES.
32-COMPLETION OF POW. SUPP. & PROTECT. S/S FINAL DES.
33-START OF POSITION SENSORS S/S FINAL DES.
34-COMPLETION OF POSITION SENSORS S/S FINAL DES.
35-START OF CONTROLS S/S FINAL DES.
36-COMPLETION OF CONTROLS S/S FINAL DES.
37-START OF SUPPORT STRUCT. S/S FINAL DES.
38-COMPLETION OF SUPPORT STRUCT. S/S FINAL DES.
39-START OF MANUFACT. ENG. FINAL DES.
40-COMPLETION OF MANUFACT. ENG. FINAL DES.
41-START OF VERIF. TESTING IN FINAL DES.
42-COMPLETION OF VERIF. TESTING IN FINAL DES.
43-START OF F.D. PHASE PROGRAM MANAGEMENT
44-COMPLETION OF F.D. PHASE PROGRAM MANAGEMENT
45-START OF MANUF., INSTAL, C.O. PHASE
46-COMPLETION OF MANUF., INSTAL, C.O. PHASE
47-START OF ENG. SUPPT. OF MAN., INST. & C.O. PHASE
48-COMPLETION OF ENG. SUPPT. OF MAN., INST. & C.O PHASE
49-START OF MACHINES & TOOLING
50-COMPLETION OF MACHINES & TOOLING
51-START OF CONDUCTOR PROCUREMENT (ALL MAGNETS)
52-START OF MAGNET DEWARS & COMPONENTS (ALL MAGNETS)
53-START CONDUCTOR DELIVERY
54-START COIL WINDING & DELIV. OF DEWARS & COMPON.
55-CONDUCTOR DELIVERY COMPLETE & START COIL ASSEMBLY
56-COMPLETE DELIVERY OF DEWARS & COMPON.
57-COIL ASSEMBLY COMPLETE
58-START REFRIGERATOR PROCUREMENT
59-START STORAGE DEWAR PROCUREMENT
60-START PIPING PROCUREMENT
61-COMPLETE DELIVERY OF COMPON.
62-START POWER SUPPLY PROCUREMENT
63-START DELIVERY, FAB. & TEST
64-COMPLETE DELIVERY, FAB. & TEST
65-START COMPON. PROCUREMENT
66-COMPLETE ELECTRO-OPTICAL S/S
67-COMPLETE EPS
68-START COMPON. PROC. & SOFTWARE PROG.
69-COMPLETE COMPON. DELIVERY
70-START S/S INTEGRATION
71-COMPLETE HARDWARE/SOFTWARE INTEG.
72-START COMPON. PROCUREMENT
73-DELIVERY OF COMPON. TO SITE
74-START REMAINING VERIF. TESTING
75-COMPLETE REMAINING VERIF. TESTING
76-START FINAL FACT. INSP. & TEST
77-COMPLETE FINAL FACT. INSP. & TEST
78-START BOX, PACK, SHIP TO SITE
79-COMPLETE BOX, PACK, SHIP TO SITE
80-BENEFICIAL OCCUPANCY
81-START POWER SUPP. S/S INSTALL.
82-START CRYO S/S INSTALL.
83-START MAGNETS INSTALL.
84-COMPLETE INSTALL.
85-START C.O. & ACCEP. TESTING
86-COMPLETE C.O. & ACCEP. TESTING
87-START MANUF., INSTAL, C.O. PHASE MGMT.
88-COMPLETE MANUF., INSTAL, C.O. PHASE MGMT.

The alternative to advanced procurement is, of course, extending the program duration so as to eliminate the overlap in the above areas. In this case the extension would be 1 year. In selecting the advanced procurement mode, GE reflects confidence that the risk incurred is low. In the Magnets area, for instance, the conductor design can be completed relatively quickly during Preliminary Design and early Final Design, since it is likely to be virtually identical to (or possibly simpler than) an existing design. In the Power Supplies and Cryogenics areas, after completion of design specifications during the Final Design Phase, the procurement activities prior to completion of Final Design are primarily "paper work", time-consuming, but not costly. Furthermore, the time spent in evaluating vendors, in carrying out a detailed proposal activity, and "spreading" the hardware among vendors to obtain the best price for each type of unit could actually save money. Initial power supply deliveries following this activity would be the smaller, off-the-shelf units likely to be required in whatever results from the Final Design phase.

While most of the line items in the given schedule are self explanatory, the items 1.1.9, 1.2.9 and 1.3.13, Verification Testing, are nomenclature familiar to today's superconducting magnet industry, and possibly need explanation to others. A brief discussion of Verification Testing is given in Appendix C.

For manufacturing the Magnets, procurement and installation of additional manufacturing equipment and tools, and modification of existing items would take one year. The key new item would be a vertical winding machine to wind the layer wound coils. Modification of existing winding stations to accommodate the size and weight of the MSBS coils would be necessary. One station would require significant strengthening to handle the drag and magnetization coils.

Winding and assembly times have been estimated based on winding rate data from other large superconducting magnets and on models developed for the fabrication of a similar system of large solenoidal magnets. The elapsed time of one year for each operation is based on the use of four winding stations, as described above, and a similar number of assembly stations.

Magnet dewars for MSBS, as in other programs, are purchased from outside vendors, based on specifications issued during Final Design. Multiple vendors, possibly four (one for each type of vessel) would be used. Initial deliveries would be used for verification testing and quality assurance, with all dewar deliveries completed in time for final factory test of assembled magnets.

Testing of each coil is estimated to take two months, including pumpdown, cooldown, test operations, and warmup. Two coils are assumed to be tested in parallel, with two more being prepared for testing at the same time.

All major Cryogenics and Power Supply components are also purchased from outside vendors, based on procurement specifications issued during Final Design. Since these components are generally large, after the vendors' designs have been approved and their components completed, testing will be carried out at the vendors' locations. After passing acceptance levels, these components will be shipped to the installation site, installed and checked out. Should individual components (such as a power supply or helium storage dewar) be required to supplement facilities for factory testing of coils, they will be routed through the factory prior to shipping to the installation site.

The shipping and installation schedule is based on incremental shipment and installation of coils, power supplies, and cryogenic components as they are completed. The availability of an adequate seasonal shipping window for the magnetization and drag coils, which must be shipped by barge for Cases 1 and 2, is also assumed.

The very large scale helium liquefaction plants required for Cases 1 and 2, Alternative E, as well as the large cryogenic and gas storage units will require on-site construction, as will the piping and wiring. These are planned to begin immediately after beneficial occupancy, utilizing the incremental shipment of relevant equipment.

11.2 POTENTIAL SCHEDULE VARIATIONS

The schedule of Figure 11.1 applies to Case 1, Alternative E.

The schedule for Case 2 is expected to be virtually the same as for Case 1. The coil winding process time would be reduced significantly, but the elapsed time would be driven by the delivery of the magnet dewar components. The magnet dewars for Case 2 are somewhat smaller in cross-section than for Case 1 but are comparable in overall size and complexity and acceleration of delivery is probably not realistic.

For Case 3, the size of the magnet dewars is reduced significantly and the delivery cycle for the vessels may be reduced by three months. The winding time for the epoxy-impregnated coils is significant because of the large number of turns required and the time for the impregnation process, but can be held to a year through the use of parallel operations, and started earlier because it is not dependent on dewar component deliveries. Thus, a net time of three months can be saved through coil winding. Three additional months can be picked up during the assembly, testing, and shipping cycle so that the total schedule is 6 months shorter than the Case 1 or 2 schedules.

The 6 month difference could be taken from the front end of the magnet tasks, which means delaying the ordering of conductor until later in the design cycle. Based on past experience, such an option is not advisable. The limited superconductor production capability is easily perturbed, and such perturbations can result in major program delays.

For the Design Concepts reported,the schedule effects of selecting Alternative F and G (reduced and eliminated forced model oscillations) are not to shorten the magnet schedule appreciably, since the amounts of conductor remain about the same. However, within the magnet schedule, the selection of Alternative G (elimination of forced model oscillation) could enable the use of stainless steel dewars rather than non-metallic dewars. While the schedule would not be shortened appreciably, the schedule risk would be reduced, since the steel dewars are already well-proven technology.

Since the overall schedule is primarily set by the magnet manufacturing schedule, the total schedule can be reduced by the power supply and cryogenics areas no more than the amounts already shown. However, within the power supply manufacturing schedule, significant reductions can occur as the selection moves from Case 1 to Cases 2 and 3, and from Alternative E to Alternatives F and G. Reductions in maximum voltage from 8.0 KV power supplies to as low as 10V, tend toward easier, though still custom, power supply design. The power supply schedule for Cases 2 and 3 and Alternatives F and G can, thus, likely be reduced by 6 months. When taken from the front end of the power supply schedule, this reduces the required power supplies lead time for advanced procurement, thus, tends to reduce the overall risk.

In the cryogenics area, the requirement for on-site construction is the major schedule factor. Alternatives F and G for all cases offer possibilities of standard design, thus, some schedule shortening. However, the piping, liquefier, and tank installations offer only small schedule savings, so that the cryogenics schedule may be shortened by possibly 6 months for these cases. Although this does not affect the overall schedule, if cut from the beginning of the cryogenics schedule, it does eliminate cryogenics as an advanced procurement.

11.3 SCHEDULE RISKS

The significant elements of the Magnet system contributing to schedule risk are the following:

- o superconductor
- o insulation
- o dewars

In the past, superconductor vendors have encountered difficulties because of inadequate resources, process failures, or lack of availability of raw materials (primarily NbTi). Careful evaluation of vendor capabilities, production plans and schedules, and past performance and continuous on-site monitoring of the vendor's performance against his plan will help to minimize the possibility of schedule slips. In addition, the overall schedule incorporates six months slack time in conductor delivery to allow for the possibility of schedule slips and enable the overall program schedule to be maintained.

Availability of NbTi is of concern because there is, at present, only one commercial domestic supplier of this material. NbTi represents only a small fraction of the vendor's business and deliveries have occasionally been erratic. Furthermore, since the total market is relatively small, a single major magnet program in an area such as fusion, MHD, or energy storage may tie up production capacity for an extended period. Again, early procurement of NbTi would tend to reduce the risk of a schedule slip in this area and could also provide additional margin for conductor fabrication slips by making the material available to the vendors well in advance of the 6-month procurement cycle assumed in the schedule.

Reduction in conductor complexity which could be achieved through the reduction of forced oscillation is not expected to significantly decrease the schedule risk.

Schedule risks in the fabrication of the insulation arise primarily from the limited resources and experience of the vendors. As in the case of the superconductor, a thorough program of vendor qualification and surveillance will reduce this risk. In addition, the experience gained by vendors on fabrication of similar insulation for LCP, CDIF, and other large superconducting magnet programs should add measurably to their ability to perform on schedule.

The schedule risk for the non-metallic dewars, if Alternative E is required, is of a slightly different nature. The schedule presented appears adequate for the fabrication of the dewars assuming that design and fabrication approaches which satisfy the performance requirements can be developed and verified during the design phase, or before, and implemented during fabrication. However, the present understanding of the problems which may be encountered during this development is sufficiently incomplete that assurance of such success is not presently possible. Failure to accomplish this development, or the inability to implement it in production, could have a significant impact on the overall program schedule. Development of a better definition of dewar requirements and the approaches required to solve them should be undertaken immediately to minimize the schedule risk associated with this problem.

The reduction of forced oscillation requirements could eliminate this schedule risk by making the use of metal dewars feasible. Although the fabrication and QC operations for metal dewars are similarly complex and time-consuming (multipass welding, in-process weld inspection, heat treating, surface finishing, helium leak testing, etc.), they are much better understood and characterized, and no development would be required to meet the recommended schedule.

For the power supplies and cryogenic systems, the schedule risk stems from not approving advanced procurement activities. Without an adequate time for the planned vendor solicitations and evaluations, the pressure of meeting final hardware delivery dates can face the prime contractor with the hard choice of high priced vendors in whom high confidence in meeting schedules exists vs low bidder whose schedule-meeting capabilities are questionable.

11.4 OTHER SCHEDULE ITEMS

This section has dealt primarily with the magnets, power supplies and cryogenics system. The other subsystems appear to have of little impact on the schedule. That is, the individual tasks in these areas fit well within the overall schedule, and, even if they should suffer 6 month delays, would cause no critical problem.

12.0 MSBS COST ESTIMATE

Cost estimates have been prepared for the design, fabrication, installation and checkout of the MSBS concepts presented in the foregoing sections. The methods used in preparing these cost estimates are, in general, the same methods employed in costing proposals for advanced projects in the electrical industry. The resulting costs, however, are not to be construed as a quotation to carry out the work defined in this report, nor as formal bid to perform the work.

Cost estimates presented in Figures 12.1, 12.2, 12.3, 12.4, 12.5 and 12.6 are given in 1981 dollars, and are calculated on the basis of labor rates common to the industry, and costs of major purchases of materials and components were primarily obtained as budgetary estimates from potential vendors.

12.1 ENGINEERING COSTS

Engineering cost estimates for the WBS tasks (Appendix B) of the preliminary and final design of the MSBS concepts were based on recently initiated and completed programs and a recently prepared estimate for a magnet system which is comparable in some respects to MSBS. The programs involved coils of comparable physical size and of a variety of configurations, but generally of lesser complexity than MSBS. Particular factors taken into account in adjusting the recent program data for MSBS included:

- the complexities introduced by the use of non-metallic dewars
- the commonality in design features for all the coils, particularly for Cases 1 and 2
- the need for a significant amount of systems analysis of magnetic fields and forces.

Because Power Supplies and Cryogenics systems are purchased from specialized vendors, costs for Preliminary and Final Design Engineering of this equipment reflect the design effort to develop component requirements and specifications for procurement, as well as subsequent vendor surveillance. The preliminary and detail design of such systems is performed by the vendor, and is treated as part of the purchased "materials".

Manufacturing Engineering is included as early as the Preliminary Design Phase. Experience has shown that the early attention to "producibility" provided by this function enhances the transition from design to hardware.

Figure 12.1

MSBS COST ESTIMATE (ALTERNATIVE E - 100% RFP FORCED SINUSOIDAL OSCILLATIONS, CONTROL FORCE BASED ON SIMULATION) IN $K

1.0	MSBS	CASE 1	CASE 2	CASE 3
1.1	PRELIMINARY DESIGN PHASE	1,626	1,555	1,307
1.1.1	SYSTEM ENGINEERING	150	140	120
1.1.2	MAGNET SUBSYSTEMS PRELIMINARY DESIGN	326	326	249
1.1.3	CRYOGENICS SUBSYSTEMS PRELIMINARY DESIGN	239	189	127
1.1.4	POWER SUPPLY AND PROTECTION SUBSYSTEMS PRELIMINARY DESIGN	122	122	122
1.1.5	POSITION SENSORS SUBSYSTEMS PRELIMINARY DESIGN	131	131	131
1.1.6	CONTROL SUBSYSTEMS PRELIMINARY DESIGN	87	87	87
1.1.7	SUPPORT STRUCTURES PRELIMINARY DESIGN	297	297	230
1.1.8	MANUFACTURING ENGINEERING	60	60	60
1.1.9	VERIFICATION TESTING	49	49	49
1.1.10	PRELIMINARY DESIGN PHASE PROGRAM MANAGEMENT	165	154	132
1.2	FINAL DESIGN PHASE	4,938	4,799	4,122
1.2.1	SYSTEM ENGINEERING	400	390	340
1.2.2	MAGNET SUBSYSTEMS FINAL DESIGN	805	805	622
1.2.3	CRYOGENICS SUBSYSTEMS FINAL DESIGN	696	578	426
1.2.4	POWER SUPPLY AND PROTECTION SUBSYSTEMS FINAL DESIGN	190	190	190
1.2.5	POSITION SENSORS SUBSYSTEMS FINAL DESIGN	419	419	419
1.2.6	CONTROL SUBSYSTEMS FINAL DESIGN	350	350	350
1.2.7	SUPPORT STRUCTURES FINAL DESIGN	1,037	1,037	800
1.2.8	MANUFACTURING ENGINEERING	357	357	357
1.2.9	VERIFICATION TESTING	244	244	244
1.2.10	FINAL DESIGN PHASE PROGRAM MANAGEMENT	440	429	374
1.3	MANUFACTURING INSTALLATION, CHECKOUT PHASE	440,518	146,892	43,113
1.3.1	ENGINEERING SUPPORT OF MANUFACTURING, INSTALLATION, CHECKOUT	910	899	860
1.3.2	MACHINES AND TOOLING	1,458	1,458	723
1.3.3	Z GRADIENT COILS MANUFACTURING	13,882	5,035	1,016
1.3.4	Y GRADIENT COILS MANUFACTURING	3,623	3,508	635
1.3.5	ROLL COILS MANUFACTURING	10,143	5,654	4,052
1.3.6	DRAG COILS MANUFACTURING	13,978	4,828	1,202
1.3.7	MAGNETIZATION COILS MANUFACTURING	3,356	3,088	634
1.3.8	CRYOGENICS SUBSYSTEMS MANUFACTURING	51,534	23,184	4,593
1.3.9	POWER SUPPLY AND PROTECTION SUBSYSTEMS MANUFACTURING	322,288	84,343	20,190
1.3.10	POSITION SENSORS SUBSYSTEMS MANUFACTURING	1,068	1,068	1,068
1.3.11	CONTROL SUBSYSTEMS MANUFACTURING	1,046	1,046	1,046
1.3.12	SUPPORT STRUCTURE MANUFACTURING	5,529	3,312	933
1.3.13	VERIFICATION TESTING	244	244	244
1.3.14	FINAL FACTORY INSPECTION AND TEST	2,330	2,330	1,364
1.3.15	BOX, PACK AND SHIP	621	509	123
1.3.16	INSTALLATION OF MSBS	4,909	3,635	2,551
1.3.17	CHECKOUT AND ACCEPTANCE TESTING	1,600	1,347	1,035
1.3.18	MANUFACTURING, INSTALLATION, CHECKOUT PHASE PROGRAM MANAGEMENT	1,999	1,404	844
	TOTAL	447,082	153,246	48,542

1981 $ - Fee not included

Figure 12.2

MSBS COST ESTIMATE (ALTERNATIVE F - 10% RFP FORCED SINUSOIDAL OSCILLATIONS, CONTROL FORCE BASED ON SIMULATION) IN $K

1.0	MSBS	CASE 1	CASE 2	CASE 3
1.1	PRELIMINARY DESIGN PHASE	1,354	1,354	1,165
1.1.1	SYSTEM ENGINEERING	132	132	106
1.1.2	MAGNET SUBSYSTEMS PRELIMINARY DESIGN	303	303	231
1.1.3	CRYOGENICS SUBSYSTEMS PRELIMINARY DESIGN	119	119	119
1.1.4	POWER SUPPLY AND PROTECTION SUBSYSTEMS PRELIMINARY DESIGN	61	61	61
1.1.5	POSITION SENSORS SUBSYSTEMS PRELIMINARY DESIGN	131	131	131
1.1.6	CONTROL SUBSYSTEMS PRELIMINARY DESIGN	87	87	87
1.1.7	SUPPORT STRUCTURES PRELIMINARY DESIGN	276	276	213
1.1.8	MANUFACTURING ENGINEERING	60	60	60
1.1.9	VERIFICATION TESTING	40	40	40
1.1.10	PRELIMINARY DESIGN PHASE PROGRAM MANAGEMENT	145	145	117
1.2	FINAL DESIGN PHASE	4,268	4,268	3,832
1.2.1	SYSTEM ENGINEERING	355	355	338
1.2.2	MAGNET SUBSYSTEMS FINAL DESIGN	765	765	590
1.2.3	CRYOGENICS SUBSYSTEMS FINAL DESIGN	407	407	407
1.2.4	POWER SUPPLY AND PROTECTION SUBSYSTEMS FINAL DESIGN	95	95	95
1.2.5	POSITION SENSORS SUBSYSTEMS FINAL DESIGN	419	419	419
1.2.6	CONTROL SUBSYSTEMS FINAL DESIGN	350	350	350
1.2.7	SUPPORT STRUCTURES FINAL DESIGN	985	985	760
1.2.8	MANUFACTURING ENGINEERING	357	357	357
1.2.9	VERIFICATION TESTING	144	144	144
1.2.10	FINAL DESIGN PHASE PROGRAM MANAGEMENT	391	391	372
1.3	MANUFACTURING INSTALLATION, CHECKOUT PHASE	83,730	46,979	24,255
1.3.1	ENGINEERING SUPPORT OF MANUFACTURING, INSTALLATION, CHECKOUT	910	899	860
1.3.2	MACHINES AND TOOLING	1,458	1,458	723
1.3.3	Z GRADIENT COILS MANUFACTURING	12,135	4,672	942
1.3.4	Y GRADIENT COILS MANUFACTURING	3,367	1,727	596
1.3.5	ROLL COILS MANUFACTURING	9,323	5,182	3,700
1.3.6	DRAG COILS MANUFACTURING	12,775	4,630	1,116
1.3.7	MAGNETIZATION COILS MANUFACTURING	3,123	2,889	607
1.3.8	CRYOGENICS SUBSYSTEMS MANUFACTURING	7,297	5,096	2,507
1.3.9	POWER SUPPLY AND PROTECTION SUBSYSTEMS MANUFACTURING	17,494	7,464	4,315
1.3.10	POSITION SENSORS SUBSYSTEMS MANUFACTURING	1,068	1,068	1,068
1.3.11	CONTROL SUBSYSTEMS MANUFACTURING	1,046	1,046	1,046
1.3.12	SUPPORT STRUCTURE MANUFACTURING	5,529	3,312	933
1.3.13	VERIFICATION TESTING	144	144	144
1.3.14	FINAL FACTORY INSPECTION AND TEST	2,135	2,135	1,250
1.3.15	BOX, PACK AND SHIP	621	509	123
1.3.16	INSTALLATION OF MSBS	2,476	2,476	2,476
1.3.17	CHECKOUT AND ACCEPTANCE TESTING	1,012	1,012	1,012
1.3.18	MANUFACTURING, INSTALLATION, CHECKOUT PHASE PROGRAM MANAGEMENT	1,817	1,260	837
	TOTAL	89,352	52,601	29,252

1981 $ - Fee not included

Figure 12.3

MSBS COST ESTIMATE (ALTERNATIVE G - 0% RFP FORCED SINUSOIDAL OSCILLATIONS, CONTROL FORCE BASED ON SIMULATION) IN $K

1.0	MSBS	CASE 1	CASE 2	CASE 3
1.1	PRELIMINARY DESIGN PHASE	1,329	1,329	1,165
1.1.1	SYSTEM ENGINEERING	120	120	106
1.1.2	MAGNET SUBSYSTEMS PRELIMINARY DESIGN	303	303	231
1.1.3	CRYOGENICS SUBSYSTEMS PRELIMINARY DESIGN	119	119	119
1.1.4	POWER SUPPLY AND PROTECTION SUBSYSTEMS PRELIMINARY DESIGN	61	61	61
1.1.5	POSITION SENSORS SUBSYSTEMS PRELIMINARY DESIGN	131	131	131
1.1.6	CONTROL SUBSYSTEMS PRELIMINARY DESIGN	87	87	87
1.1.7	SUPPORT STRUCTURES PRELIMINARY DESIGN	276	276	213
1.1.8	MANUFACTURING ENGINEERING	60	60	60
1.1.9	VERIFICATION TESTING	40	40	40
1.1.10	PRELIMINARY DESIGN PHASE PROGRAM MANAGEMENT	132	132	117
1.2	FINAL DESIGN PHASE	4,268	4,268	3,832
1.2.1	SYSTEM ENGINEERING	355	355	338
1.2.2	MAGNET SUBSYSTEMS FINAL DESIGN	765	765	590
1.2.3	CRYOGENICS SUBSYSTEMS FINAL DESIGN	407	407	407
1.2.4	POWER SUPPLY AND PROTECTION SUBSYSTEMS FINAL DESIGN	95	95	95
1.2.5	POSITION SENSORS SUBSYSTEMS FINAL DESIGN	419	419	419
1.2.6	CONTROL SUBSYSTEMS FINAL DESIGN	350	350	350
1.2.7	SUPPORT STRUCTURES FINAL DESIGN	985	985	760
1.2.8	MANUFACTURING ENGINEERING	357	357	357
1.2.9	VERIFICATION TESTING	144	144	144
1.2.10	FINAL DESIGN PHASE PROGRAM MANAGEMENT	391	391	372
1.3	MANUFACTURING INSTALLATION, CHECKOUT PHASE	82,851	46,746	24,139
1.3.1	ENGINEERING SUPPORT OF MANUFACTURING, INSTALLATION, CHECKOUT	910	899	860
1.3.2	MACHINES AND TOOLING	1,458	1,458	723
1.3.3	Z GRADIENT COILS MANUFACTURING	12,135	4,672	942
1.3.4	Y GRADIENT COILS MANUFACTURING	3,367	1,727	596
1.3.5	ROLL COILS MANUFACTURING	9,323	5,182	3,700
1.3.6	DRAG COILS MANUFACTURING	12,775	4,630	1,116
1.3.7	MAGNETIZATION COILS MANUFACTURING	3,010	2,889	607
1.3.8	CRYOGENICS SUBSYSTEMS MANUFACTURING	7,297	5,096	2,507
1.3.9	POWER SUPPLY AND PROTECTION SUBSYSTEMS MANUFACTURING	17,028	7,231	4,199
1.3.10	POSITION SENSORS SUBSYSTEMS MANUFACTURING	1,068	1,068	1,068
1.3.11	CONTROL SUBSYSTEMS MANUFACTURING	1,046	1,046	1,046
1.3.12	SUPPORT STRUCTURE MANUFACTURING	5,229	3,312	933
1.3.13	VERIFICATION TESTING	144	144	144
1.3.14	FINAL FACTORY INSPECTION AND TEST	2,135	2,135	1,250
1.3.15	BOX, PACK AND SHIP	621	509	123
1.3.16	INSTALLATION OF MSBS	2,476	2,476	2,476
1.3.17	CHECKOUT AND ACCEPTANCE TESTING	1,012	1,012	1,012
1.3.18	MANUFACTURING, INSTALLATION, CHECKOUT PHASE PROGRAM MANAGEMENT	1,817	1,260	837
	TOTAL	88,448	52,343	29,136

1981 $ - Fee not included

Figure 12.4

TIME SPREAD OF COSTS ($K)

ALTERNATIVE E

	YR 1		YR 2		YR 3		YR 4		YR 5		TOTAL
CASE 1	1,626	1,625	1,626	199,859	183,028	19,653	25,318	10,299	3,043	1,005	447,082
CASE 2	1,555	1,555	1,555	62,294	54,410	10,005	12,854	5,923	2,308	787	153,246
CASE 3	1,307	1,307	1,307	16,342	13,474	3,832	4,867	3,321	2,060	725	48,542

1981 $ - Fee not included

Figure 12.5

TIME SPREAD OF COSTS ($K)

ALTERNATIVE F

	YR 1		YR 2		YR 3		YR 4		YR 5		TOTAL
CASE 1	1,354	1,354	1,354	29,272	20,970	10,799	13,860	6,654	2,783	952	89,352
CASE 2	1,354	1,354	1,354	15,760	10,456	6,520	8,344	4,488	2,206	765	52,601
CASE 3	1,165	1,165	1,165	7,053	5,788	3,143	3,976	3,038	2,040	719	29,252

1981 $ - Fee not included

Figure 12.6

TIME SPREAD OF COSTS ($K)

ALTERNATIVE G

	YR 1		YR 2		YR 3		YR 4		YR 5		TOTAL
CASE 1	1,329	1,329	1,329	28,841	20,828	10,710	13,737	6,614	2,780	951	88,448
CASE 2	1,329	1,329	1,329	15,522	10,671	6,462	8,268	4,464	2,204	765	52,343
CASE 3	1,165	1,165	1,165	7,220	5,505	3,143	3,976	3,038	2,040	719	29,136

1981 $ - Fee not included

All engineering effort during the manufacture, installation, and checkout of MSBS is provided under WBS 1.3.1, Engineering Support. This integrated effort provides efficient utilization of engineering personnel carrying out quality assurance, inspection and corrective action, both within the factory and off-site (such as at vendors and/or the installation site).

12.2 MATERIALS COSTS

Based on the Case 1, 2 and 3, Alternatives E, F and G concept definitions, materials lists were assembled. Where the very preliminary nature of the concepts made it difficult to obtain vendor estimates, costs were estimated by experienced engineering, manufacturing and purchasing personnel, based on items purchased on other programs or extrapolations of cost of commercially available items.

12.3 FABRICATION COSTS

Fabrication, shipping, and installation costs for the various cases and alternatives were estimated on the basis of cost models previously developed for a system using large solenoidal coils supplemented by GE experience in shipping and installing large motor/generators and drives. Shipping costs include the assumption that the Case 1 and 2 magnetization and drag coils would be shipped by barge and all other coils by rail. Costs for coil winding and assembly reflect data available on large magnets such as the GE LCP coil and the MFTF coils. Cost estimates for assembly of dewars take into account the complexity of the closure process for the helium and vacuum vessels. Equipment and tooling costs reflect the modification and use of three existing horizontal winding stations at GE to wind the pie-wound coils and the purchase and installation of other tooling and fixtures. The cost of testing assumes that each magnet will be subjected to a full operational test prior to shipment, using MSBS electrical, cryogenic and vacuum support equipment.

12.4 COST RISKS

There is a general element of risk in the use of cost data derived from the design concept level of design detail. Vendors are reluctant to provide estimates of engineering and manufacturing effort on the basis of such data. The cost estimates are, therefore, of necessity approximate and should be so regarded.

However, GE experience and other experience in the superconducting magnet industry indicates that three specific elements of cost risk must be recognized for MSBS. The three elements which are of concern are:

- superconductor cost
- insulation cost
- non-metallic vessel cost

The superconductor is the most expensive single item in the MSBS magnet system, as is typical of large superconducting magnets. The MSBS system requires a very large quantity of conductor, about 30,000m for Case 1 coils. This quantity of material will require about 450,000 kg of superconducting wire, which represents a substantial fraction of the total yearly output of the domestic superconductor industry. The industry is in a growth period in response to other large magnet programs and has been subject to occasional problems in product quality and consistency, and lack of process repeatability. Such problems inevitably lead to cost increases as well as schedule delays as discussed in the following section. The cost risk associated with the conductor is reduced to some extent because the selected conductors will have been fabricated for other large magnet programs, so the manufacturing and quality control processes should be relatively well understood. However, an element of risk remains because of the large quantity needed versus the relatively small quantity (< 1000m) presently planned for fabrication. GE would plan several specifications to reduce cost risk. These include:

- use of fixed-price procurements
- continuous on-site monitoring of vendor performance
- use of multiple vendors

These actions will add somewhat to the initial cost of the program, but are expected to save money on an overall basis by preventing cost overruns as a result of failure to recognize and correct poor vendor performance.

There is a second element of risk in the cost of the superconductor which must be resolved. The cost of the NbTi alloy used to make superconducting wire has been escalating rapidly in the past several years, far more rapidly than the general rate of inflation. The cost of NbTi alloy alone for Case 1 is in excess of $10M at present prices. A cost increase of 10-20%, which is not unusual, thus represents a significant cost impact. To reduce the risk of such a cost increase, it is recommended that NASA consider the procurement of the full quantity of NbTi required immediately upon decision to proceed with

MSBS and provide it as government-furnished material. This would eliminate the vulnerability of the program to the cost volatility of NbTi.

The risk in the cost of the insulation material arises for much the same reason as for the superconductor. Many of the vendors are small firms whose fabrication and quality control capabilities are heavily taxed by the quantity and quality of the materials required for large superconducting magnets. GE would apply the same measures as described above, at a level appropriate to the value and criticality of the item, to reduce the risk to an acceptable level.

The nature of the cost risk engendered by the use of non-metallic dewars is somewhat different. There are a number of firms, both large and small, with outstanding technical capability in the fabrication of large non-metallic hardware. However, the lack of present design detail in this area, and the incomplete understanding of the problems which may be encountered raise the possibility that the estimated costs for the vessels, which have been estimated from volumetric scaling of the cost of the Los Alamos Scientific Laboratory dewars, may be low. A technical solution for the requirements of helium-tight low temperature seals and thermally efficient force transmission can certainly be found, but could conceivably involve the use of complex and expensive materials, processes, and testing techniques. A program of component and process development should be undertaken to delineate and resolve the technical problems associated with the use of non-metallic dewars in this application because of the potential impact on cost. It should be noted that the reduction or elimination of forced oscillation requirements may obviate the need for non-metallic dewars and the associated risks.

12.5 MSBS DAILY OPERATING COSTS

The costs of operating MSBS systems in the specified daily cycle have been estimated and are tabulated in Figure 12.7.

The three cost items included in the data are 1.) labor to operate and maintain the system, 2.) electrical power and 3.) replacement of helium leakage and nitrogen boiloff. The power costs, estimated at $.046 per KwH, are by far the largest portion of the total operating cost. This portion ranges from 99% for Case 1, Alternative E to 77% for Case 3, Alternative G. As the MSBS program progresses, more definitive power cost calculations will have to take into account the level of peak power demand as well as the energy required.

Figure 12.7

MSBS OPERATING* COSTS (DAILY)

Alternative / CASE	1	2	3
E	$1,559,200	$377,400	$66,700
F	62,200	9,000	7,600
G	59,100	8,900	7,500

*Includes Labor
Electrical Energy
Helium Make-up
Nitrogen Boiloff

Labor (for MSBS operations only) is assumed to be comprised of an average of 4 personnel spread over the specified 24 hour operating cycle, and helium losses from the cryogenic system and magnet dewars vary from 3500 liters/day for Case 1, Alternative E, to 50 liters/day for Case 3, Alternative G.

No separate overhead or fee costs have been included, and all calculations are in 1981 dollars.

13.0 CONCLUSIONS AND RECOMMENDATIONS

A number of significant conclusions have been reached as a result of the MSBS study. These conclusions are documented in Figure 13.1 and in the following section, and are intended to summarize key study results, as they impact the system technical goals, costs and schedules. In certain areas, additional effort is desirable to resolve technical problems which could not be addressed during the study, to achieve improvements in cost and schedule, or to minimize risk. In these cases, additional work has been recommended as appropriate.

13.1 CONCLUSIONS

On the basis of the present study, it has been concluded that the systems for all three cases and alternatives are feasible. Certain technical problems remain to be resolved, but all appear to be soluble in a period consistent with the timely design and fabrication of MSBS. Further development in some areas is required, but no breakthroughs or new technology are required.

The requirements for full forced model oscillation (Alternative E), although they impact the magnet system to some extent, have a far more significant impact on the magnet power supply and cryogenics systems. The demands for peak power and refrigeration capacity for Cases 1 and 2 lead to systems which are relatively large and expensive. The number and rating of the power supplies required and the size of the cryogenic plant push the state of the art, although the components are relatively standard, and would impose very large peak demands on the utility which may be unacceptable. Such demands may require additional power generation or storage. Furthermore, the reliability of the large systems requires definitive Failure Modes and Effects Analysis to ascertain the vulnerability of the large number of components. For Case 3, the power supply and cryogenic requirements are large but far more reasonable. Use of non-metallic dewars is required to eliminate eddy current losses and limit low-temperature heat loads to a reasonable level, and further development of present technology is required to achieve helium-tight low temperature seals and thermally efficient transmission of large coil-to-coil forces.

Reduction or elimination of forced oscillation requirements (Alternatives F and G), in combination with the revised requirements for control, significantly reduce the size and cost of all three systems. The most significant impact on system complexity and cost results from the greatly reduced demands on the power

Figure 13.1

CONCLUSIONS

- Concepts for all cases, Alternatives E, F and G are technically feasible.
  - Case 1, Alternative E pushes current hardware state of art in power supply, cryogenics, magnet dewars
  - Meeting roll torque requirements is a problem requiring further study
- Coils and power and cryogenic concepts for Cases 1 and 2, Alternatives E and F are relatively large and costly.
  - Due to requirements imposed by magnets providing model forced sinusoidal oscillations
- Case 3, using different coil technology (epoxy-impregnated coils) provides significant size and cost savings.
- High voltage/high current power supplies, as for Cases 1 and 2, Alternative E are not in present regular use.
  - Only the lower power units in all cases are current off-the-shelf products
  - Practice in the industry is that power supplies are custom designed for specific applications
  - Components used in design of power supplies are off-the-shelf
- Power peaks required for forced model oscillation in Cases 1 and 2 Alternative E, Case 1 Alternative F and possibly others, may be unacceptable to the utility.
  - "Buffering" by storage or rotating machinery, or in-house generation may be required.
- Standard magnet instrumentation appears satisfactory for aero data extraction.
  - .1% accuracy is standard. If .01% is required, further investigation is required
- Helium liquefiers for Case 1 Alternatives E and F are very large.
  - For Case 1 Alternative E liquefier is larger than any in use to date. However, this size unit is being built for Brookhaven National Laboratories
  - For Case 1 Alternative F, unit is smaller than an existing unit at bulk helium liquefier plant in Ulysses, Kansas
- Electronic position sensor derived from scale-up of MIT model appears to meet position accuracy requirements, but not angular accuracy.
  - Limitations of "scale-up" approach may be problem
  - Requirement for non-metallic test section wall may be problem
- Electro-optical position sensor appears to satisfy requirements, and offer other advantages.
  - Not generally limited by test section size or model shape
  - May be "portable"
  - Can provide video model coverage
- Control subsystem design concept is feasible
  - Three degrees of freedom in "longitudinal" mode, and three degrees in "lateral" mode demonstrated in simulation
  - Simulation is valuable adjunct in system design
- Facility to house MSBS is large for Cases 1 and 2.
  - Case 1 Alternative F 24,000 ft^2 indoors; 1 acre outdoors
  - Case 1 Alternative E two to three times larger

supply and cryogenic systems. The magnet conductor design can be simplified and its cost reduced while maintaining reasonable AC losses, and the reduction in the coil terminal voltage significantly reduces the technical risk in coil operation. It may also be possible to use metal rather than non-metal dewars, which would reduce cost slightly, and risk substantially, by eliminating the need for further development of non-metallic dewar technology.

The use of a fully symmetric 8 coil roll control system appears to be the most promising approach for production of roll torques in a large MSBS. However, achievement of the required roll torques has proved to be a difficult problem, and acceptable solutions have not been found for Cases 1 and 3. Further evaluation of coil locations and wing core materials is needed to achieve the required values.

The use of epoxy-impregnated adiabatically stable gradient and roll coils rather than cryostable coils appears feasible for Case 3. The higher current density achievable with this technology makes the Case 3 gradient coils very compact, improving access to the system, and also reduces the cost of the coils. Fundamental limits on the allowable stress levels in epoxy-impregnated windings probably make scaleup of this technology to tunnels larger than 4'x4' unfeasible.

Magnet instrumentation, customarily used for diagnostic purposes and magnet protection monitoring, appears to be of satisfactory accuracy for transformation to aerodynamic data. Should the need arise, however, for an order of magnitude improvement in instrument accuracy, it is very likely that such instruments can readily be obtained.

Analysis of position sensing via the Electronic Position Sensors has shown that simple scaling of the MIT EPS results in a shortcoming in attitude sensing accuracy. However, a more detailed design analysis may overcome this problem. On the other hand, the need for a non-metallic wall to eliminate shielding of EPS signals imposes test section design problems.

The Electro-Optical Position Sensor appears to offer satisfactory capability, and its concept appears to provide the added benefits of independence of test section size, portability between wind tunnels without large scale disassembly, and easy adaptation to video display of the model.

Work on the MSBS Control System has accounted for all six degrees of freedom in two separate modes - longitudinal (pitch, heave and drag) and lateral (yaw, slip and roll), and has demonstrated its feasibility via computerized simulation.

The required static and dynamic position and attitude accuracies have been met, and a PDP 11/60 microcomputer has been identified for the Control System.

In developing the Interface Requirements for MSBS, it is clear that the power and cooling requirements are large for the full forced oscillation Alternative (E) and the reduced oscillation Alternative (F). Translated into installation space, Case 1, Alternative F calls for a 3 story building of 24,000 square feet, and an acre of cryogenics gas storage, while Case 1 Alternative E essentially triples those requirements.

13.2 RECOMMENDATIONS

Although the present study has demonstrated the technical feasibility of Magnetic Suspension and Balance Systems for all three required cases, some additional work in specific areas appears desirable. This additional effort, briefly summarized in Figure 13.2, will serve to reduce the cost and/or the risk of undertaking MSBS and will help to define optimum design approaches more clearly prior to the initiation of the preliminary design phase.

First, in view of the very significant impact that the requirements for forced model oscillation have on the cost and complexity of MSBS, it is suggested that a careful review be carried out on these requirements, and on other methods for obtaining dynamic coefficients. Specific actions which would lead to major cost reductions include:

- Reduction of the frequency and/or amplitude of forced oscillations. Of the two, a reduction in frequency would be by far more beneficial since the peak coil terminal voltage and reactive power required for forced model oscillation vary as the third power of the frequency but only as the first power of the amplitude.
- Reduction in the duty cycle for forced oscillation from the presently assumed values of two hours at 100% of full load and eight hours at 25%. This would reduce the time-averaged loads on the cryogenic system and allow corresponding reductions in the liquefaction and storage capacities.
- Reduction of the number of forced oscillation modes which must be achieved simultaneously. This would reduce the peak and time-averaged loads on the cryogenic system. It might also make possible the "sharing" of a single high-voltage power supply between a number of coil sets by switching to reduce capital cost of the power supply system.

Figure 13.2

RECOMMENDATIONS

- Review requirements for simultaneous position, attitude, oscillation and for 2 hour operation at max. conditions
  - Reductions cán reduce magnet, power supply, cryogenics size and costs
- Investigate eddy current losses in metallic dewars and review need for non-metallic dewar development and test data.
- Investigate cost-effective structural design approaches for thermally-efficient multi-axis magnet supports and define test program.
- Investigate alternative model cores (main core/wings).
  - Permanent high field magnets
  - Superconducting magnets
- Investigate potential for reducing power supply costs by utilizing serial/parallel combinations, storage.
- If peak power demands are unacceptable to utility, investigate approaches and costs for "buffering".
- Ascertain aero data errors based on .1% magnet current (.2 to .14% force and torque) errors. Determine if errors < .1% are required.
- Initiate conceptual design of EPS - not limited to scale-up of MIT EPS
- Initiate design of electro-optical position sensor.
- Continue control system investigation to integrate "longitudinal" and "lateral" mode results.
- Continue control subsystem conceptual design
  - Integrate 6 degrees of freedom

If reduction of peak power demands is insufficient to alleviate utility load problems, a more thorough review of methods for controlling/optimizing the power factor should be made, including the use of energy storage methods such as the large AC motor generators in the Tokamak Fusion Test Reactor at Princeton University.

Since a limited (Alternative F) capability for forced model oscillation can be provided at little increase in cost over a "static" (Alternative G) system such a system may offer an attractive combination of technical features and cost.

After the operating characteristics of the system have been selected, a thorough analysis of the eddy current losses in metallic dewars should be performed. If the analysis shows that use of metallic dewars is not feasible, define a development and testing program to supplement the available technology in non-metallic dewars. The two key areas, as discussed in Section 3.4, are low-temperature helium-tight seals and thermal efficient force transmission members.

The few non-metallic dewars constructed to date with low-temperature joints have developed leaks after cooldown, apparently as a result of incompatibilities in thermal expansion and/or mechanical properties. Available data on non-metallic materials and bonding systems should be reviewed in order to identify promising material combinations. Joint approaches which provide adequate mechanical restraint, such as interlocking "finger" joints or multiple-overlap joints, should be developed, and assemblies should be fabricated and tested under helium pressure and mechanical loading at low temperatures.

Thermally efficient non-metallic tension supports incorporating integral thermal stations are commonly used in large superconducting magnets. However, a system of tension supports for the loads which occur on the MSBS coils would be extremely complex. The feasibility of extending this approach to rigid members which can provide multi-axis support should be investigated. One possible technique is the labyrinthine (Heim) column which can provide high multi-axis stiffness and a long thermal path. Other techniques are also available. Prototype assemblies should eventually be fabricated and tested for thermal performance under superimposed mechanical loads.

The magnetic requirements for the MSBS coils and the performance characteristics of the system are critically dependent on the behavior of the model magnetic core. Analysis of this behavior in the presence of spatially varying fields and/or fields non-collinear with the model axis is difficult and highly dependent on assumptions about the magnetic properties of the core material. Analytical and experimental determination of the magnetic behavior of the core is therefore highly desirable as an aid to both the design of the coil system and the core. Analytical work on soft iron cores should be complemented with equivalent work on high field permanent magnets and superconducting magnets, and should include core shapes other than cylindrical, such as ellipsoidal. For the most promising core approaches, a test program should be initiated. A test program should include superposition of the full range of fields and gradients required for operation of the system and measurement of the magnitude and direction of the resulting magnetization. Core positions should include the full range of angles expected during operation as a result of aerodynamic and magnetic forces and torques. Availability of this data will reduce the cost of the magnet system by eliminating the need for performance margins which would be required to compensate for uncertainties in core characteristics.

The problem of producing the roll torques required for MSBS has proven to be a difficult one, as discussed previously, and must be examined more comprehensively. Key issues which merit further study include:

- coil arrangement
- core configuration and material
- other roll control techniques

The present coil system was synthesized by starting with the gradient coils and adding the other coils as their characteristics and the system requirements became more clearly defined. The system impact of alternative coil configurations such as the placement of the roll coils "inside" the gradient coils, immediately adjacent to the tunnel walls, should be evaluated. Although more closely placed coils would be smaller in diameter to maintain the octagonal symmetry, the field scaling would be favorable since the axial field far from a solenoid scales approximately as the inverse of the radius, but as the inverse cube of the axial distance. However, the size of the gradient coils would be increased because of their larger distance from the model. The increase would probably be significant in the case of the Z-coils, which are near the peak field limit in the present system and would probably require a reduction in current density. The drag and magnetization coils would also have to be enlarged to accommodate the larger Z-coils. The increases in coil sizes could be handled by changes in design, but would lead to increases in cost for the coils and for the power supply and cryogenic systems. This cost increase, which could be significant

($\sim$ 10%) at the system level, would have to be traded off against the gain in roll capability.

The use of soft iron wing cores has been assumed in synthesizing the present roll control systems. Furthermore, it was assumed, as discussed in Section 3.3.7, that essentially the entire wing volume was available for the core. This latter assumption should be reviewed and modified if required to provide a basis for more realistic analysis. Because the analysis done to date has shown that the volume-average magnetization in the iron is relatively low ($\sim$ .5T), resulting in relatively poor utilization of the iron, the use of permanent magnet wing cores should be investigated. The relatively poor mechanical properties of high resonance materials such as the rare earth-transition metal alloys may be a problem if the shape of the core is relatively complex to conform to the shape of the wing. Epoxy-bonded or moldable alloys may provide acceptable fabrication and mechanical properties in conjunction with a useful increase in remanence.

Finally, it was concluded on the basis of brief analysis that a fully symmetric system using magnetic wing cores is the only approach capable of generating the relatively large roll torques required for MSBS. If the requirements cannot be met as a result of the additional effort described above and cannot be relaxed, then investigation of other approaches would be required. The most promising alternative appears to be the use of loops in the wings and/or tail to generate fields, preferably by induction but possibly with an on-board power source, which can then interact with externally applied fields. The wing location is advantageous since it offers the possibility of large areas and correspondingly large moments. However, it is emphasized that this and other alternatives are viewed as less promising than the 8-coil array previously chosen, and that the possibility that an innovative approach will lead to an adequate solution is small.

Because of the previous successful application of the Electromagnetic Position Sensor at MIT, it is recommended that a more detailed investigation (not limited to scale-up) be made of its application to MSBS. On the other hand, the Electro-Optical Position Sensor design could be initiated with target optimization analyses, photometric analyses, optimization of camera positions and fields of view.

The successful simulation of the "longitudinal" and "lateral" control system modes, separately, warrants continuing the area of activity by integrating the two modes into a single simulation. Once integrated, such a program should be used to determine the control system limits and/or responses to various rates, magnet current change, and variations in model aerodynamic characteristics.

13.3 CONSIDERATIONS INVOLVED IN ATTEMPTING TO ESTABLISH A FIGURE OF MERIT FOR POROUS POTTED SUPERCONDUCTING COILS VIS-A-VIS MECHANICALLY CONSTRAINED SUPERCONDUCTING COILS OF THE MSBS CONCEPTS

Attempting to reduce the comparison of epoxy-impregnated coils with the cryostatically stable counterpart coils to a "figure of merit" will be difficult if not impossible. Some of the key considerations are discussed below:

1. While it is true that, in general, the reduced voluem of potted coils versus cryostatically stable coils for the equivalent application leads to a lower materials cost, some of that advantage is lost due to the increased fabrication cost of impregnated coils.
2. A "merit factor" for potted coils in MSBS applications that accrues from their reduced size is the gain in visual access to the model.
3. Potted coils are inherently more rugged and reliable, thus offer an MSBS with higher productivity. GE's significant experience in the design and fabrication of potted magnets reduces the technical risk for the system.
4. No concept was developed for the cryostatically stable coils for use in Case 3. Thus, the comparison between the coils of Case 3 and Case 1 on a cost basis suffers from the inability to partition the costs between size difference due to test section size and the material/fabrication differences unique to the two approaches.
5. Peripheral equipment, such as Power Supplies, Cryogenic Subsystem, and support structure will vary in cost with the magnet power and size, which are functions of the two techniques being compared.

An attempt to reduce these considerations to a "figure of merit" is highly subjective, on the basis of present information, except, perhaps, for item 1.

Costs for complete potted magnets of the size approaching the limits of present and foreseeable technology can be expected to be 70 to 90 percent of those for cryostatically stable magnets.

Appendix A

SCALEUP OF EPOXY-IMPREGNATED COILS FOR MSBS

The use of adiabatically stable epoxy-impregnated coils manufactured by a proprietary GE technology has proven attractive for Case 3 MSBS gradient and roll coils. The high current density achievable in such coils (∿ 15,000 A/cm^2) allows them to be much more compact than conventional cryostable coils, thus providing significantly better system access and lower overall cost. The coil sizes required for Case 3 represent very modest extrapolation in size from a large solenoidal coil already built by GE.

In view of the advantages which result from the use of epoxy-impregnated coils, it is of interest to investigate the feasibility of applying this technology to larger tunnels. A brief study of the factors which may limit the scaleup of epoxy-impregnated coils has accordingly been performed. The two factors which are most likely to limit the scaleup of epoxy-impregnated windings are terminal voltage (both operating and discharge) and winding stresses.

The coil voltage is not a fundamental limit since it is always possible in principle to subdivide a coil into a large number of modules, each with a separate set of leads for operation and discharge, so that the voltage on each module is within the required limits. However, the need for modularization will make the coil increasingly complex and costly as the number of modules required increases. As an example, consider the direct substitution of an epoxy-impregnated winding for the large cryostable winding in the Case 1 Z-gradient coil. The parameters for a possible configuration are shown in Figure A-1. As is apparent, the winding volume is decreased dramatically as a result of the higher current density available and the ability to have the magnetic centers of the coils closer together along the tunnel axis.

Two options have been considered to estimate the voltages and the number of modules required for each Z-coil. These options are shown in Figure A-2. The first assumes an operating current of ∿ 750A, a value readily achievable with the available cabled conductor described in Section 3.2. The second assumes the use of a 3000-A conductor, which was proposed for use in a 300-MVA generator rotor but has not yet been fabricated or tested. The design limits on terminal voltage and maximum temperature on discharge are those used in Section 3. Both alternatives E (full forced oscillation) and F (10% forced oscillation) are shown.

It is evident from the number of modules shown in Figure A-2 that the use of an epoxy-impregnated winding for this application would require an unreasonable number of modules, with a pair of leads for each module, extremely complex and costly power supply and cryogenic systems. Scaleup of epoxy-impregnated windings for this application therefore does not appear attractive.

Although scaleup of epoxy-impregnated windings for use as gradient coils in the Case 1 system is apparently not attractive, the fact that they can be used for Case 3 would indicate that scaleup to an intermediate case (i.e. a transonic tunnel larger than 4'x4') may be possible. It is likely that scaleup will be limited by the allowable stress level in the winding composite. The limit has been estimated for the case in which the winding is a thin ring with a "soft" external structure, which provides minimal precompression and circumferential support for the winding so that the electromagnetic hoop stresses in the winding must be self-supported in tension. The case of a "hard" support which can provide significant precompression and also share a significant portion of the load on the winding has not yet been examined.

Definitive data on the circumferential tensile yield strength is not available. However, GE experience indicates that a working stress level of 206 MN/m^2 (30 ksi) is acceptable. The average electromagnetic stress in the windings is given by

$$\sigma = \frac{J\rho B}{2}$$

where σ = stress (N/m^2)
J = current density (A/m^2)
ρ = radius (m)
B = field (T)

If

$$B = 7.5T$$
$$J = 15 \times 10^7 \ A/m^2$$

which are reasonable values for an epoxy-impregnated coil, then

$$\rho \simeq .36m$$
$$\text{or } d \simeq .72m$$

Thus, for an unsupported winding, the diameter is limited to less than a meter.

This limit can be extended by the use of a high-modulus support ring which is shrunk onto the winding, and this case should be examined. However, it is clear qualitatively that as the diameter of the coil increases, the thickness of the ring must increase, and the overall current density of the winding/support ring assembly decreases correspondingly. This will reduce the advantages which the impregnated winding have over the cryostable winding.

Figure A-1

COMPARISON OF CRYOSTABLE AND ADIABATICALLY STABLE EPOXY-IMPREGNATED WINDINGS FOR A CASE 1 Z-GRADIENT COIL

	Cryostable	Adiabatically Stable
Winding Length (cm)	89	89
Winding ID (cm)	188	188
Winding Radial Depth (cm)	79	6
Overall Current Density (A/cm^2)	1500	15,000
Peak Field (T)	7.7	$\sim$ 8
Stored Energy (MJ)	105	77

Figure A-2

ELECTRICAL PARAMETERS OF AN EPOXY-IMPREGNATED CASE 1 Z-COIL

	Option I I_{op} = 750A State-of-Art		Option II I_{op} = 3000A Proposed for 300 MVA Superconducting Generator	
	Alternative E	Alternative F	Alternative E	Alternative F
dI/dt (A/sec)	2700	45	10800	180
L (h)	∿ 275	∿ 275	∿ 17	∿ 17
V_{op} (kV)	743	12.4	184	3.1
V_{disch} (kV) T_{max} = 200K	51	51	12.8	12.8
N (# of modules) V_{max} = 2 kV	372	26	92	7

Appendix B

WORK BREAKDOWN STRUCTURE
(WBS)

AND

TASK DESCRIPTIONS

2/20/81

MSBS WORK BREAKDOWN STRUCTURE (WBS)

1.0	MSBS
1.1	Preliminary Design Phase
1.1.1	System Engineering
1.1.2	Magnet Subsystems Preliminary Design
1.1.3	Cryogenics Subsystems Preliminary Design
1.1.4	Power Supply and Protection Subsystems Preliminary Design
1.1.5	Position Sensors Subsystems Preliminary Design
1.1.6	Control Subsystems Preliminary Design
1.1.7	Support Structures Preliminary Design
1.1.8	Manufacturing Engineering
1.1.9	Verification Testing
1.1.10	Preliminary Design Phase Program Management
1.2	Final Design Phase
1.2.1	System Engineering
1.2.2	Magnet Subsystems Final Design
1.2.3	Cryogenics Subsystems Final Design
1.2.4	Power Supply and Protection Subsystems Final Design
1.2.5	Position Sensors Subsystems Final Design
1.2.6	Control Subsystems Final Design
1.2.7	Support Structures Final Design
1.2.8	Manufacturing Engineering
1.2.9	Verification Testing
1.2.10	Final Design Phase Program Management
1.3	Manufacturing Installation, Checkout Phase
1.3.1	Engineering Support of Manufacturing, Installation, Checkout
1.3.2	Machines and Tooling
1.3.3	Z Gradient Coils Manufacturing
1.3.4	Y Gradient Coils Manufacturing
1.3.5	Roll Coils Manufacturing
1.3.6	Drag Coils Manufacturing
1.3.7	Magnetization Coils Manufacturing
1.3.8	Cryogenics Subsystems Manufacturing
1.3.9	Power Supply and Protection Subsystems Manufacturing
1.3.10	Position Sensors Subsystems Manufacturing
1.3.11	Control Subsystems Manufacturing
1.3.12	Support Structure Manufacturing
1.3.13	Verification Testing
1.3.14	Final Factory Inspection and Test
1.3.15	Box, Pack and Ship
1.3.16	Installation of MSBS
1.3.17	Checkout and Acceptance Testing
1.3.18	Manufacturing, Installation, Checkout Phase Program Management

TASK DESCRIPTIONS

MSBS TASK DESCRIPTIONS

WBS No.	Description
1.0	MSBS This Work Breakdown Structure covers the Preliminary Design, Final Design, Manufacturing, Installation and Checkout of the MSBS.
1.1	PRELIMINARY DESIGN PHASE The Tasks required in this Phase provide the in-depth comparisons, evaluations, selections and definitions of the MSBS approaches evolving from preceding design concept efforts and subsequent review, analysis, and decisions. These Tasks include System Engineering, Magnet Designs, Cryogenics Designs, Power Supply and Protection Designs, Position Sensor Designs and Controls Designs, in sufficient depth, and with sufficient supportive analysis to justify selections, and to enable expeditious transition to Final Design. In addition, Tasks are included for sufficient Manufacturing Engineering and Verification Test Planning to support credible schedule and cost estimates. Finally, a Task is provided to cover Program Management of the Preliminary Design Phase.
1.1.1	PRELIMINARY DESIGN SYSTEM ENGINEERING The System Engineering Task is required to provide the technical point of departure for the Preliminary Design, to maintain technical control of preliminary design options and compromises that affect the total MSBS, and to assure that the system evolving from the subsystem Tasks is internally and externally compatible. Performance of these functions will be the result of derivation and allocation of system and subsystem requirements (including reliability and maintainability), carrying-out of system-level analyses and trade-offs (including Failure Modes and Effects Analyses), maintaining overall system integration (including interface control), developing guidelines for system safety, and establishing and maintaining configuration controls.
1.1.2	MAGNET SUBSYSTEMS PRELIMINARY DESIGN This Task is required to develop and document the Preliminary Design of the Magnet Subsystems of the MSBS. To accomplish this work, the task provides for derivation of Magnet Subsystems/Components requirements from the allocated System/Subsystem requirements, definition of coil arrangements and configurations, establishment of conductor and magnet structures preliminary designs, and the carrying-out of sufficient trade studies and analyses (including stress analyses and life cycle analyses) to justify and verify such derivations, definitions and designs. This Task also provides the integration of the Magnet Subsystems that assures compatibility within the subsystems and mutually acceptable interfaces with other subsystems. Finally, this task provides for the internal documentation of the Magnet Subsystems Preliminary Design (including drawings, layouts and sketches).

WBS No.	Description
1.1.3	CRYOGENICS SUBSYSTEMS PRELIMINARY DESIGN This Task is required to develop and document the Preliminary Design of the Cryogenic Subsystems of the MSBS. To accomplish this work, the task provides for derivation of Cryogenic Subsystems/Components requirements from the allocated System/Subsystem requirements, establishment of helium, nitrogen, and vacuum subsystems preliminary design specifications (Type A) sufficient to enable procurement cost and schedule inquiries, and the carrying-out of sufficient trade studies and analyses (including liquefier/storage trades and cooldown analyses) to justify and verify the preliminary design specifications. This Task also provides the integration of the Cryogenic Subsystems that assures compatibility within the subsystems and mutually acceptable interfaces with other subsystems. Finally, this task provides for the internal documentation of the Cryogenics Subsystems Preliminary Design (including drawings, layouts and sketches).
1.1.4	POWER SUPPLY AND PROTECTION SUBSYSTEMS PRELIMINARY DESIGN This Task is required to develop and document the Preliminary Design of the Power Supply and Protection Subsystems of the MSBS. To accomplish this work, the task provides for derivation of Power Supply and Protection Subsystems/Components requirements (including requirements for all instrumentation for magnet protection, cooldown control, diagnostics, and operations) from the allocated System/Subsystem requirements, establishment of both Power Supply and Protection Subsystems preliminary design specifications (Type A) sufficient to enable procurement cost and schedule inquiries, and the carrying-out of sufficient trade studies and analyses (including cycle analyses) to justify and verify the preliminary design specifications. This Task also provides the integration of the Power Supply and Protection Subsystems (including instrumentation) that assures compatibility within the subsystems and mutually acceptable interfaces with other subsystems. Finally, this task provides for the internal documentation of the Power Supply and Protection Subsystems Preliminary Design (including drawings, layouts and sketches).

WBS No.	Description
1.1.5	POSITION SENSORS SUBSYSTEMS PRELIMINARY DESIGN

This Task is required to develop and document the Preliminary Design of the Position Sensors Subsystems (including an Electro-optical and two Electromagnetic Subsystems) of the MSBS. To accomplish this work, the task provides for derivation of Position Sensors Subsystems/Components requirements from the allocated System/Subsystem requirements, establishment of subsystems preliminary designs (including definition of sensor/model arrangements and subsystem configurations), and the carrying-out of sufficient trade studies and analyses (including electromagnetic sensor frequency analyses and position measurement accuracy analyses) to justify and verify such derivations, definitions and designs. This Task also provides the integration of each of the Position Sensors Subsystems that assures compatibility within the subsystems and mutually acceptable interfaces with other subsystems. Finally, this task provides for the internal documentation of the Position Sensors Subsystems Preliminary Design (including drawings, layouts and sketches).

1.1.6 CONTROLS SUBSYSTEMS PRELIMINARY DESIGN

This Task is required to develop and document the Preliminary Design of the Controls Subsystems of the MSBS. To accomplish this work, the task provides for derivation of Controls Subsystems/Components requirements from the allocated System/Subsystem requirements, definition of controls software, establishment of controls and displays preliminary designs, documentation of the Controls Computer Preliminary Design Specification (Type A) sufficient to enable procurement cost and schedule inquiries, and the carrying-out of sufficient trade studies and analyses (including cross-coupling analyses) to justify and verify such derivations, definitions and designs. Furthermore, this Task provides for Controls Subsystem simulation to demonstrate the adequacy of the Controls Subsystem Preliminary Design. This Task also provides the integration of the Controls Subsystems that assures compatibility within the subsystems and mutually acceptable interfaces with other subsystems. Finally, this Task provides for the internal documentation of the Controls Subsystems Preliminary Design (including drawings, layouts and sketches).

1.1.7 SUPPORT STRUCTURES PRELIMINARY DESIGN

This Task is required to develop and document the Preliminary Design of the Support Structures of the MSBS. To accomplish this work, the task provides for derivation of Support Structures requirements from the allocated System/Subsystem requirements, establishment of preliminary design specifications (Type A) sufficient to enable procurement cost and schedule inquiries, and the carrying-out of sufficient trade studies and analyses

WBS No.	Description
1.1.7	SUPPORT STRUCTURES PRELIMINARY DESIGN (cont.)

(including stress and life cycle analyses) to justify and verify the preliminary design specifications. This Task also provides the integration of the Support Structures that assures mutually acceptable interfaces with other subsystems. Finally, this task provides for the internal documentation of the Support Structures Preliminary Design (including drawings, layouts and sketches).

1.1.8 MANUFACTURING ENGINEERING FOR PRELIMINARY DESIGN

The requirements of this Task are to assure that the preliminary design is manufacturable, and to provide preliminary planning for the fabrication phase. This Task will provide the producibility engineering effort of reviewing preliminary design layouts, drawings, and design specifications, and recommending design changes. In addition, this Task will provide the preliminary planning for MSBS manufacturing facilities, machines and tools; fabrication and assembly processes; quality control; testing; and installation and alignment.

1.1.9 VERIFICATION TESTING FOR PRELIMINARY DESIGN

During Preliminary Design, the requirements of this Task are to identify potentially necessary Verification Tests and propose the preliminary plans for such testing. The Task will review all Preliminary Design areas against current state-of-the-art, and develop preliminary verification testing plans in sufficient depth to enable costing and scheduling of at least the following tests for the Final Design and Manufacturing Phases:

- o AC Losses Testing
- o Conductor Qualification
- o Conductor Splice Testing
- o Instrumentation Testing
- o Insulation Testing
- o Cryostat Materials and Structures Testing

1.1.10 PRELIMINARY DESIGN PHASE PROGRAM MANAGEMENT

This element of the WBS provides the necessary project planning, management, measurement, control and reporting to assure the high quality, timely, and economical accomplishment of the preliminary design of the MSBS. This effort shall include the Project Direction, Contract and Financial Management, Performance Measurement, Procurement Planning, Quality Assurance and Data Management (including Reports and Design Reviews) that assure meeting scheduled project milestones and costs, including award of long lead procurement contracts. This Task also includes the planning necessary for the subsequent Final Design, Manufacturing, Installation and Checkout Phases.

WBS No.	Description
1.2	FINAL DESIGN PHASE

1.2 FINAL DESIGN PHASE

The Tasks required in this Phase provide the analyses and detailed design definitions of the MSBS that upgrade and update the preceding preliminary design, based on subsequent NASA review, analysis, and decisions. These Tasks include System Engineering, Magnet Designs, Cryogenics Designs, Power Supply and Protection Designs, Position Sensor Designs and Controls Designs, in sufficient depth, and with sufficient supportive analysis to produce an MSBS Final Design that is ready for Manufacturing. In addition, Tasks are included for Manufacturing Engineering and Verification Testing to assure credibility of the Final Design, and to support credible subsequent Phase schedule and cost estimates. Finally, a Task is provided to cover Program Management of the Final Design Phase.

1.2.1 FINAL DESIGN SYSTEM ENGINEERING

The System Engineering Task is required to provide the technical point of departure for upgrading and updating the Preliminary Design to the Final Design, to maintain technical control of design options and compromises that affect the total MSBS, and to assure that the system evolving from the subsystem Tasks is internally and externally compatible. Performance of these functions will be the result of incorporating post-Preliminary design changes and re-allocation of system and subsystem requirements (if required), carrying-out of system-level analyses and trade-offs (including Failure Modes and Effects Analyses), maintaining overall system integration (including interface control), developing a system safety plan, and establishing and maintaining a Configuration Control program.

1.2.2 MAGNET SUBSYSTEMS FINAL DESIGN

This Task is required to develop and document the Final Design of the Magnet Subsystems of the MSBS. To accomplish this work, the Task provides for upgrading and updating of Magnet Subsystems/ Components requirements from the allocated System/Subsystem requirements (if required), final design of coil arrangements and configurations, final design of conductor and magnet structures, and preparation of component specifications. This Task also documents the integration of the Magnet Subsystems, and the interfaces that assure compatibility with other subsystems. In addition, this Task provides for the internal documentation of the Magnet Subsystems Final Design (including drawings and layouts). A key function of this Task is the identification of long lead items requiring early procurement (such as the magnet conductor).

WBS No.	Description
1.2.3	CRYOGENICS SUBSYSTEMS FINAL DESIGN This Task is required to develop and document the Final Design of the Cryogenic Subsystems of the MSBS. To accomplish this work, the task provides for upgrading and updating of Cryogenic Subsystems/Components requirements from the allocated System/Subsystem requirements (if required), establishment of helium, nitrogen, and vacuum subsystems product specifications (Type B) to enable initiation of procurement proposal requests, and the carrying-out of final analyses (including liquefier/storage sizing and cooldown analyses) to justify and verify the product specifications. This Task also documents the integration of the Cryogenic Subsystems and the interfaces that assure compatibility with other subsystems. Finally, this Task provides for the internal documentation of the Cryogenics Subsystems Final Design (including drawings and layouts).
1.2.4	POWER SUPPLY AND PROTECTION SUBSYSTEMS FINAL DESIGN This Task is required to develop and document the Final Design of the Power Supply and Protection Subsystems of the MSBS. To accomplish this work, the Task provides for upgrading and updating of Power Supply and Protection Subsystems/Components requirements (including requirements for all instrumentation for magnet protection, cooldown control, diagnostics, and operations) from the allocated System/Subsystem requirements (if required), establishment of both Power Supply and Protection Subsystems product specifications (Type B) to enable initiation of procurement proposal requests and schedule inquiries, and the carrying-out of final analyses (including use cycle analyses) to justify and verify the product specifications. This Task also documents the integration of the Power Supply and Protection Subsystems (including instrumentation) and the interfaces that assure compatibility with other subsystems. Finally, this Task provides for the internal documentation of the Power Supply and Protection Subsystems Final Design (including drawings and layouts).
1.2.5	POSITION SENSORS SUBSYSTEMS FINAL DESIGN This Task is required to develop and document the Final Design of the Position Sensors Subsystems (including an Electro-optical and two Electromagnetic Subsystems) of the MSBS. To accomplish this work, the task provides for upgrading and updating of Position Sensors Subsystems/Components requirements from the allocated System/Subsystem requirements (if required), final design of subsystems (including sensor/model arrangements and mounting configurations), and preparation of component specifications. This Task also documents the integration of each of the Position Sensors Subsystems and the interfaces assure compatibility with other subsystems. Finally, this Task provides for the internal documentation of the Position Sensors Subsystems Final Design (including drawings and layouts).

WBS No.	Description
1.2.6	CONTROLS SUBSYSTEMS FINAL DESIGN This Task is required to develop and document the Final Design of the Controls Subsystems of the MSBS. To accomplish this work, the task provides for upgrading and updating of Controls Subsystems/Components requirements from the allocated System/Subsystem requirements (if required), final documentation of controls software, final design of controls and displays, documentation of the Controls Computer Product Specification (Type B) to enable initiation of procurement proposal requests, and the carrying-out of final analyses and simulation to justify and verify the designs. This Task also documents the integration of the Controls Subsystems and the interfaces that assure compatibility with other subsystems. Finally, this Task provides for the internal documentation of the Controls Subsystems Final Design (including drawings and layouts).
1.2.7	SUPPORT STRUCTURES FINAL DESIGN This Task is required to develop and document the Final Design of the Support Structures of the MSBS. To accomplish this work, the task provides for upgrading and updating of Support Structures requirements from the allocated System/Subsystem requirements (if required), establishment of product specifications (Type B) to enable initiation of procurement proposal requests, and the carrying-out of final analyses (including stress and life cycle analyses) to justify and verify the product specifications. This Task also documents the integration of the Support Structures and the interfaces that assure compatibility with other subsystems. Finally, this Task provides for the internal documentation of the Support Structures Final Design (including drawings and layouts).
1.2.8	MANUFACTURING ENGINEERING FOR PRELIMINARY DESIGN The requirements of this Task are to assure that the Final Design is manufacturable, and to provide final planning for the fabrication phase. This Task will provide the producibility engineering effort of reviewing final design layouts, drawings, and design specifications, and recommending design changes. In addition, this Task will provide the final planning for MSBS manufacturing facilities, machines and tools; fabrication and assembly processes; quality control; testing; and installation and alignment.
1.2.9	VERIFICATION TESTING FOR FINAL DESIGN During Final Design, the requirements of this Task are to plan and carry out necessary Verification Tests. The Task will review the preliminary Verification Testing plans and all design areas against current state-of-the-art, and develop final verification testing plans for approval by NASA.

WBS No.	Description
1.2.9	VERIFICATION TESTING FOR FINAL DESIGN (cont.)

Upon approval by NASA, the following tests are expected to be carried out:

- o AC Losses Testing
- o Conductor Qualification
- o Conductor Splice Testing
- o Instrumentation Testing
- o Insulation Testing
- o Cryostat Materials and Structures Testing

1.2.10 FINAL DESIGN PHASE PROGRAM MANAGEMENT

This element of the WBS provides the necessary project planning, management, measurement, control and reporting to assure the high quality, timely, and economical accomplishment of the final design of the MSBS. This effort shall include the Project Direction, Contract and Financial Management, Performance Measurement, Procurement Planning, Quality Assurance and Data Management (including Reports and Design Reviews) that assure meeting scheduled project milestones and costs, including award of long lead procurement contracts. This Task also includes the planning necessary for the subsequent Manufacturing, Installation and Checkout Phase.

1.3 MANUFACTURING, INSTALLATION, CHECKOUT PHASE

The Tasks required in this Phase provide the high quality, timely, economical fabrication and delivery of an MSBS ready for operation. These Tasks include Engineering Support during this hardware phase, position of Machines and Tooling to fabricate and handle the MSBS, Manufacturing of all Magnets, Manufacturing of all Vacuum Vessels, Manufacturing of Cryogenic Subsystems, Manufacturing of Power Supply and Protection Subsystems, Manufacturing of Position Sensors Subsystems, Manufacturing of Controls Subsystems (including provision of software), and Manufacturing of MSBS Support Structure. In addition, provision is made for Verification Testing required to support manufacturing materials and processes. Pre-shipment Inspection and Test are provided, followed by shipment to NASA, where Tasks of Installation, Checkout and Acceptance Testing are carried out. Finally, a Task is provided to cover Program Management of the Manufacturing, Installation, Checkout Phase.

WBS No.	Description
1.3.1	ENGINEERING SUPPORT OF MANUFACTURING, INSTALLATION, CHECKOUT

During the hardware phase, this Task is required to provide for support by design engineers/manufacturing engineers/ installation engineers and operations engineers to resolve design/fabrication/assembly/testing discrepancies and problems, maintain configuration control, and manage the Safety Program. Design and Manufacturing Engineering support the Procurement and Manufacturing of the MSBS including the processing and approval of design and drawing changes, the inspections of products/processes for quality control, the documentation and resolution of the Non-Conformance Reports, and Vendor Surveillance. Installation and Operations Engineering support the on-site assembly, checkout and testing planning and preparations, including receiving inspection of MSBS Subsystems and Components, handling and storage. In addition, this Task provides for implementing and maintaining the Safety Program, including management of the program, resolving waivers and deviations, updating the Safety Plan, and carrying out safety training, as required.

1.3.2 MACHINES AND TOOLING

This Task is required to furnish both Standard Machines and Tools, normally available in large manufacturing facilities, and Special Machines and Tools, specifically designed for the MSBS manufacturing processes. No changes are made for Standard Machines and Tools. This Task provides for acquisition (including design, fabrication/procurement, modification/adaption) of Special Machines and Tools, and preparation and set-up of Machines and Tools for MSBS Manufacturing.

1.3.3 Z GRADIENT COILS MANUFACTURING

This Task is required to carry out the manufacture of the four complete Z gradient magnets. The Task covers the component acquisition process (including procurement, vendor surveillance, receiving inspection and storage), preparation for assembly into succeeding elements, all pertinent manufacturing processes (such as coil winding, splicing, bonding) and all pertinent in-process inspection and testing. Specific components and assemblies involved in this task include the conductor, insulation, coil forms and casing, vacuum vessel, auxiliary equipment (including leads, terminals, connectors, and service stack components), instrumentation, and handling fixtures.

WBS No.	Description
1.3.4	Y GRADIENT COILS MANUFACTURING

This Task is required to carry out the manufacture of the four complete Y gradient magnets. The Task covers the component acquisition process (including procurement, vendor surveillance, receiving inspection and storage), preparation for assembly into succeeding elements, all pertinent manufacturing processes (such as coil winding, splicing, bonding), and all pertinent in-process inspection and testing. Specific components and assemblies involved in this Task include the conductor, insulation, coil forms and casing, vacuum vessel, auxiliary equipment (including leads, terminals, connectors, and service stack components), instrumentation, and handling fixtures.

1.3.5 ROLL COILS MANUFACTURING

This Task is required to carry out the manufacture of the eight complete roll magnets. The Task covers the component acquisition process (including procurement, vendor surveillance, receiving inspection and storage), preparation for assembly into succeeding elements, all pertinent manufacturing processes (such as coil winding, splicing, bonding), and all pertinent in-process inspection and testing. Specific components and assemblies involved in this Task include the conductor, insulation, coil forms and casing, vacuum vessel, auxiliary equipment (including leads, terminals, connectors, and service stack components), instrumentation, and handling fixtures.

1.3.6 DRAG COILS MANUFACTURING

This Task is required to carry out the manufacture of the complete drag magnets. The Task covers the component acquisition process (including procurement, vendor surveillance, receiving inspection and storage), preparation for assembly into succeeding elements, all pertinent manufacturing processes (such as coil winding, splicing, bonding), and all pertinent in-process inspection and testing. Specific components and assemblies involved in this Task include the conductor, insulation, coil forms and casing, vacuum vessel, auxiliary equipment (including leads, terminals, connectors, and service stack components), instrumentation, and handling fixtures.

1.3.7 MAGNETIZATION COILS MANUFACTURING

This Task is required to carry out the manufacture of the two complete magnetization magnets. The Task covers the component acquisition process (including procurement, vendor surveillance, receiving inspection and storage), preparation for assembly into succeeding elements, all pertinent manufacturing processes (such as coil winding, splicing, bonding), and all pertinent in-process inspection and testing. Specific components and assemblies involved in this Task include the conductor, insulation, coil

WBS No.	Description
1.3.7	MAGNETIZATION COILS MANUFACTURING (cont.)

forms and casing, vacuum vessel, auxiliary equipment (including leads, terminals, connectors, and service stack components), instrumentation, and handling fixtures.

1.3.8 CRYOGENICS SUBSYSTEMS MANUFACTURING

This Task is required to carry out the manufacture of the complete cryogenics subsystems (including the helium subsystem, the nitrogen subsystem and the vacuum subsystem). The Task covers the component and subassembly acquisition process including procurement, vendor surveillance, pre-shipment inspection, and storage (if required). Since Cryogenics Subsystems components and subassemblies are primarily purchased items, and mainly of large size, the majority of such components and subassemblies will be shipped directly from vendor to the MSBS assembly site after pre-shipment inspection (or storage, if required). Assembly of this equipment is covered under WBS item 1.3.16, Installation of MSBS.

1.3.9 POWER SUPPLY AND PROTECTION SUBSYSTEMS MANUFACTURING

This Task is required to carry out the manufacture of the complete Power Supply and Protection Subsystems. The Task covers the component and subassembly acquisition process including procurement, vendor surveillance, pre-shipment inspection, and storage (if required). Since Power Supply and Protection Subsystems components and subassemblies are primarily purchased items, and some are of large size, the majority of such components and subassemblies will be shipped directly from vendor to the MSBS assembly site after pre-shipment inspection (or storage, if required). Selected components and subassemblies, however, will be required for in-factory magnet testing, or for assembly into succeeding elements prior to shipment to the MSBS assembly site. Final assembly of the Power Supply and Protection Subsystems is covered under WBS Item 1.3.16, Installation of MSBS. Since much of the Instrumentation of the MSBS is utilized for magnet protection, control, alarm and diagnostics, this Task is charged with the acquisition of such instrumentation, although the installation of instrumentation in the magnets is covered under WBS items 1.3.3, 1.3.4, 1.3.5, 1.3.6 and 1.3.7.

WBS No.	Description
1.3.10	POSITION SENSORS SUBSYSTEMS MANUFACTURING This Task is required to carry out the manufacture of three complete Position Sensor Subsystems - two Electromagnetic Position Sensors and one Electro-optical Position Sensor. The Task covers the component and subassembly acquisition process (including procurement, vendor surveillance, receiving inspection and storage), preparation for assembly into succeeding elements, all pertinent manufacturing processes, and all pertinent in-process inspection and testing. Specific components of the Electromagnetic Position Sensors include the excitation coils and position sensing coils, coil forms and coil form structure, electrostatic shields, and appropriate leads, wiring and signal processing. Components of the Electro-optical Position Sensor include CID (Charge Injection Device) Cameras, video data processor, model-mounted targets, appropriate leads and wiring and optional video displays - appropriate visual access through test section walls as well as lighting of the model must be available.
1.3.11	CONTROL SUBSYSTEMS MANUFACTURING This Task is required to carry out the manufacture of the complete MSBS Control System. The Task covers the component and subassembly acquisition process (including procurement, vendor surveillance, receiving inspection and storage (if required), preparation for assembly into succeeding elements, all pertinent manufacturing processes, all pertinent in-process inspection and testing, and programming and checkout of the control software. Components and assemblies involved in this Task include the Control System Computer, the Model Control Keyboard and Display, the Magnet Operational Keyboard and Display and required wiring, as well as the control software.
1.3.12	SUPPORT STRUCTURE MANUFACTURING This Task is required to carry out the manufacture of the complete Support Structure for the MSBS. The Task covers the component and subassembly acquisition process (including procurement, vendor surveillance, pre-shipment inspection, and storage (if required). Since Support Structure components and subassemblies are primarily purchased items, relatively non-complex, and some are of large size, they will be shipped directly from vendor to the MSBS assembly site after pre-shipment inspection (or storage, if required). Specific components and subassemblies of the Support Structure included intra-coil supports and fasteners, MSBS-to-Baseplates supports and fasteners, and Position Sensors-to-Baseplates supports and fasteners.

WBS No.	Description
1.3.13	VERIFICATION TESTING FOR MANUFACTURING

1.3.13 <u>VERIFICATION TESTING FOR MANUFACTURING</u>

The requirement of this Task is to implement tests required to qualify the manufacturing process. The following verification tests will be performed:

- o Structural Material - verify that the structural material and weld process yield acceptable design properties at operating temperature.
- o Conductor Qualification - verify that the process used to join the conductor core to the conductor jacket does not degrade the required critical current rating of the conductor composite.
- o Conductor Splice Qualification - verify that the process used to join conductor sections maintains the required design properties.

1.3.14 <u>FINAL FACTORY INSPECTION AND TEST</u>

The requirement of this Task is to provide final quality checks on all manufactured articles not already inspected and tested at vendors premises prior to shipment. The following inspections and tests will be performed:

All magnets - Continuity Test, Hi-Pot Test, Vacuum Test, Full Field Test, Magnetic Center Location and Recording

Protection Subsystem - Instrumentation Operability, Continuity Test

Position Sensors, Electromagnetic - Continuity Test

Position Sensors, Electro-optical - Camera Operability, Continuity Test

Control Subsystems - Test Problem Simulation, Displays Operability, Continuity Test

1.3.15 <u>BOX, PACK AND SHIP</u>

The requirement of this Task is to prepare all items not shipped from vendors for shipment to NASA and to ship it for on-schedule arrival

1.3.16 <u>INSTALLATION OF MSBS</u>

The requirements of this Task are to assemble all of the MSBS components, subassemblies, and assemblies at the Installation location, and install the MSBS on a site prepared by NASA. Based on planning carried out during the design phase under WBS item 1.2.9, this Task will provide the on-site receiving inspection, emplacing the appropriate magnet support structures, mounting the magnets, installing the cryogenic subsystems and their transfer piping, installing the power supply and protection

WBS No.	Description
1.3.16	INSTALLATION OF MSBS (cont.)

subsystems (including the circuit breakers and dump resistors) and their bus/cable circuitry, and installing the Controls Subsystems and its circuitry. This Task will also provide the utility services hook-ups to electrical power (110 and 440V). Cooling water (atmospheric and 60 psi), outside ventilation of nitrogen. Accomplishment of this Task assumes NASA will provide predetermined space in the immediate vicinity of the Wind Tunnel Test Section for the Magnet Subsystems, Liquid Helium Transfer Lines and Storage Dewar, Power Supplies buses/cables. In close proximity, NASA will need to provide space for the power supplies, circuit breakers and dump resistors, as well as the helium refrigerator/liquefier. Space for outdoor storage of liquid nitrogen and gaseous helium will be required in the general vicinity of the test section, and means for truck delivery of these items. Space for installation of the Control Subsystem will also be required in the general vicinity of test section. NASA is expected to furnish access to the electrical power and water listed above, and instrument cooling air.

1.3.17 CHECKOUT AND ACCEPTANCE TESTING

This Task requires the final assurance of the operability of the MSBS and its acceptance by NASA. Upon completion of installation, this Task covers the step-by-step operation of all subsystems at levels established to indicate readiness for full-scale operation, monitoring and recording of the performance of all subsystems, and identification of potential problem areas. After correction of potential problems, this Task covers a test operation of the total MSBS at pre-agreed levels, and upon successful completion of the test, acceptance of the MSBS by NASA.

1.3.18 MANUFACTURING, INSTALLATION, CHECKOUT PHASE PROGRAM MANAGEMENT

This element of the WBS provides the necessary project planning, management, measurement, control and reporting to assure the high quality, timely, and economical fabrication and delivery of the MSBS. This effort shall include the Project Direction, Contract and Financial Management, Performance Measurement, Procurement Management, Quality Assurance and Data Management (including Reports and Reviews) that assure meeting scheduled project milestones and costs, including award of procurement contracts, fabrication milestones, and deliveries.

Appendix C
VERIFICATION TESTING PROGRAM

The purpose of verification testing is to support the Design and Manufacturing Engineering functions by obtaining test results to verify the adequacy of the actual designs and processes to be used. Verification testing is a common, standard procedure in the superconducting magnet business for designs at the state of the art. Most features of the General Electric MSBS designs are supported by valid data or directly comparable experience, but testing is required to verify some state of the art design features and manufacturing procedures (processes). Because of the large size, number, required reliability, and cost of the MSBS coils, the failure of one or more coils to meet its performance requirements would lead to an expensive, time-consuming repair or replacement effort.

The test cycle involves identification of areas of technical concern, determination of the design requirements in these areas, and definition and planning of tests to verify adequacy of the actual designs, processes, or materials. The consequences of not performing each test are then evaluated, in terms of technical risk as well as program costs and schedule, and only those tests found to be necessary are proposed to the customer.

Proposals for the selected tests are written, including cost and schedule estimates. Approved tests are performed, and the results are reported and interpreted to the Engineering functions. Any features which are shown to be inadequate can then be redesigned and retested, so that sufficient confidence in the design is obtained. Testing for design verification tests will be completed prior to and in support of the final design review. Testing for process verification tests will be performed according to a schedule that provides information in a timely manner, as the production hardware is fabricated.

1. Report No.	2. Government Accession No.	3. Recipient's Catalog No.
NASA CR-165917		

4. Title and Subtitle	5. Report Date
Design Concepts and Cost Studies for Magnetic Suspension and Balance Systems	July 1982
	6. Performing Organization Code

7. Author(s)	8. Performing Organization Report No.
*H. L. Bloom, et al	81LSP47251
	10. Work Unit No.

9. Performing Organization Name and Address	11. Contract or Grant No.
Kentron International, Inc. Hampton Technical Center Hampton, VA 23666 (Subcontractor) General Electric Company Energy Systems Programs Dept. Schenectady, NY 12345	NAS1-16000

12. Sponsoring Agency Name and Address	13. Type of Report and Period Covered
National Aeronautics and Space Administration Washington, DC 20546	Contractor Report
	14. Sponsoring Agency Code

15. Supplementary Notes

Langley Technical Monitor: Neil A. Holmberg
Final Report - Nov. 1980 thru March 1981

*General Electric Company

16. Abstract

This report presents the final results of a study of the application of superconducting magnets for suspension and balance of wind tunnel models.

Conceptual designs are presented for Magnetic Suspension and Balance System (MSBS) configurations compatible with three high Reynolds number cases representing specified combinations of test section conditions and model sizes. Concepts, in general met initially specified performance requirements such as duty cycle, force and moment levels, model angular displacement and positioning accuracy with nominal design requirements for support subsystems. Other performance requirements, such as forced model sinusoidal oscillations, and control force magnitude and frequency, were modified during the study, at the request of the customer, so as to alleviate the magnitude of magnet, power, and cryogenic design requirements that resulted in equipment concepts that were inordinately large and/or costly.

To preserve the information developed in pursuing the above-noted performance and design permutations, the report provides configuration and cost data for concepts responsives to three sets of variations in each of the three specified cases.

Among the significant configuration results for the 9 concepts, the data shows variations in magnet 4-quadrant power supplies ranging from 10 to 8000 volts with total magnet input power of 15 to 5400 MVA, helium refrigerator/liquefiers with capacities ranging from 5000 to 700,000 liters, superconducting magnetization and drag coils whose diameters range from 3 to 10 meters. Cost results show comparable variations ranging from $29,000,000 to $447,000,000 non-recurring costs, and daily operating costs of $7500 to $1,500,000.

17. Key Words (Suggested by Author(s))	18. Distribution Statement
Magnetic Suspension, Magnetic Balance, Superconducting Magnets, Wind Tunnel Apparatus, Model Support Interference Wind Tunnel Balance	Unclassified - Unlimited Subject Category 09

19. Security Classif. (of this report)	20. Security Classif. (of this page)	21. No. of Pages	22. Price
Unclassified	Unclassified	346	A15

N-305

For sale by the National Technical Information Service, Springfield, Virginia 22161

End of Document